AFFDL-TR-70-49

STRESS AND DEFLECTON ANALYSIS OF MECHANICALLY FASTENED JOINTS

HARRY G. HARRIS
IRVING U. OJALVO
REGINALD E. HOOSON
Grumman Aerospace Corporation
Bethpage, New York

TECHNICAL REPORT AFFDL-TR-70-49

MAY 1970

AIR FORCE FLIGHT DYNAMICS LABORATORY
AIR FORCE SYSTEMS COMMAND
WRIGHT-PATTERSON AIR FORCE BASE, OHIO

NOTICE

When Government drawings, specifications, or other data are used for any purpose other than in connection with a definitely related Government procurement operation, the United States Government thereby incurs no responsibility nor any obligation whatsoever; and the fact that the government may have formulated, furnished, or in any way supplied the said drawings, specifications, or other data, is not to be regarded by implication or otherwise as in any manner licensing the holder or any other person or corporation, or conveying any rights or permission to manufacture, use, or sell any patented invention that may in any way be related thereto.

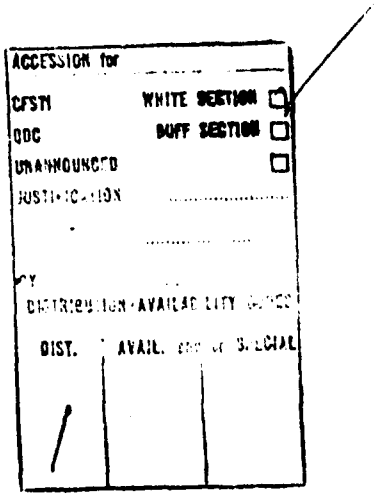

Copies of this report should not be returned unless return is required by security considerations, contractual obligations, or notice on a specific document.

400 - June 1970 - CO455 - 122-2702

AFFDL-TR-70-49

STRESS AND DEFLECTON ANALYSIS OF MECHANICALLY FASTENED JOINTS

HARRY G. HARRIS
IRVING U. OJALVO
REGINALD E. HOOSON

FOREWORD

This report was prepared by the Grumman Aerospace Corporation, Bethpage, New York, under Contract No. F 33615-69-C-1263 with the Air Force Flight Dynamics Laboratory of the Research and Technology Division, Air Force Systems Command, Wright-Patterson Air Force Base, Ohio. The work was accomplished under Project No. 1467 "Structural Analysis Methods", and Task No. 146704 "Structural Fatigue Analysis". Technical monitor on this project was Howard A. Wood. This report covers work conducted from 15 January 1969 to 15 January 1970, and was submitted for review 15 January 1970. The manuscript was released by the authors in April 1970 for publication as an RTD Technical Report.

The project engineer and principal investigator of the present effort was Harry G. Harris, Unit Leader, Structural Mechanics Section, with Alex Gomza, Assistant Chief of Structural Mechanics acting as primary consultant. In addition to the authors, the painstaking efforts of Albert J. Davidson of the Structural Mechanics Section who wrote the computer programs and Appendices A and E of the report are gratefully acknowledged. Other Structural Mechanics personnel who contributed to the technical effort are William E. Falby, Vangala S. Reddy and Barry B. Silverman.

The experimental effort was supervised by Robert Zoellner of the Elements and Materials Test Group.

All computations were performed at the Grumman Data Systems Corporation.

This technical report has been reviewed and is approved.

FRANCIS J. JANIK, JR.
Chief, Solid Mechanics Branch
Structures Division

ABSTRACT

This report presents analytical techniques for predicting both the linear and nonlinear stresses and deformations of mechanically fastened joints. The idealization used is a set of stacked parallel plates which transfer planar loads among themselves by means of transverse fasteners. The plates are treated by finite element methods of matrix structural analysis in which each element is assumed to be in plane stress for both elastic and plastic stress states. The fasteners, which are treated by short-beam theory, interact with the plates under the assumption that the plates may be represented by an equivalent elastic foundation.

Application of the present analytical techniques was made to a variety of problems including: the combined elastic-plastic behavior of plates with unloaded holes, the load-deflection behavior of single-fastener joints, the residual stress distributions in plates with squeeze rivets, the effect of fastener bending and shear deformation on the bearing stress distribution between the fastener and the plate, and the prediction of the fatigue life of typical mechanically fastened joints. In all these cases, comparisons with test results generally gave very good correlation.

Parametric studies were performed to determine the effects on stress and deflection distributions of variables such as: initial clearance or interference between fastener and hole, load level, geometry and material properties. The effect of these variables upon fatigue life of single and multi-fastener joints under realistic loadings was also assessed.

For the range of parameters studied, the effects of hole clearance and fastener interference and geometric configuration appear to play the dominant roles in determining the stress distribution and hence, the fatigue life of mechanically fastened joints.

TABLE OF CONTENTS

LIST OF TABLES

LIST OF FIGURES

LIST OF SYMBOLS

a	material constant in member equation
A	fastener cross-sectional area (in^2); constant
B	constant
C, C_1, C_2 C_3, C_4, C_5, C_6	constants
d	fastener diameter (in.)
D, D_i	diameter of hole (in.); constant
ΔD	change in diameter
e, e_1, e_2	plate edge distances measured from the hole center, (in.)
E	Young's modulus (psi)
f	nominal stress, (ksi)
f_m	mean nominal stress, (ksi)
f_{max}	maximum nominal stress, (ksi)
f_{min}	minimum nominal stress, (ksi)
G	shear modulus of fastener material, (psi)
I	fastener cross-sectional moment of inertia, ($in.^4$)
k	"spring constant" or slope of the load-deflection curve (lb./in.); foundation modulus (psi)
k_1	foundation modulus of plate layer 1 (psi)
k_2	foundation modulus of plate layer 2 (psi)
k_{eff}	effective joint stiffness (lb/in)
$K \equiv$ S.C.F.	stress concentration factor
k_{fp}	Stowell plastic stress concentration factor
K_N	Neuber stress concentration factor
K_T	theoretical elastic stress concentration factor
ℓ	beam length (in); gage length (G.L.)

M	cross sectional moment (in-lb)
M_1	cross sectional moment at beam station 1 (in-lb)
M_2	cross sectional moment at beam station 2 (in-lb)
M_H	cross sectional moment at head attachment (in-lb)
N	cycles to failure
p	radius of hole or notch in Neuber equation, (in.)
P	applied load; squeeze rivet applied load, (lb.)
P_i	redundant radial load; load at a particular offset of δ_i in the load-deflection curve, (lb.)
P_j	load at an offset of δ_j (lb.)
P_o	statically determinate radial load in contact problem, force transmitted by fastener-held joint (lb.)
P^*	by-pass load in multi-fastener joint, (lb.)
P_u	ultimate load, (lb.)
P_2	load at an offset of 0.002 inches, (lb.)
P_5	load at an offset of 0.005 inches, (lb.)
P_{12}	load at an offset of 0.012 inches, (lb.)
q	distributed plate-interaction load per unit of fastener length (lb/in)
Q	cross sectional shear; fastener transfer load in multi-fastener joints, (lb.)
S, S_W	hole spacing, (in.); hole spacing across plate width, (in.)
S_L	hole spacing along plate length, (in.)
W, W_1, W_2	plate width, (in.)
x	fastener axial coordinate, (in.)
$\bar{x}$	fastener axial coordinate with shift in origin, (in.)
X	cartesian coordinate
y, y_1, y_2	relative beam deflections, (in.)
Y	cartesian coordinate

β	fastener cross sectional shearing-angle rotation (radians)
$\bar{\beta}$	fastener-plate bending stiffness parameter (in^{-4})
γ	fastener-plate shearing stiffness parameter (in^{-2})
γ_1, γ_2	fastener-plate shearing stiffness parameters (in^{-2})
δ	displacement, (in)
δ_e	elastic component of displacement, (in)
δ_p	plastic component of displacement, (in)
δ_o	correction to p vs. δ curve, (in)
δ_T	overall joint deflection, (in)
δ_{Ti}	total displacement corresponding to P_i on load-deflection curve, (in)
δ_{Tj}	total displacement corresponding to P_j on load-deflection curve, (in)
Δ	denotes incremental quantity (dimensionless)
ϵ	strain, in/in
ϵ_a	strain amplitude, in/in
ϵ_{elr}	elastic strain range, in/in
ϵ_{max}	maximum strain, in/in
ϵ_t	equivalent fully reversed strain amplitude in/in
ϵ_{tr}	equivalent fully reversed strain range in/in
ϵ_1	major principal strain; strain range for initial stage of unload, in/in (Fig. 55)
ϵ_2	intermediate principal strain; strain range for final stage of unload, in/in (Fig. 55)
ϵ_3	minor principal strain, in/in
$\bar{\epsilon}$	"effective strain", (in/in)
$\epsilon^{(k)}$	uniaxial strain at k^{th} cycle, (in/in)
$\bar{\epsilon}^p$	plastic component of "effective strain", (in/in)
η	applied loading cycles

θ	angular measure around hole circumference
λ	cross sectional shear parameter (dimensionless)
ν	Poisson's ratio (dimensionless)
σ	stress, (ksi)
σ_f	stress at fracture in static test, (ksi)
σ_{max}	maximum stress, (ksi)
σ_{maxR}	value of σ_{max} when $E/k \rightarrow \infty$
σ_{min}	minimum stress, (ksi)
σ_m	mean stress at edge of hole or notch, (ksi)
σ_{net}	net section stress, (ksi)
σ_0	mean net section stress due to interference, (ksi)
$\sigma_{appl.}$	net section stress due to applied load, (ksi)
σ_r	radial stress
σ_R	ratio of σ_{max} to σ_{maxR}
σ_θ	circumferential stress, (ksi)
$\sigma_1, \sigma_2, \sigma_3$	principal stresses
$\bar{\sigma}_N^{(k)}$	effective stress of the N^{th} element at k^{th} cycle
$\sigma_{3N-2}^{(k)} = \sigma_x^{(k)}$	for the N^{th} element at k^{th} cycle
$\sigma_{3N-1}^{(k)} = \sigma_y^{(k)}$	for the N^{th} element at k^{th} cycle
$\sigma_{3N}^{(k)} = \tau_{xy}^{(k)}$	for the N^{th} element at k^{th} cycle
$\sigma^{*(k)}$	relaxed uniaxial stress at k^{th} cycle
$\Delta\sigma_1$	stress range for initial stage of unload, ksi (Fig. 55)
$\Delta\sigma_2$	stress range for final stage of unload, ksi (Fig. 55)
Ψ	cross sectional rotation, (radians)

Matrices:

$\{D_A\}$	allowable relative radial displacements
$\{D_B\}$	relative radial displacement caused by by-pass load
$\{P\}$	load vector
$\{P^{(k)}\}$	load vector at the k^{th} cycle
$\{\delta\}$	nodal displacement vector
$\{\delta^{(k)}\}$	nodal displacement vector at the k^{th} cycle
$\{\epsilon_i\}$	initial strain vector
$\{\epsilon_i^{(k)}\}$	initial strain vector at the k^{th} cycle
$\{\Delta_r\}$	relative radial displacement vector
$\{\sigma\}$	stresses of all elements
$\{\sigma^{(k)}\}$	stresses at the k^{th} cycle
$\{\mathfrak{L}\}$	loading conditions
$[A]$	flexibility coefficients of hole for unit radial loads
$[D]$	influence coefficients relating induced strains to nodal displacements
$[D_L]$	relative radial displacements for various loadings in statically determinate structure
$[G]$	influence coefficients relating induced strains to element stresses
$[\Delta]$	influence coefficients relating applied loading to nodal displacements
$[\Gamma]$	influence coefficient relating applied loading to element stresses.

CHAPTER 1. SUMMARY OF PRESENT EFFORT

1.1 Introduction

The accurate structural analysis of mechanically fastened joints is an important aspect in the efficient design of aircraft structures where minimum weight is a prime consideration. As a first step in such an analysis, it is necessary to know the distribution of the applied loads among the different fasteners in a multi fastener joint. Previous investigations (Refs. 1 and 2) have developed convenient, practical methods for determining such gross load distributions in multi fastener joints. However, one of the necessary input quantities for the use of such methods is the load-displacement relationship for an appropriate single fastener joint. In the studies of Refs. 1 and 2 recort to test data was made in obtaining the input information necessary for such gross analysis methods.

In addition, another input to these procedures is the proper spring constants representing the sheet material between fasteners. The spring constants involve uniformly loaded "effective widths" because of the non uniform stress fields that exist in the sheets in the vicinity of the fasteners. Here again the techniques of Refs. 1 and 2 employ semi-empirical inputs to account for the plate spring constants needed in the analysis.

The methods developed in the present study provide an alternative to the empirical approach by supplying analytical predictions of the plate-fastener spring constants for the complete range of loading up to and beyond yielding, using nonlinear planar analyses. Methods are also developed for predicting the non-planar elastic portion of the load-deflection curve of a single fastener. A more general inelastic procedure for predicting the inelastic portion of this load-deflection curve is also indicated but not implemented. The total joint deformation resulting from both plate and fastener deformations are then determined and some analytical results are compared with those obtained from a concurrent, small scale experimental program.

After the transfer loads and by pass loads for the individual fasteners are obtained by procedures such as those of Refs. 1 and 2, the peak stresses

that occur in the vicinity of the fastener holes must still be determined. These total peak stresses are particularly significant in fatigue studies. The procedures presented in this report, which employ matrix methods of structural analysis in conjunction with finite element techniques, enable the determination of these stresses in plates having either loaded or unloaded holes. Furthermore, the effects of fastener bending and shear deformations on the distribution of bearing stress between fastener and plate, through the plate thickness, are analyzed and the resulting increases in the peak bearing stress determined.

To determine the applicability of the analytical results obtained, the fatigue analysis prediction of an aluminum joint with both hole clearance and interference fit is made. Finally, a comparison is made of the analytical life prediction of an actual titanium joint with test results showing the effect of clearances for a spectrum type loading.

1.2 Methods of Analysis

1.2.1 General

A mechanically fastened joint is, in general, a highly redundant structure in which the mechanism of load transfer creates a nonlinear, three-dimensional, combined elastic-plastic stress state. Since the exact analysis of such problems is clearly beyond the present state of the art, a more modest approach, based upon justifiable engineering simplifications, is employed.

Basically, the approach taken is to create a series of two-dimensional plate idealizations which include as variable parameters the important planar effects such as material properties, geometric configuration, hole clearance and interference fit. In addition, a one-dimensional model capable of accounting for fastener shear and bending, head stiffness effects and bearing stress variation through the plate thickness is used. This component analogue to simulate the actual mechanically fastened structure is illustrated schematically in Fig. 1.

1.2.2 Two-Dimensional Problems

The planar problems are treated by the finite element method of structural analysis. Two types of problems are considered in the present study: (1) elastic-plastic analysis of plates with unloaded holes, and (2) elastic nonlinear contact problem analysis of plates with holes loaded by

rigid circular pins having arbitrary initial fit conditions. The analysis of problems of the first type is given in Chapter 2 and problems of plates with loaded holes are treated in Chapter 3

1.2.3 Three-Dimension Effects

The three-dimensional fastener-plate interaction is approximated through idealization of this system as a short beam on an elastic foundation. The fastener deformations are treated by various beam theories which include either shear or bending effects, while the plates are replaced by a continuous set of mutually uncoupled springs whose moduli are determined from the concurrent two-dimensional finite-element study described in Section 1.2.2.

1.3 Application of Present Analytical Results

1.3.1 Effective Width and Inelastic Stiffness of Plates with Holes

An elastic-plastic planar analysis capable of generating "spring constants" for the plates in multi-fastener joint analyses as described in Refs. 1 and 2 is applied to several plates with unloaded holes. The stiffness characteristics of these structures are evaluated at load levels in the elastic and plastic regions. From the planar finite element analysis the "effective width" of the plate is determined. Present results reveal that this parameter is strongly influenced by the hole spacing-to-hole diameter ratio (S/D) and to the hole spacing-to-plate width ratio (S/W). For usual hole spacing, say of the order of 4D, it is found for the values of S/W considered, that the effective width of the plate is approximately 75 to 90 percent of the original width.

1.3.2 Prediction of Load-Deflection Behavior for Single Fasteners in Single and Double Shear

The bending and shear deflections in a fastener are evaluated separately by solving the differential equations for a beam on an elastic foundation, where the modulus of the foundation is the local spring constant of the plate. The cases considered are a fastener in antisymmetrical single shear and a fastener in symmetrical double shear. The relative magnitudes of the shear and bending deformations are estimated for several cases through numerical applications. In addition, the effects of head fixity are estimated through consideration of the two limiting cases, i.e., a rigidly clamped head and one with negligible rotational resistance.

The effects of fastener flexibility on the bearing stresses between fastener and plate through the plate thickness are examined. The increase in the bearing stress, at some plate thickness locations, above the nominal bearing stress obtained with a rigid fastener are evaluated for a range of fastener diameter to plate thickness ratios and the results presented in graphical parametric form. If shear rigidity of the plate in the thickness direction may be neglected, these local increases in bearing stress result in corresponding increases in all the plate stresses at the same plate thickness locations.

1.3.3 Fatigue Analysis Under Constant Amplitude and Spectrum Loading

The effect of fastener fit (ie. clearance and interference) on fatigue life of mechanically fastened joints is studied for conditions of constant amplitude and spectrum type loading. In general, results indicate that fatigue life is reduced for cases where there is a clearance between fastener and hole and increased where there is an interference fit. The degree of improvement or reduction in fatigue life is shown to be a function of the amount of clearance or interference in the joint.

There appears to be a fairly uniform decrease in fatigue life in going from a neat fit condition up to clearances of approximately 2% dia., after which the effect is progressively less significant. For interference fit cases, results indicate the possibility of an optimum interference for a given stress level and joint geometry. It should be noted however, that excessive amounts of interference may be detrimental to fatigue life.

1.3.4 Correlation With Experimental Results

(1) Static Tests

Overall joint flexibilities for single fasteners in double shear are determined both experimentally and analytically. A comparison of the results reveals a reasonable correlation for the modest number (15) of tests performed. Both tests and analytical predictions reveal a greater sensitivity of results with the type of fit between fastener and hole (i.e., loose or interference) rather than with the fastener material employed.

(2) Fatigue Tests

Fatigue test data for double-shear and multi fastener aluminum alloy and titanium alloy joints, which include both constant amplitude and spectrum type fatigue loading, are compared to analytical predictions based on the results of this study. Although the data exhibit a fairly large scatter, the trend to reduction in fatigue life as clearance between fastener and hole is increased is clearly demonstrated. Improvement in fatigue life is generally obtained in going from a neat fit or clearance to an interference fit, but there are optimum degrees of interference for given stress levels and joint geometries. It is notable that all the basic trends are predictable by analysis.

Limited experimental test data are also presented to show the effect of clamp-up due to installation torque on fatigue life. A multi fastener double-shear aluminum alloy joint was tested in constant amplitude fatigue for conditions of normal clamp-up and no clamp-up. Considerable increases in fatigue life are shown for the clamp-up condition.

1.4 Conclusions and Recommendations

Analytical methods for studying the complex structural three-dimensional stress and deflection behavior of mechanically fastened joints have been presented in this report. These techniques have proved to be very useful in obtaining basic data so as to gain a better understanding of the problem and to narrow down the most important parameters which affect structural joint behavior. The results of planar analyses of plates with loaded and unloaded holes have provided input information for both static load-deformation characteristic studies and fatigue life predictions of joints.

An adequate engineering method of determining the separate effects of fastener shear and bending flexibility on overall joint flexibilities and local stress distributions has been developed. For the cases considered, the effects of bending flexibility were generally less significant than the effects of shear flexibility.

Possible extensions of the techniques presented include a more refined beam theory to include the effects of fastener shear and bending simultaneously, as well as countersink head effects and clamp-up force upon overall joint compliance and stress concentration.

It is concluded from these studies that the fatigue lives of mechanically fastened joints are significantly affected by the degree of clearance or interference between the fasteners and holes. Basic trends shown in experimental joint fatigue test data have been reasonably well predicted by the fatigue analysis. It was also possible to account for certain aspects of joint fatigue behavior through a study of the elastic stress variation around plate holes, as related to nominal stress level and hole location in the joint.

It is concluded that clearances between fasteners and holes will reduce fatigue life beyond that obtained with a neat fit condition. In addition the effect on an interference fit will generally improve fatigue life, although behavior under this condition is not as predictable as in the case of clearance fits. This is due to the degree of plasticity encountered as a result of the initial interference fit. Trends shown by the fatigue analysis, backed up by limited test data, indicate the possibility of the existence of an optimum interference for a given joint geometry, and that additional interference beyond these levels may tend to reduce fatigue life.

A limited study of the effect of clamp-up in a joint has shown that fatigue life can increase significantly as a result of clamp-up. This effect can be accounted for by analysis if a reasonable estimate of the magnitude and distribution of frictional forces is made.

It is recommended that further attention be given to the prediction of stress distribution in the region of fastener holes in joints, for the conditions of clearance and interference fits. For the interference cases in particular, extension of the present work to include the effects of plasticity would result in a closer representation of the stress-strain behavior at a hole or notch. If the strain amplitude in a fatigue cycle can be estimated to a reasonable degree of accuracy, the use of strain-life data enables a good estimate of fatigue life to be made. The trends indicated by the qualitative analysis methods employed in the present study are sufficiently well defined to show the value of a continuing effort in this field.

CHAPTER 2 INELASTIC ANALYSIS OF PLATES WITH UNLOADED HOLES

2.1 Introduction

The elastic-plastic analysis of planar structures having stress concentrations caused by unloaded holes is considered in this section. To perform such analyses two computer programs (based on finite element methods) are used. The first is an elastic analysis used to generate influence coefficients relating the applied loading and plastic strains to the stresses and displacements throughout the structure. The second step in the analysis procedure is an incremental plasticity program to follow the load well into the inelastic range. For this purpose a previously available computer program designated here as the Grumman-Air Force plasticity program was modified and expanded to accommodate the present computational requirements. This program is fully documented in the present report.

2.2 Inelastic Stress and Deflection Analysis of Planar Structures

2.2.1 Basic Considerations

The Grumman-Air Force program which forms the basis of the present plasticity analyses is fully documented in Ref. 3. The theoretical background of the program and the necessary modifications to provide for an inelastic deflection analysis capability are summarized here.

The program uses the "initial strain" method of plastic analysis where plastic strains are interpreted as initial strains. The basis of the method resides in the formulation of the stiffness analysis problem as a series of linear analyses each of which involves representation of a state of initial strain in the structure. The general formulation for this type of problem can be written in matrix form:

$$\{\sigma\} = [\Gamma]\{P\} + [G]\{\epsilon_i\} \qquad (1)$$

Here, the σ's are the stress values which characterize the state of stress in the respective elements of the structure. These may be defined, in a given element, e.g., at its centroid, or at nodal points of the finite element idealization. The matrix $[\Gamma]$ relates the stresses $\{\sigma\}$ to the applied loading

{P}, on the basis of a conventional elastic matrix displacement analysis of the structure. The matrix [G] relates the stresses to the initial strains $\{\epsilon_i\}$.

A similar expression to the element stresses can be written for the generalized nodal displacements since these must be determined at each step of the loading in order that a complete analysis of a structural joint can be made. This equation takes the form:

$$\{\delta\} = [\Delta]\{P\} + [D]\{\epsilon_i\} \tag{2}$$

In this expression the values of the nodal displacements $\{\delta\}$ are computed in an analogous fashion to the stresses at each step in the load increment. The matrix $[\Delta]$ is the flexibility matrix relating displacements to applied loads {P}, and the matrix [D] relates nodal displacements to the initial strains. Both the $[\Delta]$ and [D] martices are determined from an elastic analysis of the structure together with the matrices $[\Gamma]$ and [G] needed for the stress analysis. These four matrices then act as inputs to the plasticity program.

In the present approach, the initial strains ϵ_i are taken as the plastic strains ϵ^p at the specified load level. The load is applied incrementally and the above linear analyses are applied for each increment. An examination of the numerical techniques used to solve such nonlinear problems reveals two possible approaches: (1) a non iterative step-by-step calculation in which all quantities, including the initial (plastic) strains, ϵ_i, are incremented and (2) an alternate iterative procedure for any particular load level. The first approach, which is the most straightforward, is the one used in this analysis.

Two methods for the non iterative step-by-step procedure have been suggested in Ref. 4 but subsequent evaluation of these methods (Ref. 3) indicates that only one of them is free from inherent computational instabilities. In this method the stresses in the plate are expressed by the following modified form of

$$\{\sigma^{(k)}\} = [\Gamma]\{P^{(k)}\} + [G]\{\epsilon_i^{(k-1)}\} \tag{3}$$

where k is the load increment designation. In a similar fashion the computations for the displacements can be made by rewriting Eq. 2 in the form

$$\{\delta^{(k)}\} = [\Delta]\{P^{(k)}\} + [D]\{\epsilon_i^{(k-1)}\} \qquad (4)$$

where k is the same load increment designation as before. In Eqs. 3 and 4 the stresses and displacements in the k^{th} increment are expressed in terms of the initial (inelastic) strains from the $(k-1)^{th}$ increment.

The actual method used for determining the stresses and strains in the k^{th} increment is the "constant strain" method, which is illustrated in Fig. 2 for a uniaxial stress-strain case. The method proceeds as follows. One enters the k^{th} increment with applied loads $\{P^{(k)}\}$ and initial strains $\{\epsilon^{(k-1)}\}$, the latter evaluated during the preceding increment. The first operation of the k^{th} increment is to determine an approximation to $\{\sigma^{(k)}\}$ from Eq. 3 by direct substitution. Referring to Fig. 2 point A is thus determined with stress-strain coordinates $\sigma^{(k)}$ and $\sigma^{(k)}/E + \epsilon^{p(k-1)}$. Since point A will probably not lie on the stress-strain curve of the material, the stress at point A is relaxed to $\sigma^{*(k)}$ (while the total strain is held constant, i.e., "constant strain"), corresponding to point B, which does lie on the stress-strain curve. Point B, then, defines the final, corrected values of stress, $\sigma^{*(k)}$, and initial strain, $\epsilon_i^{(k)}$, in the k^{th} cycle, as indicated in Fig. 2.

2.2.2 Isotropic Elastic-Plastic Analysis

In the general biaxial stress state which is of interest in the analysis of planar structures, the notion of an "effective" stress-strain relationship as shown in Fig. 3 is used in conjunction with the Von-Mises yield criterion and the Prandtl-Reuss flow relations of incremental plasticity theory.

The biaxial analysis employs the same step-by-step procedure described above, with modifications for biaxial stress states. It can be summarized in the following algorithm for the k^{th} load level:

1. Obtain the stress components at each node using the basic Eq. (3) by assuming the initial strains from the previous load level.

2. Using these stresses, calculate an "effective" stress at each node.

3. Assuming that the effective stress-strain relation for the material, modified by including the elastic strain, corresponds to data measured in a simple uniaxial tension test, determine the "effective" strain corresponding to the effective stress. Calculate the corresponding effective plastic strain and the increment in effective plastic strain over the previous load level.

4. Using the incremental flow relations, calculate the inelastic strain increments. The proportionality constant in these equations is the ratio of the effective plastic strain increment to the effective stress.

At this point in the calculation, the applied load can be incremented again and the cycle repeated. The details in implementing each of these four steps in the algorithm follows:

Step (1) When calculating the stresses $\sigma_N^{(k)}$ at the node point, N, for the k^{th} load level using the initial strains from the $(k-1)^{th}$ load level in Eq. (3), it is convenient to identify the three stress components (one shear and two normal) at the node point by means of subscripts 3N, 3N-1, and 3N-2, as follows:

$$\begin{Bmatrix} \cdot \\ \cdot \\ \cdot \\ \sigma_N^{(k)} \\ \cdot \\ \cdot \\ \cdot \end{Bmatrix} = \begin{Bmatrix} \cdot \\ \cdot \\ \cdot \\ \sigma_{3N-2}^{(k)} \\ \sigma_{3N-1}^{(k)} \\ \sigma_{3N}^{(k)} \\ \cdot \\ \cdot \\ \cdot \end{Bmatrix} \qquad (5)$$

The stresses are thus arranged in groups of three components at each node point N.

Step (2) We now calculate the corresponding effective stresses $\bar{\sigma}_N^{(k)}$ for each of the nodes from the Von-Mises expression:

$$\bar{\sigma}_N^{(k)} = \left[\left(\sigma_{3N-2}^{(k)}\right)^2 - \left(\sigma_{3N-2}^{(k)}\right)\left(\sigma_{3N-1}^{(k)}\right) + \left(\sigma_{3N-1}^{(k)}\right)^2 + 3\left(\sigma_{3N}^{(k)}\right)^2\right]^{\frac{1}{2}} \qquad (6)$$

Note that by definition $\bar{\sigma}_N^{(k)}$ must be positive and is proportional to the octahedral shear stress. This expression together with the stress-strain data constitutes the strain hardening criterion.

Step (3) Assuming that the effective stress-strain curve ($\bar{\sigma}$ vs. $\bar{\sigma}/E + \bar{\epsilon}^P$) is the same as the tensile stress-strain for the material of interest, we use the curve, together with the constant strain method, to determine the corrected (relaxed) value of $\bar{\sigma}_n^{(k)}$ and the corresponding effective plastic strain $\bar{\epsilon}_N^{p(k)}$. The increment in the effective plastic strain $\Delta\bar{\epsilon}_n^{p(k)}$ over that of the preceding interval will be either positive or zero, depending upon whether plastic loading or elastic unloading is taking place. Thus

$$\Delta\bar{\epsilon}_N^{p(k)} = \bar{\epsilon}_N^{p(k)} - \bar{\epsilon}_N^{p(k-1)} \qquad (7a)$$

when $\bar{\sigma}_N^{(k)}$ is greater than any previous $\bar{\sigma}_N$ (inelastic strain increasing), and

$$\Delta\bar{\epsilon}_N^{p(k)} = 0 \qquad (7b)$$

when $\bar{\sigma}_N^{(k)}$ is smaller than a previous $\bar{\sigma}_N$.

Step (4) The increments in the ordinary plastic strain components may now be obtained using a Prandtl-Reuss incremental relationship.

$$\Delta\epsilon_{3N-2}^{p(k)} = \frac{\Delta\bar{\epsilon}_N^{p(k)}}{\bar{\sigma}_N^{(k)}}\left[\sigma_{3N-2}^{(k)} - 1/2\ \sigma_{3N-1}^{(k)}\right] \qquad (8a)$$

$$\Delta\varepsilon^{p(k)}_{3N-1} = \frac{\Delta\bar{\varepsilon}^{p(k)}_N}{\bar{\sigma}^{(k)}_N}\left[\sigma^{(k)}_{3N-1} - 1/2\ \sigma^{(k)}_{3N-2}\right] \tag{8b}$$

$$\Delta\varepsilon^{p(k)}_{3N} = \frac{\Delta\bar{\varepsilon}^{p(k)}_N}{\bar{\sigma}^{(k)}_N}\left[\sqrt{3}\sigma^{(k)}_{3N}\right] \tag{8c}$$

The total, ordinary plastic strain components are obtained by addition,

$$\begin{Bmatrix} \vdots \\ \varepsilon^{p\ (k)}_{3N-2} \\ \varepsilon^{p\ (k)}_{3N-1} \\ \varepsilon^{p\ (k)}_{3N} \\ \vdots \end{Bmatrix} = \begin{Bmatrix} \vdots \\ \varepsilon^{p\ (k-1)}_{3N-2} \\ \varepsilon^{p\ (k-1)}_{3N-1} \\ \varepsilon^{p\ (k-1)}_{3N} \\ \vdots \end{Bmatrix} + \begin{Bmatrix} \vdots \\ \Delta\varepsilon^{p\ (k)}_{3N-2} \\ \Delta\varepsilon^{p\ (k)}_{3N-1} \\ \Delta\varepsilon^{p\ (k)}_{3N} \\ \vdots \end{Bmatrix} \tag{9}$$

These components together with the new applied loads $P^{(k+1)}$ may be substituted in Eq. (3) to obtain $\sigma^{(k+1)}_N$ in the next load cycle.

2.2.3 Computer Program

The computer program which incorporates the theory described above is explained in Appendices A through D. Appendix A is essentially a user's manual for the program and describes the various options available. The logic of the program is given by means of extensive flow charts in Appendix B. The complete FORTRAN listing of the program is given in Appendix C. By necessity, the IBM 7094 version of the program provided for the Flight Dynamics Lab is small because of core limitations. Nevertheless, with a maximum number of 34 plastic nodes available, a moderate size stress concentration problem can still be run. An example of the output of the program is given in Appendix D which presents the results of a two hole aluminum plate at only three of the total of 150 load increments used in the solution up to a maximum load of 18,000 lbs.

2.3 Results and Discussion

2.3.1 Finite Element Idealizations

For the planar structural analyses of the present study, the finite element approach was used. The analysis technique, described in Section 2.2, requires an elastic analysis of the structure to be made in order to generate the four influence input matrices for the plasticity analysis. The Grumman COMAP-ASTRAL structural analysis program was used for this purpose. The details of this program will not be presented in this report but can be found in Refs. 5 and 6 . Three different finite elements, available in the COMAP-ASTRAL library of elements, were examined and compared in the early stages of the study. These included the constant strain triangular element, the constant strain quadrilateral element (composed of four constant strain triangles), and a linearly varying strain triangle. The comparison of the three elements showed excellent convergence properties for the linearly varying strain triangle and somewhat slower convergence for the constant strain elements. However, the quadrilateral has a decided advantage over the triangle because more refinement in the grid size can be accomplished, for topological reasons, by using the same number of quadrilaterals as triangles for any particular structure. At the time when the work of the present effort was performed the COMAP-ASTRAL program did not have a matrix stacking procedure for the induced strain matrices and therefore considerably more data handling would have been necessary in using the linearly varying strain triangular element. For this reason, the constant strain quadrilateral element was used in all the parametric studies of this chapter. In the case of the constant strain elements the induced strain matrix reduces to a straight-forward matrix multiplication and is easily accomplished in COMAP, which is basically a matrix manipulation package.

2.3.2 Rectangular Plates

The mathematical model used to study the effective width of a plate which is part of a structural joint, as well as the effect of fastener spacing, is shown in Fig. 4 . Due to symmetry, only a quadrant of the plate shown need be analyzed. Note that the grid chosen has a greater refinement near the region of high strain gradient, which for this type problem is perpendicular to the direction of the load. The number of elements used in this idealization

was 54. This is close to the maximum of 60 allowed for the IBM-360 version of the plasticity program used, in which all computations are done in core. Table 1 and Fig. 4 give the geometric properties of the six plate problems analyzed in this series. A graphical option in the input data, when using the Grumman structural analysis program COMAP-ASTRAL, permits the use of a graphical check to the input. Using this option to check the geometry and member data, plots of the six plates were made by means of an Orthomat drafting machine as shown in Figs. 5 and 6 . All the plates were assumed to be of 2024-T4 aluminum alloy having the stress-strain curve shown in Fig. 7 .

The output of the plasticity program includes all the nodal displacements and all the element centroidal stresses (when using constant strain elements) or nodal stresses (when using the linearly varying strain triangular element) at all increments of loading. From these results both the load-deflection characteristics and stress concentration factors of the structure can be computed. For purposes of illustration of the analytical results, the net section tangential stress distributions at various load levels are shown in Fig. 8 for plate problem P 1.1. The mean net section stress is also indicated in Fig. 8 at each level of load. The effects of plasticity are such that a leveling in the peak stresses at the hole boundary occurs as the load increases. The stress concentration factor, which is the maximum stress divided by the net section stress, decreases with load as shown in Fig. 9 . Note also from this figure that the theoretical stress concentration factor is underestimated by about 20% using this particular idealization.

The load-deflection characteristics of plate No. P 1.3 shown in Fig. 10a. At any level in the loading the tangent to the load-deflection curve indicates the stiffness, k, of the structure. This has been plotted vs. applied load in Fig. 10b and shows a considerable drop in stiffness at a load level above 7 kips. Data such as the above can be readily used in the multi fastener joint analyses described in Refs. 1 and 2 which require the spring rates of the plate between fasteners as an input.

One of the objectives of the present study was the analytic determination of the "effective width" of a strap in tension pierced by several holes. The load-deflection curve obtained by finite element analysis is used to determine

the elastic spring constant, k_e, shown in Fig. 11 for the three plates with an S/W ratio of 2. Fig. 12 shows similar load-deflection results for three plates with an S/W ratio of 1. An "effective width" can be computed using the relations:

$$k_e = \frac{A_e E}{S}$$

and $$A_e = (W - D_e)t = W_e\, t$$

where,

A_e is the "effective" cross sectional area

E is the Young's modulus

S is the spacing of the holes or pitch

W is the distance between fastener lines

D_e is the "effective diameter"

W_e is the "effective width"

and t is the plate thickness

Using the values of k_e obtained from Figs. 11 and 12, values of the "effective width" were computed. The results are shown in Fig. 13 for the six plates analyzed. It should be noted from Fig. 13 that as the fastener spacing to diameter ratio (S/D) decreases, the "effective width" decreases rapidly. At the "standard" spacing of 4D for example, the value of the "effective width" is between 75 and 90 percent of the original width for the two S/W ratios shown. The corresponding value of D_e for an S/D of 4 is 0.38D for S/W = 1 and 0.60D for S/W = 2. This appears much lower than the 0.80D recommended by McCombs et. al. (Ref. 1) as a semi-empirical value.

2.3.3 Plates Tapered in Width

A series of four tapered plate analyses were performed in order to study the effect of taper in width on the stiffness characteristics of the plate. A summary of the geometric properties of the plates is given in Table 2. The idealization used on this symmetric structure is shown in Fig. 14 using constant stress quadrilateral elements. Orthomat drawings of the four problems were made to check the geometry and member data input. These are shown in Figs. 15 to 18 . The four tapered plates are assumed to be made of 2024-T4 aluminum alloy and have the stress strain behavior shown in Fig. 7. No

yielding is assumed below a stress level of 40,000 psi. The stress distribution across the two net sections of plate P 3.1A, as a function of applied load, is shown in Fig. 19 where the mean net section stress is also indicated. In Fig. 20 the variation of the stress concentration factor with increasing applied load is shown. The same decreasing effect with increasing load mentioned in connection with plate P 1.1 (Fig. 9) is obtained in this case also. The load-deflection characteristics of the four plates are summarized in Fig. 21 . The effect of decreasing taper and the resulting decrease in net-section area shows a substantial reduction in the elastic modulus, k_e, as the taper is decreased from 1:4 (P 3.1B) to 1:16 (P 3.3B) the k_e drops from 432,000 lb/in to 343,000 lb/in. Plate P 3.3B has a relatively low carrying capacity compared to the other three. An examination of the development of yield zones with increasing load as shown in Fig. 21 will explain this behavior. At a load level of 5,200 lb. the yielded elements have transversed the whole net section of the edge holes with the resulting reduction in stiffness. The strain hardening modulus of 2024-T4 aluminum alloy is taken to be 360,000 psi (Fig. 7), which is approximately 30 times smaller than the elastic modulus. Hence, when the net section elements have yielded, the overall stiffness values will be very low compared to the elastic range stiffnesses.

CHAPTER 3 PLATES WITH LOADED HOLES

3.1 Nonlinear Contact Problem - Elastic Analysis

3.1.1 Introduction

In a typical multi-fastener joint under load the stress distribution around a particular hole is very complex and depends on a variety of geometric, material and manufacturing parameters. This chapter treats the problem of plates loaded by fasteners having either initial clearance or interference. A basic assumption in the analyses to be presented is that the stress distribution across the plate thickness is constant. This restraint will be relaxed in Chapter 4 which analyzes the three dimensional effects causing a non-uniform distribution across the plate thickness.

The load transfer from one plate of a joint to another through a fastener creates a nonlinear contact problem. The reason is that as the load in the joint changes the area of contact between the plate and the fastener changes and hence there is gradual load redistribution. The amount of redistribution is a function of the load level and the initial amount of clearance or interference between the fastener and the hole. Frictional effects also play an important role on the area of contact but for the present analysis these are assumed negligible so that the load direction at any point on the contact surface is always assumed to be radial in direction. Only radial compressive loads are permitted in the analysis.

3.1.2 Analytical Model

The mathematical model chosen in order to study the local effects of the load transfer and by-pass load around a single fastener is shown in Fig. 23. This analysis assumes that a region around the fastener can be isolated from the rest of the joint (Fig. 23a) in which the stresses influenced primarily by the fastener are localized. Another assumption is that the plate structure is symmetric and is loaded symmetrically as shown in Fig. 23b. The problem is one where on a specified number of contact points around the periphery of the hole the redundant radial reactions must be determined for a given load level and a particular initial fit condition.

Using the notation shown in Fig. 23b an expression can be written for the relative radial displacements between the plate and the rigid

fastener. This expression takes the form:

$$\{\Delta_r\} = [A]\{P\} + [D_L]\{\mathfrak{L}\} + \{D_A\} + \{D_B\} \qquad (10)$$

where,

$\{\Delta_r\}$ are the relative displacements or "gaps" that exist between the plate and the fastener,

$[A]$ is the flexibility matrix for unit radial load,

$\{P\}$ are the redundant radial loads which exist on the contact surface,

$[D_L]$ are the relative radial displacements that exist in the statically determinate structure ($P_i \equiv 0$) for various loading conditions, $\{\mathfrak{L}\}$,

$\{\mathfrak{L}\}$ load levels or loading conditions,

$\{D_A\}$ set of relative radial displacements caused by initial clearance or interference between the fastener and the plate hole,

$\{D_B\}$ relative radial displacements in the statically determinate structure caused by the applied by-pass load, P^*.

The condition for obtaining the redundants P is to set the relative radial displacements to zero.

$$\{0\} = [A]\{P\} + [D_L]\{\mathfrak{L}\} + \{D_A\} + \{D_B\} \qquad (11)$$

$$\text{Thus,} \quad \{P\} = -[A]^{-1}\left\{[D_L]\{\mathfrak{L}\} + \{D_A\} + \{D_B\}\right\} \qquad (12)$$

If any of the P's are positive (tensile) these are put to zero. By a trial and error procedure the redundants are computed such that all are compressive and the computed relative radial displacements create a compatible deflected condition between the plate and the fastener. The details of the various steps used to generate the matrices needed for solving the contact problem are given in Appendix I .

3.1.3 Computer Program

The iterative solution of Equation 12 is accomplished by means of the nonlinear contact program documented in Appendices E through H. Appendix E

explains the use of the program. Extensive flow charts of the program are provided in Appendix F and the FORTRAN listing is given in Appendix G. A sample problem output is shown in Appendix H for illustrating the form of the output. The case run is the aluminum plate Problem P 2.3 with fit condition C2 which is equivalent to a $\frac{\Delta D}{D}$ of 0.4 percent. The initial lack of fit indicated in the program refers to the percentage based on the radius of the hole, not the diameter. Once the components of the radial loads are obtained as illustrated in Appendix H for each load level, these are then applied to the plate structure to determine the elastic stress and displacement distribution throughout.

3.1.4 Effect of Load Level and Fit on the Elastic Stress Distribution

(1) Aluminum Plates

Using the analysis techniques described in Section 3.3.1 and Appendix I, four Aluminum joints loaded by means of a single rigid fastener were studied. The geometric properties of these are given in Table 3. Orthomat drawings, used as a means of checking the input, were made and are shown in Figs. 24 and 25. Problem P 2.1 has the same geometry as the double shear single fastener joints used in the test program and described fully in Chapter 7. Results of the analysis to be presented in this section coupled with the three dimensional effects caused by fastener bending and shear given in Chapter 4 will be used as a comparison of the present analysis with the experimentally determined load deflection curve.

The effects of load level and initial fit on the load distribution at the contact surface between the fastener and the plate are illustrated in Figs. 26 to 28 for plate P 2.1. In these figures the loads on the rigid fastener are drawn vectorially to scale for three different load levels: 500 lb., 2000 lb. and 8000 lb. applied load. It should be noted that the loads acting on the plate structure are equal and opposite to those shown in these figures. For the initial lack-of-fit cases it can be seen that as the load increases the fastener deforms into the plate with the consequence that more and more points around the periphery come into contact. The effect of interference fit on the load distribution is to create a pre-compression on the fastener or a pre-tension or hoop stresses around the periphery of the hole. As the load of the fastener is increased the initial load distribution changes

and for the smaller values of interference ($\frac{\Delta D}{D}$ = 0.004 and 0.02) the applied load is enough to pull the fastener away from the top of the hole (Fig. 28).

The variation of the maximum tangential stresses at the net section at different load levels is illustrated in Figs. 29 to 31 . Fig. 29 gives the maximum tangential stress distribution for a clearance of $\frac{\Delta D}{D}$ = 0.004 of plate P 2.1 and Fig. 30 gives the distribution for a clearance of $\frac{\Delta D}{D}$ = 0.02.

The variation of tangential stress at a section $\theta = 81^{\circ}$ for four different interference fits is illustrated in Fig. 31 . These results although obtained from an elastic analysis can still be very useful for generating stress concentration factors needed in a fatigue analysis. The application of these results to fatigue analysis of typical joints is illustrated in Chapter 5. The stress concentration factors vary with amount of clearance and level of load as illustrated in Figs. 32 to 34 for problem P 1.1 to P 1.3 respectively. Note from these figures that the clearance increases the stress concentration factor substantially and hence it may be anticipated that the fatigue life of the joint will consequently be decreased .

In the case of interference fit fasteners the stress concentration factor, as defined in this study (maximum stress divided by net section stress), must be modified. At zero applied load a substantial tensile tagential stress can exist at the edge of the hole depending on the magnitude of the interference and the position around the hole. The method of defining stress concentration factors for interference fit fastener was to use the net section stress, σ_{net}, as follows:

$$\sigma_{net} = \sigma_0 + \sigma_{appl.} \qquad (13)$$

where,

σ_0 = mean net section stress at zero applied load

$\sigma_{appl.}$ = mean net section stress corresponding to the applied load

Using this approach the modified stress concentration factor for plate P 2.3 with an interference fit $\frac{\Delta D}{D}$ = 0.004 was computed at six different cross sections and plotted vs. increasing applied net section stress in

Fig. 35. The results of Fig. 35 indicate that for a net section stress below 25 ksi the critical section is at 9° to the direction of load. As the load increases, however, the critical section rotates by 90°. This phenomenon can be explained by the fact that at a net section stress above 25 ksi the fastener has completely overcome the radial clamping effect of interference and is beginning to pull from the top of the hole. This has also been observed experimentally in Ref. 7 .

For the same plate a ten times larger interference ($\frac{\Delta D}{D} = 0.04$) indicates similar trends but at much higher net section stresses as shown in Fig. 36. A plot of maximum modified stress concentration factor vs. applied net section stress is shown in Fig. 37 for the same plate with three different interference fits.

Another important aspect of the plate with a single loaded fastener analysis is the use of the plate "spring constant" as input to the study of three dimensional effects (Chapter 4). The load-deflection curves of two of the aluminum joints are shown in Figs. 38 and 39 for all the different initial fit conditions indicated.

(2) Titanium Plates

The problem of a two fastener titanium joint in double shear was also analyzed using the contact problem program. The dimensions of the outer plates of the joint are shown in Fig. 40 together with the finite element model used in the analysis. Results of the effect of different clearances on the stress concentration factor are presented in Fig. 41 with increasing net section stress. The effect of load on the stress concentration factor with increasing load is not as large as in the case of the aluminum joints (Figs. 32 to 34) which had a different geometry. The results of Fig. 41 were used in Chapter 5 to compare the analytical fatigue life predictions with actual spectrum test results. The comparison of these is shown in Fig. 61 and the experimental work pertaining to the titanium joint is described in Section 7.2.2.

3.2 Elastic and Plastic Interference Stresses in Plates With Squeeze Rivets

3.2.1 Introduction

In order to increase the fatigue life of joints, a variety of techniques have been proposed including the use of interference fit fasteners. Several commercial fasteners using this technique have now become available. The difficulty in using some of these fasteners, however, is the need for special drills and tools for their installation.

A cheaper alternative is to squeeze a relatively soft rivet into the joint hole under a large enough force to obtain appreciable plastic flow in the rivet with enough radially outward bulging of the rivet to produce yielding in a substantial region of the plate surrounding the hole.

When the squeeze force is released, the rivet and plate spring back, with the radial spring-back of the plate tending to exceed that of the rivet at the hole boundary. The result is to create an interference fit between the rivet and the plate and a state of residual stresses in the plate which some test results indicate gives a beneficial effect on the fatigue life of the joint.

This study was undertaken in order to study the effect of material selection and squeeze force on the resulting residual stresses around the rivet hole.

3.2.2 Method of Analysis

As a first step in the solution procedure, a plastic analysis of the plate, into which the rivet is squeezed, is performed. The specific analyses in this section were made using a finite element plasticity program developed for the government by Grumman and presented in Refs. 8 and 9. Basically the initial strain approach used in the inelastic stress and deflection analysis program described in Chapter 2 is used in this program also. However, the program has additional capabilities in being able to handle complete stress reversal into the plastic range (not merely elastic unloading). In addition it can account for the Bauschinger effect, which in the case of uniaxial stress is characterized by a reduction in compressive yield stress due to prior yielding in tension and vice versa, and is thus significant for unloading and reversed loading situations.

The idealization in the analysis is shown in Fig. 42 . The axisymmetric model, representing one quarter of the structure is composed of 144 planar triangular elements in which stress and strain vary linearly.

The rivet is assumed to be a cylindrical structure which fits neatly into the plate hole prior to squeezing under high pressure. During squeezing it is assumed to undergo plastic deformations based on the deformation theory of plasticity. In Ref. 10 both incremental and deformation plasticity theories were used to study a shear lag problem in which the answers obtained by the two theories agreed very well. The rivet and plate structures are coupled by means of a semi-graphical technique described fully in Ref. 11. Basically the method combines the stress strain behavior of the two structures at the point of contact to obtain a compatible solution during maximum squeezing or subsequent unloading.

3.2.3 Results of Analysis and Discussion

(1) Aluminum Plate with Aluminum Rivet

An elasto-plastic analysis was made of a 3/8 in. thick aluminum plate made from 2024-T351 alloy. A 3/8 in. diameter rivet of the same material was squeezed with a 20 kip force. The objective of this study is to determine the residual stress distribution in the plate when the squeeze force is removed.

The finite element solution for the idealization shown in Fig. 42 is presented in Fig. 43 together with the solutions of the coupled structure (plate and rivet). Fig. 43 shows the variation in the circumferential stress, σ_θ, at the hole boundary with increasing applied radial stress, σ_r, at the hole boundary during loading and subsequent unloading from several values of σ_r. The corresponding positions of the yield boundary for each of these radial stresses is shown in Fig. 44.

It is seen from Fig. 43 that yielding occurs when the radial stress exceeds 23,000 psi. As the radial stress increases beyond 23,000 psi the circumferential stress first shows a relatively small increase and then begins to decrease. If the applied radial stress

is then reduced, the plate first unloads elastically, along lines parallel to the original elastic loading. Fig. 43 shows the straight line elastic reduction in circumferential stress. As the unloading proceeds, the initially tensile circumferential stresses change sign and become compressive. Further unloading can cause these circumferential compressive stresses to become large enough to result in yielding opposite to that which occurred during loading. The effect of yielding during loading on yielding in the opposite direction during unloading is accounted for by assuming an ideal Bauschinger effect. Still further unloading causes additional yielding, with a consequent reduction in the magnitude of the circumferential stress at the hole boundary as shown in Fig. 43 .

A plot of the variation of circumferential stress with distance from hole edge is shown in Fig. 45 for the peak squeeze force condition (σ_r = 53.2 ksi) and two levels of unloading. The curve for σ_r = -38.5 ksi is the solution taking into account the plate-rivet interference. The curve for complete unloading to σ_r = 0 and the rivet removed, including the Bauschinger effect, is also shown.

(2) Titanium Plate with Steel Rivet

Residual stresses were evaluated for the case of an annealed titanium plate (Ti-6 Al-6V-2Sn) into which a 3/8 in. A286 steel rivet was squeezed with a 66 kip force. The plate has the same configuration as the aluminum plate in the previous problem. The variation of the circumferential stress at the edge of the hole with increasing radial stress and subsequent unloading from 3 levels of radial stress is shown in Fig. 46 . The yield surface boundary for these same levels of radial stress is shown in Fig. 47 .

The relationship between applied squeeze force and the residual circumferential and radial stresses at the hole boundary is shown in Fig. 48 (a) and (b) respectively. Two curves are shown in each case to account for the fact that the applied squeeze force is not known exactly since all the force is not transmitted to the shank of

the rivet. In the present analysis it is assumed that the axial stress in the rivet shank is somewhere between one-half to two-thirds of the nominal squeeze stress, P/A. This assumption appears to be reasonable in the case of protruding head rivets.

In Fig. 49 the computed interference fit, ΔD, (the change in the rivet diameter) is shown as a function of the squeeze force for the same two assumed values of the axial rivet shank stress used in Fig. 48. Since the interference has a direct relation to the beneficial effects gained in improving fatigue life, a plot such as Fig. 49 can be extremely useful. From it, the necessary squeeze force to obtain a given interference can be read directly.

The computed interference for the titanium plate shown in Fig. 49 is compared to some experimental results obtained from the Grumman Corporate Titanium Program. The experimental values were obtained by measuring the diameter of the rivet before squeezing and after the load is removed. To get the final change in diameter, the rivets were cut free of the plate and measured at various locations along their shank. These experimental results cannot be compared directly to the computed curves of Fig. 49 because they were obtained using countersunk rivets that were squeezed into a Ti-6Al-4V annealed plate. Nevertheless, they do indicate a trend similar to that of the analytical results.

3.2.4 Conclusions

The nature of the plate circumferential residual stresses caused by squeeze rivets can change depending on the magnitude of the squeeze force and the type of rivet material used. Interference fit fasteners, however, generally create tensile tangential residual stresses by expanding the hole into which they are applied.

The results shown in Fig. 48 for the titanium plate problem can be very useful in controlling the squeezing force during manufacture. For the particular materials and geometric properties chosen, Fig. 48 gives the range

of expected circumferential and radial residual stresses in the plate at the hole boundary. These stresses can be used in predicting the fatigue life of the joint.

From Fig. 49 it is seen that the method of analysis can be a valuable aid in predicting the amount of interference to be expected. By correlating the interference to the joint fatigue life through testing, the results of Fig. 49 could be used to indicate appropriate values of squeeze force needed to achieve the desired interference fit.

It is concluded from this study that the squeezing technique can be useful in increasing the fatigue life of joints and further correlations with fatigue tests should be made. Of particular interest would be a test program using protruding head rivets to measure the interference fit caused by different values of the squeeze force. The protruding head rivet with a cylindrical shank of constant cross-section corresponds closer to the three dimensional model used in the present analysis. Attempts to evaluate the actual rivet shank stress during the driving operation should also be made.

CHAPTER 4. THREE DIMENSIONAL EFFECTS CAUSED BY FASTENER BENDING AND SHEAR - (LINEAR ANALYSIS)

4.1 General

Because of the extreme complexity of the general nonlinear three dimensional mechanical fastener problem, the preceding analyses were directed towards obtaining strictly planar solutions. These planar solutions might be considered applicable to the plates in a symmetrical double-shear joint, in which the nominal stress is uniform through the plate thickness. The planar solutions might also be assumed to apply to individual thin layers in single-shear joints (in which the nominal stress varies linearly through the plate thickness) provided that the layers are chosen sufficiently thin to put each individual layer in a planar stress condition.

In obtaining the planar solutions the effects of fastener shear and bending deformation and fastener rotation were assumed secondary while the fastener was taken as both rigid and cylindrical. In addition many other effects such as fastener head shape, countersink, clamp-up force, and contact friction were also neglected. In this section, the influence of fastener deformation on stress distribution through the plate thickness and overall joint load deflection characteristics are estimated by means of an engineering-type approximation. In this treatment, the fastener is assumed to act as a short beam with either shear or bending deformations present, but not both existing simultaneously.

The fastener-plate interaction is idealized as a beam resting on a continuous set of mutually uncoupled springs such that the bearing forces per unit of axial length are directly proportional to the fastener's transverse, centerline displacements. The assumption that the springs are not coupled is equivalent to assuming that the plate's transverse shear stiffness may be neglected, and different layers in the plate slide past each other freely.

Solutions for the load distribution of a fastener in both single and double shear are obtained for the linear spring rates obtained in Chapter 3. A more detailed nonlinear analysis of the current beam-on-elastic-foundation idealization is presented in Appendix J. This more detailed analysis outlines how one may include combined shear and bending effects simultaneously, both nonlinear

and nonuniform spring rates, as well as nonuniform beam effects (such as those arising from tapered shanks or countersunk heads).

Numerical results are presented for the simplified linear beam bending and shear theories with clamped and free conditions at the fastener heads. The ratio of maximum bearing stress to nominal bearing stress through the sheet thickness is plotted as a function of fastener-diameter to sheet-thickness ratio for several joint configurations. In addition, experimentally determined joint load-deflection curve data are compared with the analytical predictions based upon the method of this chapter.

4.2 Structural Idealization

For many engineering applications, the problem of a beam interacting with an elastic medium can be treated by adopting the Winkler hypothesis which states that the local transverse beam displacement is directly proportional to the local load intensity per unit of length. The loads and displacements are related through the "foundation modulus", k. The classical treatment of the problem, in which only beam bending effects are included, is discussed in many texts (e.g. Refs. 12 and 13). In a more in-depth treatment of this subject, Hetenyi, Ref. 14, demonstrates that its applicability to foundations with shear continuity, such as the plates comprising our joints, is greater with increasing $(EI)_{fastener}/k$ stiffness ratio and that it yields results which are closer to the more accurate three dimensional case (i.e. beam on a three-dimensional half-space) than does a two-dimensional (i.e. beam on a two-dimensional half-space) elasticity solution.

Timoshenko, Ref. 12, distinguishes among three groups of beams which include bending effects only: "short" ($\bar{\beta}\ell<0.6$), "medium" ($0.6<\bar{\beta}\ell<5.0$) and "long" ($\bar{\beta}\ell>5.0$) where ℓ is the beam length and

$$\bar{\beta}^4 = \frac{k}{4(EI)_{beam}}$$

For short beams, which correspond to the present idealization of the fastener, Timoshenko claims that bending can be entirely ignored and that the beam can be considered as absolutely rigid in comparison with the foundation. However, it is well known that shear effects are generally more

important than bending effects for short beams and so a higher order beam theory* should be considered for such applications. Crandall, Ref. 15, Essenburg, Ref. 16, and Hess, Ref. 17, have treated various more accurate beam theories in conjunction with a Winkler foundation. Their results show that for softer foundations, $E/k > 1$ (which corresponds to the fastener problem), shear effects in the beam decrease in importance and the behavior of the beam approaches that predicted by elementary beam theory.

The present section attempts to estimate some of the higher order effects associated with fastener flexibility. To achieve this, two simplified beam theories which separate the bending and shear effects in the fastener, are used. In concluding these preliminary remarks, we note that the remarkably wide range of practicability of the elementary beam formulas stems from the fact that these formulas provide excellent approximations to the elasticity solutions in a large number of problems, Ref. 18.

4.3 Beam Equations

The most elementary and useful beam idealization which includes the effects of both bending and shear is called the Timoshenko beam, Ref. 19. In a manner similar to that used in elementary beam theory, this theory assumes plane sections before loading remain plane after loading. However, unlike simple bending theory, the normal to the beam center line, at any given section, before loading, will differ from the normal to the deflected center-line, after loading, by a shearing angle, β, caused by the local shear, Q. The relationship is expressed by

$$\frac{Q}{\lambda GA} = \beta \qquad (14)$$

where G is the material's shear modulus and A is the beam cross-sectional area.

---

* The various technical beam theories are engineering approximations to the mathematically precise theory of linear elasticity. The technical theories which include shear-deflection, excluded in elementary beam theory, are generally referred to as "higher-order" beam theories.

The parameter λ is dependent on the geometry of the beam cross-section and relates β to the nominal average shearing angle of the cross-section. For circular cross-section beams, Cowper, Ref. 20, gives

$$\lambda = \frac{6\,(1 + \nu)}{7 + 6\nu} \tag{15}$$

where ν is Poisson's ratio for the beam material.

The linear equilibrium equations for a beam element, regardless of which beam theory is used, (reference Figure 50a)

$$\frac{dM}{dx} + Q = 0 \tag{16}$$

$$\frac{dQ}{dx} + q = 0 \tag{17}$$

where M is the internal moment, q is the external loading per unit of length, and x is the axial coordinate. For a Winkler foundation with spring modulus k we have

$$q = -k\,y \tag{18}$$

where y is the transverse deflection relative to a rigid portion of the foundation. The usual linear beam hypothesis of plane section behavior yields

$$\frac{M}{EI} = \frac{d\Psi}{dx} \tag{19}$$

where Ψ is the rotation of a normal to the beam center line caused by loading (reference Figure 50b). If β were zero, Ψ and $\frac{dy}{dx}$ would coincide. Hence, from purely kinematic considerations

$$\beta = \frac{dy}{dx} - \Psi \tag{20}$$

Combination of Eqs. (14) through (20) yields the appropriate Timoshenko beam equations for interaction of a circular cross-section beam with a Winkler foundation. It should be noted that up to this point no assumptions as to property variation along the beam have been made. Therefore, to further simplify the problem, the assumption is made that EI, k and GA are independent of x (the more general case is discussed in Appendix J). The resulting equation is:

$$\frac{d^4y}{dx^4} - \frac{k}{\lambda GA}\frac{d^2y}{dx^2} + \frac{ky}{EI} = 0 \qquad (21)$$

Two simplified cases, the first corresponding to the classical beam theory in which shear effects are ignored, and the second corresponding to pure shear theory in which bending effects are ignored, are considered below.

4.3.1 Classical Beam Bending Theory: Ignoring shear deformations (i.e. $\beta = 0$) is equivalent to setting the shear flexibility $(\lambda GA)^{-1}$, to zero in Eq. (14). Once this is done, the classicial beam on elastic foundation equations result:

$$\Psi = \frac{dy}{dx} \qquad (22a)$$

$$M = EI\frac{d^2y}{dx^2} \qquad (22b)$$

$$\frac{d^4y}{dx^4} + \frac{k}{EI}y = 0 \qquad (22c)$$

The general solution to Eq. (22c) takes the form

$$y = \cosh \bar{\beta}x\,(A\cos\bar{\beta}x + B\sin\bar{\beta}x) + \sinh\bar{\beta}x\,(C\cos\bar{\beta}x + D\sin\bar{\beta}x) \qquad (22d)$$

where the values of A, B, C and D are determined by boundary conditions on the beam and the solution for Ψ may be obtained by differentiation of the solution as indicated by Eq. (22a).

4.3.2 Shear Beam Theory: In a manner similar to that used in eliminating shear effects, beam bending deflection may be eliminated by setting the bending flexibility, $(EI)^{-1}$, to zero. Eq. (19) gives:

$$\frac{d\Psi}{dx} = 0 \tag{23a}$$

Differentiating Eqs. (14) and (20), and substituting into Eqs. (17) and (18) gives:

$$\frac{d^2y}{dx^2} - \frac{k}{\lambda GA} y = 0 \tag{23b}$$

The general solution to Eq. (23b) is

$$y = E \sinh \gamma x + F \cosh \gamma x \tag{23c}$$

where $\gamma = \sqrt{\frac{k}{\lambda GA}}$

and E and F may be determined by again satisfying the boundary conditions. The solution for Ψ is readily obtained by integration of Eqs. (16) and (23a) between limits x_1 and x_2, and substitution of Eqs. (14) and (20) to yield:

$$M_1 - M_2 = \lambda GA \left((x_2 - x_1) \Psi - y_2 + y_1\right) \tag{23d}$$

where, $M_i = M\,(x = x_i)$, $y_i = y\,(x = x_i)$, $i = 1, 2$

Particular solutions of the beam bending and shearing cases are given in the following subsections.

4.4 Fastener in Single Shear

4.4.1 Fastener with Negligible Head Stiffness

To demonstrate typical results from application of the above idealization to a fastener in single shear for an anti-symmetrical structural joint (see Figure 51(a)*, several cases are investigated below.

(1) Bending Theory: The boundary conditions associated with Eqs. (21) are

$$Q(0) = P_0, \quad M(0) = 0, \quad Q(t) = 0, \quad M(t) = 0.$$

The resultant bearing load distribution on the plate (and fastener) is

$$-\frac{ky}{P_0/t} = \frac{qt}{P_0}$$

$$\frac{qt}{P_0} = 2\bar{\beta}t\left\{\frac{\sinh\bar{\beta}t\cos\bar{\beta}x\cosh\bar{\beta}(t-x) - \sin\bar{\beta}t\cosh\bar{\beta}x\cos\bar{\beta}(t-x)}{\sinh^2\bar{\beta}t - \sin^2\bar{\beta}t}\right\} \quad (24)$$

(2) Shear Theory: Applying the same boundary conditions as for the bending theory to Eqs. (23) yields

$$-\frac{ky}{P_0/t} = \frac{qt}{P_0} = -\gamma t\left\{\frac{\sinh\gamma x + \sinh\gamma(t-x) - \gamma t\cosh\gamma(t-x)}{\gamma t\sinh\gamma t + 2(1-\cosh\gamma t)}\right\} \quad (25)$$

(3) Rigid Fastener: For a rigid beam, force and moment equilibrium considerations yield

$$-\frac{ky}{P_0/t} = \frac{qt}{P_0} = 2\left(2-3\frac{x}{t}\right) \quad (26)$$

It should be noted that both Eqs. (24) and (25) can be shown to approach Eq. (26) in the limit as the fastener becomes essentially rigid compared

---

* Note, that although the springs in Figure 51 are pictured as compression springs acting at the bearing surface of the fastener, the spring constant is actually dependent upon the overall elastic properties of the plate in a complex state of stress involving both tension and compression.

to the foundation. This result may be achieved through consideration of the series-expansions of the cosh and sinh functions, letting γ and $\bar{\beta}$ approach zero, and performing appropriate limiting processes.

Numerical results, corresponding to Eqs. (24) through (26), for a typical set of parameters are presented in Table 4.

As can be seen from Table 4, for the realistic parameters employed, the fastener performs in an essentially rigid manner and, both shear and bending effects, acting separately, cause only a slight perturbation upon this behavior. However, shear flexibility is the more important factor of the two since its effects are an order of magnitude greater than those due to bending for the parameters used in Table 4. Therefore, in the subsequent solution for the clamped head fastener in single shear, below, principal attention will be given to the solution of the shear beam theory, since it is anticipated that bending effects are negligible.

4.4.2 Fastener With Clamped Head

It should be noted that the assumed highly-flexible-head performance of the previous configuration permits an overall cocking action of the fastener relative to the plate, provided the plate has negligible transverse shear stiffness (as was initially assumed). However, if the fastener has stiff head-attachments which tend to clamp the plate locally, then the fastener is prevented from rotating at the ends relative to the plate. Thus, the limiting case becomes $\Psi = 0$ at the ends of the fastener. In addition, the head is assumed to exert no net shear upon the fastener. Under these conditions, the resultant bearing load distribution on the plate and fastener using shear beam theory is:

$$-\frac{ky}{P_0/t} = \frac{qt}{P_0} = \gamma t \ \frac{\cosh \gamma(t-x)}{\sinh \gamma t} \qquad (27)$$

and the corresponding rigid fastener solution is $qt/P_0 = 1$. Results are presented in Table 5 for the same typical paramters as were used in Table 4.

4.5 Fastener in Double Shear

The idealization considered for the fastener in double shear (Reference Figure 52) is to divide the top half of the fastener into two shorter beams joined by appropriate compatibility conditions. For the symmetrical case, the shear beam theory yields Ψ as constant (from Eq. (19). Therefore, for the symmetrical case, $\Psi = 0$ regardless of head effects.

The solution for this case is obtained through solution of Eqs. (23) together with the boundary conditions:

$$Q(0) = 0,\ Q\left(\frac{t_1}{2}\right) = P_0/2,\ Q\left(\frac{t_1}{2} + t_2\right) = 0,$$

and is given as

$$\frac{qt_1}{P_0} = \gamma_1 t_1 \frac{\cosh \gamma_1 x}{2 \sinh\left(\frac{\gamma_1 t_1}{2}\right)} \qquad 0 \le x \le \frac{t_1}{2} \qquad (28a)$$

$$\frac{q(2t_2)}{P_0} = -\lambda_2 t_2 \frac{\cosh \gamma_2\left(\frac{t_1}{2} + t_2 - x\right)}{\sinh \gamma_2 t_2} \qquad \frac{t_1}{2} \le x \le \frac{t_1}{2} + t_2 \qquad (28b)$$

where $\gamma_1 = \sqrt{\frac{k_1}{\gamma GA}}$, $\gamma_2 = \sqrt{\frac{k_2}{\gamma GA}}$

The corresponding bending solution with free and clamped heads is obtained from the general solutions

$$y = C_1 \cos\bar{\beta}_1 x \cosh\bar{\beta}_1 x + C_2 \sin\bar{\beta}_1 x \sinh\bar{\beta}_1 x \qquad 0 \le x \le \frac{t_1}{2} \qquad (29a)$$

and

$$y = \cos\bar{\beta}_2\bar{x}\ (C_3 \cosh \bar{\beta}_2\bar{x} + C_4 \sinh \bar{\beta}_2\bar{x}) + \sin \bar{\beta}_2\bar{x}\ (C_5 \cosh \bar{\beta}_2\bar{x} + C_6 \sinh \bar{\beta}_2\bar{x})$$

$$\frac{t_1}{2} \le x \le \frac{t_1}{2} + t_2 \qquad (29b)$$

where $\bar{x} = \frac{t_1}{2} + t_2 - x$;

The constants C_1 and C_2 may be determined through the boundary conditions

$$M(0) = \frac{P_0(t_1 + t_2)}{4} \quad \text{and} \quad \frac{Q(t_1)}{2} = \frac{P_0}{2}$$

The constants C_3 through C_6 may be determined by the boundary conditions $Q(\bar{x}=0) = 0$, and $M(\bar{x}=0) = 0$ (for a very flexible fastener) or $\Psi(\bar{x}=0)=0$ (for a rigidly clamped fastener head), and compatibility conditions on Q and Ψ at $x=\frac{t_1}{2}$.

Typical numerical results using Eqs. (28) and (29) are presented in Table 6. It should be noted that although the shear theory produces greater fastener flexibility effects, the difference from the bending theory results are far less pronounced than was the case for the fastener in single shear. This indicates that fastener bending is as important a factor as shear is for such configurations.

4.6 Parametric Study:

The ratio of peak bearing stress for a flexible fastener versus peak bearing stress for a rigid fastener may be employed as a stress concentration factor to account for variations in bearing load through the plate thickness. A series of bearing stress ratio curves as functions of fastener diameter to plate thickness ratio are presented in Figures 53 and 54. Results for two values of E/k, which represent approximate practical limits for this parameter, are presented. As can be expected, the stiffer fastener to plate ratios (i.e. higher E/k) and larger D/t ratios yield results which approach those for a rigid fastener.

It should be noted that the bearing stress in each plate lamina is a measure of the two dimensional stress state level in the lamina, as given in Chapters 2 and 3. Thus, the bearing stress ratios presented in Figures 53 and 54 may be viewed as stress concentration factors, caused by fastener flexibility, over and above the plate stress concentrations resulting from the purely two dimensional plate-fastener considerations of Chapter 3.

4.7 Comparison of Tests with Theory

Overall joint flexibilities for single fasteners in double shear, for a given gage length, were determined both experimentally and by the methods of this section. A series of 15 tests were performed on aluminum-plate, symmetrical, double-shear lap joints using titanium fasteners. Twelve (12) of these specimens were joined by loose fitting fasteners and the remaining three (3) by interference-fit fasteners. A more complete description of the tests and parameters investigated, such as plate friction and fastener clamp-up, is presented in Chapter 7.

The analytical model used for comparison purposes is the shear beam of Section 4.5 (Eqs. (28) and Figure 52). However, since the elastic foundation supports for the center and outside plates are assumed fixed in that model, we must add rigid body displacements to each segment idealization to obtain the total joint deflection, δ_T. This is equivalent to obtaining the differences in displacements, relative to the fastener, of the foundations in the center and outside plates, in the planes common to both (i.e. $x = \frac{t_1}{2}$). Thus,

$$\delta_T = y_1 \left(x = \frac{t_1}{2}\right) - y_2 \left(x = \frac{t_1}{2}\right)$$

which by virtue of Equations (28) yields

$$\delta_T = \frac{P_0}{2\lambda GA} \left(\frac{1}{\gamma_1 \tanh \frac{\gamma_1 t_1}{2}} + \frac{1}{\gamma_2 \tanh \gamma_2 t_2} \right) \qquad (30)$$

Since the plates joined in the tests were of the same material and the thicknesses satisfied the relationship

$$t_1 = 2t_2$$

Equation (30) reduces to

$$\delta_T = \frac{P_0 \gamma}{k \tanh \frac{\gamma t_2}{2}}$$

Thus, the effective joint stiffness, k_{eff}, becomes

$$k_{eff} = \frac{P_0}{\delta_T} = \frac{k \tanh \frac{\gamma t_1}{2}}{\gamma} \tag{31}$$

which, in the limit, as the ratio of plate stiffness (k) to fastener stiffness (γGA) approaches zero, becomes

$$\lim_{\gamma \to 0} \quad k_{eff.} = \frac{kt_1}{2} \tag{32}$$

Equations (31) and (32) were used to generate effective stiffnesses for both titanium and steel fasteners joining aluminum plates. The plate stiffness was varied to account for various conditions of fit; i.e. loose, neat, and interference. Numerical results for these cases are presented in Table 7 and the corresponding stiffness for the linear portion of the experimental results (summarized from Appendix K) are presented in Table 8.

The last three columns of Table 7 show the effect of increasing the fastener to plate stiffness ratio, as well as the relative importance of including the three dimensional effect of fastener flexibility upon the overall joint stiffness. However, it should be noted that the effects of fastener-to-hole fit, which can be observed by comparing the loose, neat, and interference fit results, are more significant in establishing the joint's net compliance.

A comparison of results between Tables 7 and 8 reveals excellent agreement for the loose fitting titanium fasteners and good agreement for the interference fit titanium fasteners. However, it should be noted that the variation of measured results from test to test, for similar conditions of fit, varied significantly and, that Table 8 gives only average values. In addition, the definition for the elastic plate modulus, k_e, is somewhat arbitrary in the case of the interference fit fasteners (Fig. 75) because of the highly non-linear nature of the virgin load-deflection curve for all levels of loading. (The method used in obtaining the k_e values for these types of curves was to define k_e to be the secant modulus to an arbitrary value of the load level equal to 1/3 of the ultimate load, P_u, sustained by the joint.)

CHAPTER 5 APPLICATION OF RESULTS TO FATIGUE ANALYSIS OF JOINTS

5.1 Introduction

The fatigue strength of a discretely fastened joint is dependent to different degrees on various parameters within the joint. Of major importance to fatigue life is the magnitude and range of stress and strain at critical points within the joint. The stress distribution is largely related to joint geometry, but is influenced to significant degrees by various other parameters, such as type and order of loading, clamp-up forces, variation in fit between different fasteners in a multi-fastener joint and clearance or interference between fastener and hole. Fatigue strength is also influenced by fretting, which can occur as a result of relative movement between fastener shank and hole surface or between the inner and outer members of a joint. This phenomenon is difficult to include in a fatigue strength calculation, except by the use of empirically determined fatigue strength reduction factors. The effects of in-plane loads induced by frictional forces due to clamp-up are also difficult to assess except by experimental procedures.

Of the many factors which affect the fatigue life of a mechanically fastened joint, clearance or interference between fastener and hole is one of the most important. In addition, it is also a joint parameter that can be controlled in design and manufacture. Fatigue tests have shown that fatigue life is generally reduced as a result of increasing clearance, and improved when there is an interference fit. If the degree of reduction or improvement in fatigue life is reasonably well established it is possible to use various fits to advanta . For example, increased hole tolerances in certain areas may result in a saving in production costs. Also, the necessity of otherwise using interference fit fasteners to increase fatigue life can be evaluated.

The present investigation is, therefore, largely concerned with the effect of changes in stress distribution due to geometry and fit, as they influence the calculation of fatigue strength. Except as inherent properties of the

test results, fretting and clamp-up are neglected.

Some examples of test data demonstrating the effect of clearance and interference are presented in References 21 and 22 for constant amplitude loading. However, the number of systematically run test programs to evaluate the effect of clearance and interference fits on fatigue life is limited, and such data as are available are usually confined to constant amplitude tests where residual stress effects are not present to complicate the results. In spectrum fatigue loading, the effects of residual stresses induced as a result of high loads in the spectrum must be considered.

In the application of the results of the present study to the fatigue analysis of joints, two specific joint configurations have been considered. The fatigue life of these joints has been investigated for conditions of clearance and neat fit, for typical aircraft maneuver spectrum loadings. In addition, constant amplitude fatigue life predictions have been made for conditions of neat fit and interference on one joint configuration. The methods of fatigue analysis are described in the following section.

5.2 Method of Fatigue Analysis for Joints with Neat Fits and Clearance Fits

5.2.1 Constant Amplitude Loading

The fatigue life prediction method of Reference 23 which has been used in this analysis is based on the strain cycling concepts of Manson, Peterson and others (References 24 and 25), who employed constant strain amplitude, fully reversed strain cycling data to establish relationships between total strain amplitude and cycles to failure, for unnotched specimens tested in fatigue at zero mean stress. The method of Reference 23 gives a procedure for extending the approach to cover cases other than zero mean stress. In using the method, the basic assumption is made that the material at the edge of a hole or other stress raiser will fail in fatigue at the same life as an unnotched specimen subjected to the same strains. It is therefore necessary to establish the strain range at the critical section of the notch. For a given load cycle, stress-strain variation at the critical fatigue section (generally the region of maximum stress concentration) is established using several approximations. The procedure is illustrated in Figure 55 , for the condition in which the applied maximum stress is tensile, and the minimum stress is zero in the fatigue cycle.

For values of minimum applied stress other than zero, a modification of this procedure is given in Reference 23. The nominal applied stress in the loading cycle varies from 0 to f_{max} (Figure 55), Point A. The corresponding stress at the notch root is assumed to vary from 0 to σ_{max}, (point B), where σ_{max} is given by the expression

$$\sigma_{max} = K_{fp} f_{max} \tag{33}$$

K_{f_p} is a plastic stress concentration factor calculated by the Stowell formula (Reference 26). The strain, ε_{max}, corresponding to σ_{max}, is obtained from a cyclic stress-strain curve similar to Figure 56. When the section is unloaded, the material at the edge of the notch is assumed to unload in two stages. In calculating the first stage from the point B to the point C, the elastic part of the unload cycle, use is made of the Neuber factor, K_N, which is given for a circular hole by the formula:

$$K_N = 1 + \frac{K_T - 1}{1 + \frac{a}{\sqrt{\rho}}} \tag{34}$$

where K_T = elastic stress concentration factor

a = material constant

ρ = radius of hole or notch

The elastic unload stress increment is given by the expression:

$$\Delta\sigma_1 = \frac{K_N f_{max}}{2} \tag{35}$$

with a corresponding unload strain of: $\Delta\varepsilon_1 = \frac{\Delta\sigma_1}{E}$. (36)

To determine the remaining part of the unloading cycle at the notch (to point D), it is assumed that the material follows the same cyclic stress-strain curve as during initial loading, and that the strain at the notch will decrease by an additional amount:

$$\Delta\varepsilon_2 = \frac{\varepsilon_{max}}{2} \tag{37}$$

with a corresponding stress increment, $\Delta\sigma_2$, obtained from the cyclic stress-strain curve.

The strain amplitude at the notch will be: $\varepsilon_a = \frac{\varepsilon_1 + \varepsilon_2}{2}$ (38)

The minimum stress at the notch, at point D, is given by:

$$\sigma_{min} = \sigma_{max} - (\Delta\sigma_1 + \Delta\sigma_2) \tag{39}$$

The mean stress at the notch will be:

$$\sigma_{mean} = \frac{\sigma_{max} + \sigma_{min}}{2} \tag{40}$$

Subsequent applications of the same load cycle are assumed to follow the same loop, i.e., D,B,C,D shown in Figure 55. At the end of the loading cycle (at point D), there will be a residual compressive stress at the notch, which is equal to σ_{min} (Eq. 39). This residual stress may have a significant beneficial effect on fatigue under spectrum loading, as discussed in Section 5.2.2.

In calculating fatigue damage, use is made of constant amplitude, fully reversed strain cycling data. The calculated strain amplitude at the notch, ϵ_a, is therefore modified by the use of a Goodman type correction, to obtain an equivalent fully reversed strain amplitude.

$$\epsilon_t = \frac{\epsilon_a}{1 - \frac{\sigma_m}{\sigma_f}} \tag{41}$$

where

ϵ_t = equivalent fully reversed strain amplitude; ϵ_a = strain amplitude;

σ_m = mean stress in cycle and σ_f = stress at fracture for the material

The life is then obtained by entering the strain-life curve for the material. Such a curve for aluminum alloy, 7075-T6, is shown in Figure 57. The life of the element is then determined by applying Miner's linear damage rule:

$$\Sigma \frac{n}{N} = 1 \tag{42}$$

5.2.2 Spectrum Loading

The method for predicting the fatigue life of a joint subjected to spectrum loading is basically similar to that used for predicting constant amplitude fatigue life. The cyclic strain amplitude corresponding to any particular load level in the spectrum is determined exactly as for the case of constant amplitude loading, independent of the previous load levels that were applied. The cyclic mean stress corresponding to any given load level is also independent of the previous loading history, provided that the previous applied loads were all equal to or lower than the subsequent loads. If, however, any of the previous applied loads were higher than the subsequent applied load, then relatively large residual compression stresses remaining from the previous higher loads would tend to reduce the cyclic mean stress in the subsequent load cycles. The amount of this reduction is directly related to differences in residual stress

levels, as explained in Reference 23.

In general, the types of assumptions made in the empirical fatigue analysis procedures described above, both for constant amplitude loading and for spectrum loading, were based on qualitative, physical reasoning. The specific details, however, were determined so as to obtain a best fit with available fatigue test data. Further discussion is given in Reference 23.

5.3 Method of Fatigue Analysis for Joints with Interference Fits

In the case of joints with neat fit pins or with pins having positive clearance the fatigue analysis method described in Section 5.2 gives generally satisfactory results. One of the principal reasons for this is that for initial loading into the plastic range, the use of the Stowell formula for determining the plastic strains and stresses at the edge of a hole with a known elastic stress concentration factor, will give sufficiently accurate results in such joints. Subsequent unloading is largely elastic and can, therefore, also be determined with good accuracy.

In general, the Stowell formula applies quite well to cases where there is no initial self-balancing system of stresses, such as those resulting from the use of a pin with an interference fit in a joint. However, for joints with interference fit pins the plastic stresses and strains that result from the combined effects of interference fit loads and applied loads cannot be accurately predicted with the use of the Stowell formula, especially for large interferences which cause local plasticity even before any external load is applied.

Because a simple, reasonably accurate procedure has not yet been developed for approximating the plastic stresses and strains around the holes in a joint with interference fit pins, a much simpler version of the fatigue analysis procedure described in Section 5.2 has been used to determine, at least qualitatively, if not quantitatively, the effects of different interference fits on the fatigue life of a joint. This simplified procedure makes use of the elastic strain distributions shown in Tables 9 through 12 , in conjunction with the cyclic stress-strain and strain-life curves shown in Figures 56 and 57. This procedure can be illustrated by considering the elastic stresses (Table 12) at $\theta = 81^{\circ}$ (Fig. 58) for a point on the hole circumference in the aluminum alloy joint of Fig. 68.

Assuming an elastic modulus of $E = 10 \times 10^6$ psi for simplicity, the elastic strain amplitude at $\theta = 81°$ when cycling from no load to an 8000 lb load is 0.00375. This elastic strain amplitude is then modified to account for mean stress effect by the use of the Goodman type correction discussed in Section 5.2.1, thereby obtaining the equivalent fully reversed strain amplitude. The value of σ_m is obtained by determining the average of stresses corresponding to the maximum and minimum elastic stress in the cycle from the cyclic stress-strain curve for 7075-T6 aluminum alloy (Fig. 56). In this case, the elastic strains are 0.01087 and 0.01837, the corresponding stresses are 60 ksi and 71 ksi, and the mean stress is 65.5 ksi. The resulting value of ϵ_t from Equation 41 , is 0.00935. The fatigue life at $\theta = 81°$ obtained by entering the fully-reversed strain-life curve (Fig. 57) with this value of ϵ_t is 1200 cycles.

It should be emphasized that this simplified fatigue analysis procedure can be regarded as giving only qualitative results, and it may be concluded that improved methods for determining plastic stresses and strains in joints with interference fits are needed to obtain good quantitative results.

As will be discussed later in Section 5.4, interference fits result in non-linear variations of edge-of-hole stresses with applied load (the actual variation approaches a bi-linear variation). Also, the initial interference stresses may vary considerably around the hole circumference, depending on the joint geometry. The result is that, especially under spectrum loading conditions, it may be necessary to examine several locations around the circumference to determine which is fatigue critical.

5.4 Discussion of Results

5.4.1 Joints with Clearance Fits

Figure 59 shows the calculated fatigue life for clearance fits in an aluminum alloy joint similar to that shown in Fig. 68 with a 3/4" Dia. fastener (See also Fig. 24). The fatigue analysis has been performed for a typical maneuver loading spectrum, to a zero 'g' base, using the method described in Section 5.3. Four conditions of fastener-hole fit are considered, i.e. neat fit, 0.4% dia 2.0% dia and 4.0% dia. The curves show the variation of service

life with limit stress level in the spectrum. For a limit stress level of 35 ksi (a typical design stress level for a 7075-T6 aluminum alloy wing), results indicate that fatigue life decreases as a result of going from a neat fit to a clearance fit. Much of the reduction in life occurs in the range between a neat fit and a clearance equal to about 2% of the pin diameter as indicated in Figure 60 where service life is plotted against % clearance for a constant limit stress level. Similar indications are evident in the constant amplitude test data of Reference 21.

Figure 61 shows a similar calculation for a 6Al-6V-2Sn titanium alloy joint (Figs. 79 and 39). together with a limited quantity of test data. The joint represents a configuration used in a particular design investigation, in which a number of specimens were tested to a simplified fighter aircraft maneuver spectrum, (somewhat more severe than that used for obtaining the curves in Figure 59). Test data for clearance of 1.2% and 2.4% diameter are presented. Considerable scatter is evident in the test results. Fatigue predictions show a significant reduction in life in going from a neat fit to a 2.4% dia clearance. At a limit stress level of 90ksi, for example, the calculated life is reduced from 18700 hours to 12000 hours. The reduction is less than that calculated for the case of the aluminum alloy joint previously discussed (the curves in Figure 59 indicate that at a limit stress of 29 ksi, the life of the aluminum joint would be reduced from 19000 hours for a neat fit condition to 3300 hours for a 2.4% clearance condition), but this is mainly due to the joint configuration, as reflected in the stress concentration factors shown in Figures 33 and 40. The fatigue predictions for the titanium joint show good general correlation with test data.

5.4.2 Joints with Interference Fits

As discussed in Section 5.3, a simplified approach has been used in fatigue predictions for the interference fit cases. The aluminum alloy joint discussed in Section 5.4.1 has been analyzed for constant amplitude cyclic loading. The neat fit, 0.4% and 2.0% interferences have been considered, and the results are presented in Figure 62. The calculations show the fatigue strength at a point on the hole circumference at 81° from the axis of applied load.

It should be noted that the curves for 0.4% interference and 2.0% interference show increased fatigue life over the neat fit for the entire range of net section stresses considered. However, a comparison of the degree of improvement in fatigue life between the 0.4% and 2% curves indicates that larger increases in fatigue life are obtained with the smaller interference when the applied stresses are less than about 47ksi. At this stress level, the two curves cross at a life of about 3000 cycles. Below 47 ksi the 0.4% interference joint shows somewhat longer lives. This behavior would indicate that at any given stress level in this particular joint, there may be a limiting degree of interference, beyond which fatigue life would decrease with increased interference.

In order to further examine this result, Figures 63 and 64 have been plotted. Figure 63 shows the variation of elastic strain at the edge of the hole with the applied net section stress, for two points on the hole circumference, at 45° and 99° to the axis of applied load. Curves are plotted for the 0.4% D and 2.0% D interference conditions. These plots are obtained directly from the data given in Tables 9 through 12. Figure 64 shows edge elastic strain variation with nominal stress at the edge of a hole at a point that is 81° from the applied load axis. This location was the one considered in calculating the constant amplitude fatigue curves shown on Figure 62.

An indication of the effects of interference fit on the elastic behavior at the edge of the hole is obtained from an examination of the curves in Figs. 63 and 64. It can be seen from these figures that. for each value of θ, the initial slope of the curves (a measure of the rate of change in the elastic strain at the hole with change in the elastic stress on the net section) is the same for the 2% D interference case as for the 0.4% D interference case. However, as the applied stress is increased, the initial interference condition is eventually overcome and the slope of the curves approaches the slope that would be obtained in a neat fit (0% interference) case. The applied stress level at which the initial interference is overcome increases with increasing interference. The significance of this behavior,

as it affects fatigue life, may be better understood by examining in detail some of the calculations that were made in obtaining the constant amplitude fatigue curves in Fig. 62.

Consider, for example, the elastic strain ranges at the edge of the hole for 2.0% and 0.4% interference when the net section stress varies from 0 to 47 ksi (the cross over point for these two interferences on the constant amplitude fatigue curves in Fig. 62). The elastic strain ranges at the edge of the hole at $\theta = 81^{\circ}$, obtained directly from Tables 9 through 12, are as follows:

Interference % Dia.	ϵ_{el_r}
0.0	0.014
0.4	0.0096
2.0	0.00625

As would be expected, the strain range at the edge of the hole in the joint decreases with increasing interference. However, as discussed in Section 5.2 the fatigue life of either joint depends not only on the strain range but also on the mean stress. Therefore, when the values of ϵ_{el_r} are corrected for mean stress effects using Equation 41 (which can be applied to strain range or strain amplitude), the resulting "equivalent" fully reversed cyclic strain ranges are:

Interference % D	ϵ_{el_r}
0.0	0.0200
0.4	0.01564
2.0	0.01558

Because the "equivalent" strain ranges for the two interference fits are essentially equal, the corresponding fatigue lives, (obtained by entering the strain-life curve in Fig. 57 with the strain amplitude $\epsilon_t = \epsilon_{t_r}/2$), are also equal, and are approximately three times the life of the neat fit joint.

At net section applied stresses greater than 47 ksi, the "equivalent" fully reversed strain ranges are lower for the 2.0% D interference than for the 0.4% D, resulting in longer fatigue lives for the larger interference. For example, at a net section applied stress of 55 ksi, the 0.4% D interference strain range is 0.01205, while the 2.0% D interference strain range is 0.0073. The corresponding "equivalent" strain ranges, when the effect of mean stress has been accounted for, are 0.0205 and 0.0184 resulting in a longer fatigue life for the 2.0% D interference case (Fig. 62). The strain range for the neat fit joint, at the same applied stress level is 0.0164, but when the mean stress correction is applied, the "equivalent" fully reversed strain range becomes 0.0242 and the corresponding fatigue life is lower than for either of the interference fit cases.

At lower values of applied stress, 30 ksi for example, both the 0.4% D and 2.0% D interferences show improvement in fatigue life. However, the considerably larger mean stress correction for the 2% interference case predominates so that the improvement in it's fatigue life is consequently less than that shown by the 0.4% D interference case.

From an examination of the curves in Fig. 64 and the above calculations it becomes obvious that when a load is applied to a joint, the resulting increase in stress and strain at the edge of the hole is smaller in the case of an interference fit than in the case of a neat fit. This tends to increase the fatigue life of joints with interference fits. However, when the interference fit becomes large, the mean tensile stress at any point on the hole periphery also becomes large, and this tends to decrease the fatigue life. There would, therefore, appear to be optimum amounts of interference for different applied stress levels. This appears to be partly born out by the test data shown in Fig. 7 of Ref. 27, which showed that the constant amplitude fatigue life of a small lug with a taper pin increased with increasing pin interference up to a certain point, and then showed a significant reduction at higher interferences.

5.5 Conclusions

1. The fatigue life of a discretely fastened joint is reduced if there is a loose fit between fasteners and holes. This reduction increases significantly up to a point where the clearance is between 1% and 2% of the fastener diameter, after which the rate of reduction in fatigue life becomes noticeably less. Limited test data tend to substantiate this.

2. Increases in local stress due to clearance, and resulting reduction in fatigue life may vary significantly with joint geometry. A well designed joint with standard proportions could be less affected than one with undesirable geometrical characteristics, such as extremely short edge distance.

3. Variations in fit between different fasteners in the same group will affect fatigue life. The analysis presented in this report can account for such variations in fit where these are known.

4. The degree to which interference fits between fastener and hole will affect the fatigue life of a joint is a function of the amount of interference, the joint geometry and the applied stress levels in the fatigue loading cycle. In general, interference fits will improve fatigue life, but the improvement is related to the joint geometric parameters mentioned above, and there would appear to be optimum amounts of interference for different applied stress levels, (as discussed in Section 5.3). It is possible that excessive interference may be detremental to fatigue life.

5. The trends shown by the fatigue analysis in general are of considerable interest. The availability of the very detailed elastic stress data generated in this report, if utilized to the fullest extent, offers an attractive prospect of extensive parametric study. Extension of the present work to include plasticity effects would result in a greatly increased capacity for the analytical prediction of joint fatigue life.

6. Existing methods of fatigue analysis are not fully adequate for the condition of interference fit. However, a more accurate knowledge of the stress-strain behavior at the edge of a notch would undoubtedly permit a better fatigue analysis to be made.

CHAPTER 6. FASTENER-SHEET LOAD-DEFLECTION DATA

6.1 Introduction

Of considerable importance to the analysis of multi-fastener joints is the determination of the "spring constants" or the slopes to the load-deflection curve of the individual fasteners in combination with the local sheet. This has been pointed out by previous investigators (Refs. 1, 2 and 28) who have treated the joint as a set of springs and attempted to determine experimentally the particular spring constants needed in their analyses. In Ref. 2 the fastener experimental load-deflection curve was approximated by a "Ramberg-Osgood" type expression and in Refs. 1 and 28 an incremental piecewise linear approximation to the curve was used in the analysis.

The lack of a tabulated set of data for a variety of fastener-sheet combinations was considered a major shortcoming in the analysis of load distribution in multi-fastener joints of any type. In this chapter a method for approximating the load-deflection curve of individual fasteners is presented. Comparisons using this approximation show good correlation with experimental data. Tabulations of several hundred load-deflection curves found in the literature and covering a large variety of fastener types and plate combinations are also presented.

6.2 Parametric Representation of Fastener-Sheet Load-Deflection Curves

A typical load-deflection curve is shown in Fig. 65 . The initial portion of the curve denoted by the letters OA is usually linear and rises to only a small percentage of the total load carrying capacity of the fastener. For fasteners with small tolerances and a small clamping action, the portion of the curve OA represents the frictional effects in the joint. This aspect has been studied experimentally and comparisons of its effect on the load-deflection curve are presented in Chapter 7. The portion of the curve denoted by AB represents the effect of initial clearance or "slop".

A modification to the initial portion of the generally complex curve (Fig. 65) is proposed in order to simplify the application of load-deflection data to load distribution analyses.

This modification consists of extending the linear portion of the curve to cut the δ axis at zero load as shown in Fig. 65 at point O'. The offset is designated δ_o and depending on the nature of the curve can be positive or negative. An expression for the displacement at any load level can be obtained after the modification to the curve has been made. Writing the total displacement across the fastener, δ, as a combination of an elastic and a plastic part we have:

$$\delta = \delta_e + \delta_p = \frac{P}{k_e} + A\left(\frac{P}{F_j}\right)^B \tag{43}$$

where,

$$\delta_e = \frac{P}{k_e} \tag{44}$$

and

$$\delta_p = A\left(\frac{P}{P_j}\right)^B \tag{45}$$

and A and B are constants.

The quantities k_e, P_i and P_j are defined in Fig. 65. The value of k_e is easily obtained from an automatic load-deflection trace. By choosing appropriate offsets δ_i and δ_j, from the initial corrected linear part of the curve we define the corresponding values of P_i and P_j. The two constants A and B in Eq. 43 can then be determined from the following expressions:

$$A = -\delta_e + \delta_j \tag{46}$$

and

$$B = \frac{\ln\left(\frac{-\delta_o + \delta_i}{-\delta_o + \delta_j}\right)}{\ln\left(\frac{P_i}{P_j}\right)} \tag{47}$$

The main difference between the method proposed here and the "Ramberg-Osgood" type curve proposed in Ref. 2 is the method of obtaining the values P_i and P_j at the "knee" of the curve. Gehring and Maines (Ref. 2) recommend P_i to be chosen at a secant modulus of 0.7 k_e to be consistent with the yield defined by Ramberg - Osgood (Ref. 29) and the point P_j is selected "as far out on the curve as practicable". It appears preferable and much easier construction-wise to use direct offsets parallel to the linear slope of the modified curve at finite displacements as shown in Fig. 65 to accomplish the same thing. Because we are more interested in the region near the knee of the curve (moderate plasticity) rather than at failure (large plasticity) this appeared to be a good technique.

6.3 Evaluation of the Accuracy of the Proposed Parametric Load-Deflection Curve

Before the proposed method of parametric representation of load-deflection curves was applied to existing experimental data, an evaluation of its accuracy was made. Fig. 66 shows in solid line an experimentally obtained autometic load-deflection curve of a single Hi-Lok fastener in double shear. Using the method described in Section 7.2 two parametric approximations to the curve were obtained using two different sets of offset points. In the first curve (designated by crosses) offsets at 0.002 and 0.005 inches were used. The second curve (circles)was obtained using offsets at 0.005 and 0.012 inches. It appears from the comparison shown in Fig. 66 that both parametric approximations are good representations of the experimental curve over the useful range. However, as would be expected, the second approximation shows better correlation to the experimental curve in the inelastic range.

Another comparison is shown in Fig. 67 which correlates three different parametric curves to the original experimental curve. It is seen from the equations of the three curves that as the constant B increases from 5.65 to 9.76 the knee of the curves becomes sharper and the parametric curve deviates from the test curve. The two curves with the lower values of B appear better approximations to the particular experimental curve. It is suggested that in tabulating data by the parametric procedure an attempt be made to see which offsets give a better correlation for each group of fasteners analyzed. In

the results given in Appendix K this procedure was followed.

6.4 Summary of Existing Load-Deflection Data

A tabulation of several hundred load-deflection curves are presented in Appendix K. Data published in Refs. 1 and 30 are presented as well as Grumman unpublished test data (Ref. 31). Use of new commercially available fastening systems, so widespread in the aircraft industry at the present time, necessitates a large accumulation of such data as those presented in Appendix K. However, due to the unavailability of test results in the open literature, the scope of the tabulation shown is somewhat limited. It is hoped that future tabulations and additions of this type can be made available to other interested users in the near future.

The format used in presenting the data of Appendix K is shown on pg. 255 together with the definition of the various symbols. The table gives the following: information concerning the plates making up the joint (Cols. 1 to 7); information concerning the fastener data (Cols. 8 to 13); measured interference or clearance (Cols. 14 to 16); the computed load-deflection parameters (Cols. 17 to 22) and test information and identification (Cols. 23 to 28). Pages 255 and 256 summarize the data presented by Mc Combs et al. (Ref. 1) for single and double shear single fastener joints. On page 257 is given a summary of the single fastener double shear tests of the present study. Pages 258 to 264 summarize the results of Grumman data obtained in a Corporate titanium study (Ref. 31). The code used in describing each test is shown in Cols. 27 and 28 and on top of page 258.

CHAPTER 7 EXPERIMENTAL PROGRAM

7.1 Introduction

The main purpose of the experimental program was the verification of the analytical methods described in Chapters 2 to 5. In addition, the experimental results pointed out the relative importance of some of the parameters which influence the structural behavior of mechanically fastened joints. Two types of tests are described: static strength and fatigue. The static strength tests were performed on single fastener and multi-fastener joints and the fatigue tests were performed on multi-fastener joints. Some of the results presented herein were obtained under other Grumman Independent Research and Development programs and were not part of the present contract. However, the results are pertinent to the present analytical study and are presented for illustrative purposes.

7.2 Static Strength Tests

7.2.1 Single Fastener Load Deflection Curves

(1) Description of the Tests

The configuration for the double shear test specimen chosen is shown in Fig. 68. A view of the test set up prior to testing is shown in Fig. 69. Note the extensometer device used for obtaining the automatic trace of the load-deflection curve across the joint. Table 13 gives a summary of the 15 static strength tests which were performed. All fasteners had a nominal diameter of 0.25 inches.

The method of testing followed closely the Grumman procedures used in obtaining fastener design allowables and is described in Ref. 32. The specimen is given a very small initial load of the order of 100 to 300 lbs. prior to start of test. The specimen is then loaded slightly beyond the beginning of its inelastic behavior and then unloaded. Reloading of the specimen then follows and a second unloading is made at a deflection of approximately 0.010 inches greater than the first. These two unloading cycles are chosen with the help of visual observation of the continous load-deflection trace and are intended to bracket the 0.012 inch offset point which is used to obtain the allowable yield load of the fastener.

A typical failed specimen is shown in Fig. 70 which shows the large local deformation causing ovalization of the holes and the excessive bending deformations in the broken titanium Hi-Lok fastener

(2) Results and Discussion

An attempt was made to determine the influence of gage length on the load-deflection curve of the single flush Hi-Lok fastener joint shown in Fig. 69. Three "identical" specimens having a single Hi-Lok fastener in double shear were tested by the procedure described above. The only variable in these three specimens was the length over which the deformations across the fastener were recorded by the extensometer. Three lengths were used in the study 2, 4 and 6 inches. The results are shown in Fig. 71. Although no definite trend is indicated the results do point to the fact that a fair amount of scatter can be expected in the load-deflection characteristics of seemingly identical specimens installed under normal production conditions.

The results of a limited study of the effect of friction coefficient on the faying surfaces of a joint are shown in Figs. 72 to 74. Fig. 72 shows the results of tests on joints made from plates as received with no special finish. The flush Hi-Lok installation torque is of the order of 65-80 in.-lbs. causing a small bi-linear effect in the elastic portion of the load-deflection curve with the change in slope occurring at an applied load of approximately 500 lbs. By finishing the plates with a standard protective alodine treatment used at Grumman the point at which the bi-linear effects occurs is shown to be about 1000 lbs. in the three tests shown in Fig. 73. This indicates an increase in the friction coefficient over the natural finish of Fig. 72 since the same Hi-Lok fasteners were used in both cases.

By Teflon coating the faying surfaces, the friction coefficient is reduced to practically zero, hence the break in the initial portion of the bi-linear curve occurs at a much lower load (approximately 100 lbs.) as shown in Fig. 74. It should be noted however, that for all three types of surface finish, the effect of a relatively small clamp-up (65-80 in.-lbs) has a very small effect on the over-all load deflection characteristics of the fastener.

The results of three tests using a single $\frac{1}{4}$" interference Hi-Lok-Hi-Tigue fastener in double shear are shown in Fig. 75. Comparing these results

with the tests using normal flush Hi-Lok fasteners having a small clearance due to the manufacturing tolerances, two things stand out. The load-deflection curve is nonlinear almost from the start of loading and the elastic modulus measured by the value of k_e is also much higher.

7.2.2 Multi-Fastener Joints

An example of a multi-fastener joint is shown in Figure 76 . The configuration is representative of a structural element fatigue test on a wing center line splice. The material of the outer plates is aluminum alloy, 7075-T6 clad and the inner plate is aluminum alloy 2024-T3511. The fasteners are $\frac{1}{4}$" dia. Hi-Loks. Three conditions of fastener-hole fit were tested, neat fit, 0.002" clearance and 0.004" clearance. In addition, the effects of clamp-up as applied to the fasteners due to installation torque, were studied. Tests were conducted with the fasteners lightly torqued by hand as against the normal installation torque used in manufacturing assembly.

The static behavior of the joint when assembled with the normal clamp-up is clearly demonstrated in Fig. 77, where the load-deflection curve for the joint over a 4 inch gage length shows a marked breaking point. The joints with clearance, as distinct from the neat fit, show the break in slope more clearly. In all three cases, the break occurs at a significant percentage of the joint ultimate strength. The relative effect of clamp-up and clearance on the fatigue strength of the joint is illustrated in Fig. 78. The fatigue life tends to decrease as clearance is increased, for the specimens without clamp-up. A considerable increase in fatigue life is obtained when normal fastener clamp-up is present.

A second double shear joint specimen is shown in Fig. 79. This configuration has two fasteners on a line, perpendicular to the applied load line. The material is titanium alloy, 6Al-6V-2 Sn annealed sheet. Joints assembled with 1/4" dia. Taper-Lok fasteners were tested with interference fits of 0.0018" and 0.0042". Joints with 1/4" Hi-Lok fasteners were tested with clearances of 0.003" and 0.006". A typical aircraft manuever load spectrum was used in all the tests.

Test results are presented for the interference fit specimens in Fig. 80. The data show substantial increases in fatigue life for the 0.0042" interference case over the 0.0018" interference case. Several specimens were tested after a 14 day exposure to a 3.5% NaCl solution, but the effect on

fatigue did not appear to be significant, based on very limited data.

Test results for the clearance fit specimens are presented in Fig. 81. The data show considerable scatter, and the results for the 0.003" clearance and the 0.006" clearance overlap to the extent that a separate scatter band for each condition has not been defined. These test results are also discussed briefly in Section 4 of Chapter 5, where fatigue life predictions for the joint are presented.

REFERENCES

1. McCombs, W. F., McQueen, J. C. and Perry, J. L., "Analytical Design Methods for Aircraft Structural Joints", AFFDL-TR-67-184, Air Force Flight Dynamics Laboratory, Wright-Patterson Air Force Base, Ohio, January 1968.

2. Gehring, R. W. and Maines, C. H., "A Redundant-Force Method for the Inelastic Analysis of Mechanically Fastened Joints", U. S. Naval Air Engineering Center Report No. NAEC-ASL-1103, January 1967.

3. Jensen, W. R., Falby, W. E., and Prince, N., "Matrix Analysis Methods for Anisotropic Inelastic Structures", Air Force Technical Report AFFDL-TR-65-220, Air Force Flight Dynamics Laboratory, Wright-Patterson Air Force Base, Ohio, April 1966.

4. Padlog, J., Huff, R. D. and Holloway, F. G., "Unelastic Behavior of Structures Subjected to Cyclic, Thermal and Mechanical Stressing Conditions", WADD Tech. Report 60-271, December 1960.

5. Grumman Aerospace Corporation, IDEAS Manual, Vol. IIA, Chapter 7, September 1968.

6. Wennagel, G. J., Mason, P. W., and Rosenbaum, J. D., "IDEAS, Integrated Design and Analysis System", paper presented at the ASE Aeronautic and Space Engineering and Manufacturing Meeting, Los Angeles, Calif., Oct. 7-11, 1968.

7. Lambert, T. H. and Brailey, R. J., "The Influence of the Coefficient of Friction on the Elastic Stress Concentration Factor for a Pin Jointed Connection" The Aeronautical Quarterly, Feb. 1962, pp. 17-29.

8. Isakson, G., Armen, H., Jr., and Pifko, A., "Discrete-Element Methods for the Plastic Analysis of Structures," NASA Contractors Report, CR-803, October 1967.

9. Armen, H., Jr., Isakson, G., and Pifko, A., "Discrete-Element Methods for the Plastic Analysis of Structures Subjected to Cyclic Loading," Grumman Research Department Report RE 28LJ, February 1967; also presented at the joint AIAA/ASME 8th Materials, Structures, Structural Dynamics Conference, Palm Springs, California, March 1967.

10. Lansing, W., Jensen, W., and Falby, W., "Matrix Analysis Methods for Inelastic Structures," Proc. of (First) Air Force Conference on Matrix Methods in Structural Mechanics, AFFDL TR66-80, Air Force Flight Dynamics Laboratory, Wright-Patterson Air Force Base, Ohio, November 1965.

11. Harris, H. G., Armen, H., Jr., and Pifko, A.B., "A Method for Determining the Stress Distribution in Plates with Squeeze Rivets," Structural Mechanics Report, Report No. 000-STMECH-029, Grumman Aerospace Corporation, Bethpage, New York, April 1969.

12. Timoshenko, S., Strength of Materials, Part II, 2nd Ed., Van Nostrand New York (1941).

13. Den Hartog, J. P., Advanced Strength of Materials, McGraw-Hill, New York (1952).

14. Hetenyi, M., Beams on Elastic Foundation, U. of Michigan Press, Ann Arbor (1946).

15. Crandall, S. H., "The Timoshenko Beam on an Elastic Foundation", Proceedings of the Third Midwestern Conference on Solid Mechanics, 1957, pp. 146-159.

16. Essenburg, F., "Shear Deformation in Beams on Elastic Foundations", J. of Applied Mechanics, Vol. 29, No. 2, 1962, pp. 313-317.

17. Hess, M. S. "Eigenfunction Solution for Beam on Elastic Foundation", J. of Applied Mechanics, Vol. 36, 1969, pp. 799-802.

18. Boley, B. A. and Tolins, I. S., "On the Stresses and Deflections of Rectangular Beams," J. of Applied Mechanics, Vol. 23, Trans. ASME, Vol. 78, 1956, pp. 339-342.

19. Fung, Y. C., Foundations of Solid Mechanics, Prentice-Hall, New Jersey (1965).

20. Cowper, G. R., "The Shear Coefficient in Timoshenko's Beam Theory", J. of Applied Mechanics, Vol. 33, No. 2, 1966, pp. 335-340.

21. Aubrey, C. and McLean, J. L. - "The Effect of Hole Clearance on the Fatigue Life of Aluminum Lugs" - Canadian Aeronautics and Space Journal, June 1964.

22. Heywood, R. B. - Designing Against Fatigue of Metals (Figures 9.14 and 9.15) - Reinhold Publishing Co., New York 1962.

23. Silverman, B. S., Hooson, R. E. and Saleme, E. - "Fatigue Prediction Methods Based on Strain Cycling" Grumman Advanced Development Report No. FSR-AD2-01-68.3, Grumman Aerospace Corporation, Bethpage, N.Y., May 1968.

24. Manson, S. S., and Hirshberg, M. H. -"Fatigue Behavior of Materials Under Strain Cycling in the Low and Intermediate Life Range", NASA TN-D-1574, April 1963.

25. Peterson, R. E., "Fatigue of Metals - Part 3 - Engineering and Design Aspects", Materials Research and Standards, February 1963.

26. Stowell, E. Z., "Stress and Strain Concentration at a Circular Hole in an Infinite Plate", NACA TN 2073, 1950.

27. Smith, C. R., "Design Tips for Preventing Fatigue Failures", Figure 7, Assembly Engineering, March 1968.

28. Lee, W. and Villalba, I. P., "Method for Calculating Shear Lag Type Load Distributions in Multiple Fastener Joints", Report No. GF-145, Grumman Aerospace Corporation, Bethpage, N.Y. June 8, 1956.

29. Ramberg, W. and Osgood, W. R., "Description of Stress-Strain Curves by Three Parameters", NACA T. N. 902, July 1943.

30. Villalba, I., Tsongas, A. G. and Torczyner, R., "Fastener Allowables and Load Deflection Curves", Vols. I and II, Grumman Report No. 000 - STMECH - 021/022, Grumman Aerospace Corporation, Bethpage, New York, August 1968.

31. Corporate Titanium Program Report on Fastener Evaluation, Grumman Aerospace Corporation, Bethpage, New York, 1968 (Unpublished).

32. Moon, D. P., and Hyler, W. S. "MIL-HDBK-5 Guidelines for the Presentation of Data" Technical Report AFML-TR-66-385, Air Force Material Laboratory, Wright-Patterson Air Force Base, Ohio, February 1967.

Problem No.	Diam. D_1 & D_2 (in.)	Width W (in.)	Spacing S (in.)	e Edge Dist. (in.)	Thick-ness t (in.)	$\frac{S}{W}$	$\frac{W}{D}$	$\frac{e}{D}$	$\frac{D}{t}$	$\frac{S}{D}$
1	2	3	4	5	6	7	8	9	10	11
P 1.1	.25	2	4	1	.125	2	8	4	2	16
P 1.3	.50	2	4	1	.125	2	4	2	4	8
P 1.6	.75	2	4	1	.125	2	2.67	1.33	6	5.33
P 1.2	.25	2	2	1	.125	1	8	4	2	8
P 1.4	.50	2	2	1	.125	1	4	2	4	4
P 1.5	.75	2	2	1	.125	1	2.67	1.33	6	2.67

Table 1 Summary of Plate Problems With Two Unloaded Holes

Problem No.	Diam. D_1 to D_6 (in.)	Taper	Spacing Along Width S_W (in.)	Spacing Along Length S_L (in.)	Edge Dist. Plate ℄ Holes e_1 (in.)	Edge Dist. End Holes e_2 (in.)	Thickness t (in.)	$\frac{S_W}{D}$	$\frac{S_L}{D}$	$\frac{e_1}{D}$	$\frac{e_2}{D}$	$\frac{D}{t}$	℄ Width W_1 (in.)	Width Across Edge Holes W_2 (in.)	$\frac{W_1}{D}$	$\frac{W_2}{D}$
1	2	3	4	5	6	7	8	9	10	11	12	13	14	15	16	17
3.1A	.250	1:4	.5	1	.75	.5	.125	2	4	3	2	2	2	1.5	8	6
3.1B	.125	1:4	.5	1	.75	.5	.125	4	8	6	4	1	2	1.5	16	12
3.2B	.125	1:8	.5	1	.5	.375	.125	4	8	4	3	1	1.5	1.25	12	10
3.3B	.125	1:16	.5	1	.375	.3125	5 .125	4	8	3	2.5	1	1.25	1.125	10	9

Table 2 Summary of Tapered Plate Problems with Six Unloaded Holes

Problem Number	Diameter D (in.)	Width W (in.)	Edge Distance e (in.)	Thick-ness t (in.)	$\frac{W}{D}$	$\frac{e}{D}$	$\frac{D}{t}$
P2.1	.25	.9375	.625	.125	7.5	2.5	2
P2.2	.50	.9375	.625	.125	3.75	1.25	4
P2.3	.75	.9375	.625	.125	2.5	.835	6
P2.4	.75	.9375	1.6	.3	2.5	2.13	2.5

Table 3 - Summary of Geometric Parameters of Aluminum Plates with Single Rigid Fastener

x/t	Flex. Beam (Rigid in Shear) Eq. (24)	Shear Beam (Rigid in Bending) Eq. (25)	Completely Rigid Beam Eq. (26)
0	4.003	4.032	4.000
.1	3.401	3.410	3.400
.2	2.800	2.796	2.800
.3	2.199	2.190	2.200
.4	1.599	1.588	1.600
.5	0.998	0.990	1.000
.6	0.399	0.395	0.400
.7	-0.201	-0.200	-0.200
.8	-0.800	-0.795	-0.800
.9	-1.399	-1.392	-1.400
1.0	-1.998	-1.992	-2.000

Table 4 - Load Interaction Parameter $\frac{qt}{P_0}$ for a Fastener with Negligible Head Stiffness in Single Shear (Ref. Figure 51a) ($E = 30 \times 10^6$ psi, $\nu = 0.3$, $k = 7.68 \times 10^6$, $t = 0.125$ in, $d = 0.25$ in.)

x/t	Shear Beam (Rigid in Bending)	Completely Rigid Beam
0	1.078	1.000
.1	1.056	
.2	1.036	
.3	1.018	
.4	1.029	
.5	0.990	
.6	0.980	
.7	0.972	
.8	0.966	
.9	0.962	
1.0	0.961	1.000

Table 5 - Load Interaction Parameter $\frac{qt}{P_0}$ for a Rigid-Head Fastener in Single Shear (Ref. Fig. 51 b)
($E = 30 \times 10^6$, $\nu = 0.3$, $k = 7.68 \times 10^6$ psi, $t = 0.125$ in, $d = 0.25$ in)

	x/t_1	Completely Rigid Beam	Free & Clamped Heads Shear Beam (Rigid in Bending)	Clamped Head Bent Beam (Rigid in Shear)	Free Head Bent Beam (Rigid in Shear)
inner plate	0	1.000	0.990	0.995	0.995
	.1	↓	0.991	0.996	0.996
	.2		0.995	0.997	0.997
	.3		1.001	1.000	1.000
	.4		1.009	1.005	1.005
	.5	1.000	1.020	1.010	1.010
outer plates	.5	1.000	1.020	1.009	1.015
	.6	↓	1.009	1.004	1.009
	.7		1.001	1.000	1.003
	.8		0.995	0.997	0.997
	.9		0.991	0.995	0.991
	1.0	1.000	0.990	0.995	0.985

TABLE 6 - Load Interaction Parameter, $\frac{qt_1}{P_0}$ or $\frac{q(2t_2)}{P_0}$,

for a Fastener in Double Shear (Reference Fig. 52)

($E = 30 \times 10^6$ psi, $\nu = 0.3$, $k_1 = 7.68 \times 10^6$ psi, $k_2 = 7.68 \times 10^6$ psi, $t_1 = 0.125$ in, $t_2 = 0.0625$ in, $d = 0.25$ in.)

Type Fit	Plate Stiffness (Refer to Fig. 38) $k \times 10^{-6}$(psi)	Joint Stiffness $k_{eff} \times 10^{-6}(\frac{lb}{in})$		
		Titanium Fastener	Steel Fastener	Rigid Fastener
Loose	4.255	.416	.512	.535
Neat	5.330	.610	.635	.670
Interference	6.966	.778	.816	.876

Table 7 - Analytical Results for the Double Lap Joints Tested

Type Fit	Linearized Joint Stiffness $k_{eff} \times 10^{-6}(\frac{lb}{in})$
	Titanium fastener
Loose	.420 (avg. of 12 tests)
Interference	.803 (avg. of 3 tests)

Table 8 - Summary of Experimental Results Presented in Appendix K

Load Level (lbs)	Net Section Applied Stress (psi)	Maximum Tangential Stress at Edge of Hole in psi			
		$\theta = 9^\circ$	$\theta = 45^\circ$	$\theta = 81^\circ$	$\theta = 99^\circ$
2	14.2	25.62	28.34	42.60	45.56
500	3555	6404.9	7092	10,669	11,390
1000	7111	12,810	14,185	21,338	22,781
2000	14,222	25,620	28,369	42,676	45,562
4000	28,444	51,239	56,739	85,351	91,123
8000	56,888	102,479	113,477	170,702	182,247
9000	63,999	115,288	127,662	192,040	205,027
10000	71,111	128,098	141,847	213,378	227,809

Table 9 Elastic Stresses for Neat Fit Case

Load Level (lbs)	Net Sect. Appl. Str. (psi)	Maximum Tangential Stress at Edge of Hole in psi					
		$\theta = 9^\circ$	$\theta = 27^\circ$	$\theta = 45^\circ$	$\theta = 63^\circ$	$\theta = 81^\circ$	$\theta = 99^\circ$
2	14.232	50,615	36,062	28,281	23,732	21,764	22,330
500	3,555	49,842	39,140	32,934	28,759	26,433	25,973
1000	7,111	29,066	42,231	37,606	33,807	31,121	29,631
2000	14,222	48,993	47,791	45,456	42,185	38,956	35,890
4000	28,444	68,526	67,655	66,120	64,410	64,831	73,709
8000	56,888	119,532	120,634	122,547	127,133	149,354	164,939
9000	63,999	132,342	133,946	136,731	142,912	170,692	187,720
10000	71,111	145,152	147,257	150,916	158,690	192,030	210,500

Table 10 Elastic Stresses for the Case of $\Delta D/D = 0.4\%$ Interference

Load Level (lbs)	Net Section Applied Stress (psi)	Maximum Tangential Stress at Edge of Hole in psi			
		$\theta = 9^\circ$	$\theta = 45^\circ$	$\theta = 81^\circ$	$\theta = 99^\circ$
2	14.2	253,087	141,330	108,744	111,593
500	3555	252,315	145,984	113,413	115,236
1000	7111	251,538	150,656	118,101	118,893
2000	14,222	249,986	159,999	127,477	126,209
4000	28,444	246,882	178,686	146,229	140,839
8000	56,888	240,673	216,059	183,733	170,100
9000	63,999	240,752	223,206	190,762	175,591
10000	71,111	244,964	227,282	194,780	179,448

Table 11 Elastic Stresses for the Case of $\Delta D/D = 2.0\%$ Interference

Load Level (lbs)	Net Section Applied Stress (psi)	Maximum Tangential Stress at Edge of Hole in psi			
		$\theta = 9^\circ$	$\theta = 45^\circ$	$\theta = 81^\circ$	$\theta = 99^\circ$
2	14.2	506,178	282,644	217,469	223,172
500	3555	505,404	287,296	222,138	226,815
1000	7111	504,629	291,968	226,827	230,472
2000	14,222	503,077	301,312	236,203	237,787
4000	28,444	499,972	319,998	254,954	252,418
8000	56,888	493,764	357,371	292,458	281,679
9000	63,999	492,211	366,715	301,835	288,994
10000	71,111	490,659	376,058	311,210	296,309

Table 12 Elastic Stresses for the Case of $\Delta D/D = 4\%$ Interference

Specimen No.	Finish on Faying Surfaces	Hole Diameters: Outer Plate A in.	Hole Diameters: Middle Plate B in.	Hole Diameters: Outer Plate C in.	Fastener Diam. in.	Fastener Installation Torque in.-lbs.	Component Part Designation
HL-1	None	———	.2514	———	———	65-80	GB510A-4-9 -GN512H-4
-2			.2515				
-3	None	———	.2514	———	———		
-4	Alodine 823-011	———	.2511				
		———	.2510	———	———		
-5		———	.2510	———	———		
-6	Alodine 823-011	———	.2510	———	———		
-7	Teflon	———	.2512	———	———		
-8		———	.2513	———	———		
-9	Teflon	———	.2510	———	———		
-10	None	.2509	.2509	.2510	.2492		
-11	None	.2509	.2509	.2510	.2492		
-12	Teflon	.2509	.2509	.2510	.2491		GB510A-4-9 -GN512H-4
HT-1	None	———	.2518	———	———		HLT-1170-8-9
-2	None	———	.2514	———	———		
-3	None	———	.2515	———	———	65-80	HLT-1170-8-9

Table 13 Single Fastener Tests - Physical Description

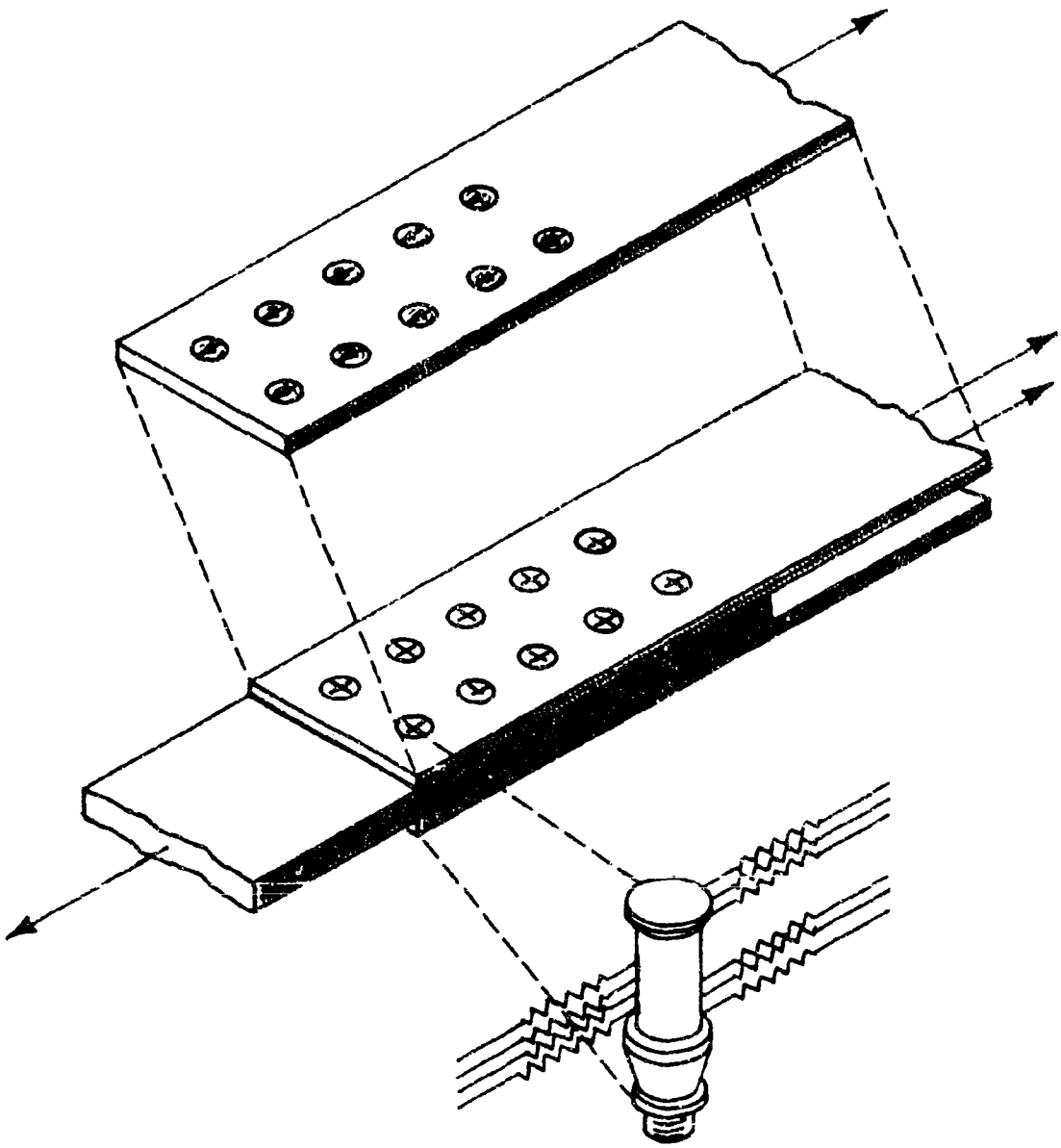

Fig. 1 Schematic Representation of Mechanically Fastened Structural Joint Showing the Method Used to Decompose the Structure for Analysis Purposes

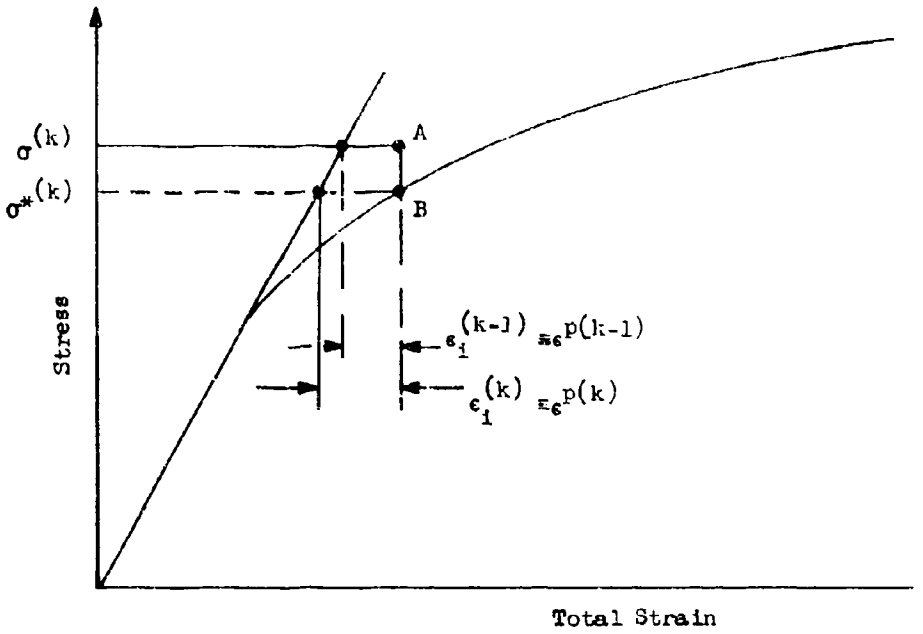

Fig. 2 Illustration of the Constant Strain Method for a Uniaxial Stress Case

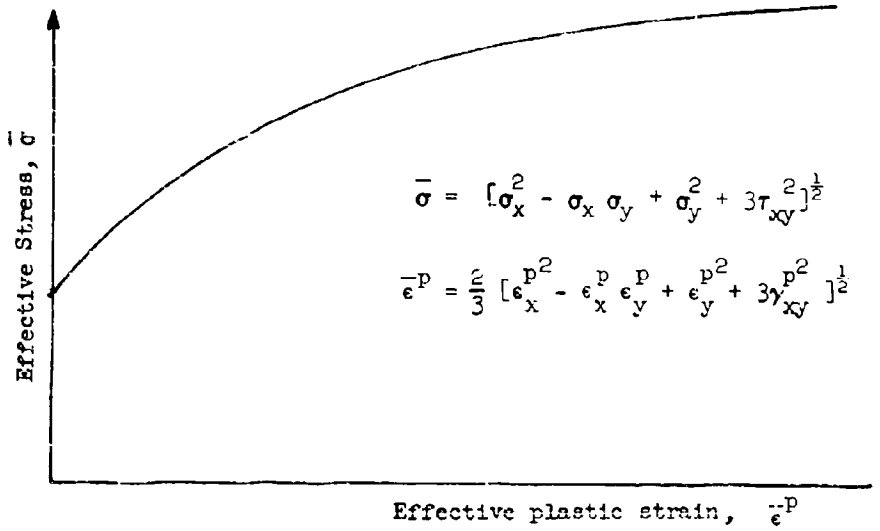

$$\bar{\sigma} = [\sigma_x^2 - \sigma_x \sigma_y + \sigma_y^2 + 3\tau_{xy}^2]^{\frac{1}{2}}$$

$$\bar{\epsilon}^p = \frac{2}{3}[\epsilon_x^{p2} - \epsilon_x^p \epsilon_y^p + \epsilon_y^{p2} + 3\gamma_{xy}^{p2}]^{\frac{1}{2}}$$

Fig. 3 Effective Stress-Strain Curve

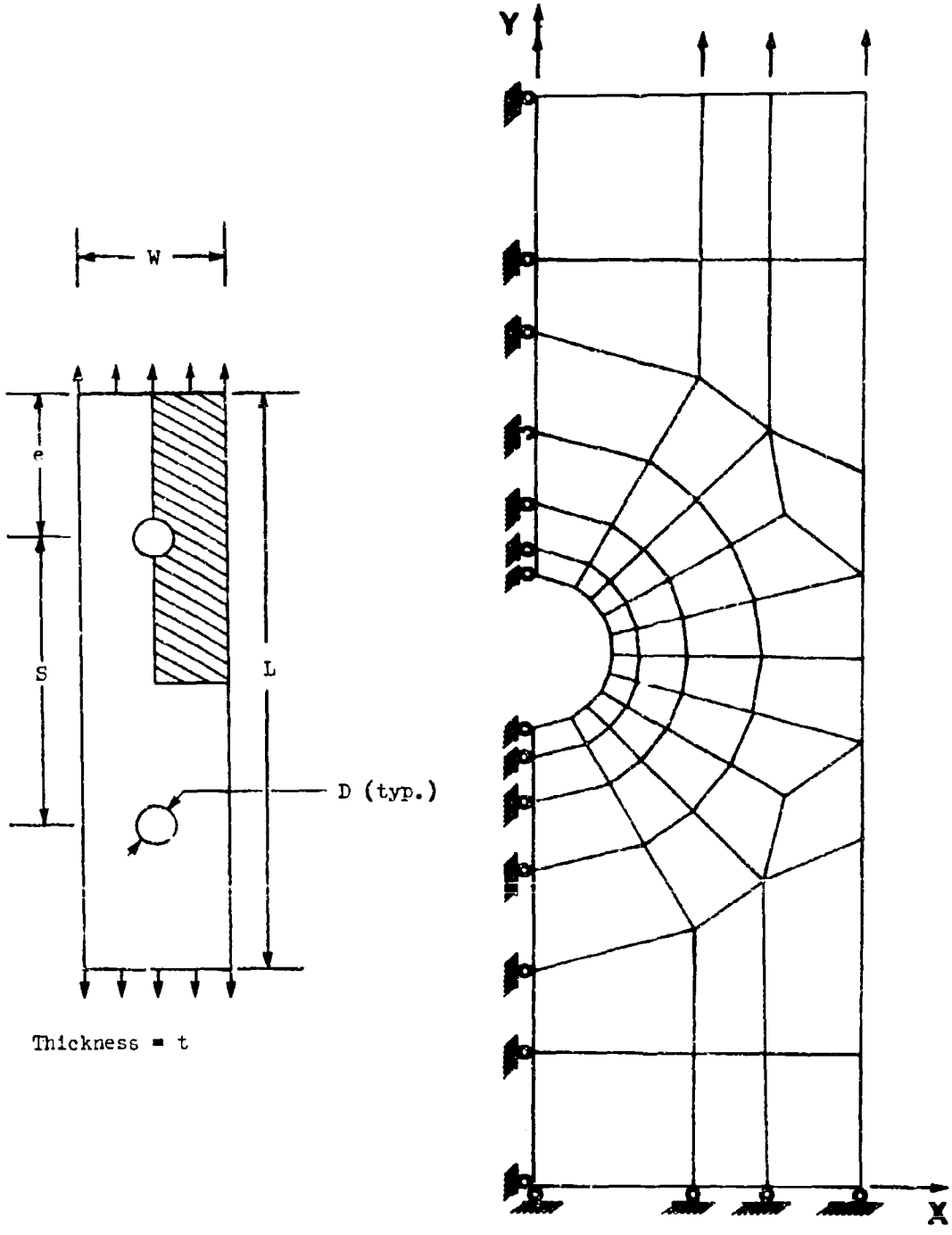

Fig. 4 Model for Determination of Effective Width and Effects of Fastener Spacing

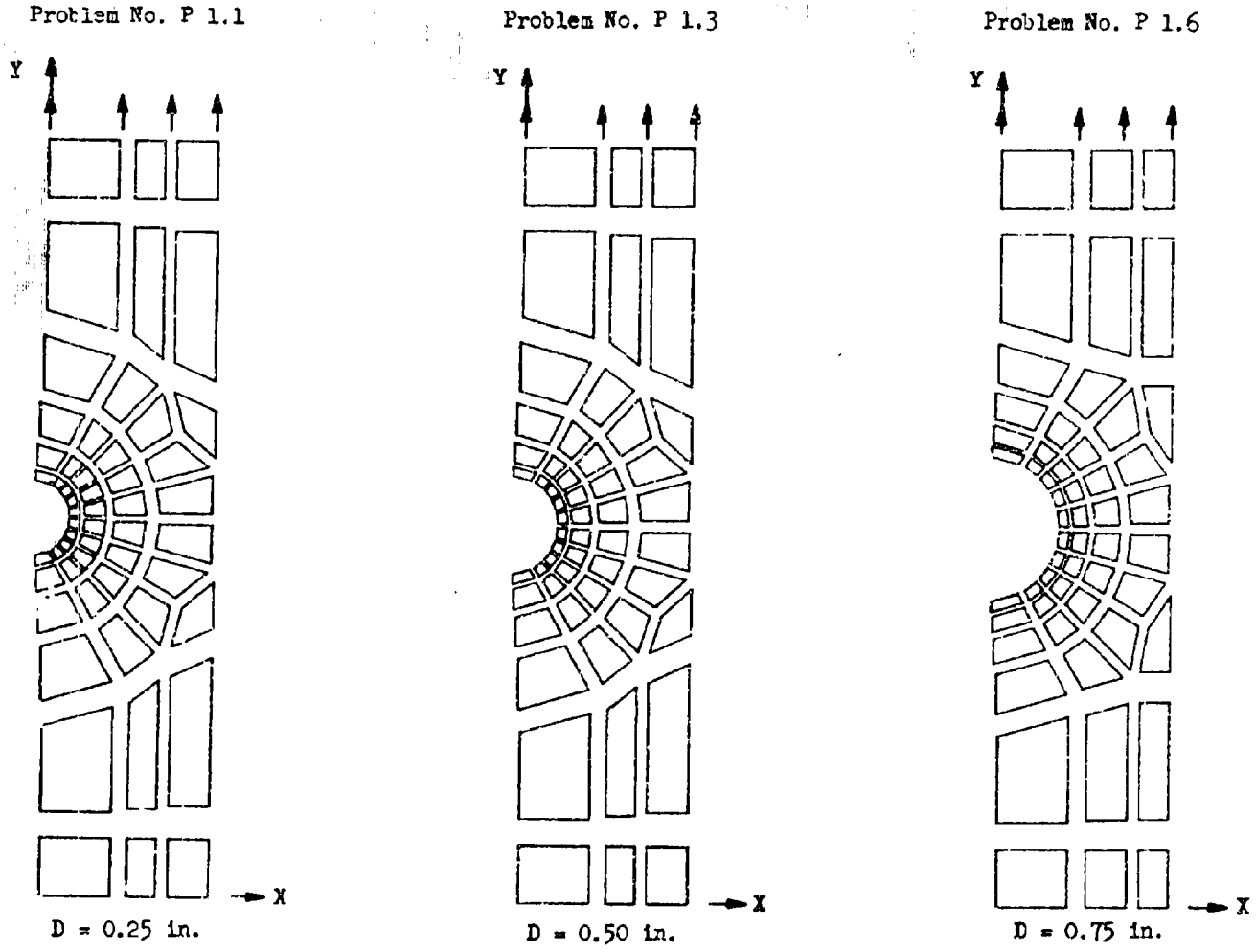

Fig. 5 Idealizations of Two Hole Plates in 2024-T4 Aluminum with S/W = 2

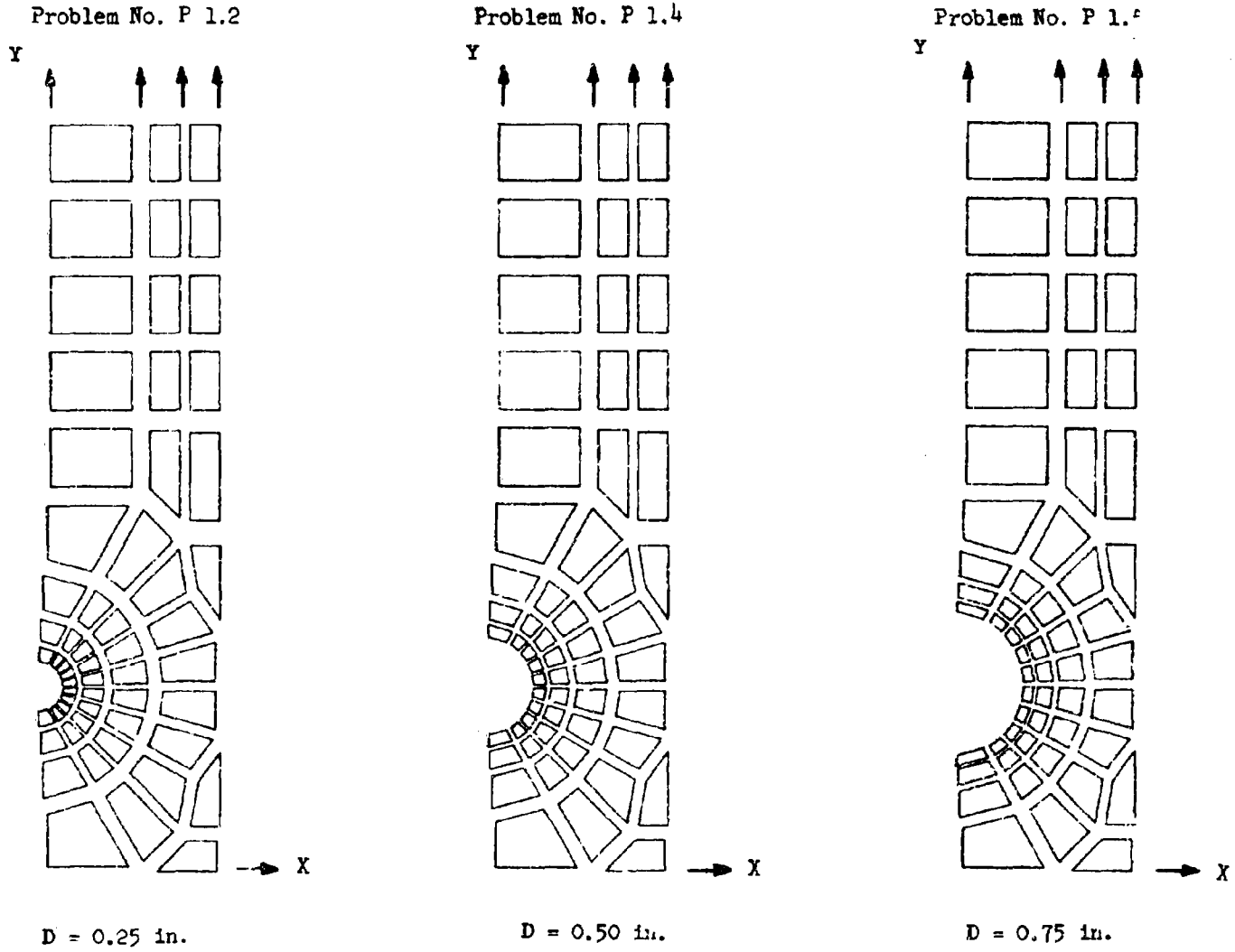

Fig. 6 Idealizations of Two Hole Plates in 2024-T4 Aluminum with S/W = 1

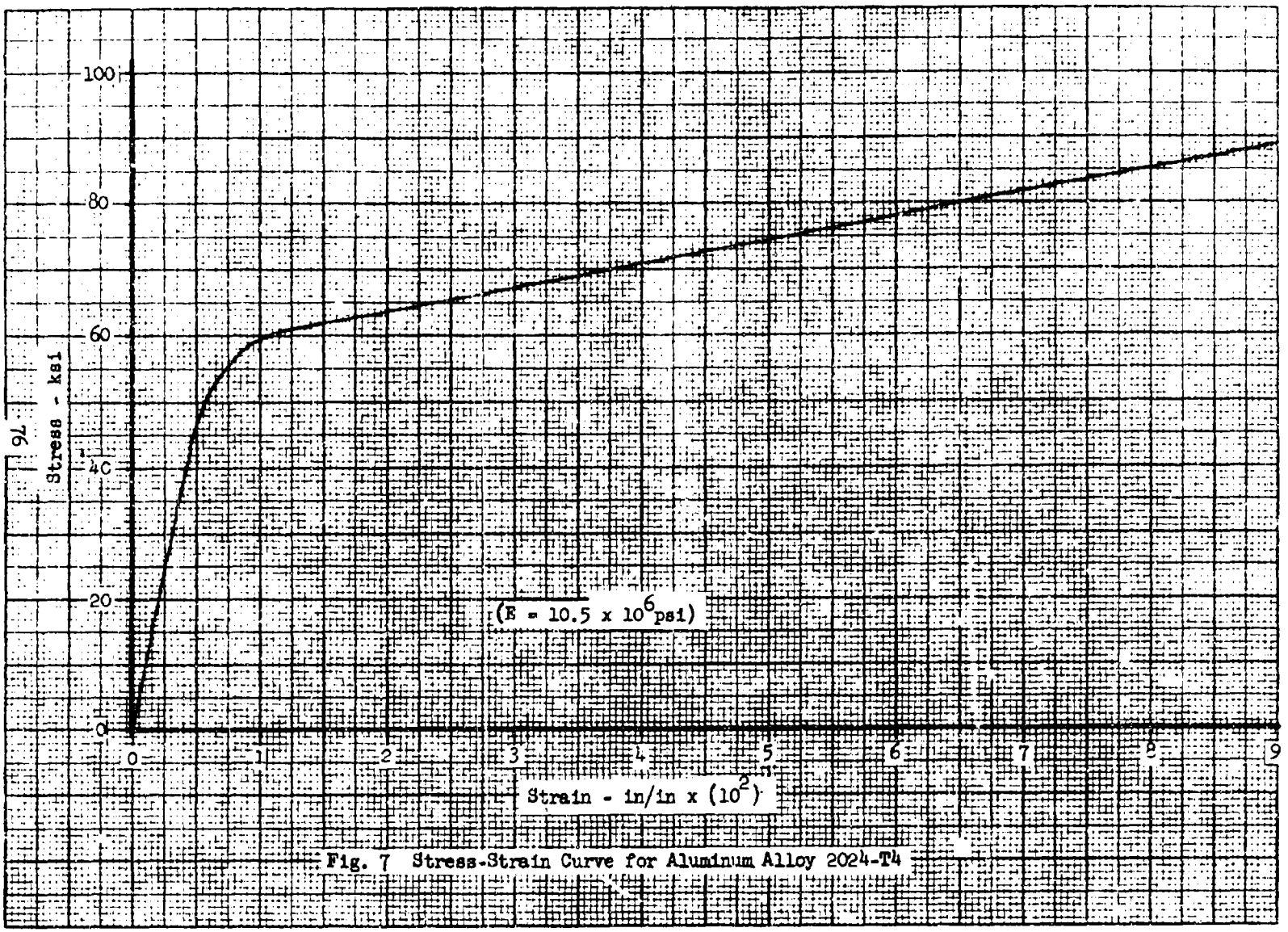

Fig. 7 Stress-Strain Curve for Aluminum Alloy 2024-T4

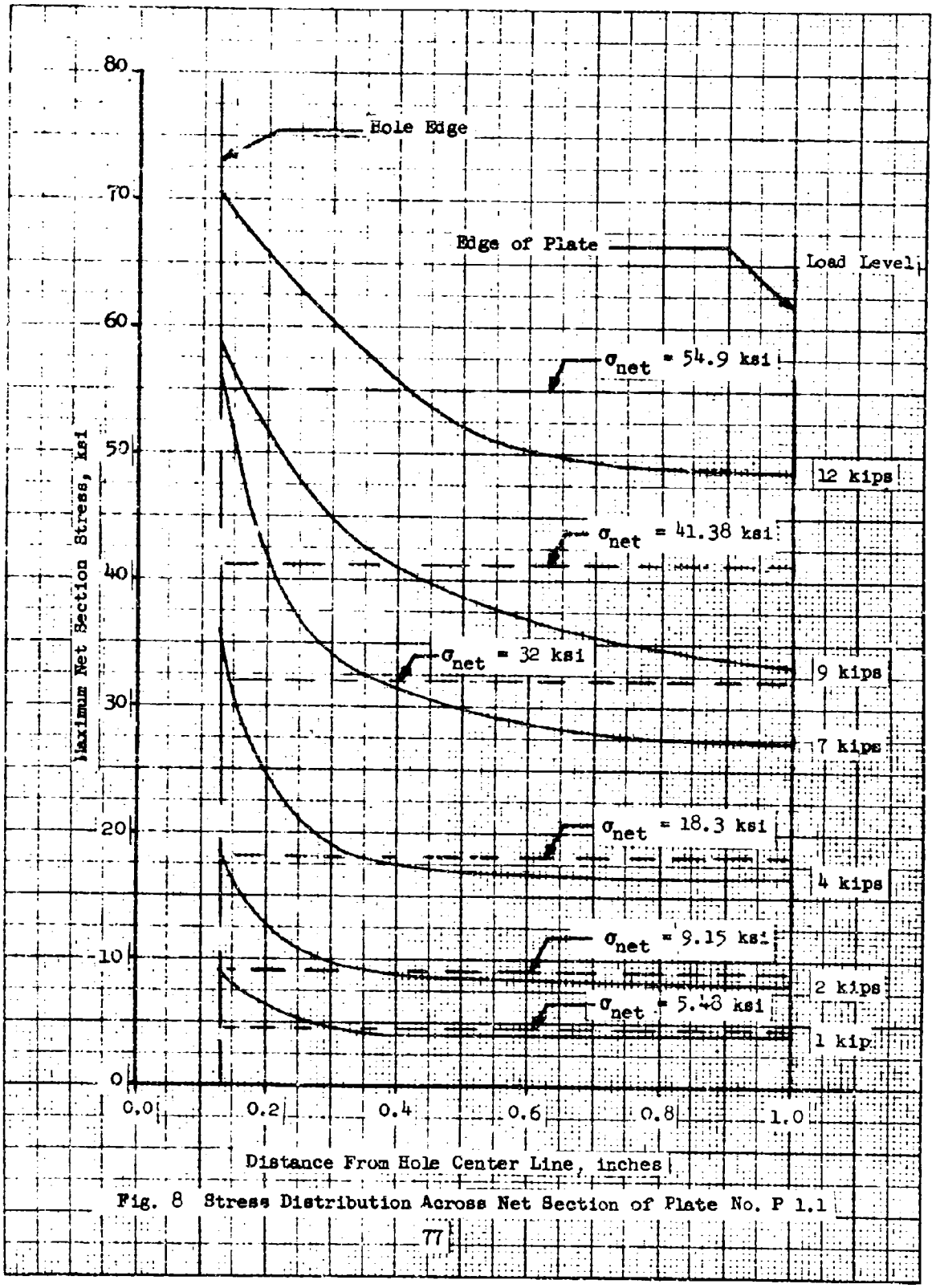

Fig. 8 Stress Distribution Across Net Section of Plate No. P 1.1

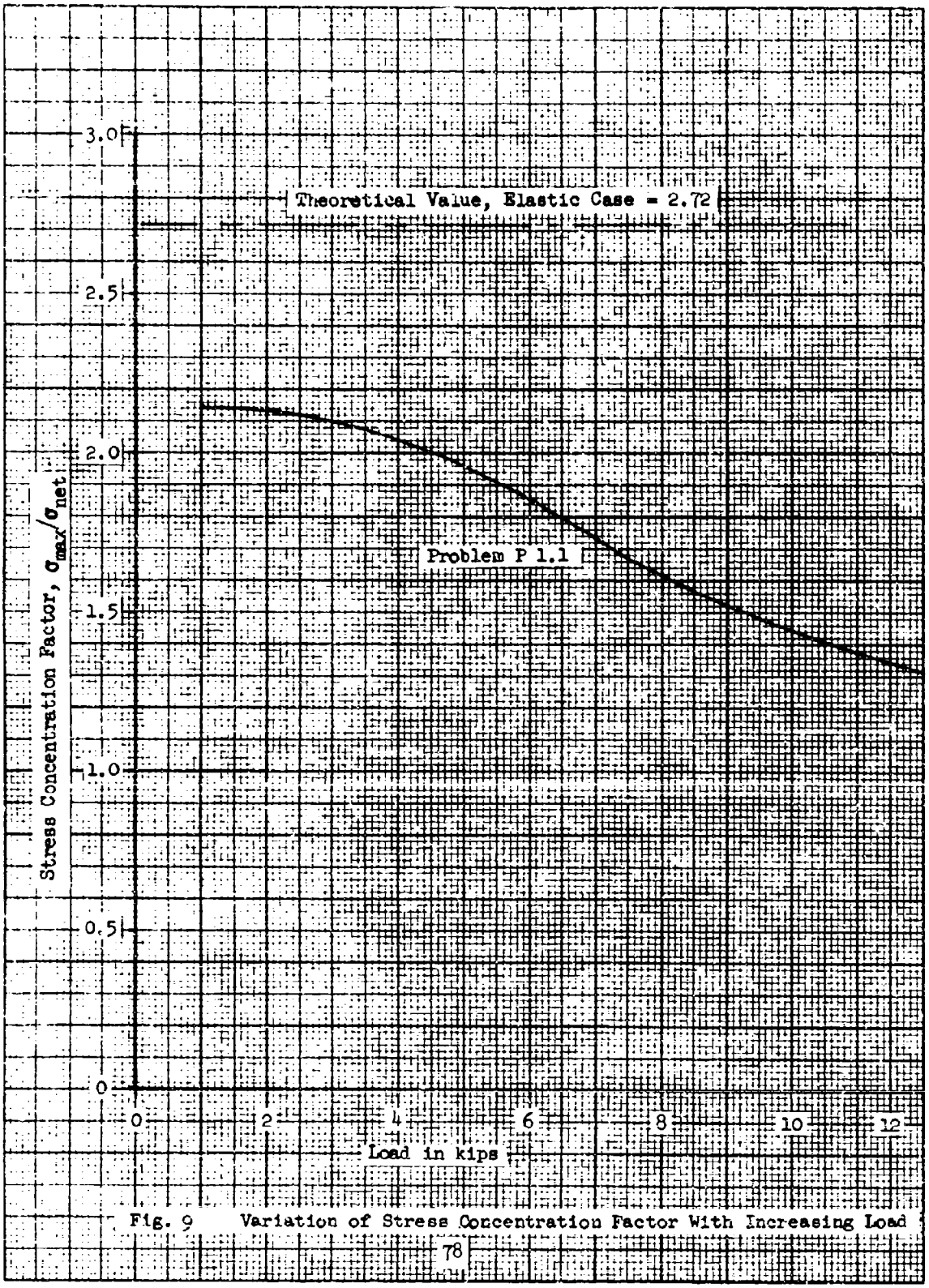

Fig. 9 Variation of Stress Concentration Factor With Increasing Load

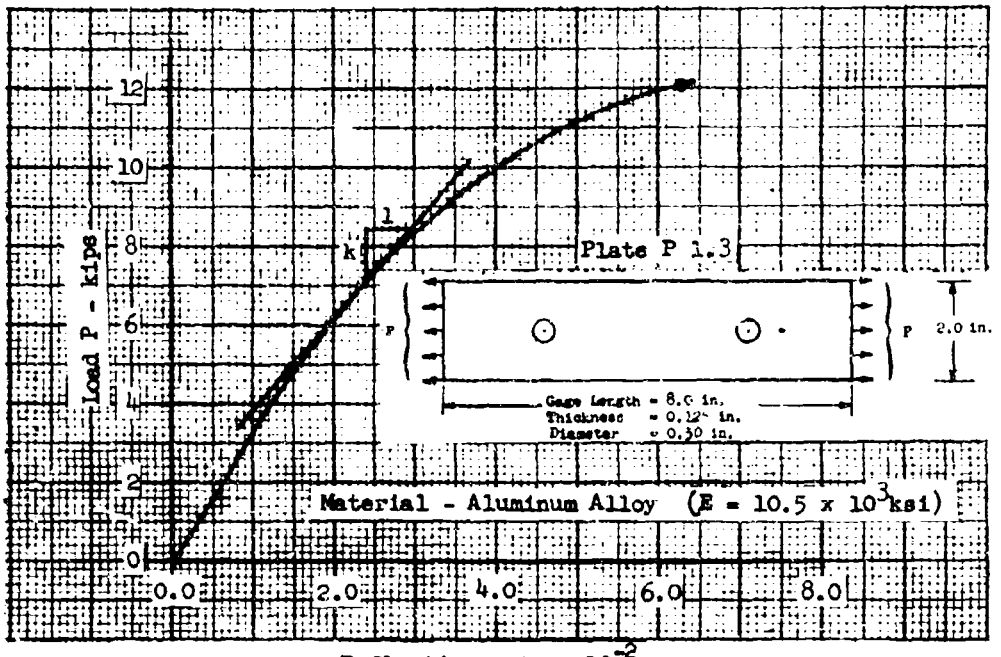

(a) Load-Deflection Curve

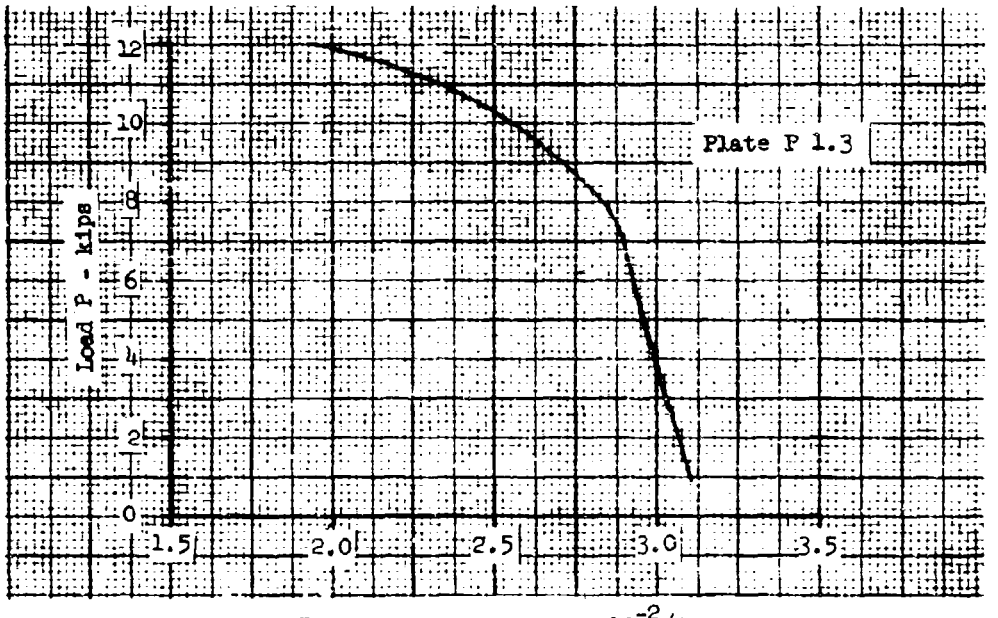

(b) Load vs. Tangent Modulus

Fig. 10 Variation in Stiffness or Slope of the Load-Deflection Curve with Increasing Load.

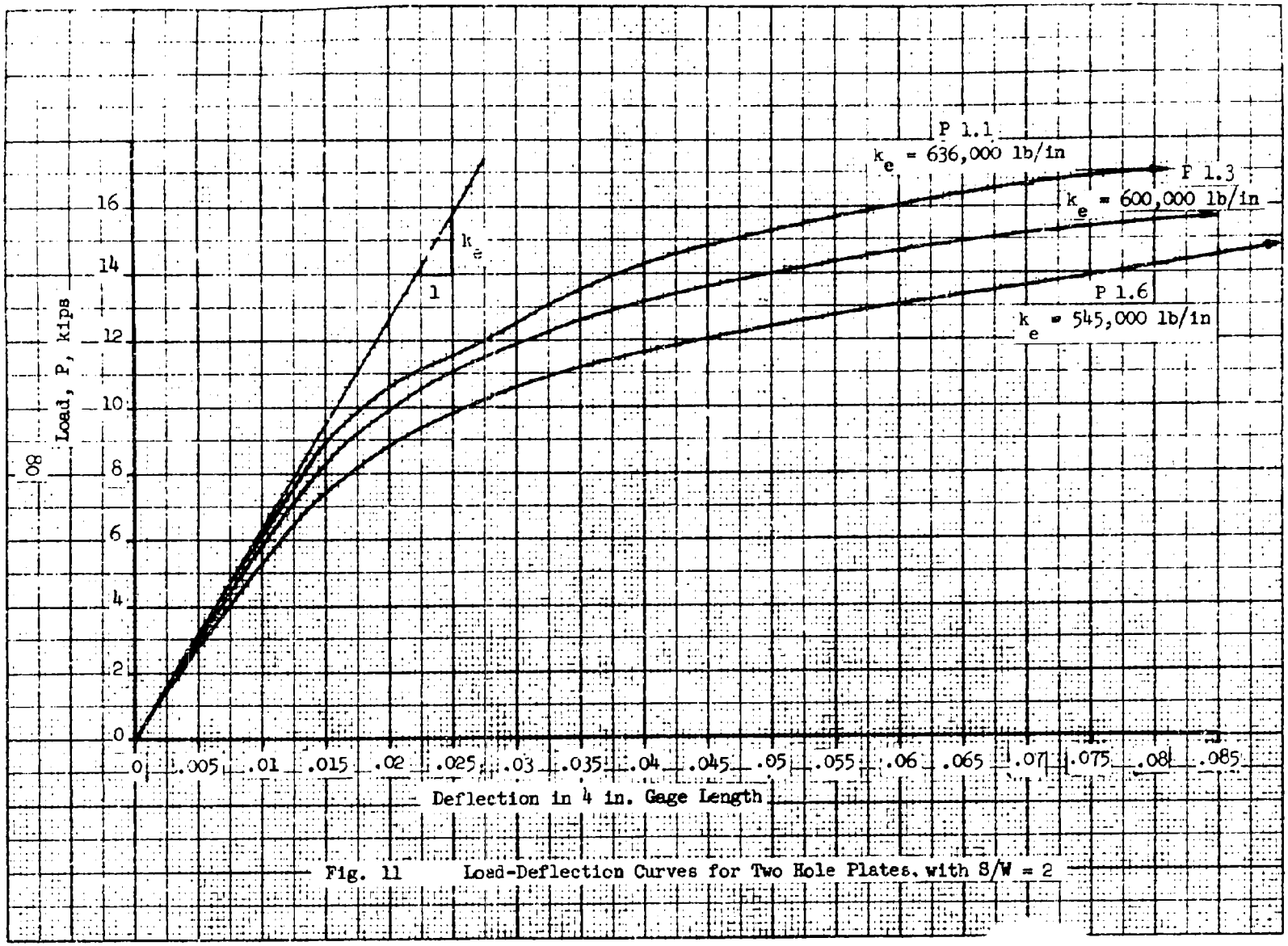

Fig. 11 Load-Deflection Curves for Two Hole Plates with S/W = 2

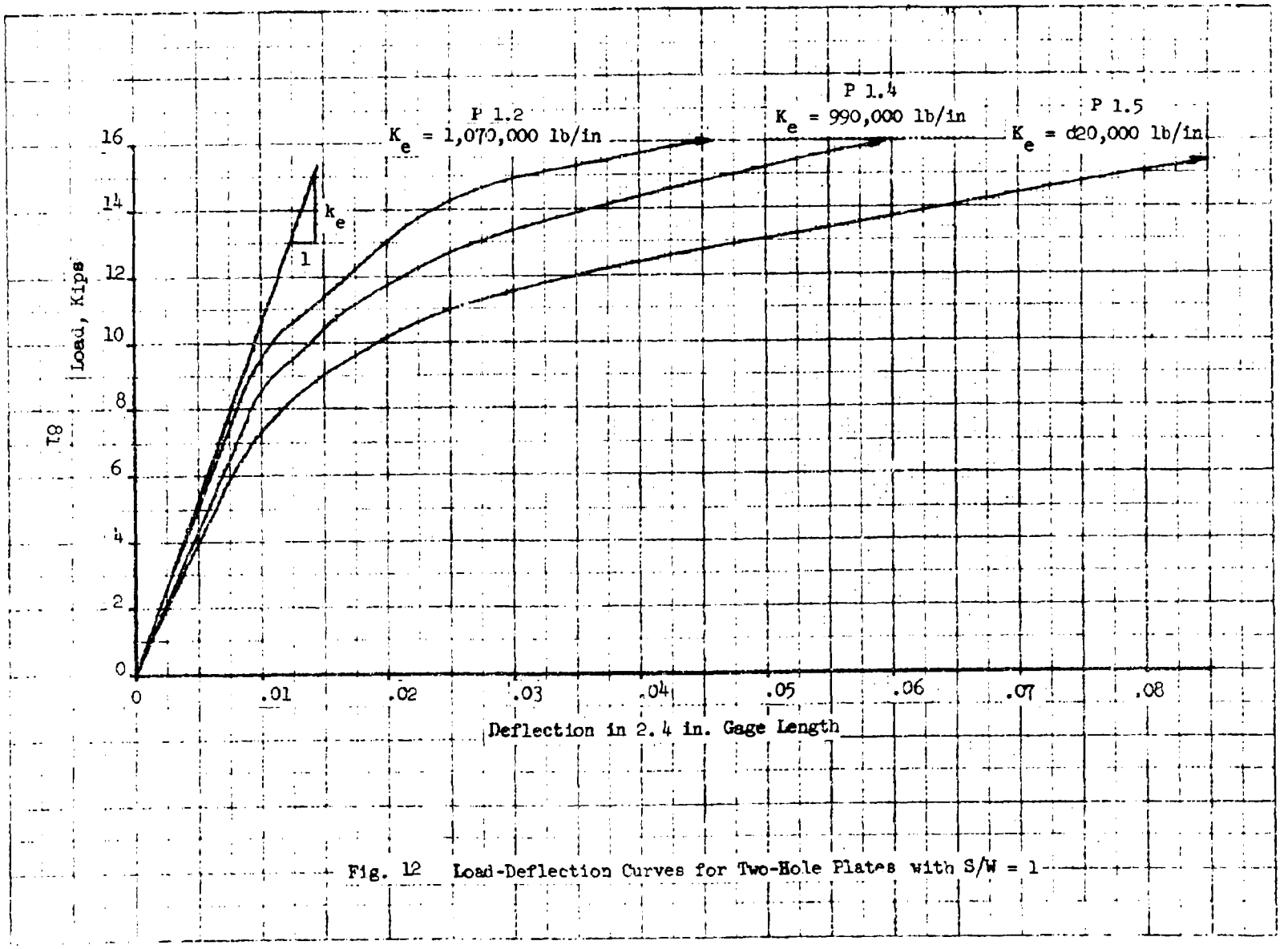

Fig. 12 Load-Deflection Curves for Two-Hole Plates with S/W = 1

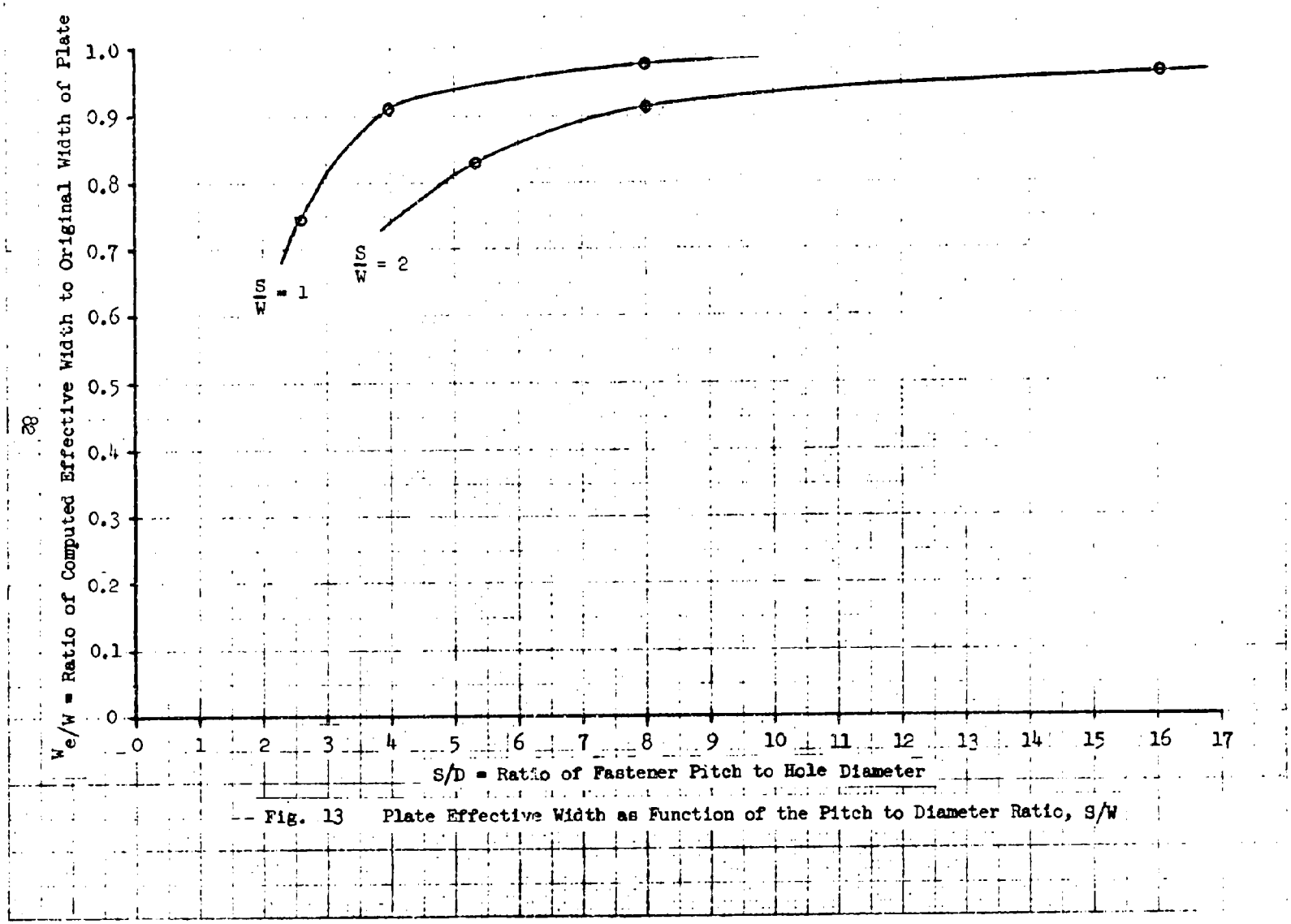

Fig. 13 Plate Effective Width as Function of the Pitch to Diameter Ratio, S/W

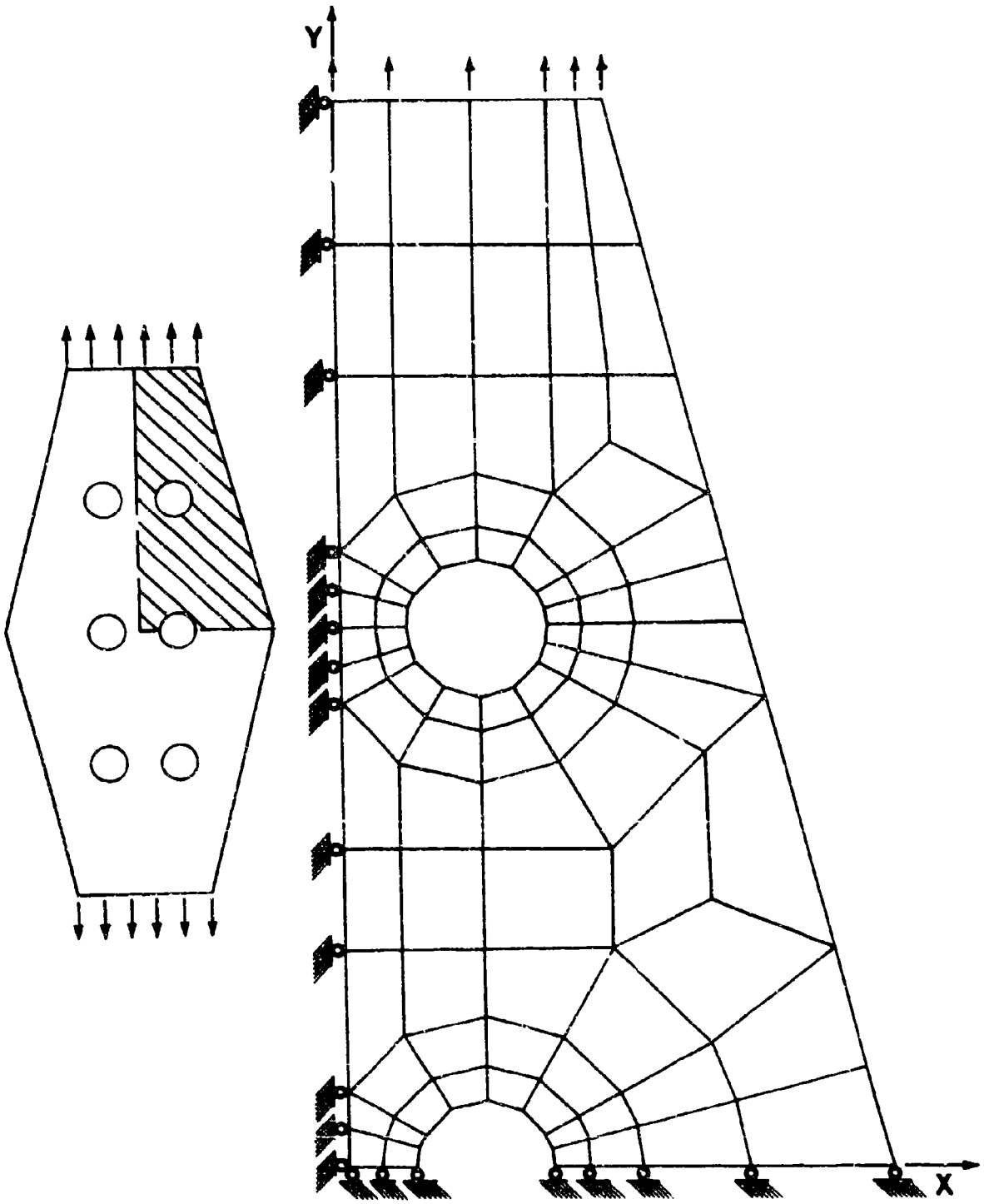

Fig. 14 Idealized Model for Evaluation of Effects of Width Taper

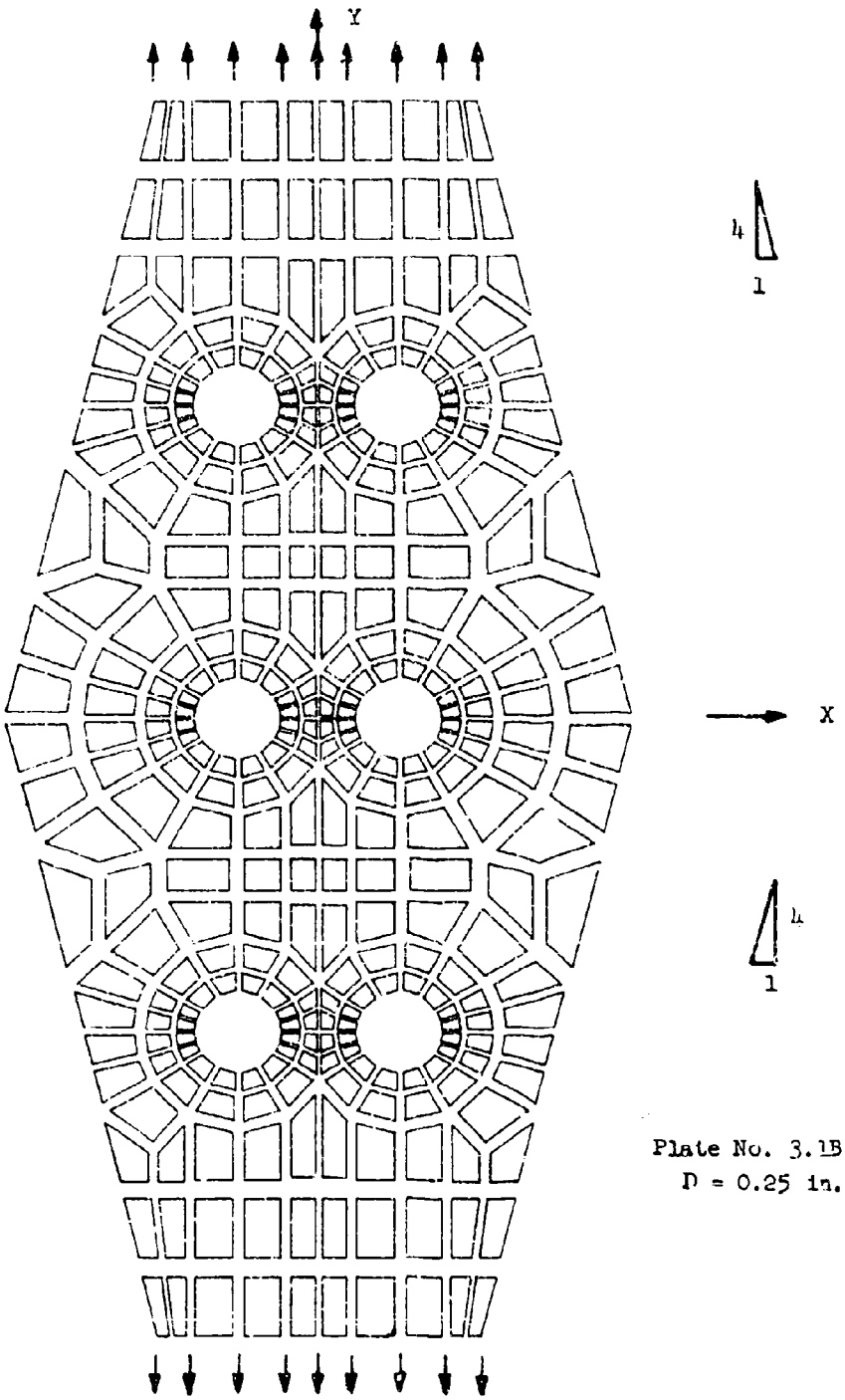

Fig. 3.5 Idealization of Tapered Plate with Taper of 1:4 and D = 0.25 in.

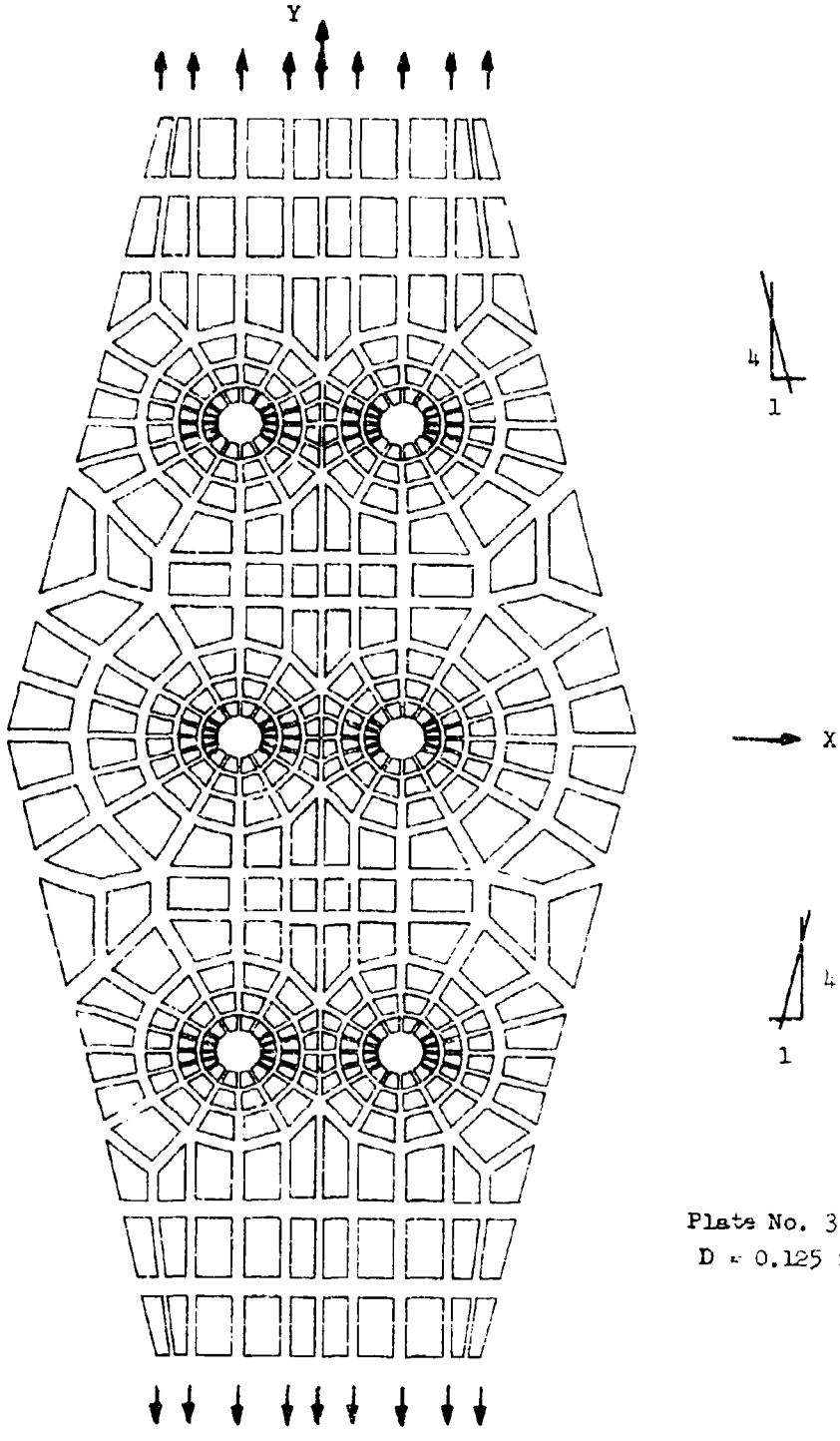

Fig. 16 Idealization of Tapered Plate with Taper of 1:4 and D = 0.125 in.

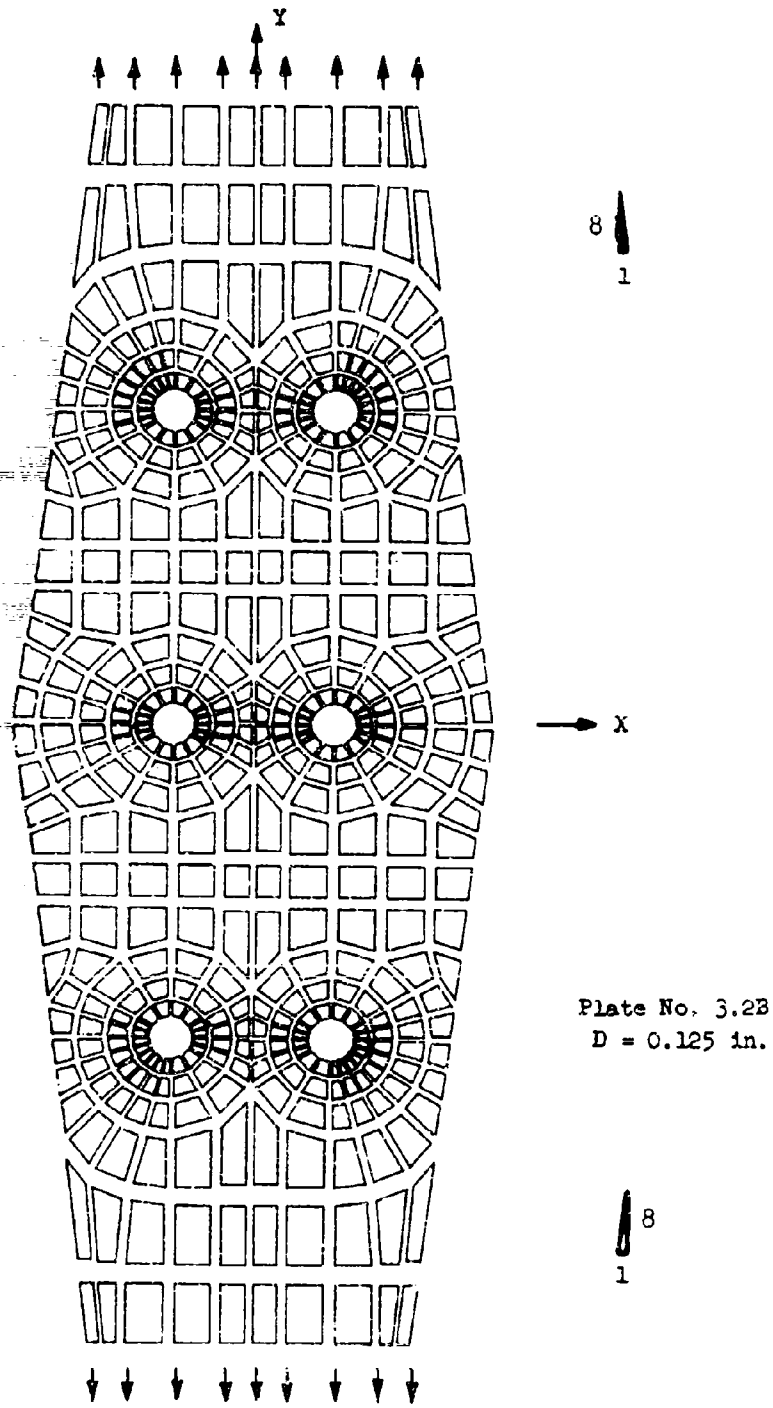

Fig. 17 Idealization of Tapered Plate with Taper of 1:8 and D = 0.125 in.

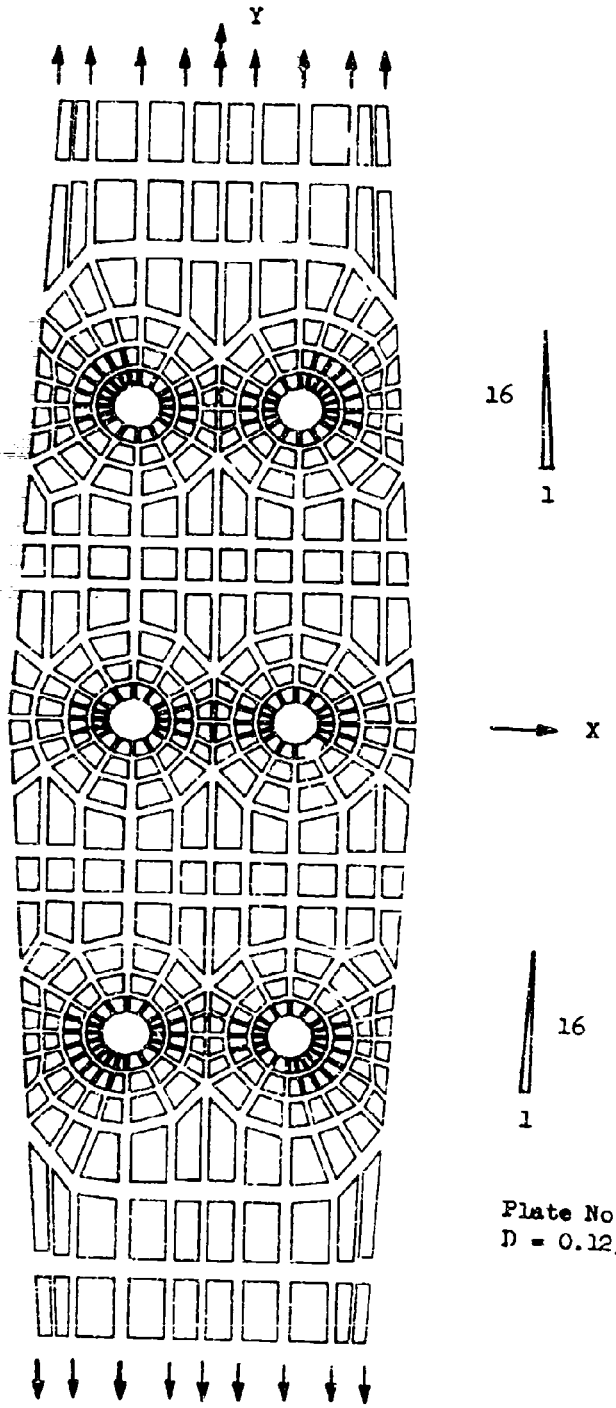

Fig. 18 Idealization of Tapered Plate with Taper of 1:16 and D = 0.125 in.

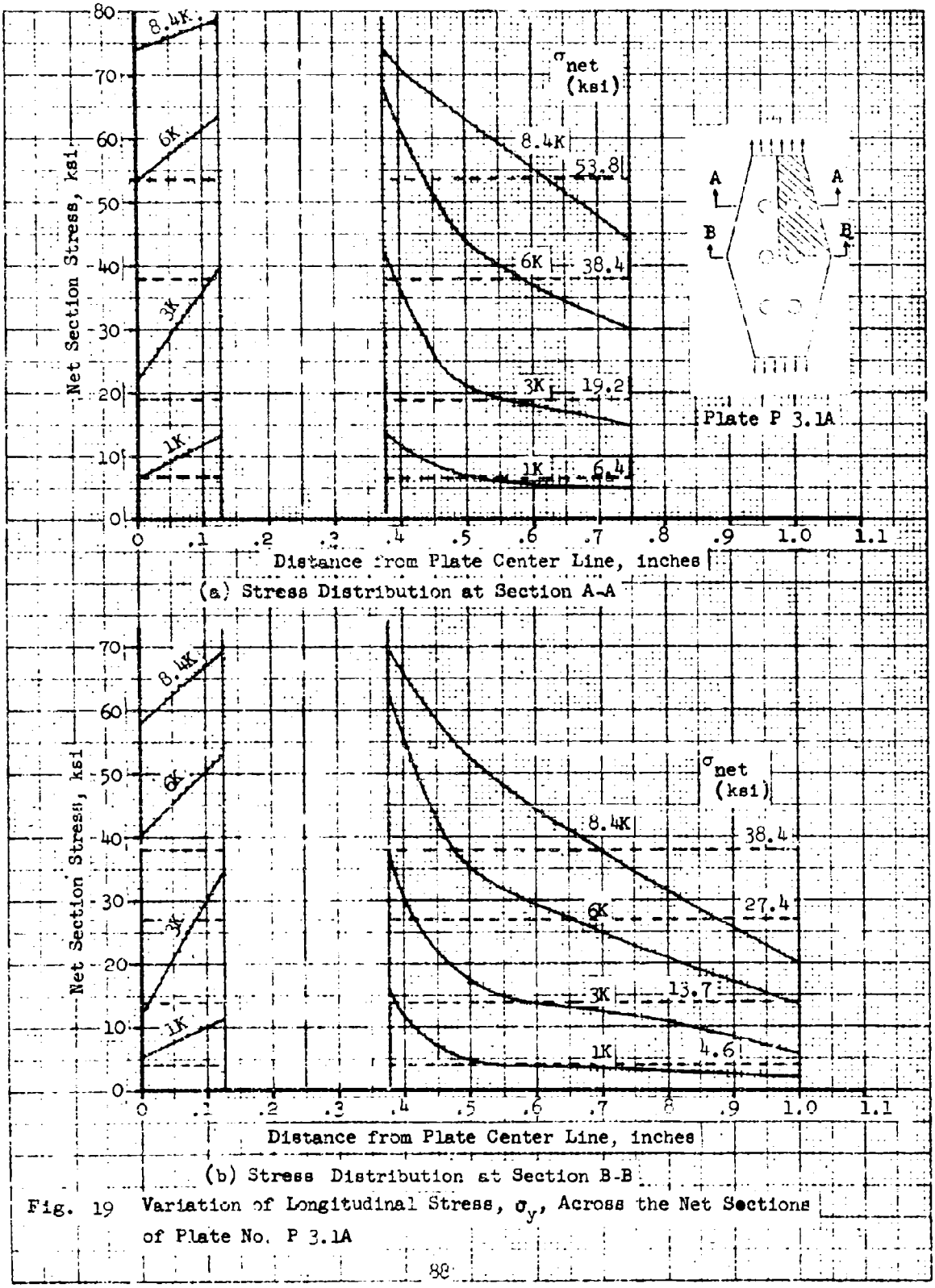

Fig. 19 Variation of Longitudinal Stress, σ_y, Across the Net Sections of Plate No. P 3.1A

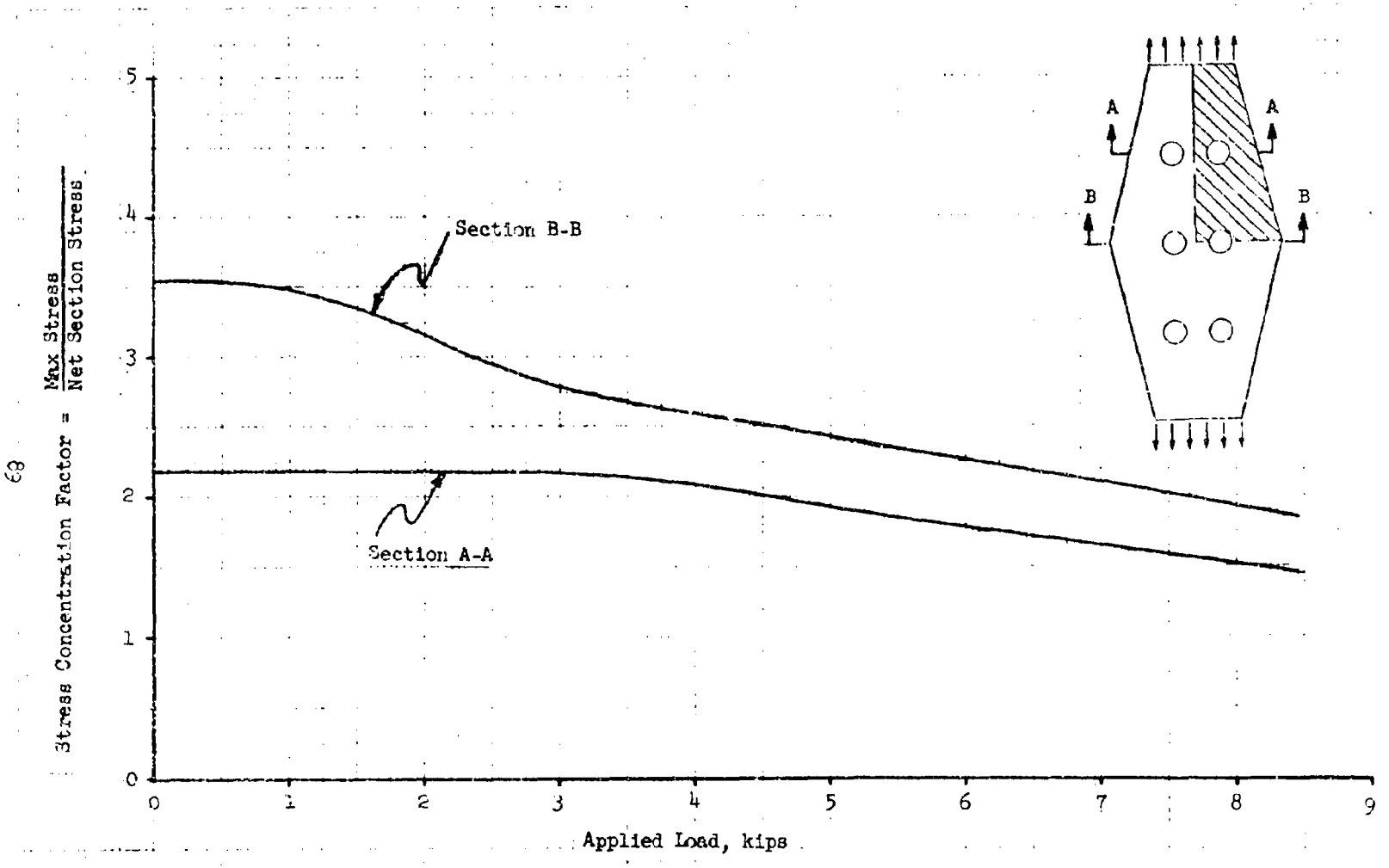

Fig. 20 Variation of Stress Concentration Factors with Load for Tapered Plate P 3.1A

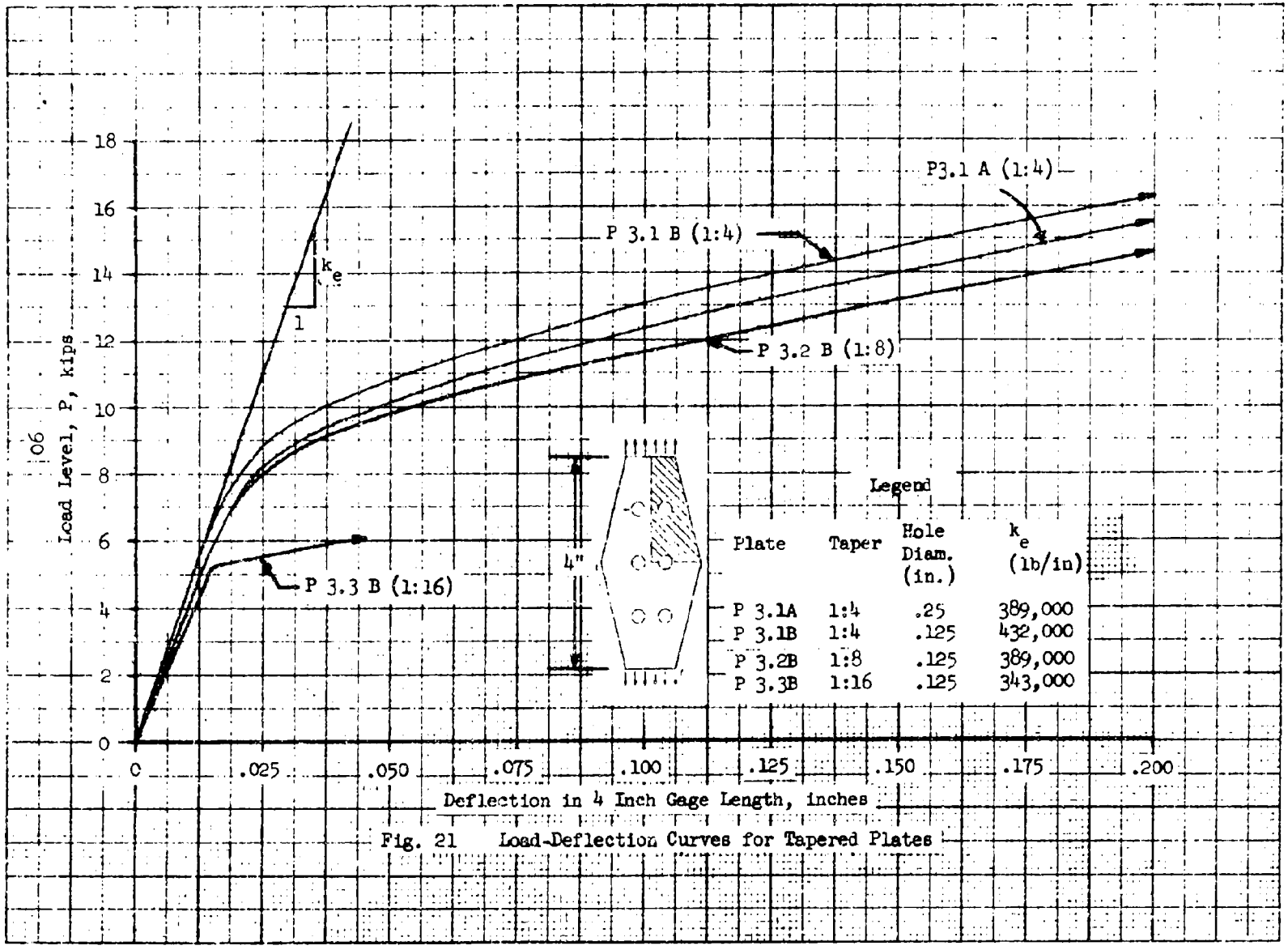

Fig. 21 Load-Deflection Curves for Tapered Plates

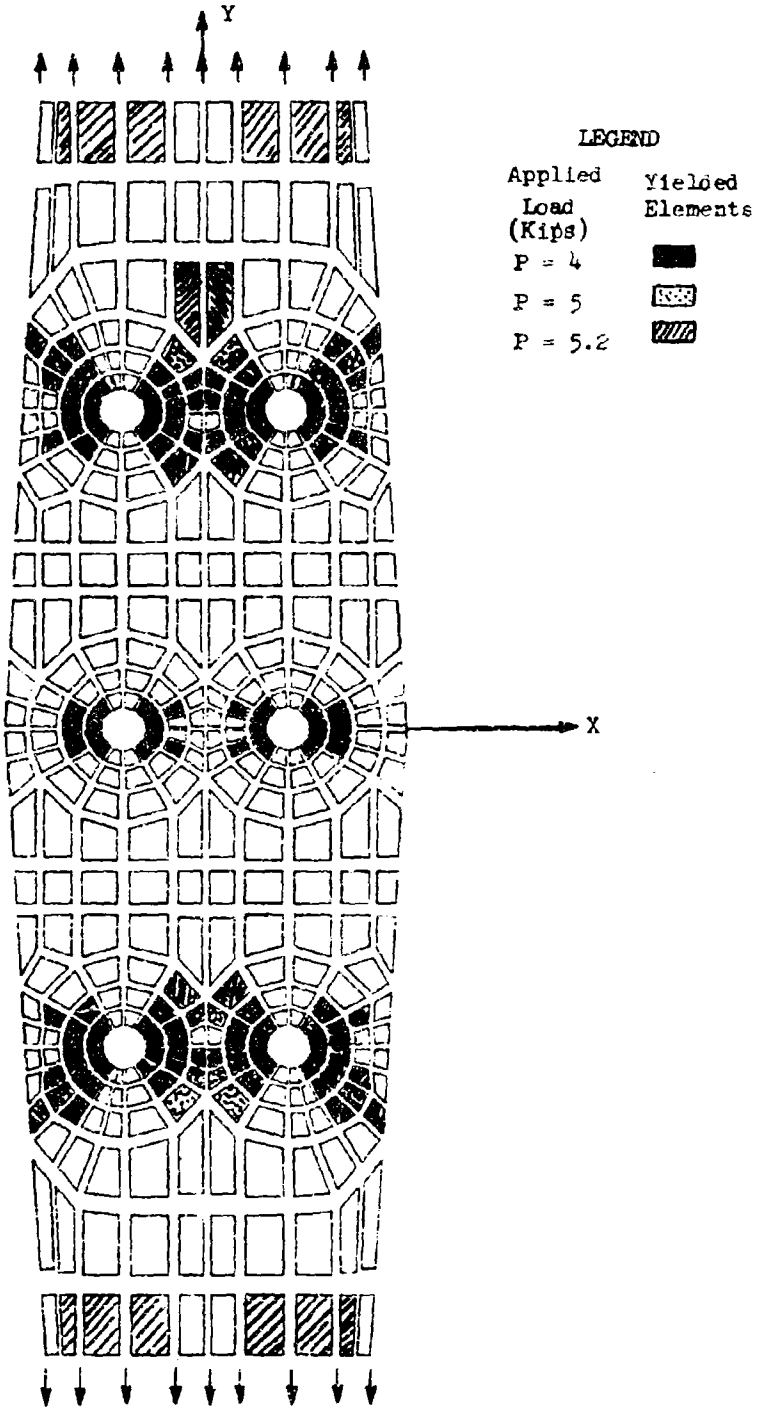

Fig. 22 Progression of Yield Zones with Increasing Applied Load, Plate P 3.3B

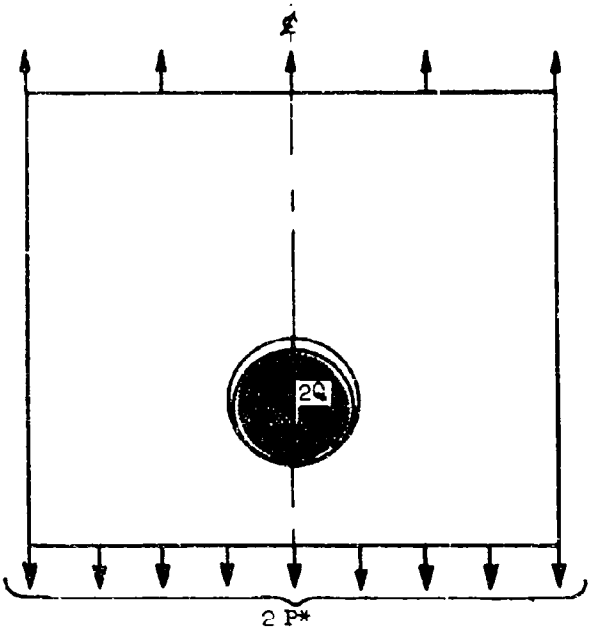

(a) Region Around a Typical Fastener

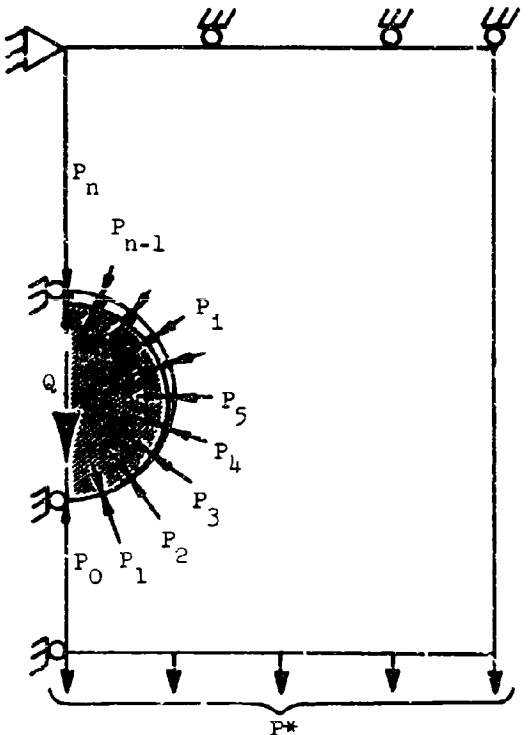

Q = Transfer Load

P* = By-pass Load

(b) Idealization Used

Fig. 23 Mathematical Model of Plate Loaded Through a Fastener

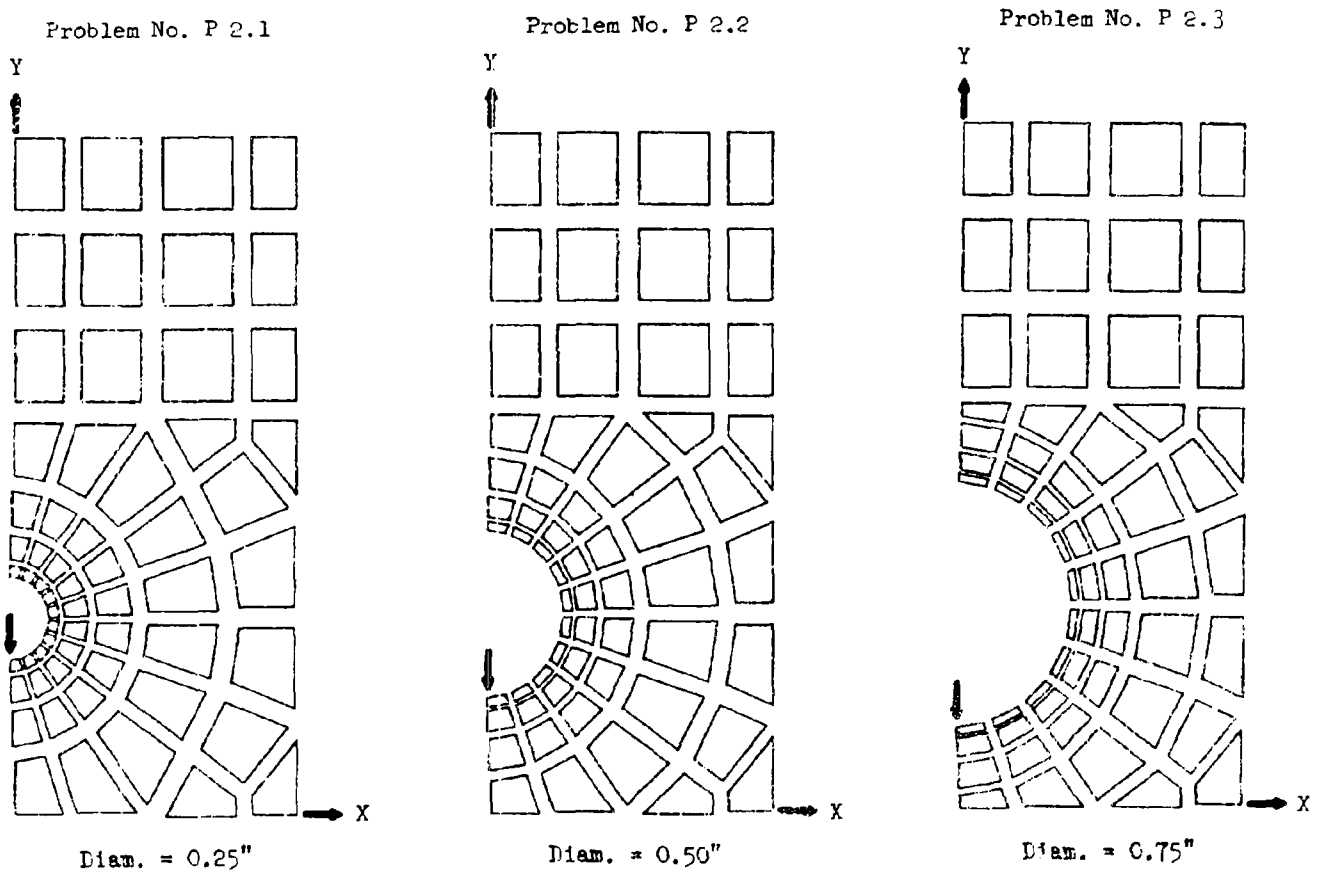

Fig. 24 Finite Element Idealizations of Aluminum Joints With e = 0.625 Inches

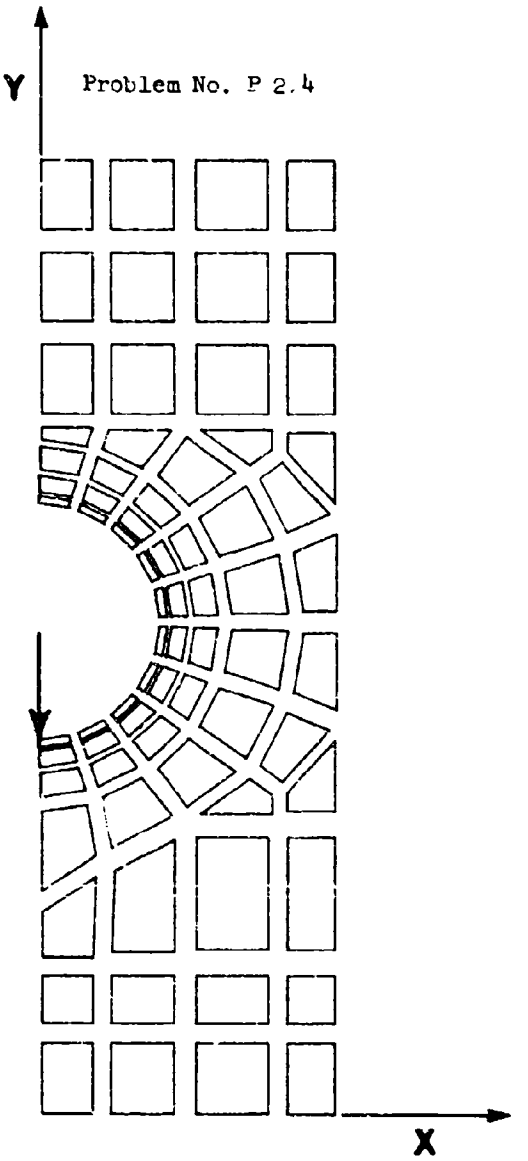

Fig. 25 Finite Element Idealization of Aluminum Joint With e = 1.6 Inches

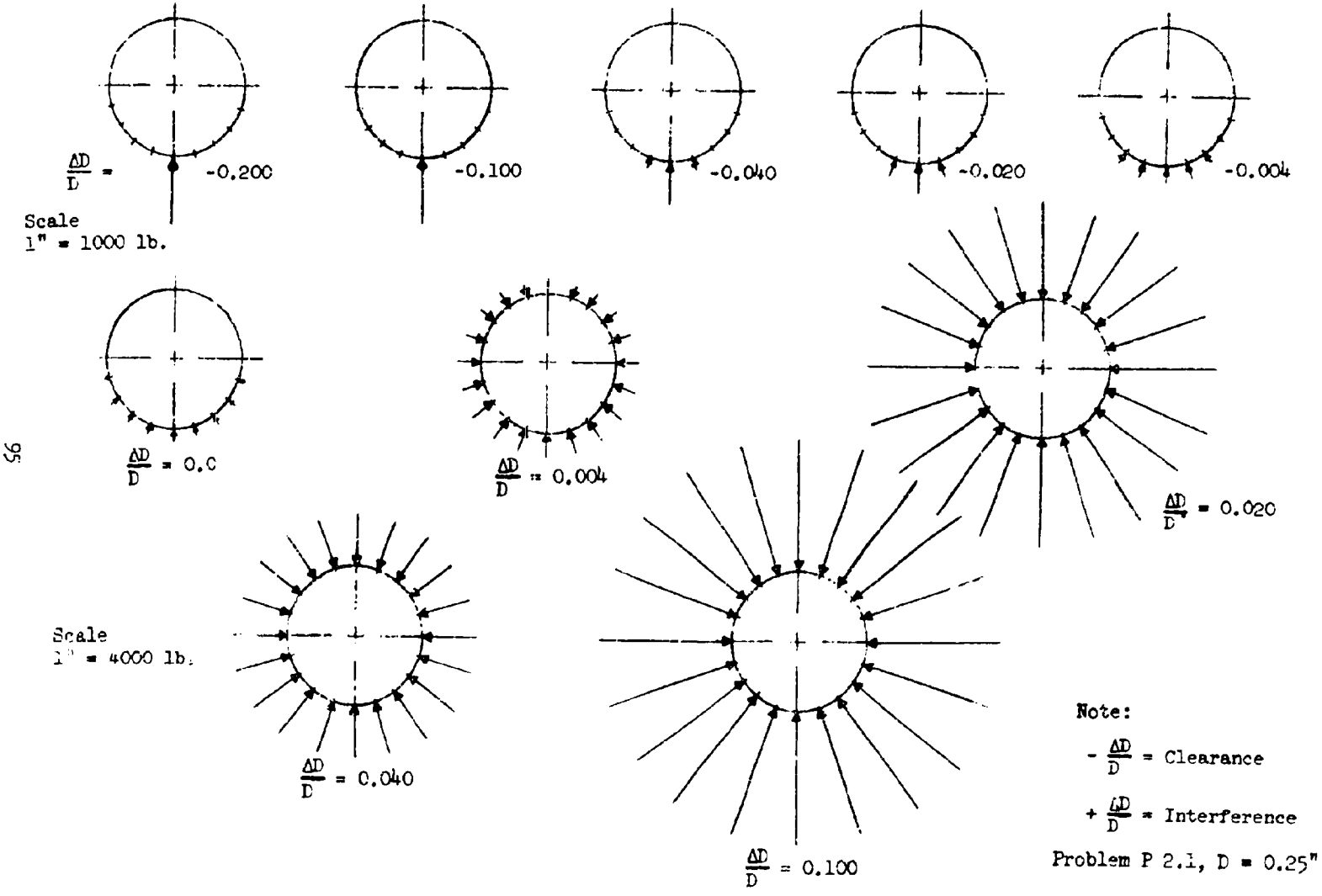

Fig. 26 Load Distribution Around Fastener at 500 lb. Applied Load

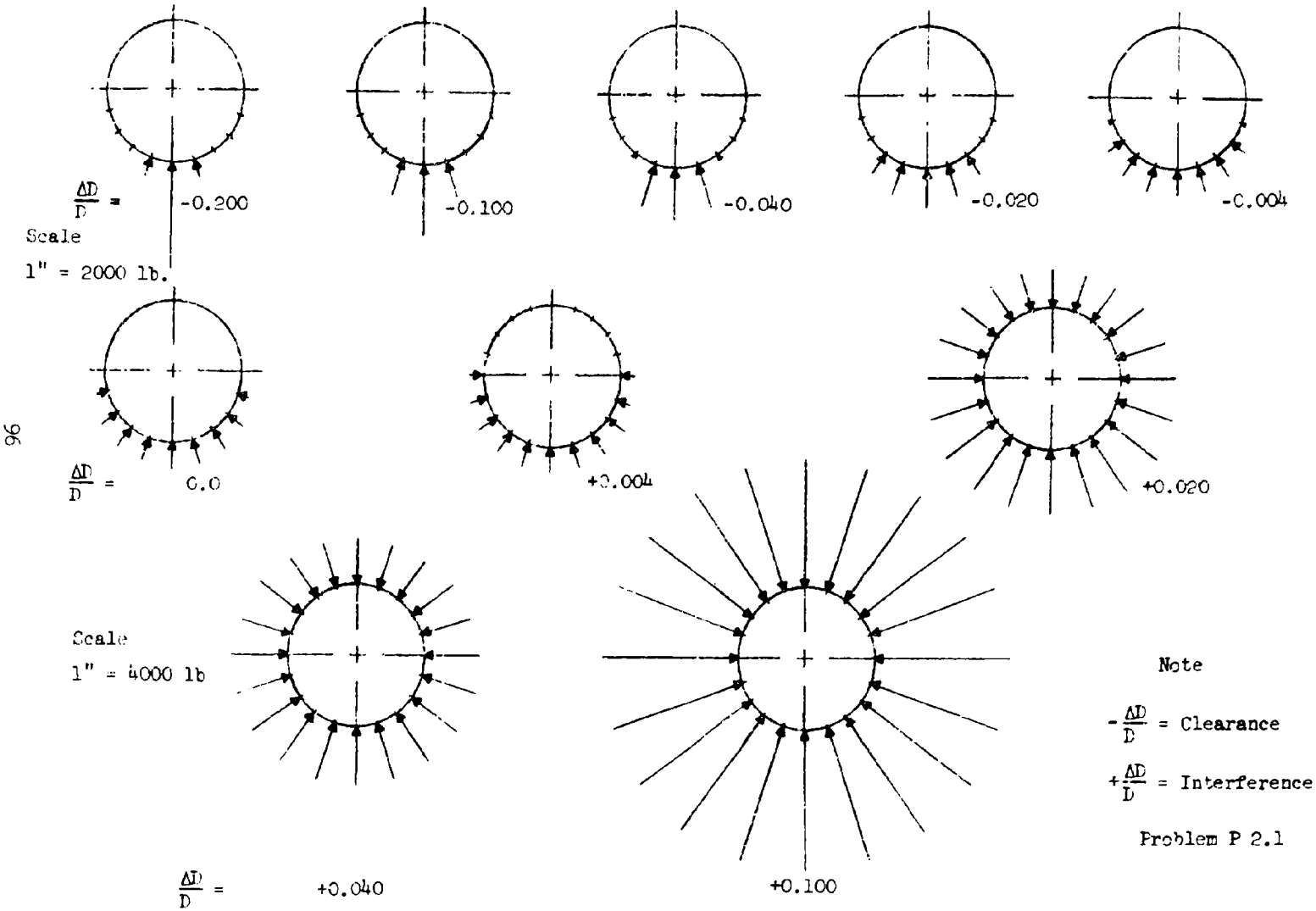

Fig. 27 Load Distribution Around Fastener at 2000 lb Applied Load

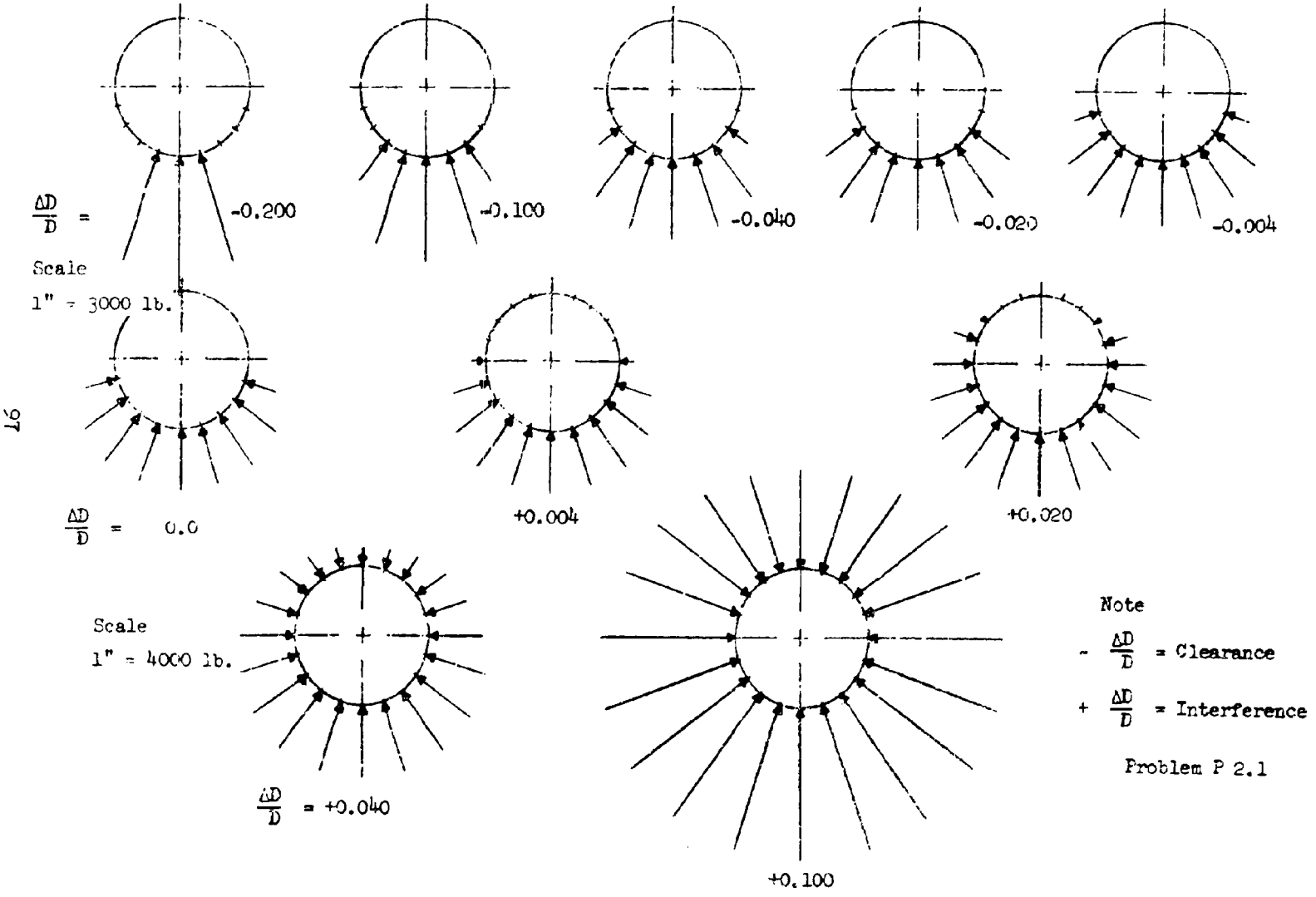

Fig. 28 Load Distribution Around Fastener at 8000 lbs. Applied Load

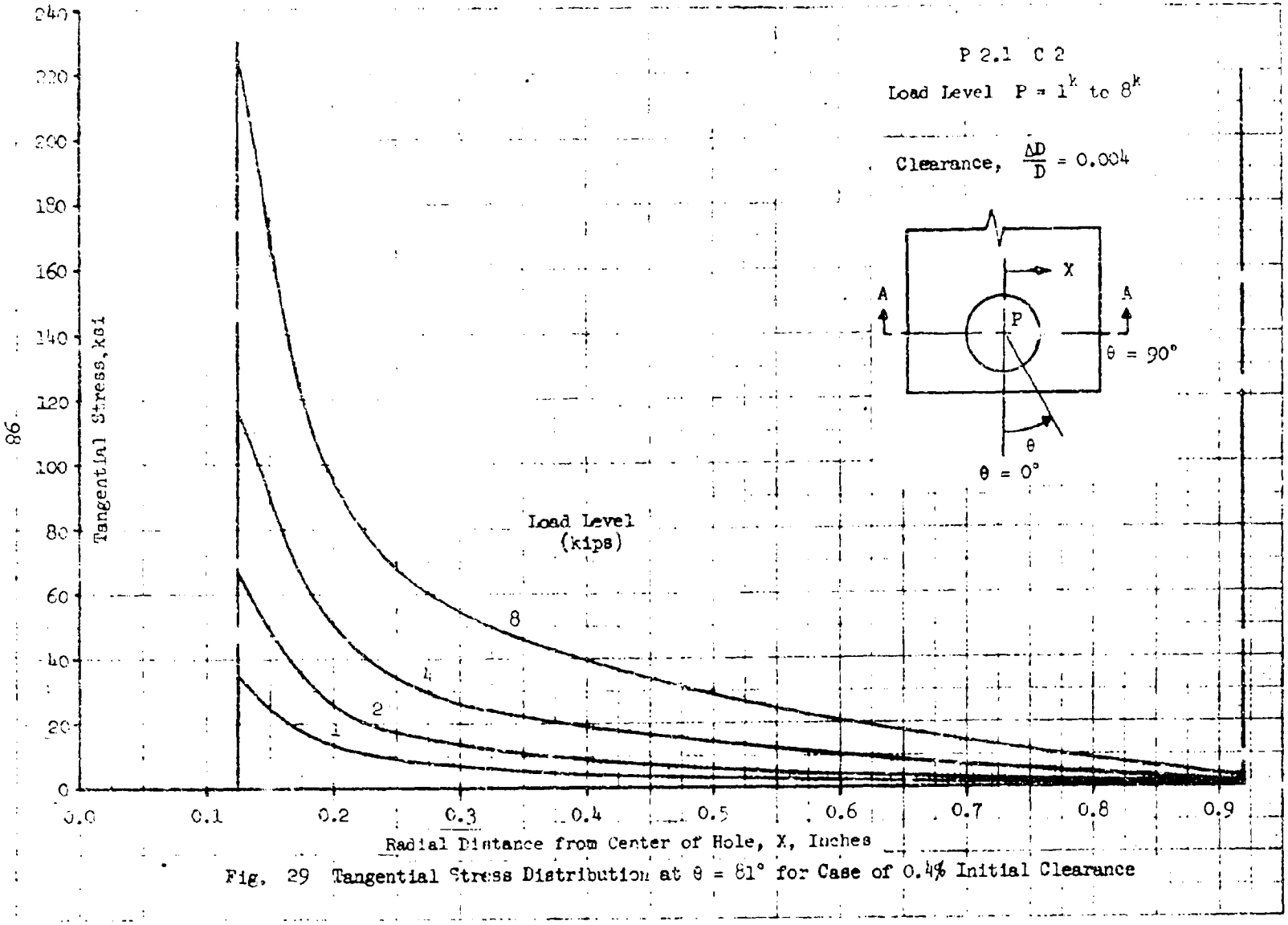

Fig. 29 Tangential Stress Distribution at θ = 81° for Case of 0.4% Initial Clearance

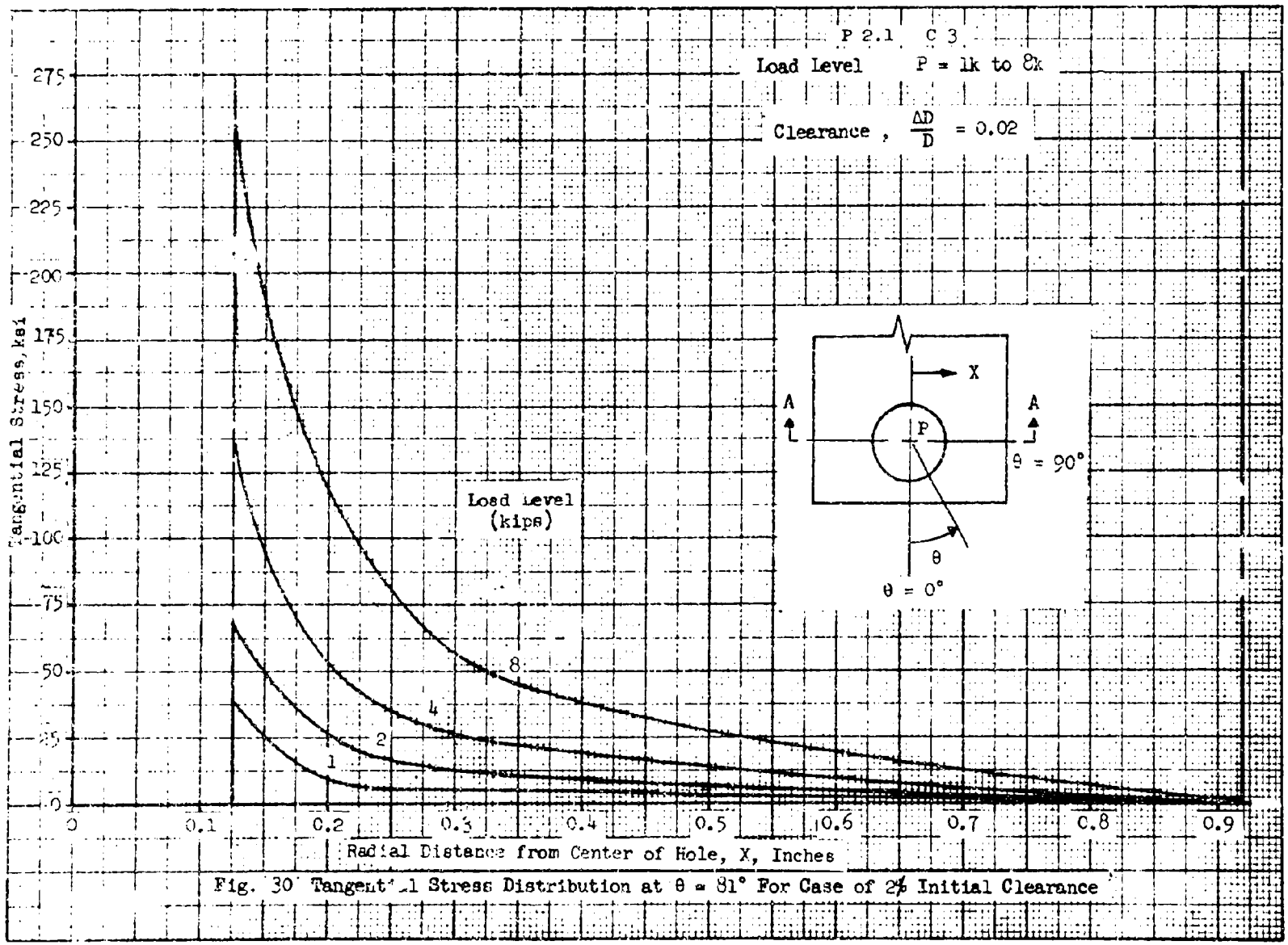

Fig. 30 Tangential Stress Distribution at θ = 81° For Case of 2% Initial Clearance

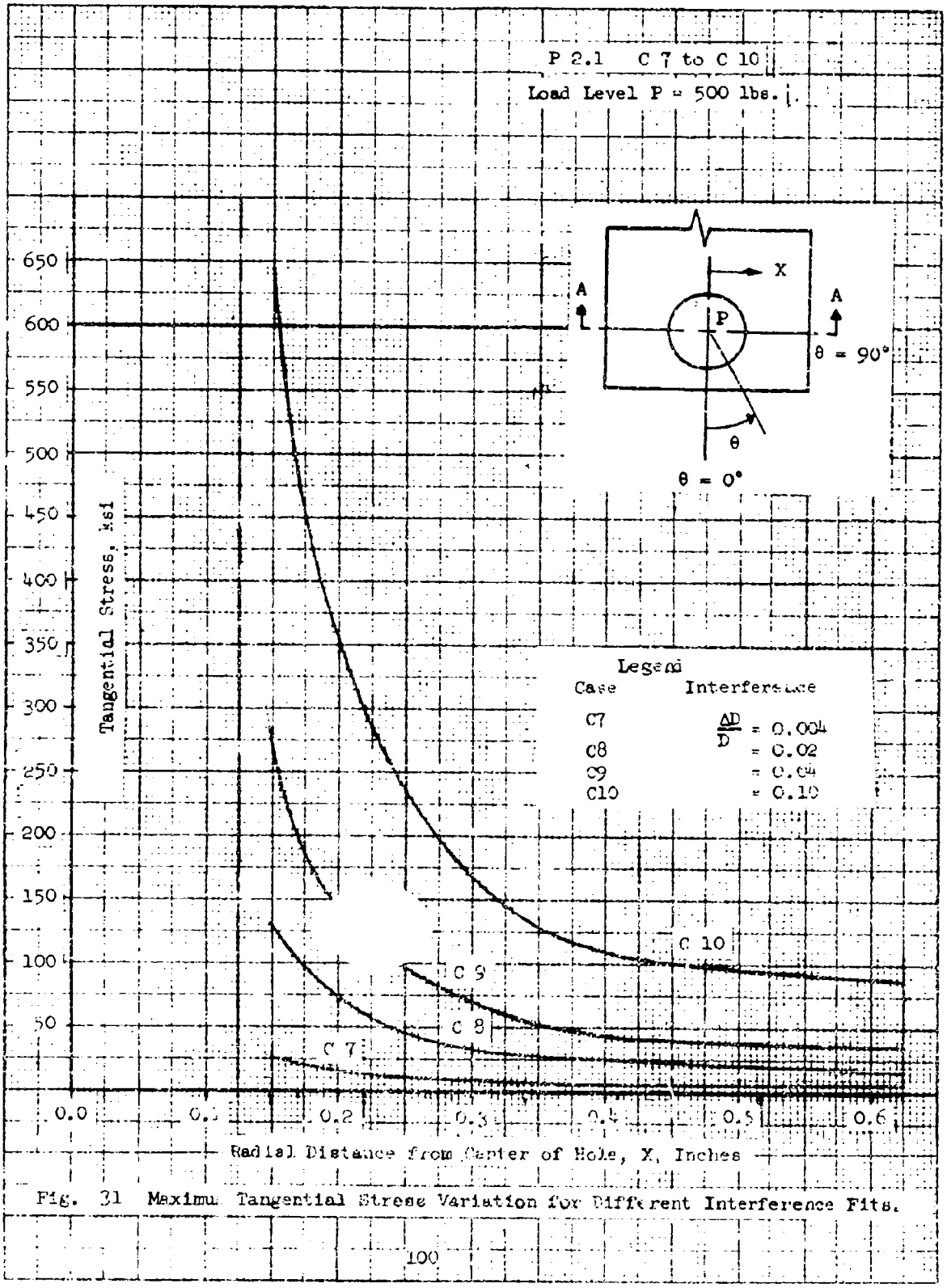

Fig. 31 Maximum Tangential Stress Variation for Different Interference Fits.

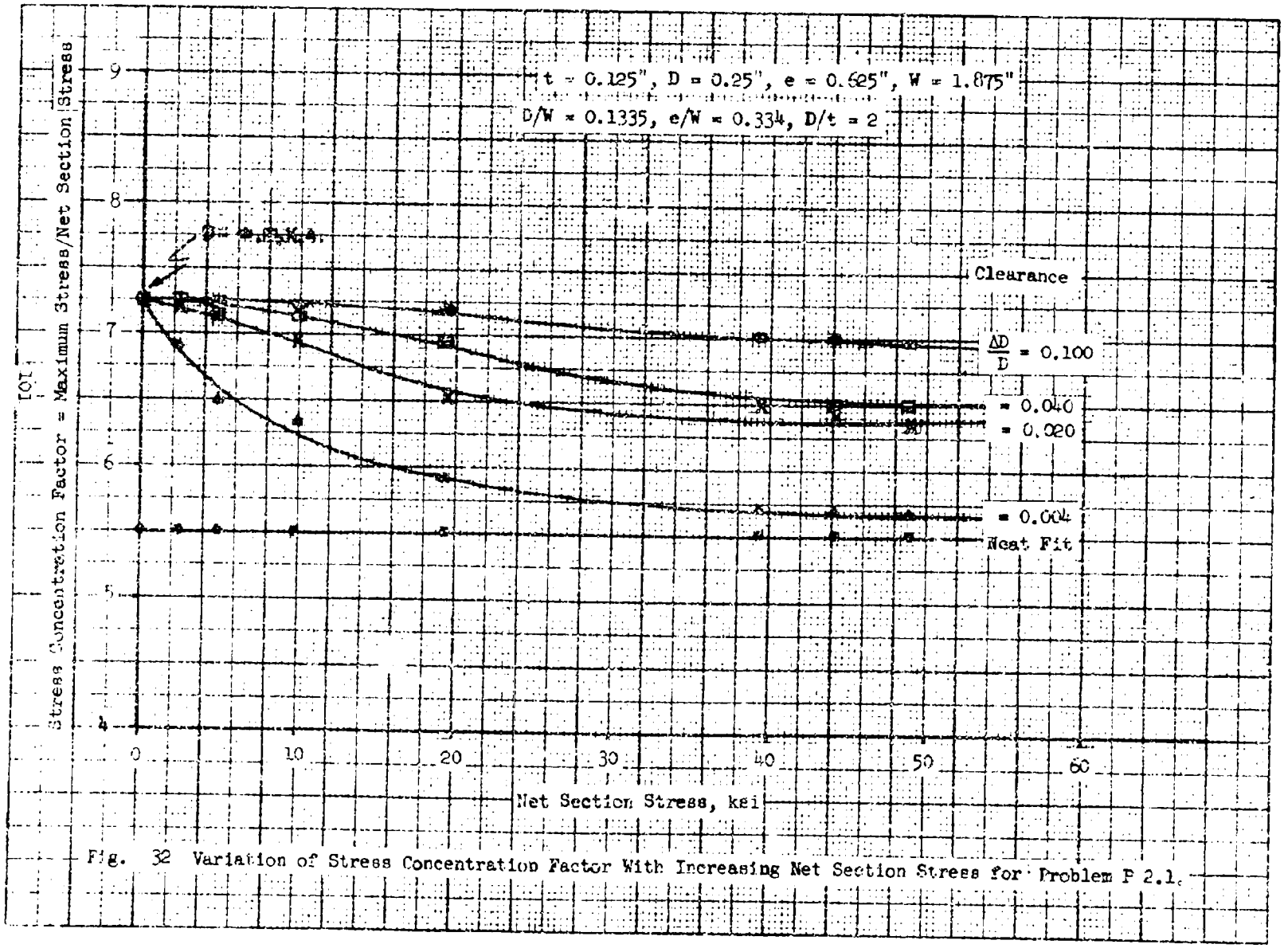

Fig. 32 Variation of Stress Concentration Factor With Increasing Net Section Stress for Problem P 2.1.

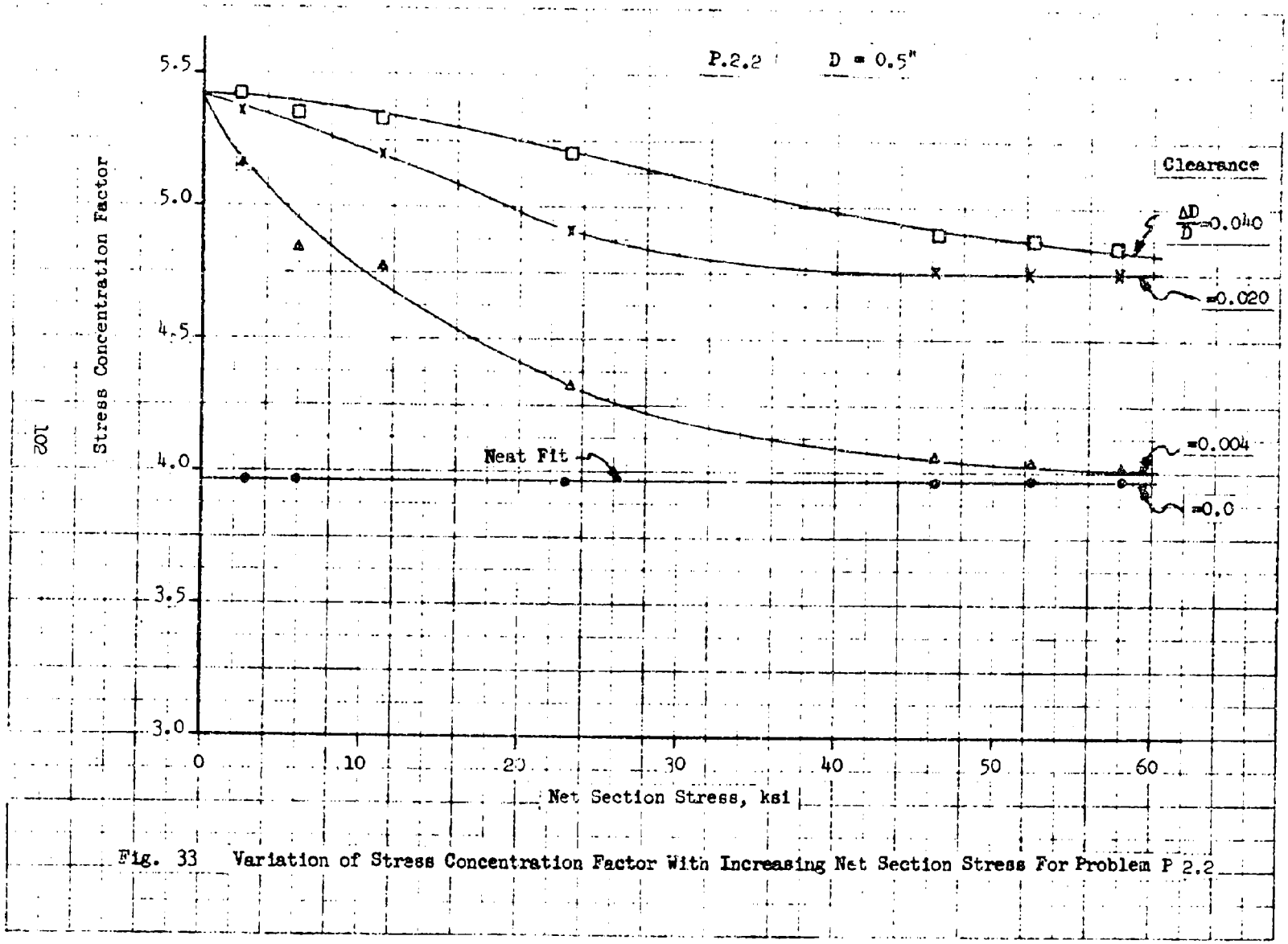

Fig. 33 Variation of Stress Concentration Factor With Increasing Net Section Stress For Problem P 2.2

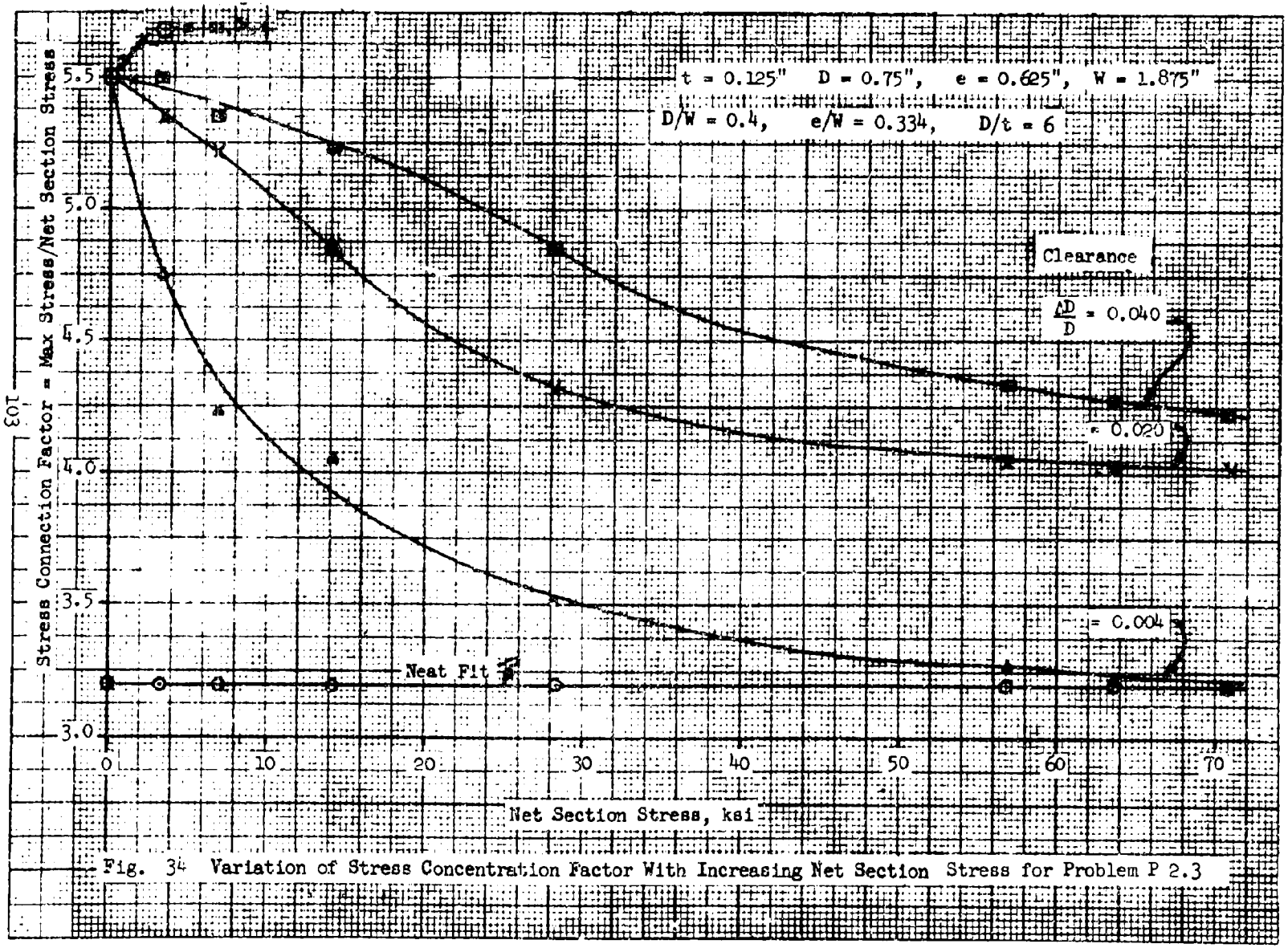

Fig. 34 Variation of Stress Concentration Factor With Increasing Net Section Stress for Problem P 2.3

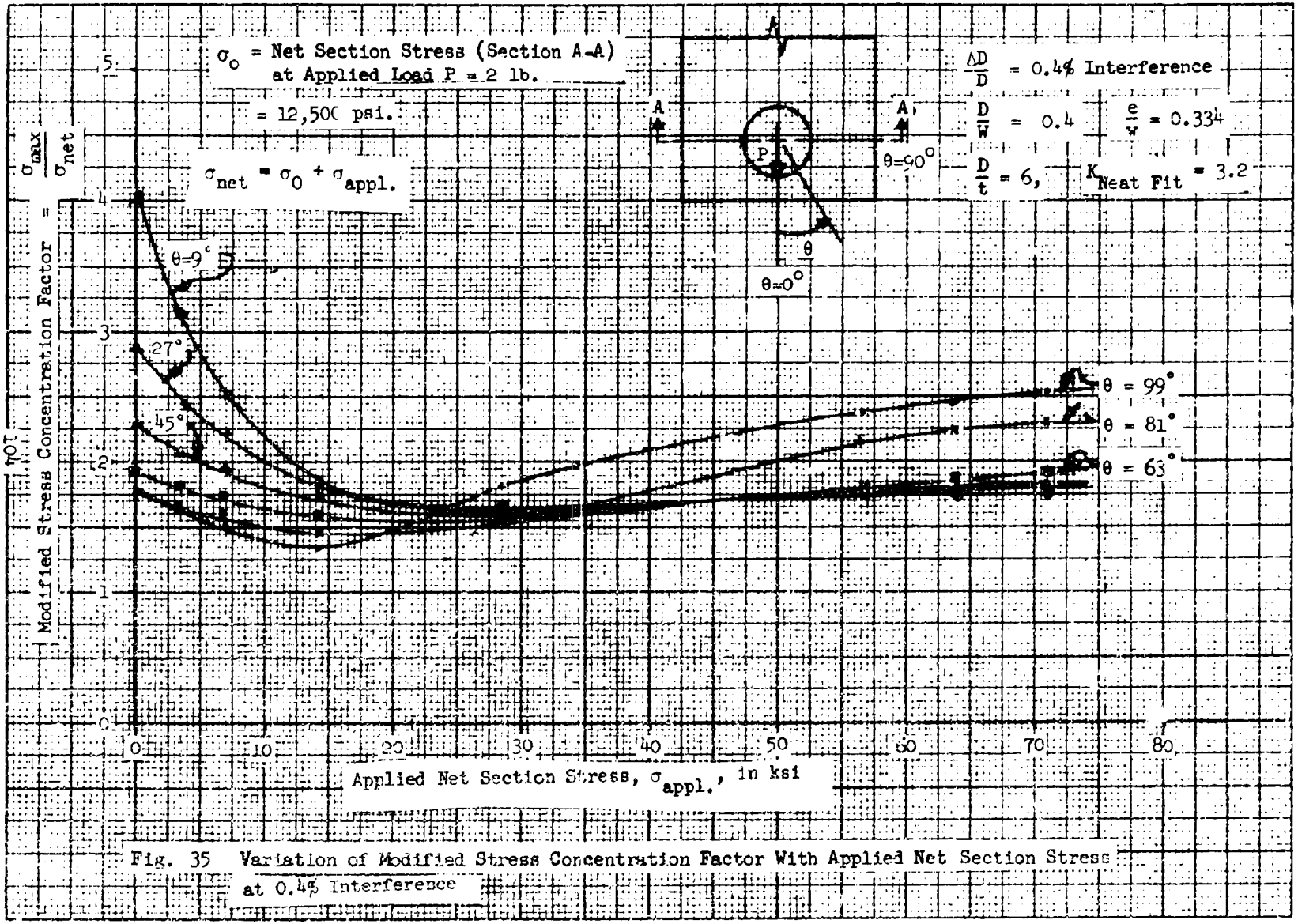

Fig. 35 Variation of Modified Stress Concentration Factor With Applied Net Section Stress at 0.4% Interference

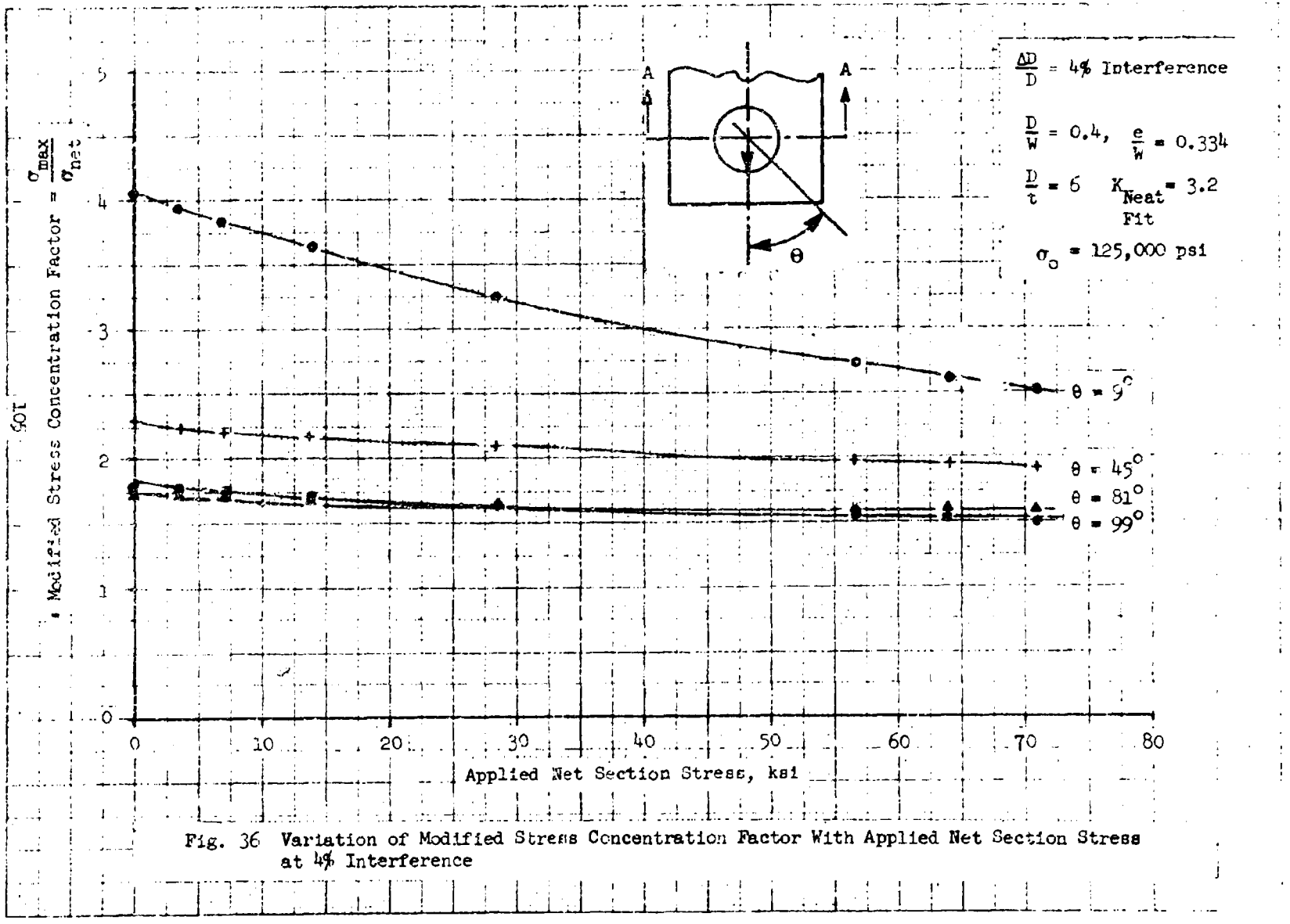

Fig. 36 Variation of Modified Stress Concentration Factor With Applied Net Section Stress at 4% Interference

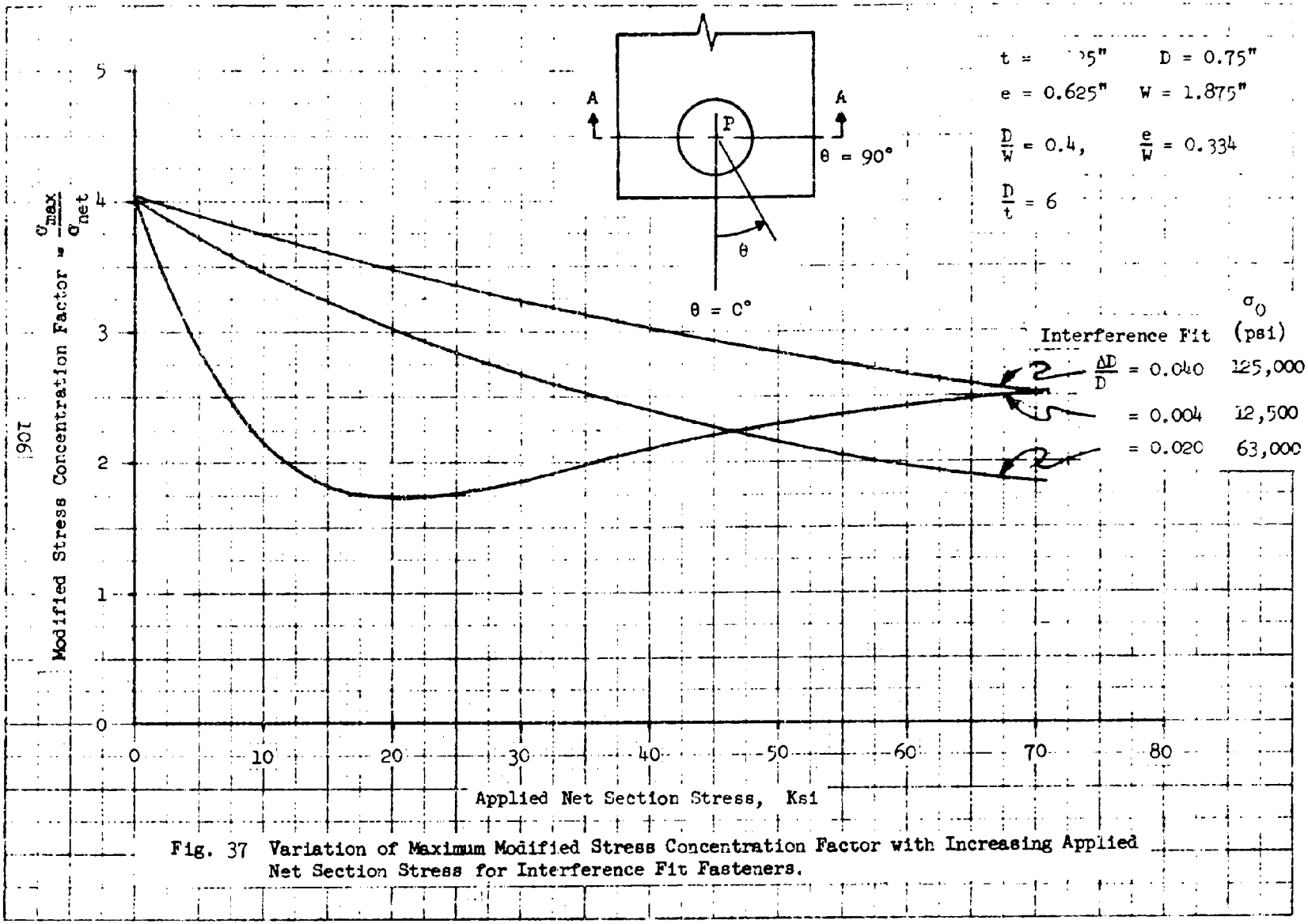

Fig. 37 Variation of Maximum Modified Stress Concentration Factor with Increasing Applied Net Section Stress for Interference Fit Fasteners.

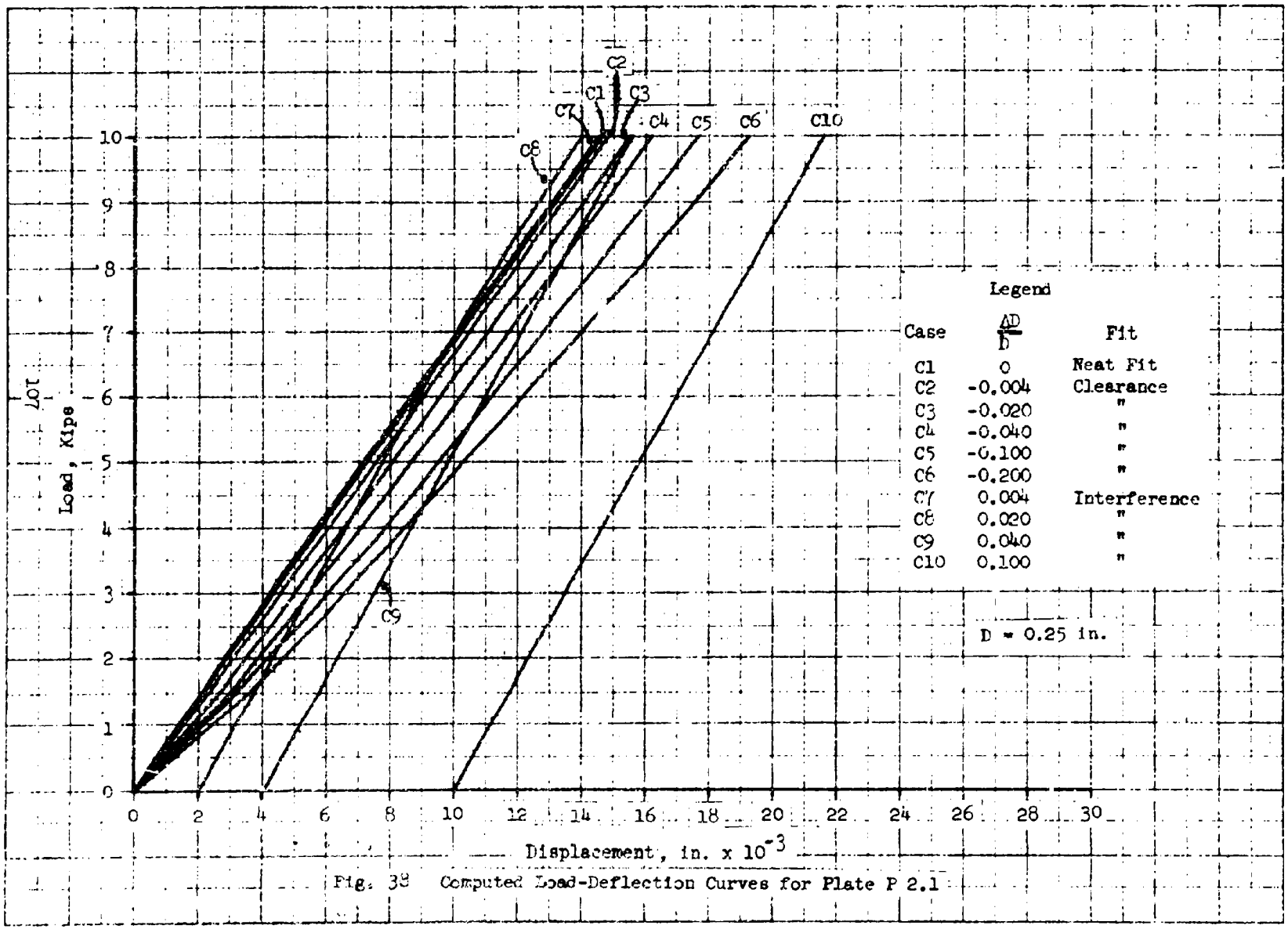

Fig. 38 Computed Load-Deflection Curves for Plate P 2.1

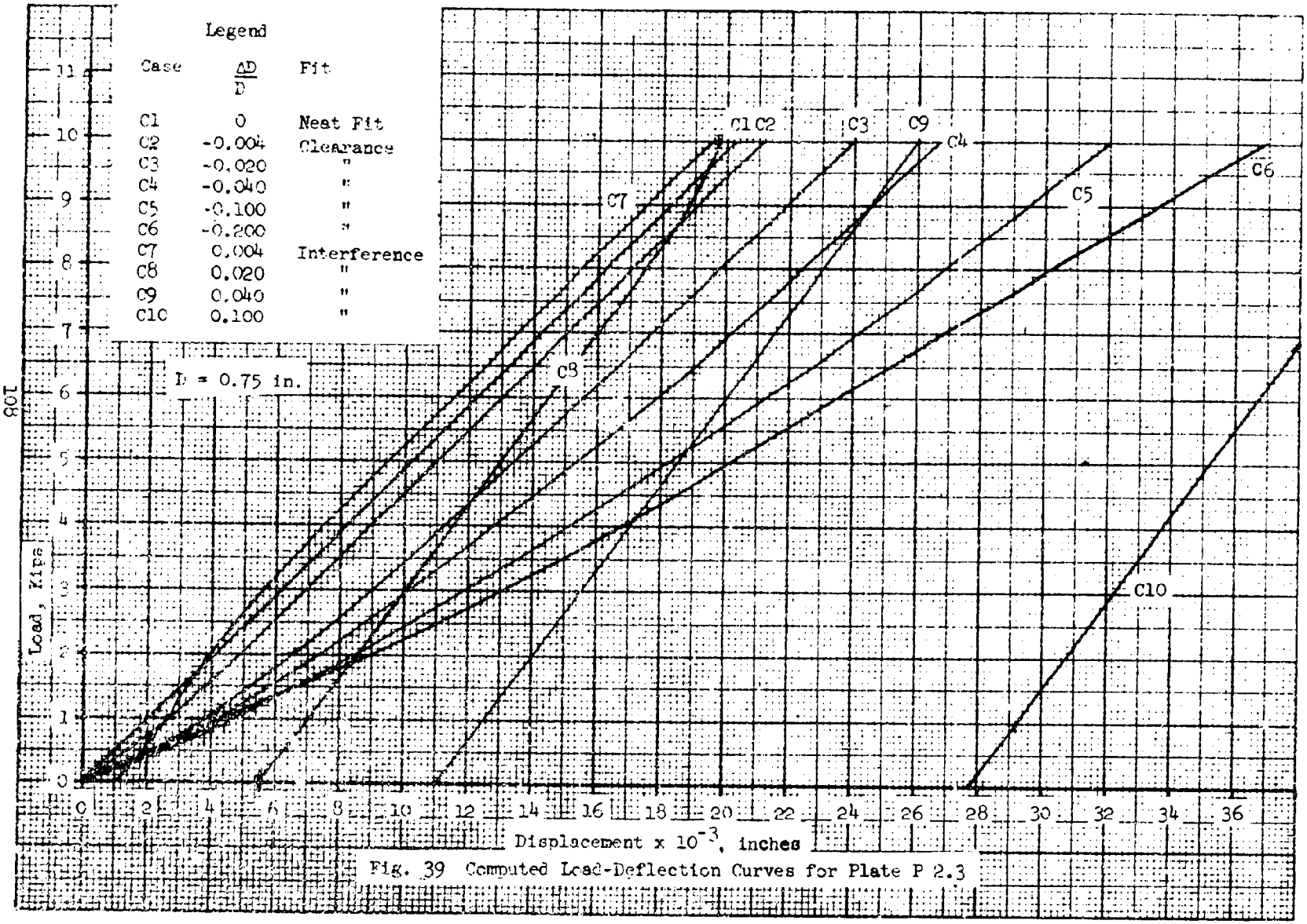

Fig. 39 Computed Load-Deflection Curves for Plate P 2.3

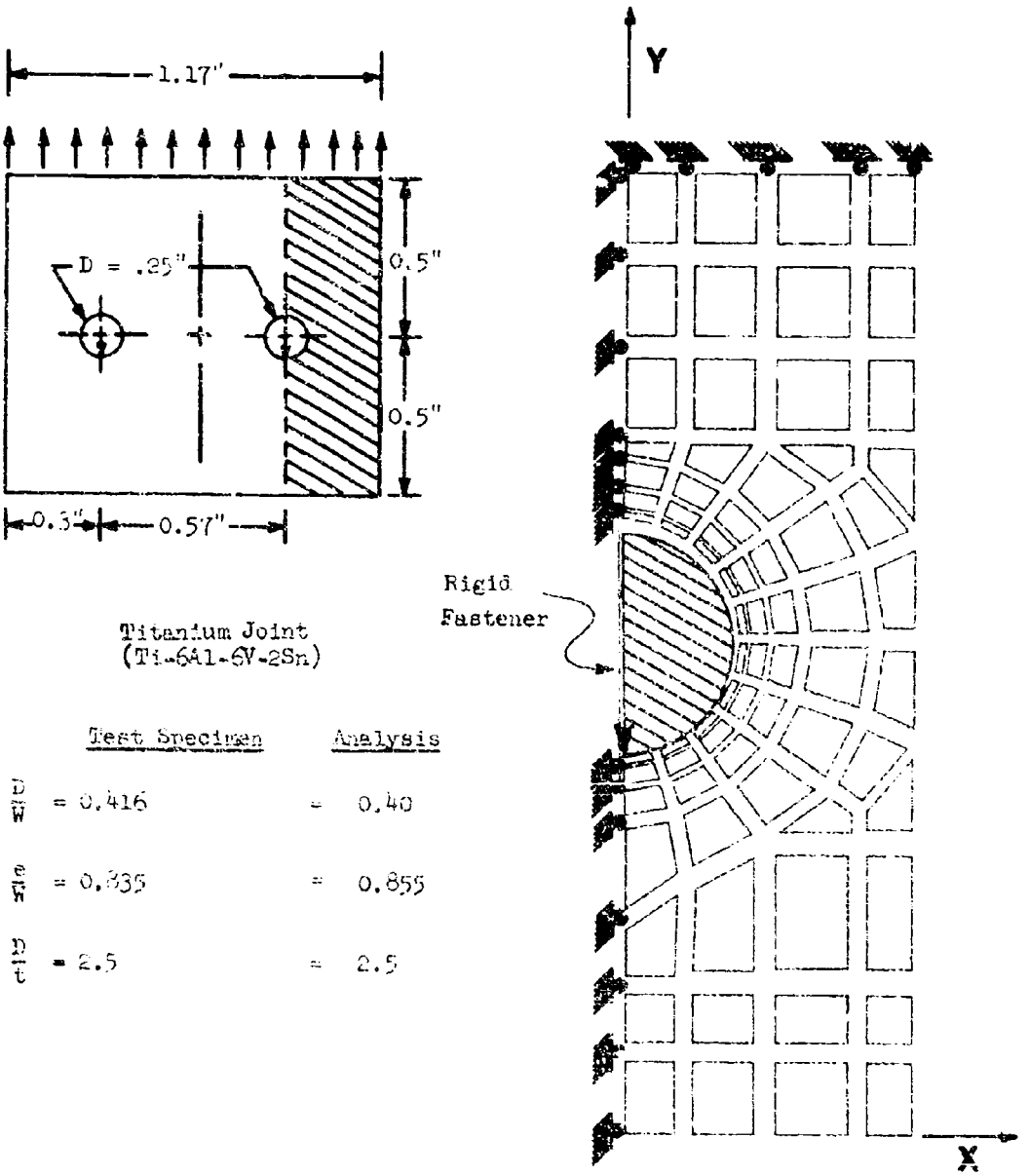

Titanium Joint
(Ti-6Al-6V-2Sn)

	Test Specimen	Analysis
$\frac{D}{w}$	= 0.416	= 0.40
$\frac{w}{e}$	= 0.835	= 0.855
$\frac{D}{t}$	= 2.5	= 2.5

Fig. 40 Dimensions of Tested Titanium Joint and Idealization Used in the Analysis

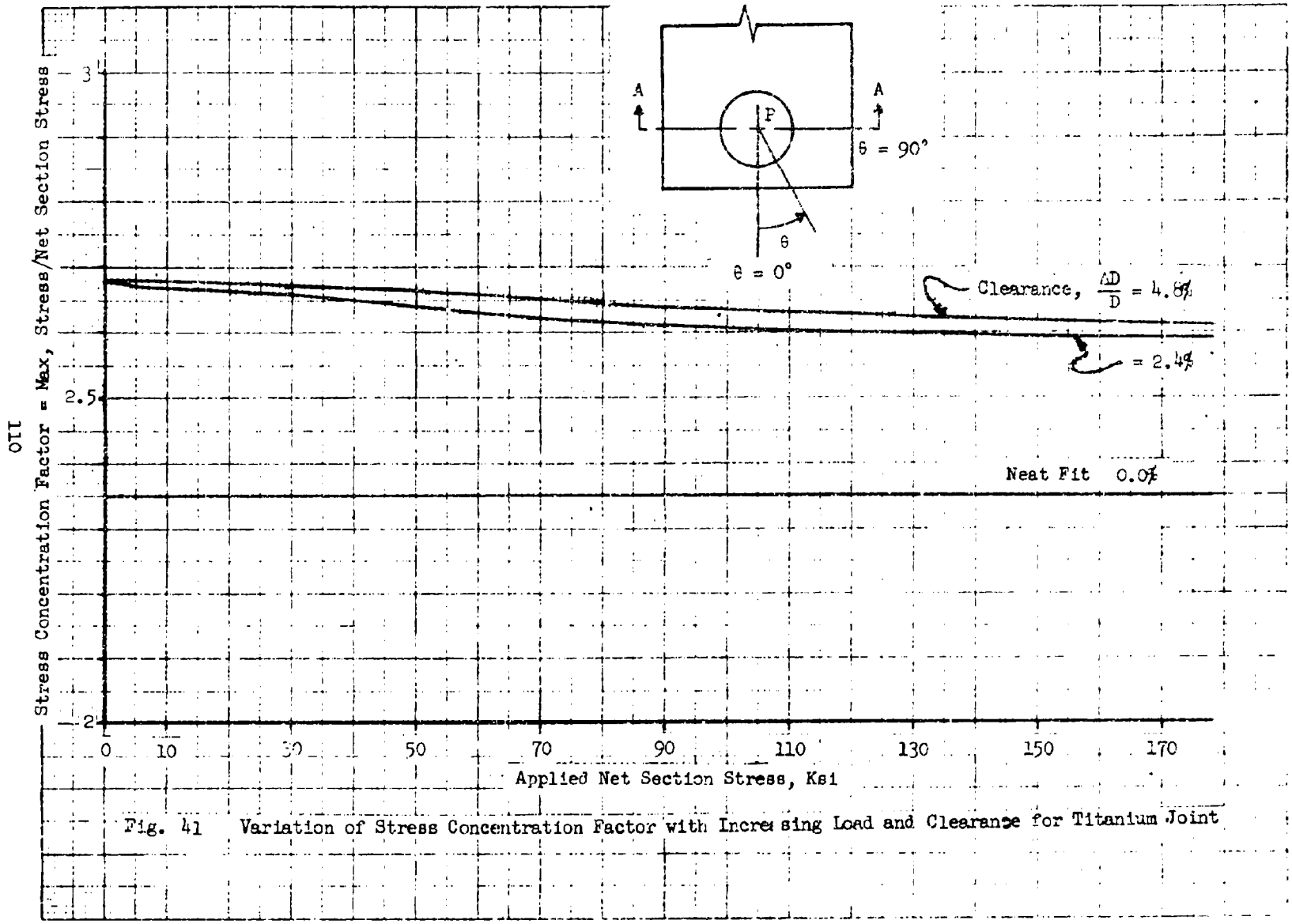

Fig. 41 Variation of Stress Concentration Factor with Increasing Load and Clearance for Titanium Joint

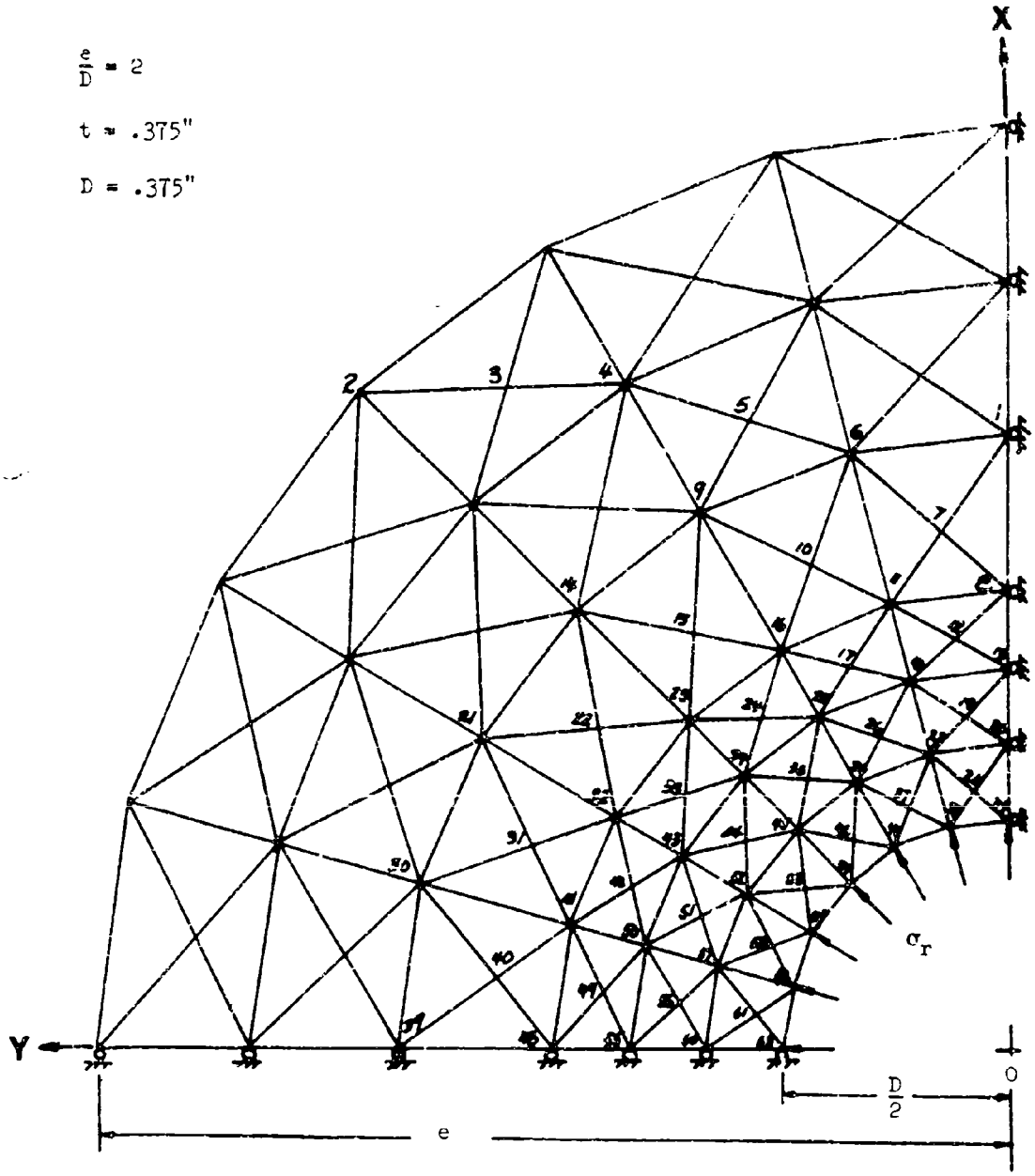

Fig. 42 Mathematical Model Used in the Analysis of Axi-symmetrically Loaded Plate.

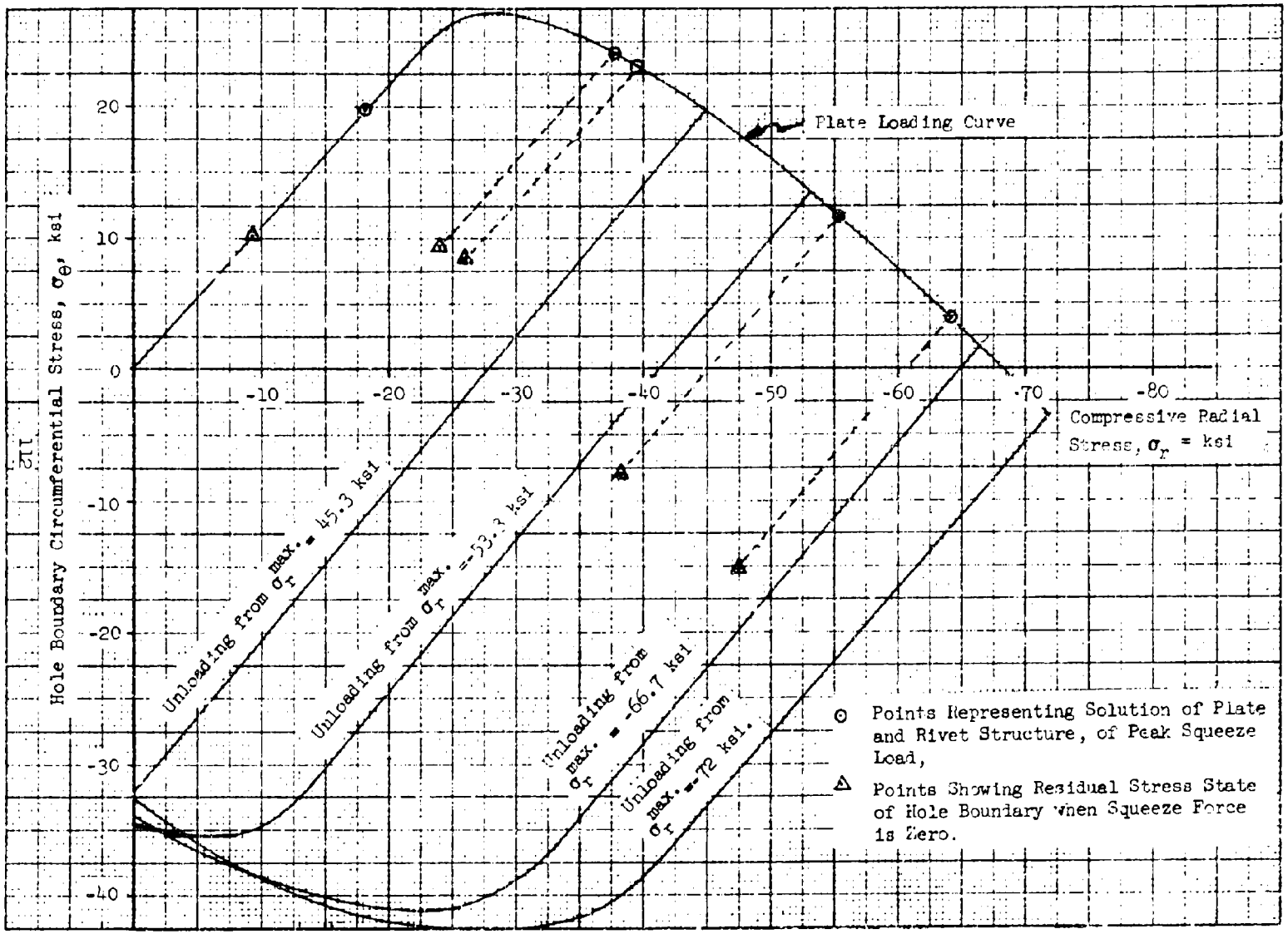

Fig. 43 Circumferential Stress vs Compressive Radial Stress at the Hole Boundary (2024-T351 Al. Plate)

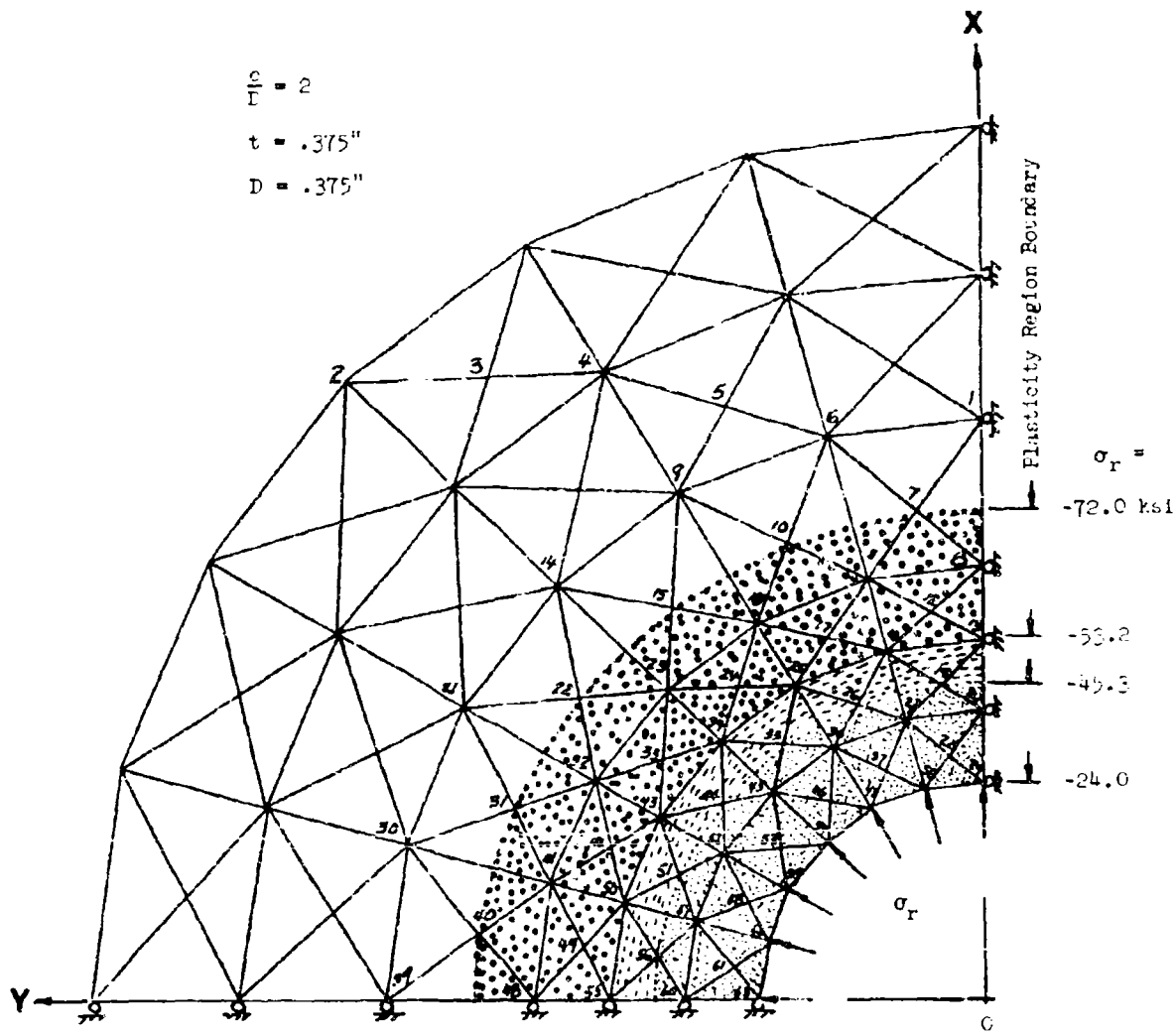

Fig. 44 Growth of the Plasticity Region in a 2024-T351 Aluminum Plate with Increasing Radial Stress

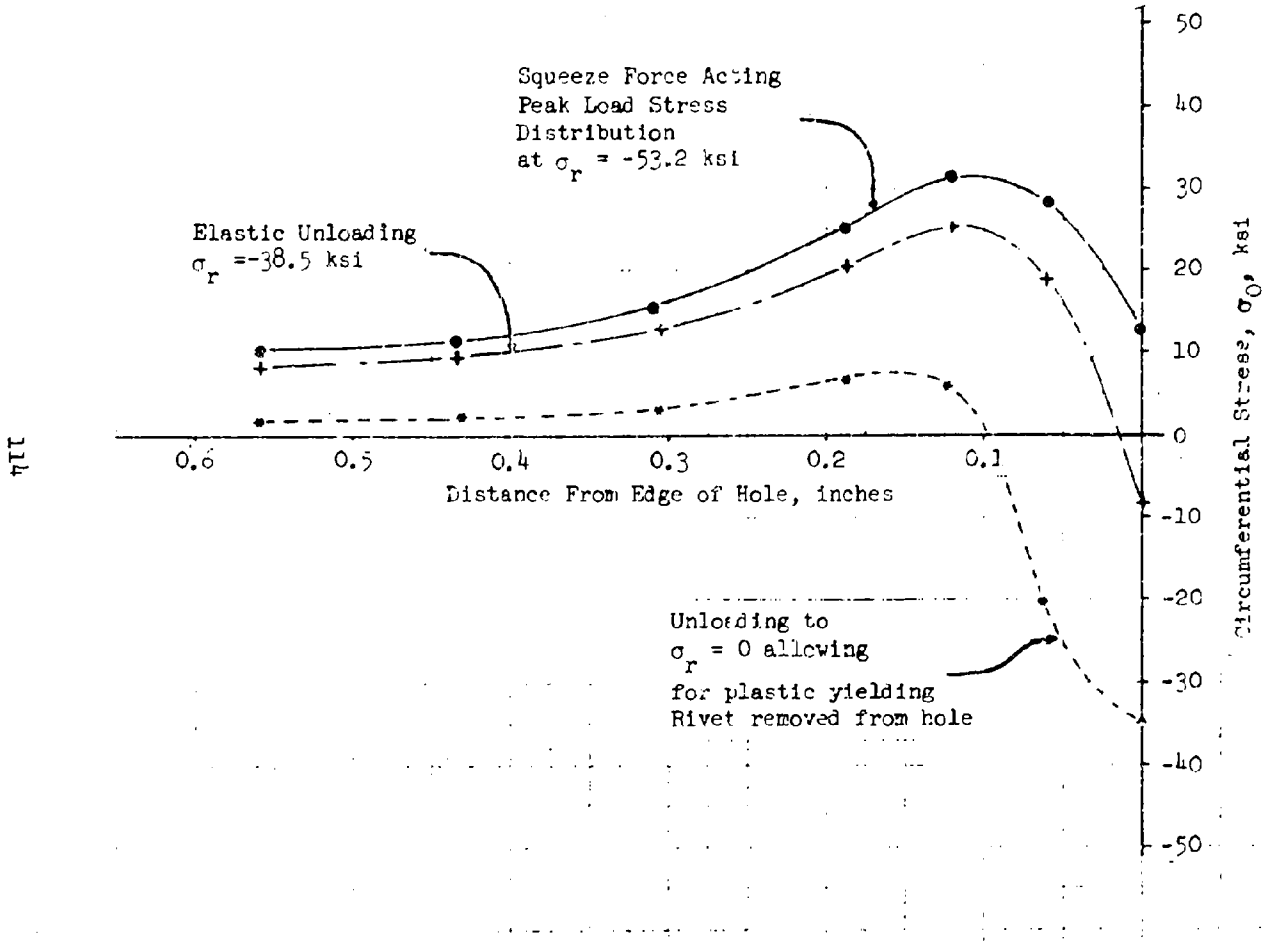

Fig. 45 Circumferential Stress Distribution, σ_θ, Acr[illegible] Aluminum P[illegible]ate For Two Types of Unloading

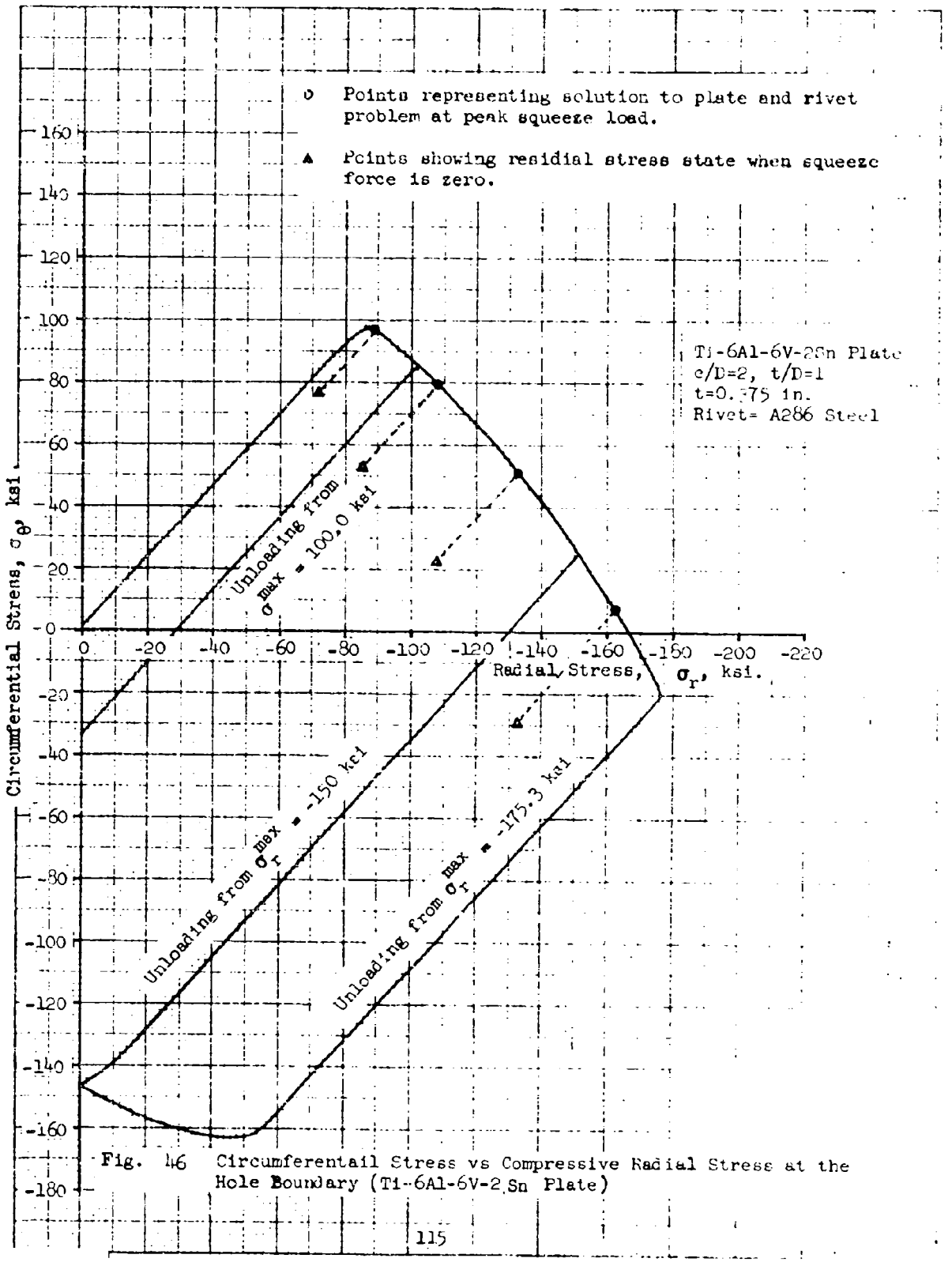

Fig. 46 Circumferentail Stress vs Compressive Radial Stress at the Hole Boundary (Ti-6Al-6V-2Sn Plate)

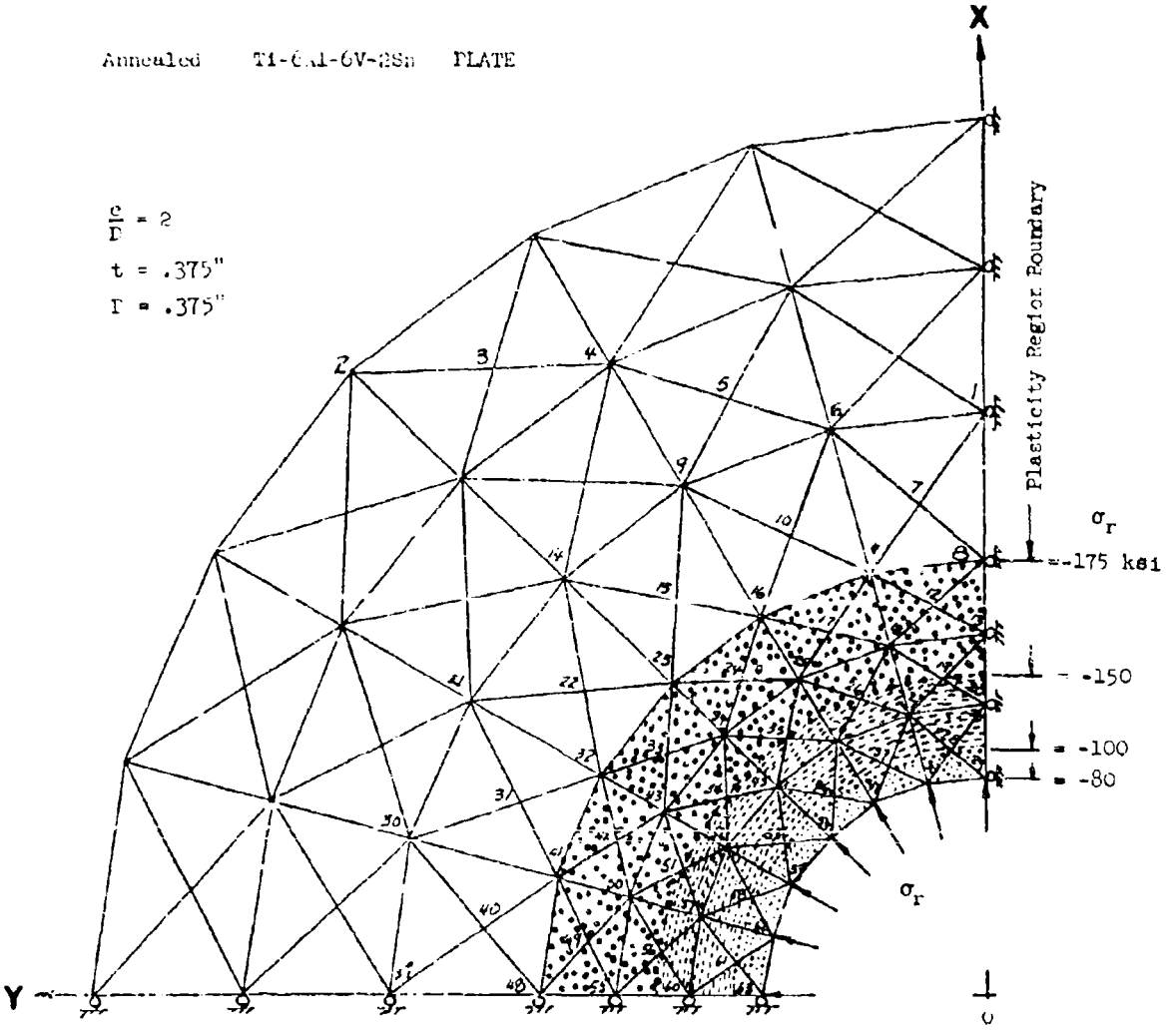

Fig. 47 Growth of the Plasticity Region in the Annealed Titanium Plate with Increasing Radial Stress

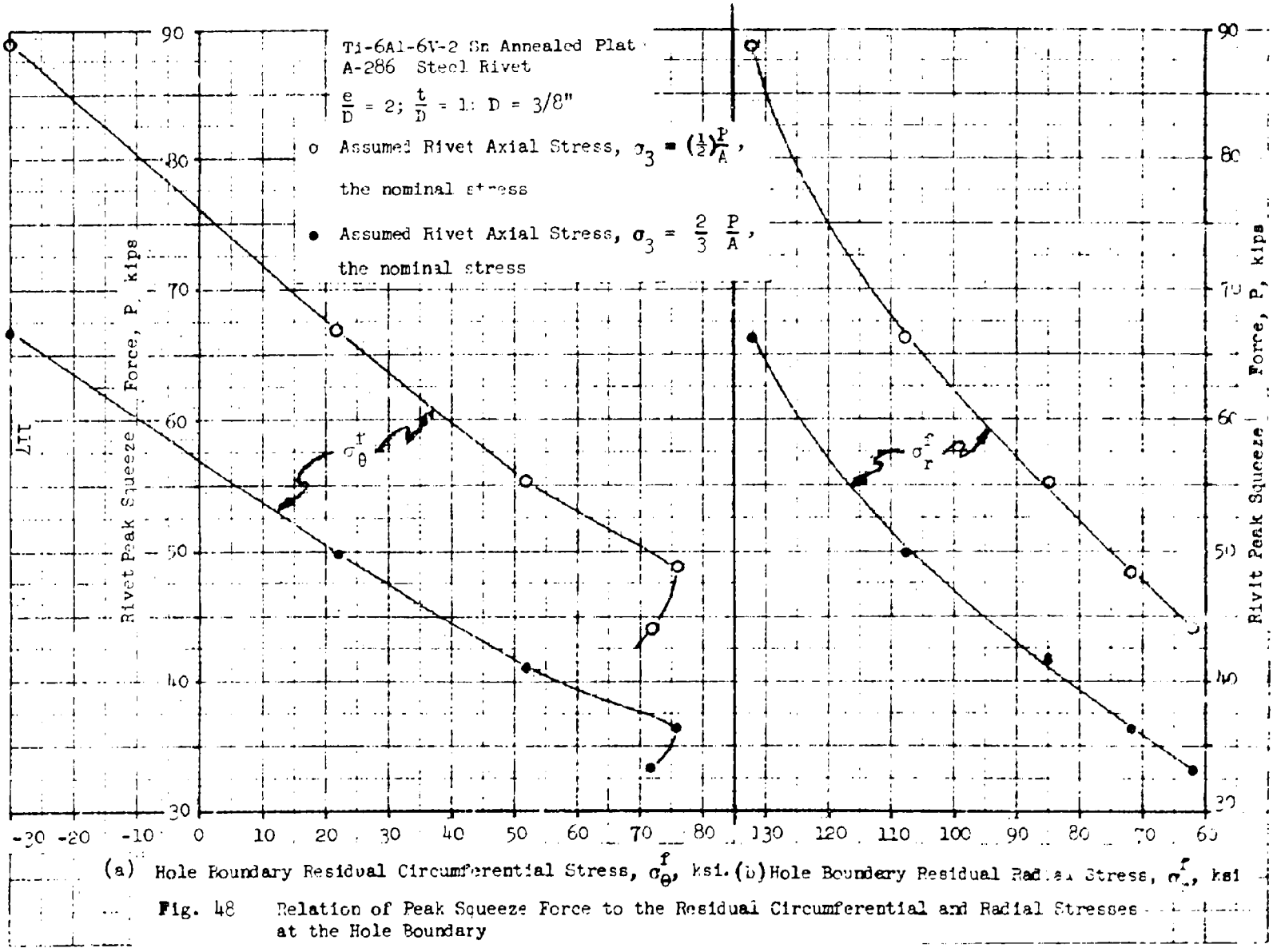

Fig. 48 Relation of Peak Squeeze Force to the Residual Circumferential and Radial Stresses at the Hole Boundary

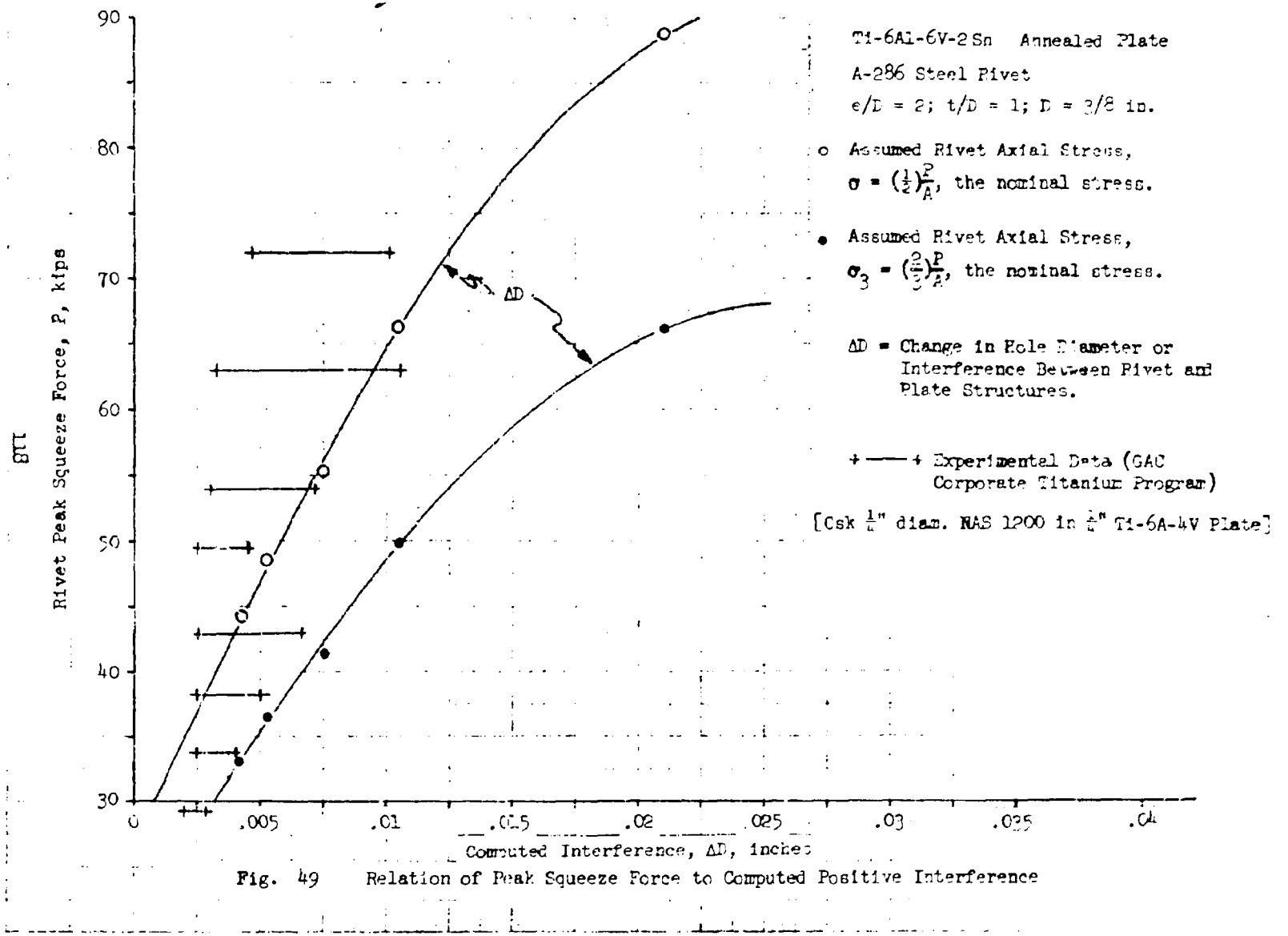

Fig. 49 Relation of Peak Squeeze Force to Computed Positive Interference

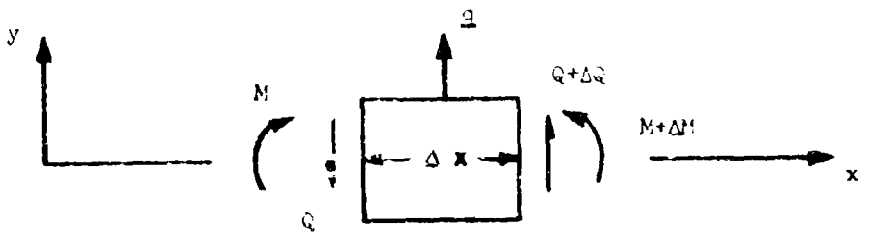

(a) Forces and Moments

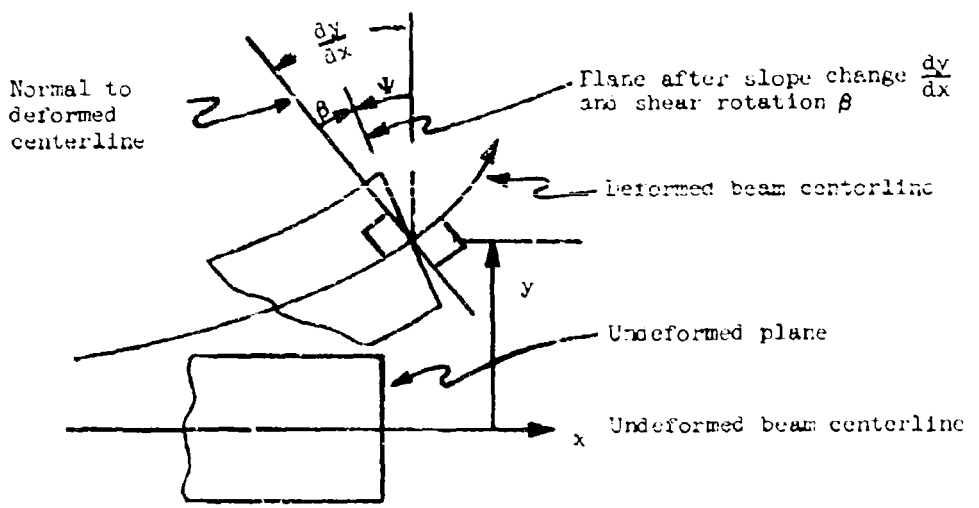

(b) Kinematics of Deformation

Fig. 50 Equilibrium and Deformation of a Typical Beam Element

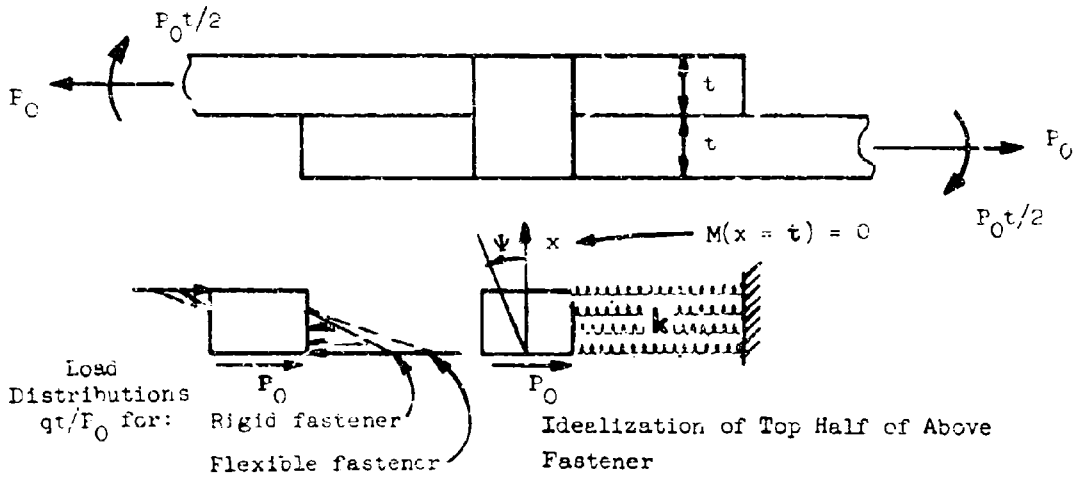

(a) Fastener With Negligible Head Stiffness

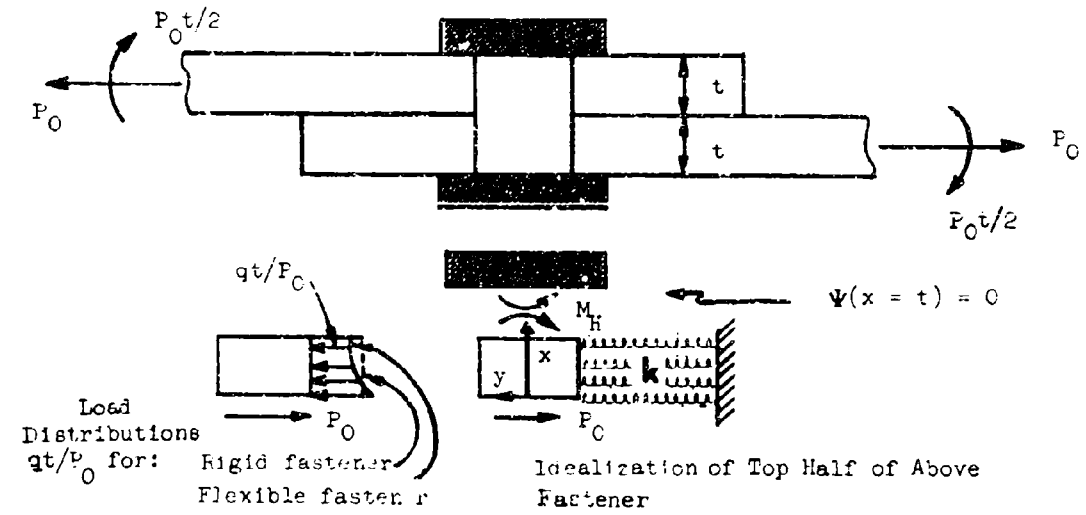

(b) Clamped Head Condition

Figure 51 Fastener in Single Shear with Idealizations and Typical Solutions

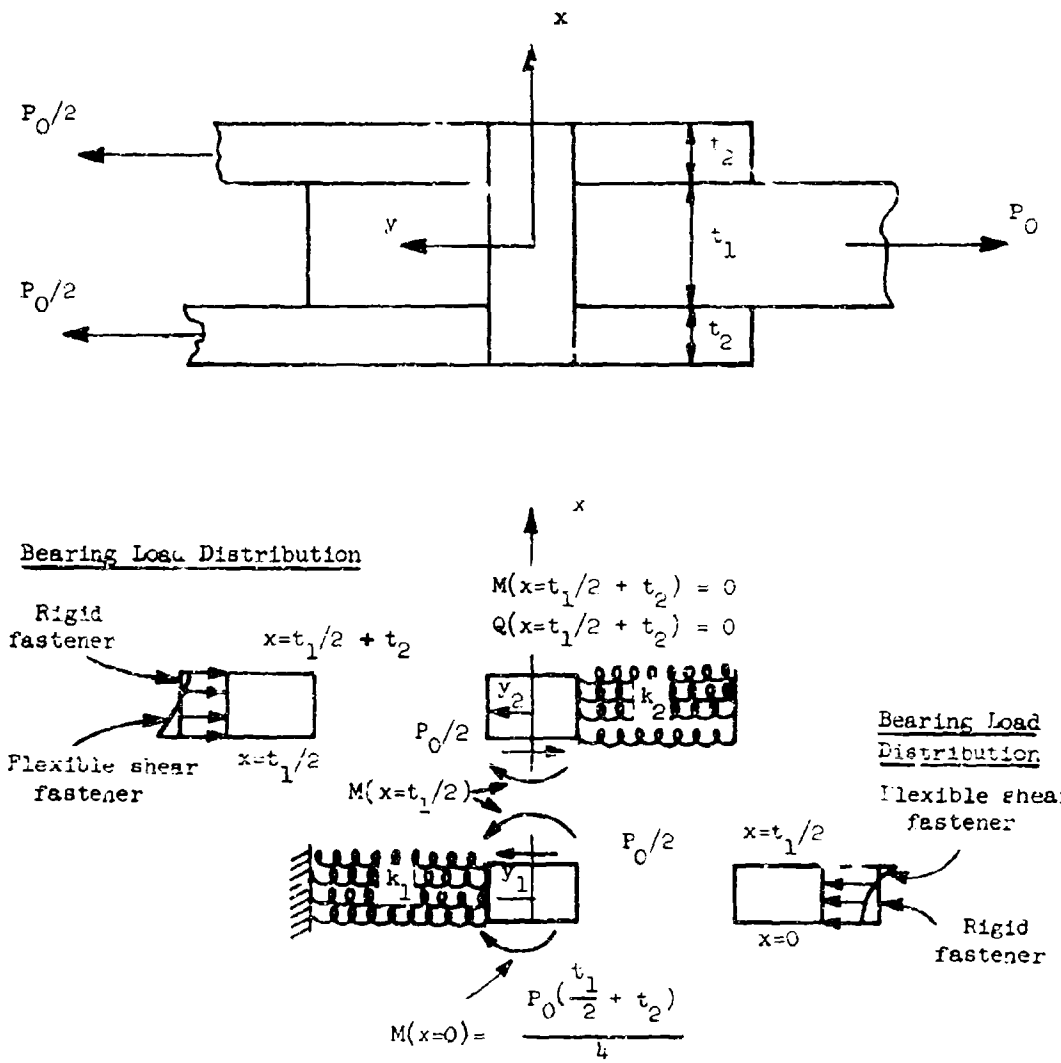

Figure 52 Fastener in Symmetrical Double Shear with Idealization and Typical Solution.

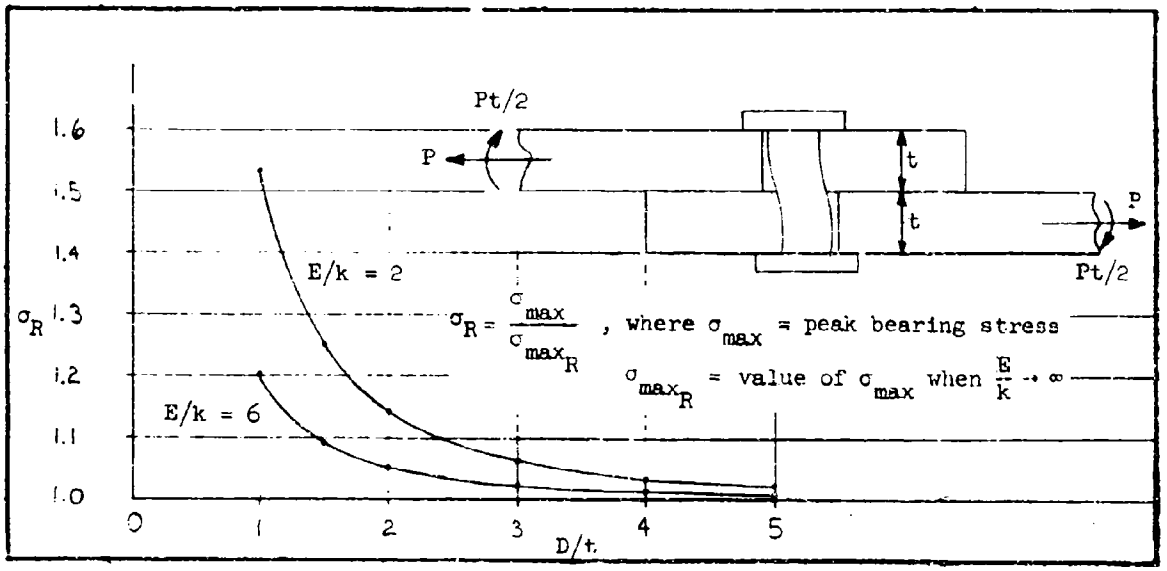

(a) Single Shear, Clamped Fastener Head

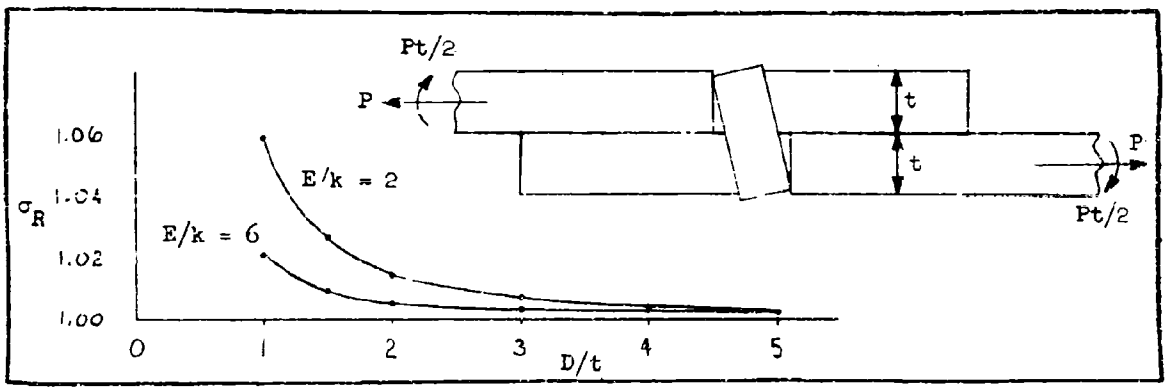

(b) Single Shear, Free Fastener Head.

Fig. 53 Effect of Fastener Stiffness on Peak Bearing Stress

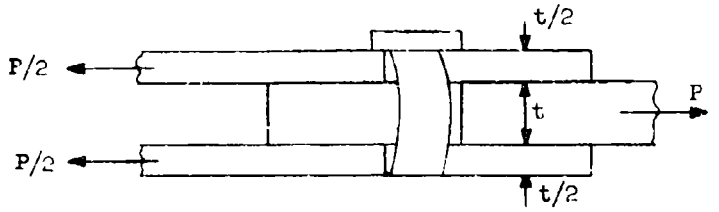

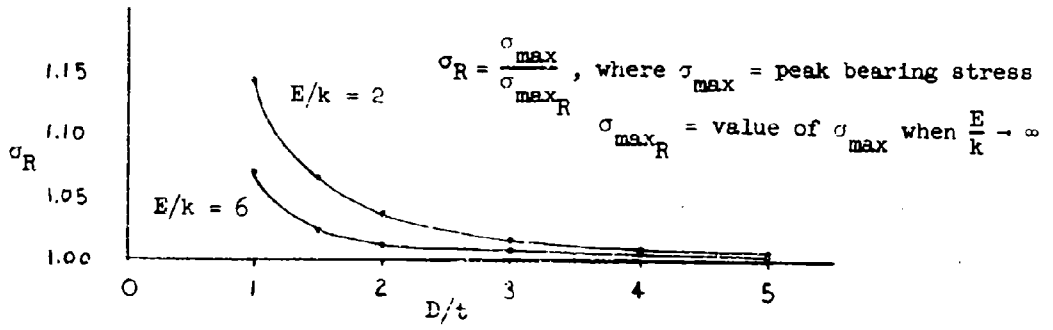

Fig. 54 Effect of Fastener Stiffness on Peak Bearing Stress
(Double Shear Case With Arbitrary Fastener Head End Conditions)

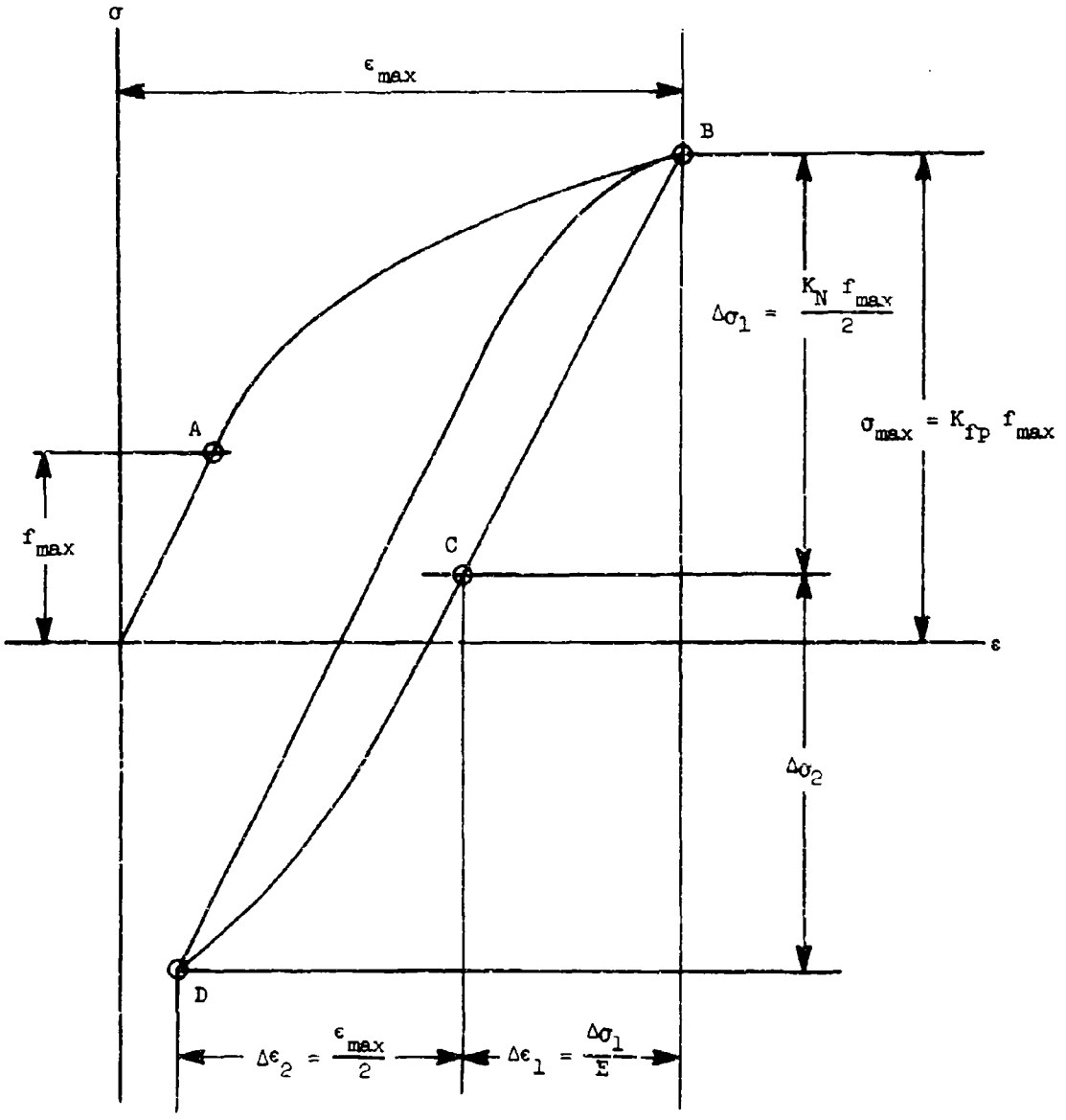

Fig 55 Stress-Strain Cycle at Edge of Notch

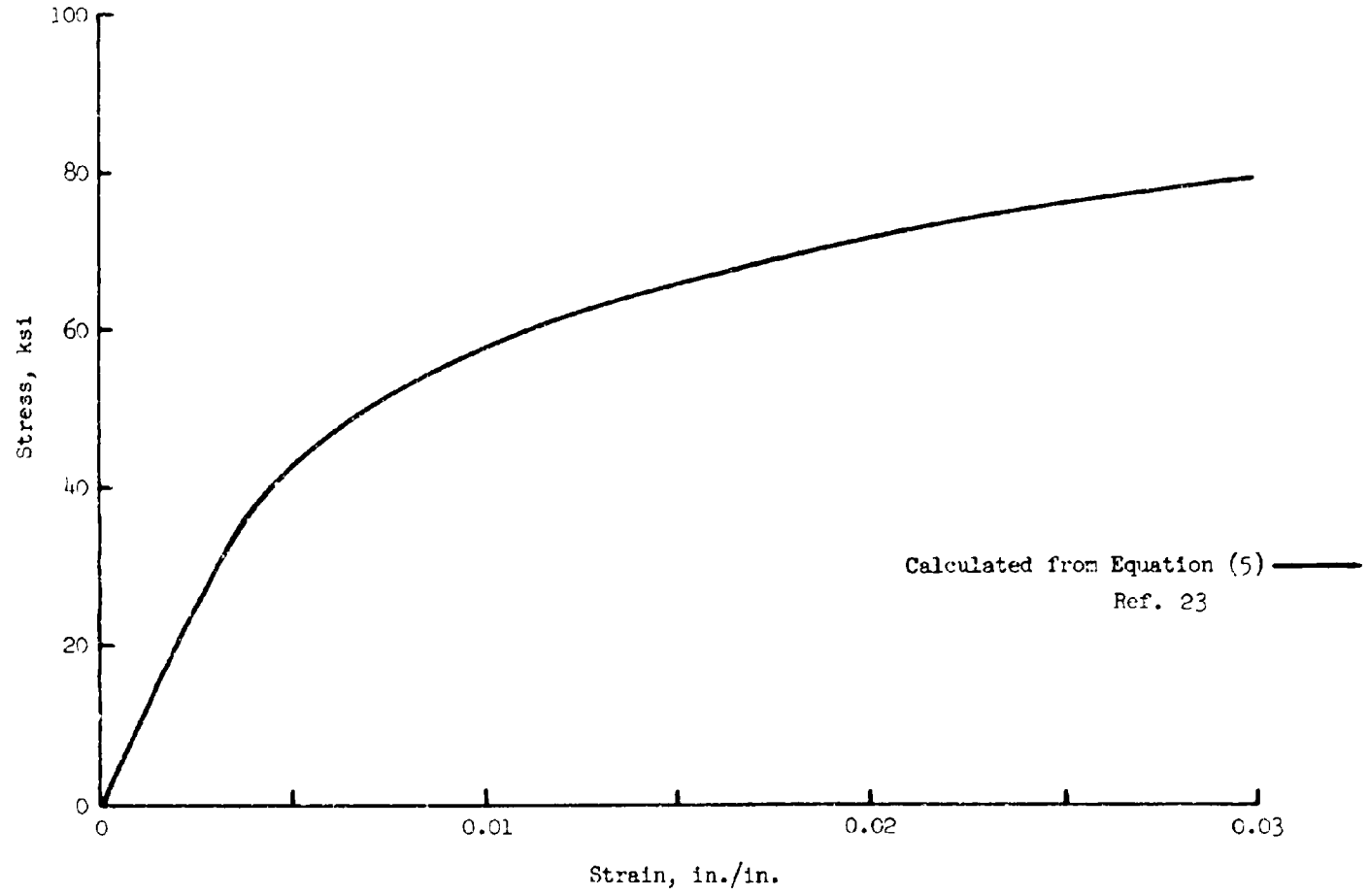

Fig. 56 Cyclic Stress - Strain Curves - 7075-T6 Aluminum Alloy

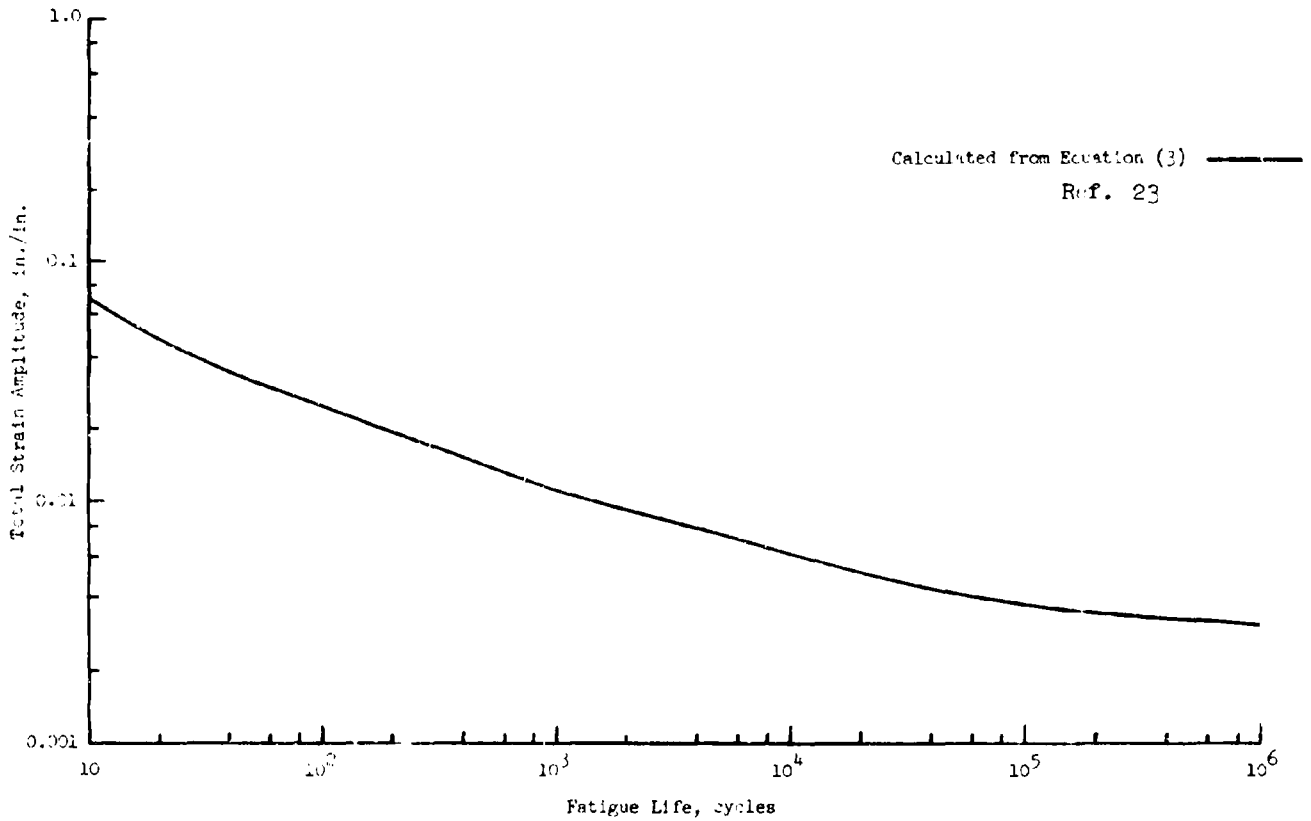

Fig. 57 Variation of Total Strain Amplitude with Fatigue Life for Completely Reversed Cyclic Loading - 7075-T6 Aluminum Alloy

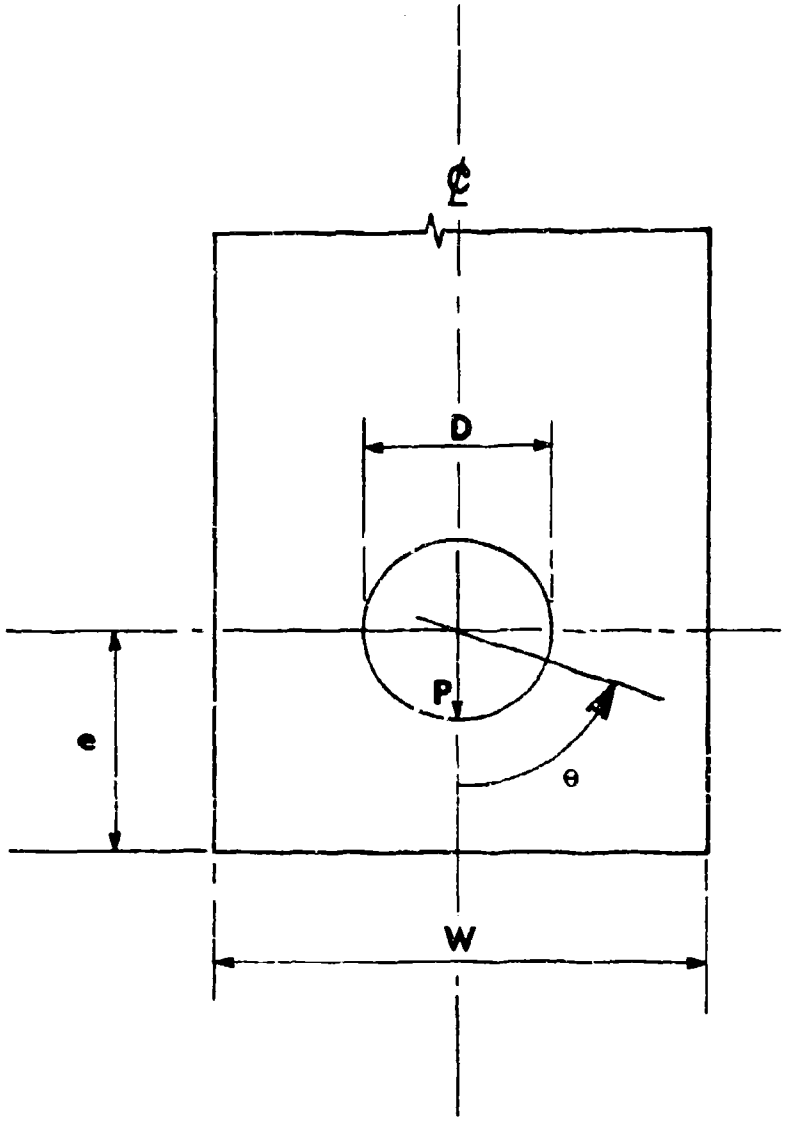

Fig. 58 Typical Element Geometry

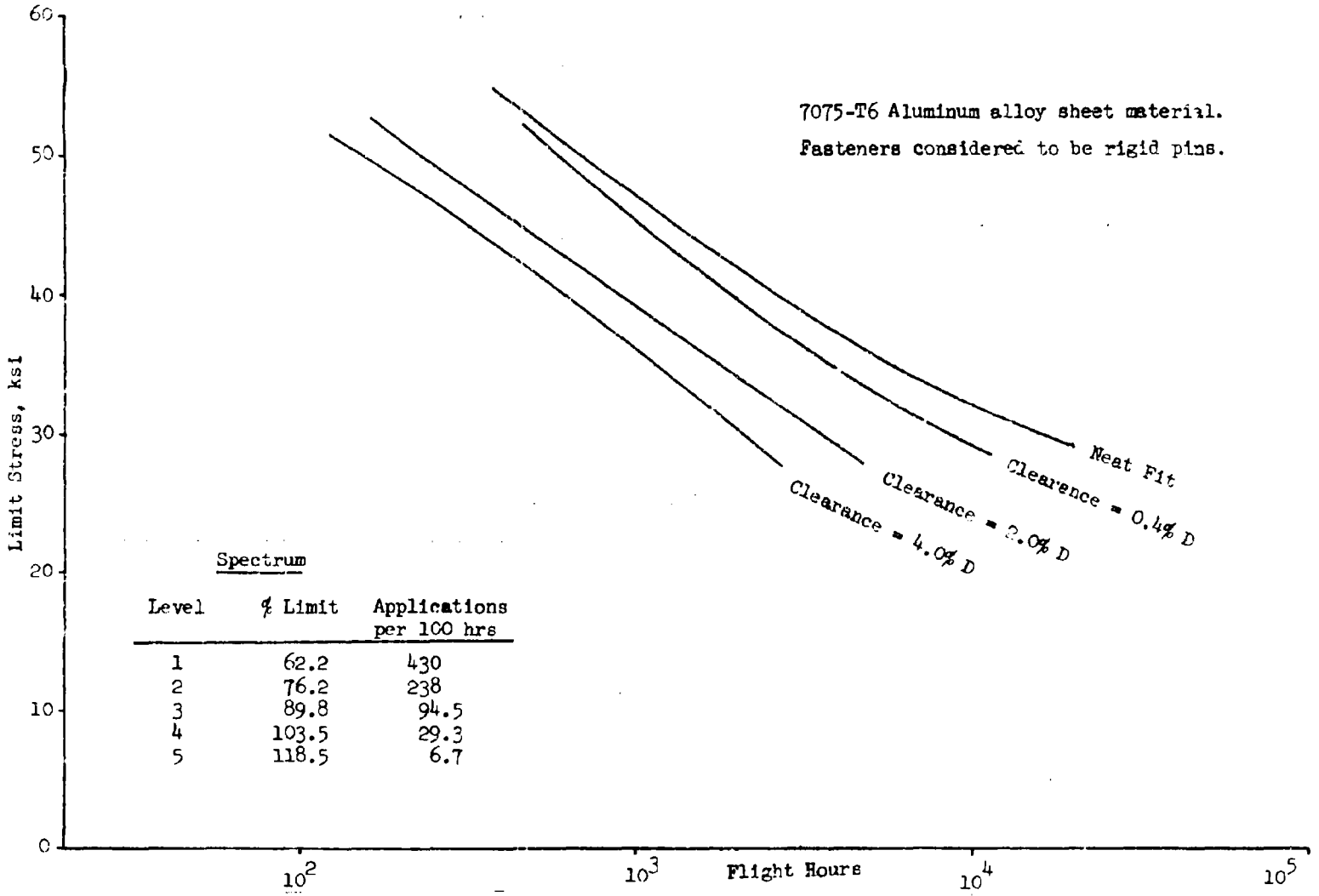

Spectrum

Level	% Limit	Applications per 100 hrs
1	62.2	430
2	76.2	238
3	89.8	94.5
4	103.5	29.3
5	118.5	6.7

Fig. 59 Spectrum Fatigue Life Predictions For Aluminum Alloy Joint

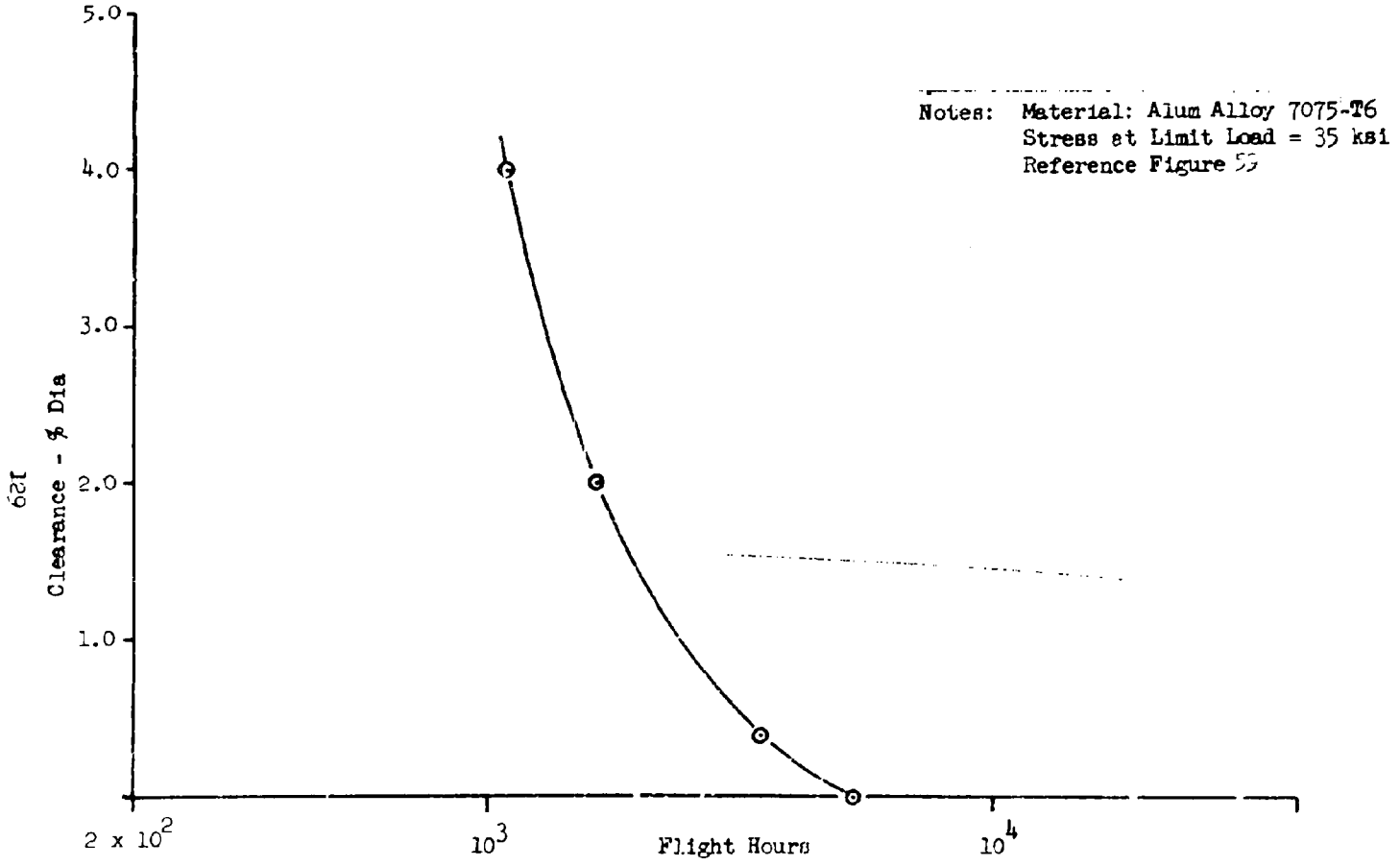

Fig. 60 Effect of Hole Clearance on Spectrum Fatigue Life

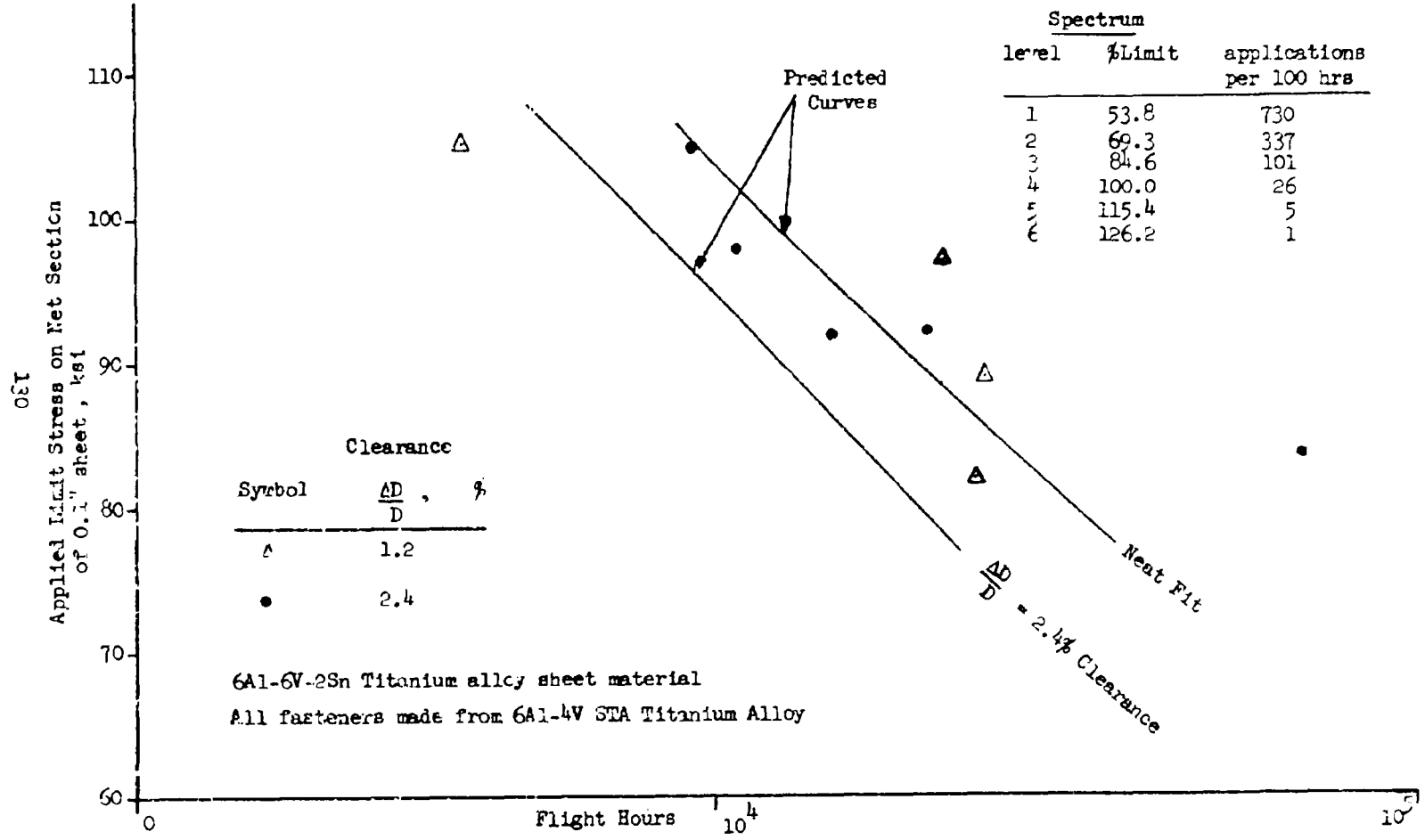

Fig. 61 Comparison of Spectrum Fatigue Life Predictions With Test Results For Titanium Alloy Joint

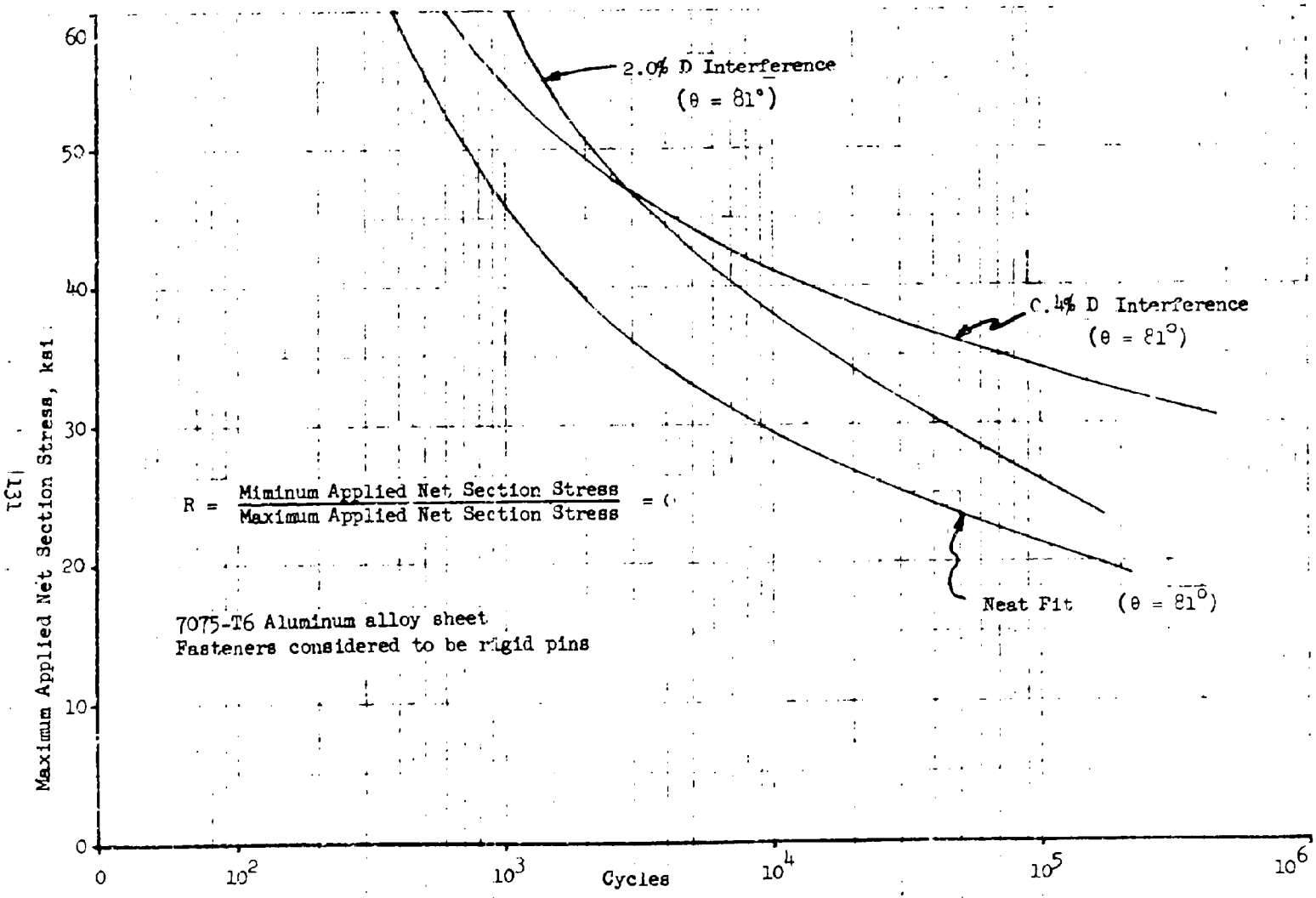

Fig. 62 Constant Amplitude Fatigue Life Predictions for Aluminum Alloy Joint

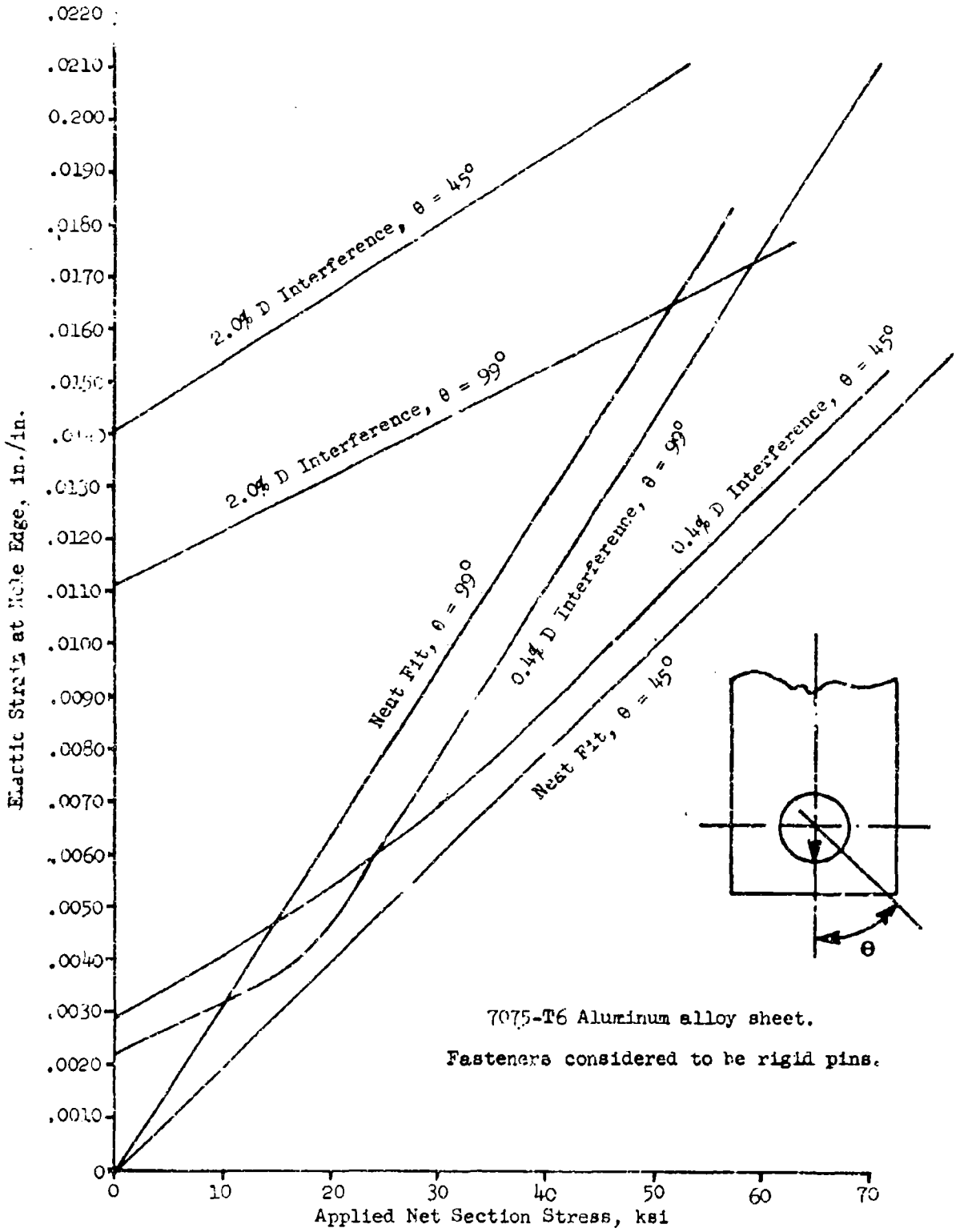

7075-T6 Aluminum alloy sheet.

Fasteners considered to be rigid pins.

Fig. 63 Variation of Elastic Strain at the Hole Edge With Applied Net Section Stress for Interference and Neat Fits

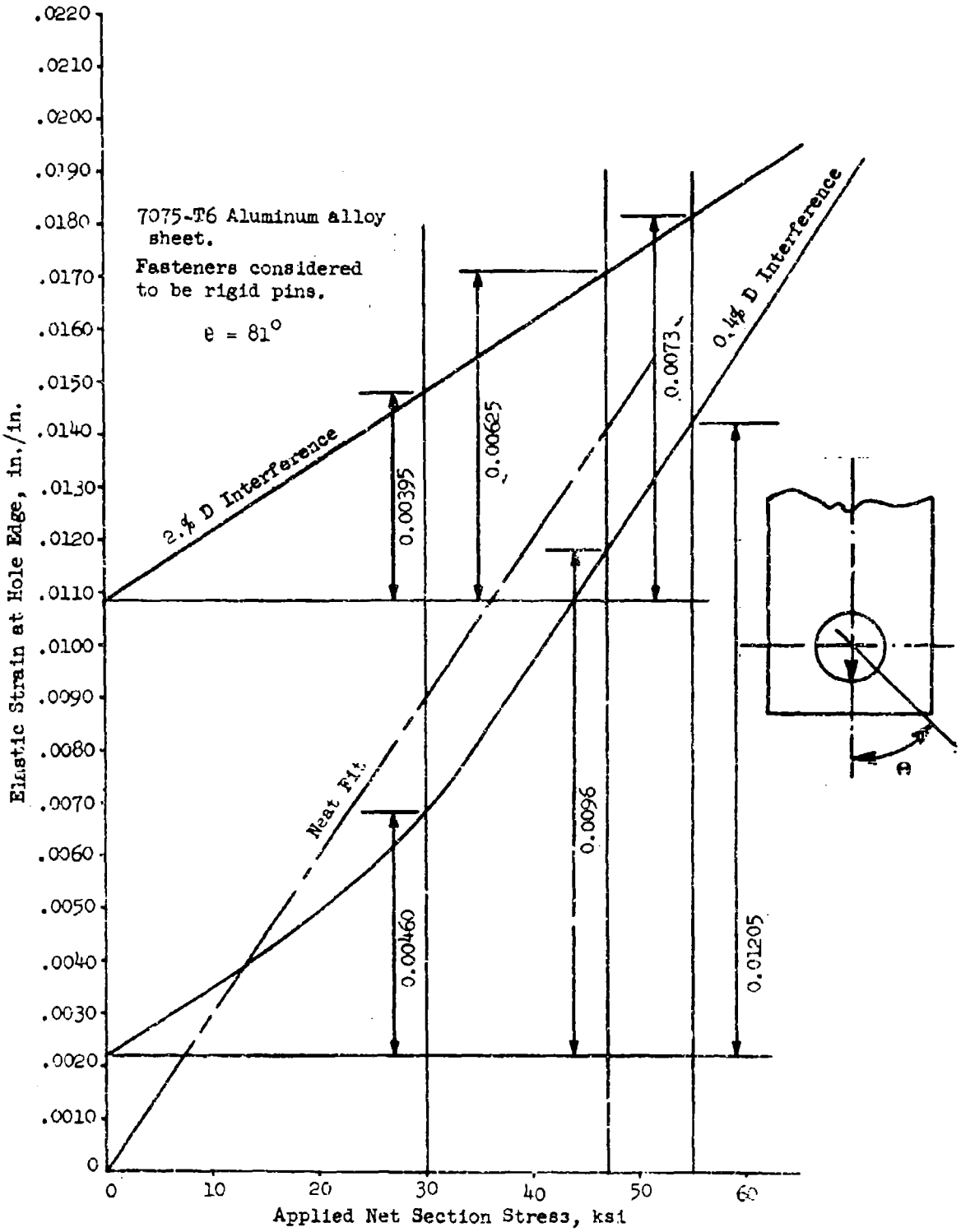

Fig. 64 Variation of Elastic Strain at the Hole Edge With Applied Net Section Stress for Interference and Neat Fits

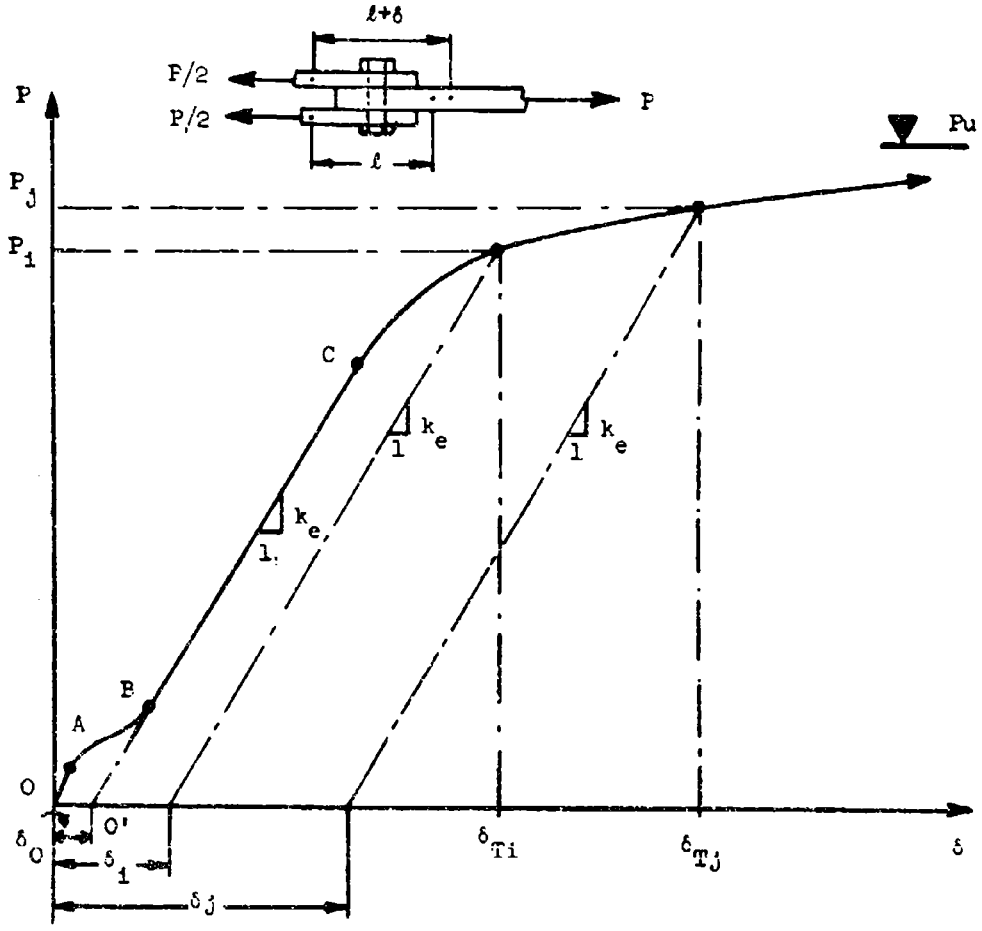

Fig. 65 Typical Load-Deflection Curve for Single Fastener Joint.

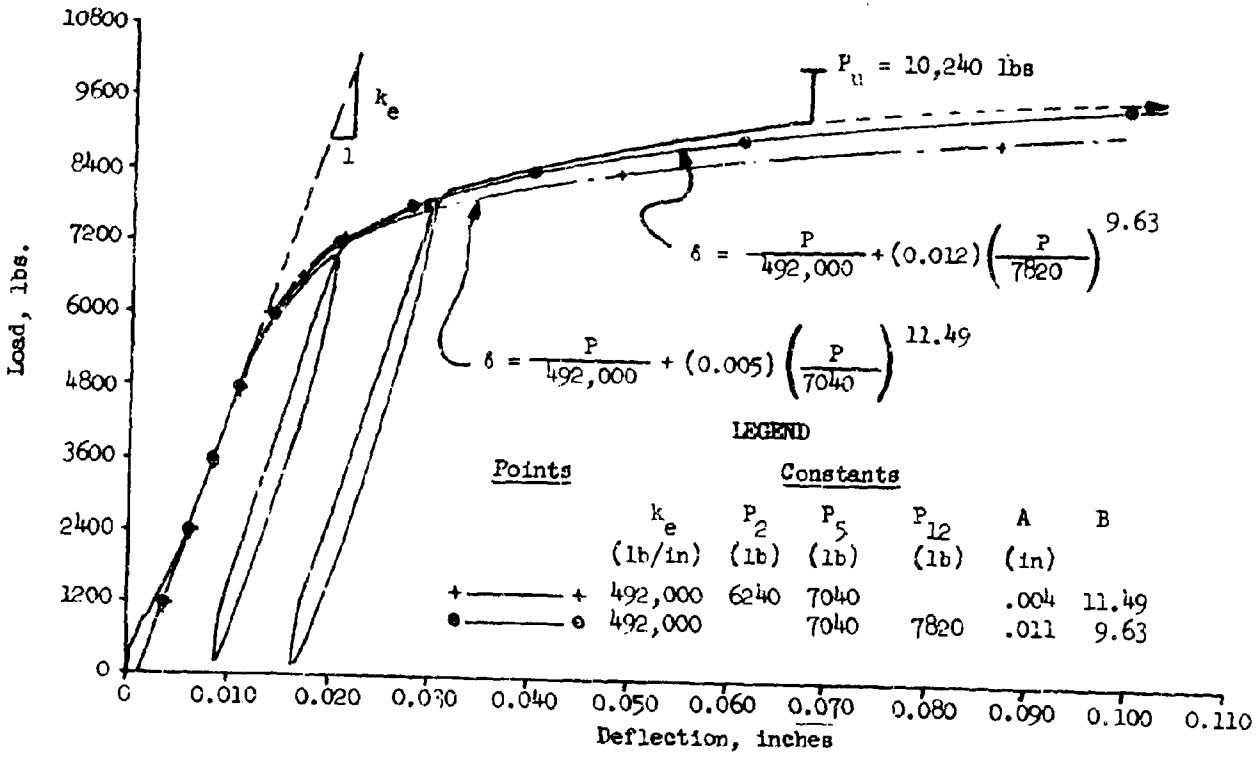

Fig. 66 Comparison of Experimental and Parametrically Derived Joint Load-Deflection Curves.

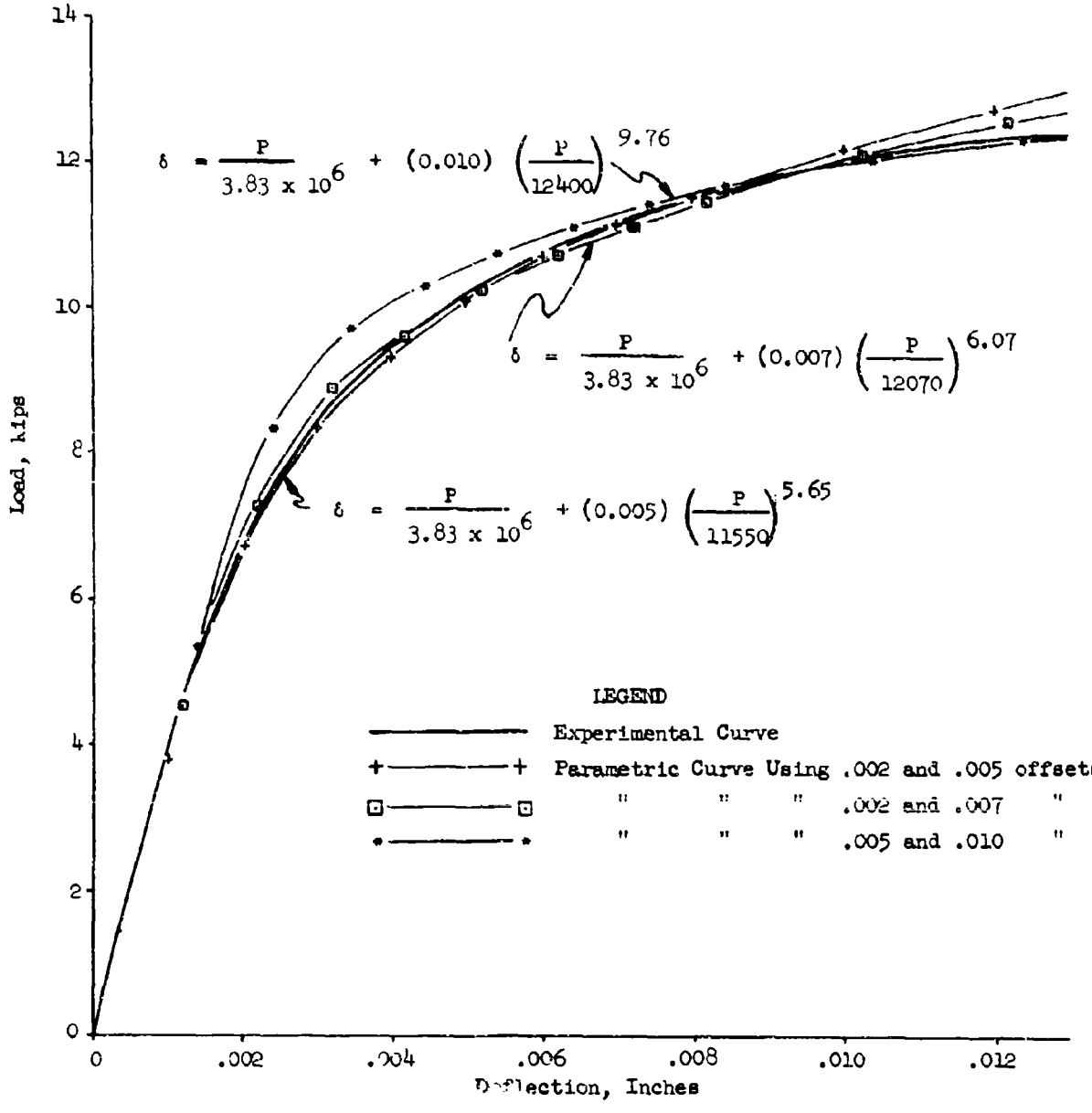

Fig. 67 Comparison of Three Parametric Curves With Experimentally Determined Load-Deflection Curve.

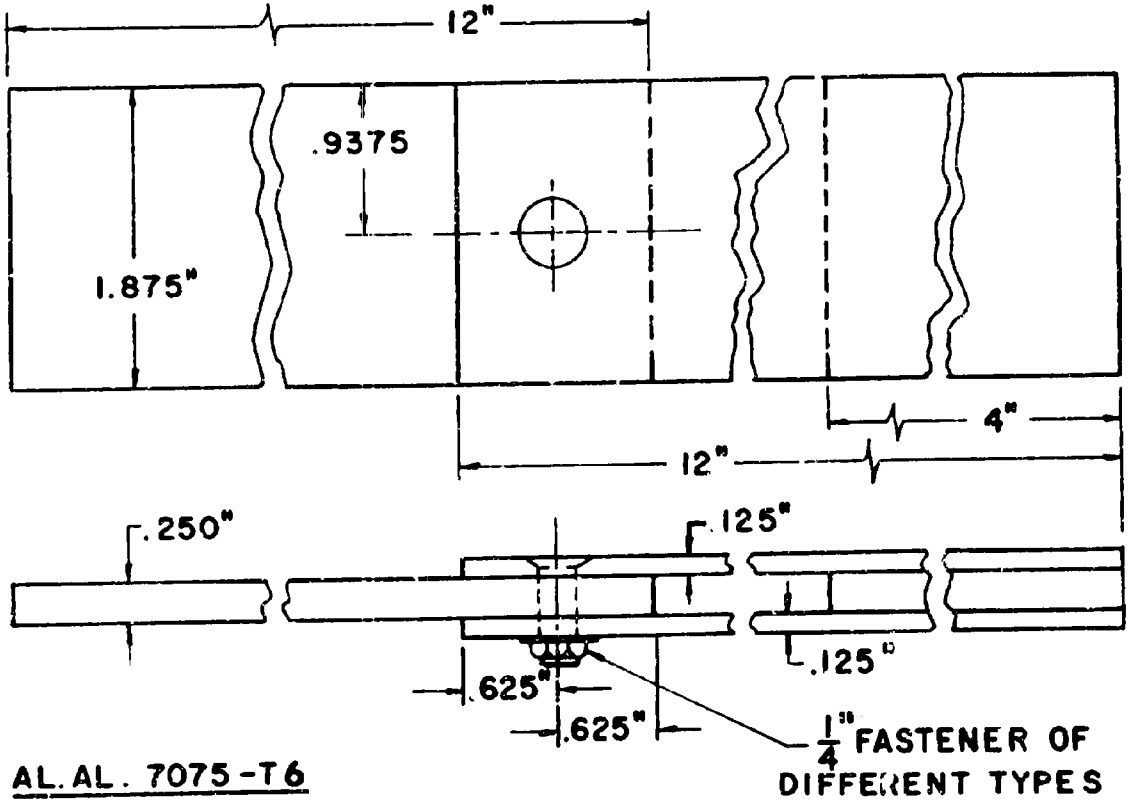

Fig. 68 - Test Specimen for Single Fastener in Double Shear

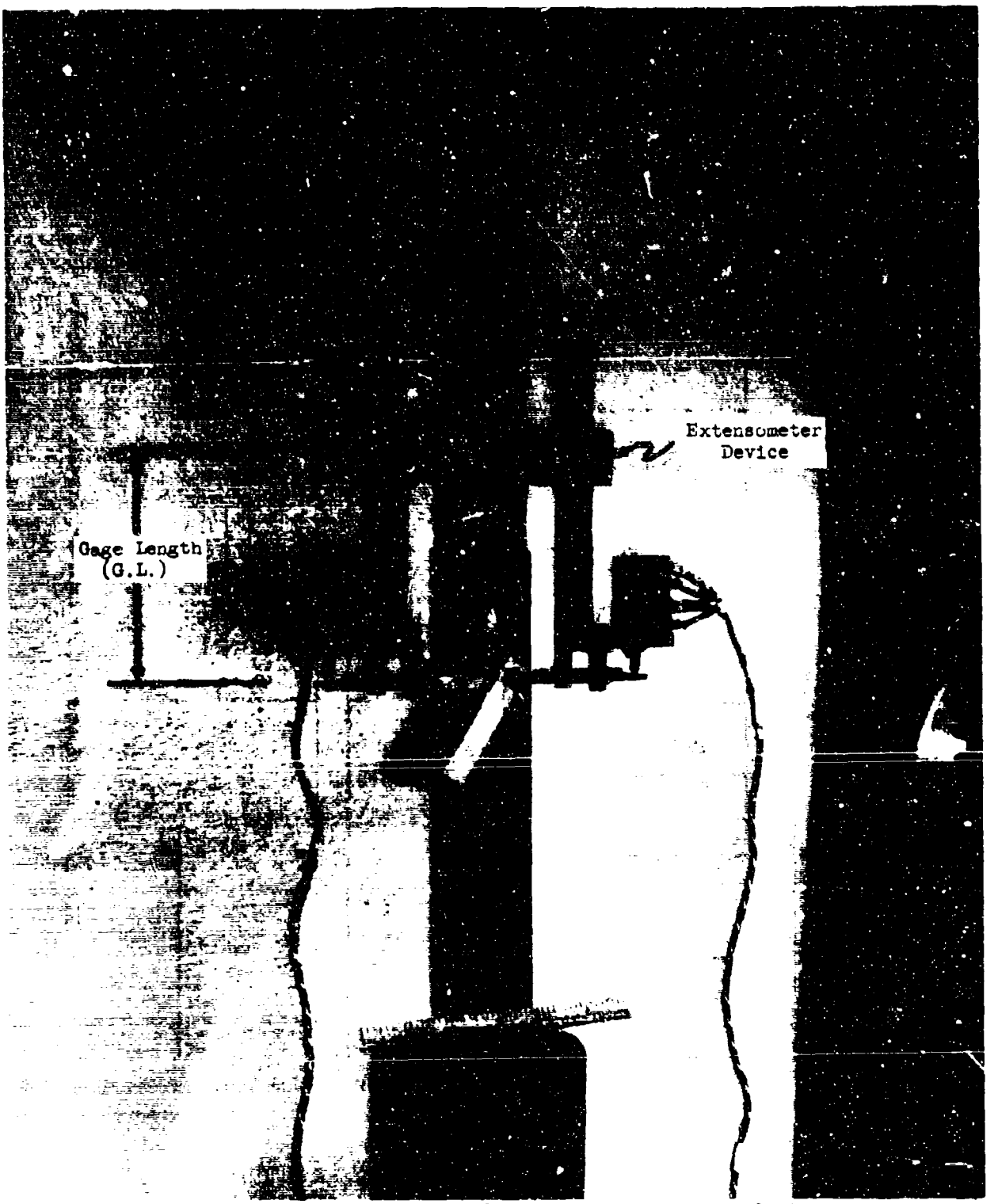

Fig. 69 Test Set Up for Single Fastener Joint in Double Shear

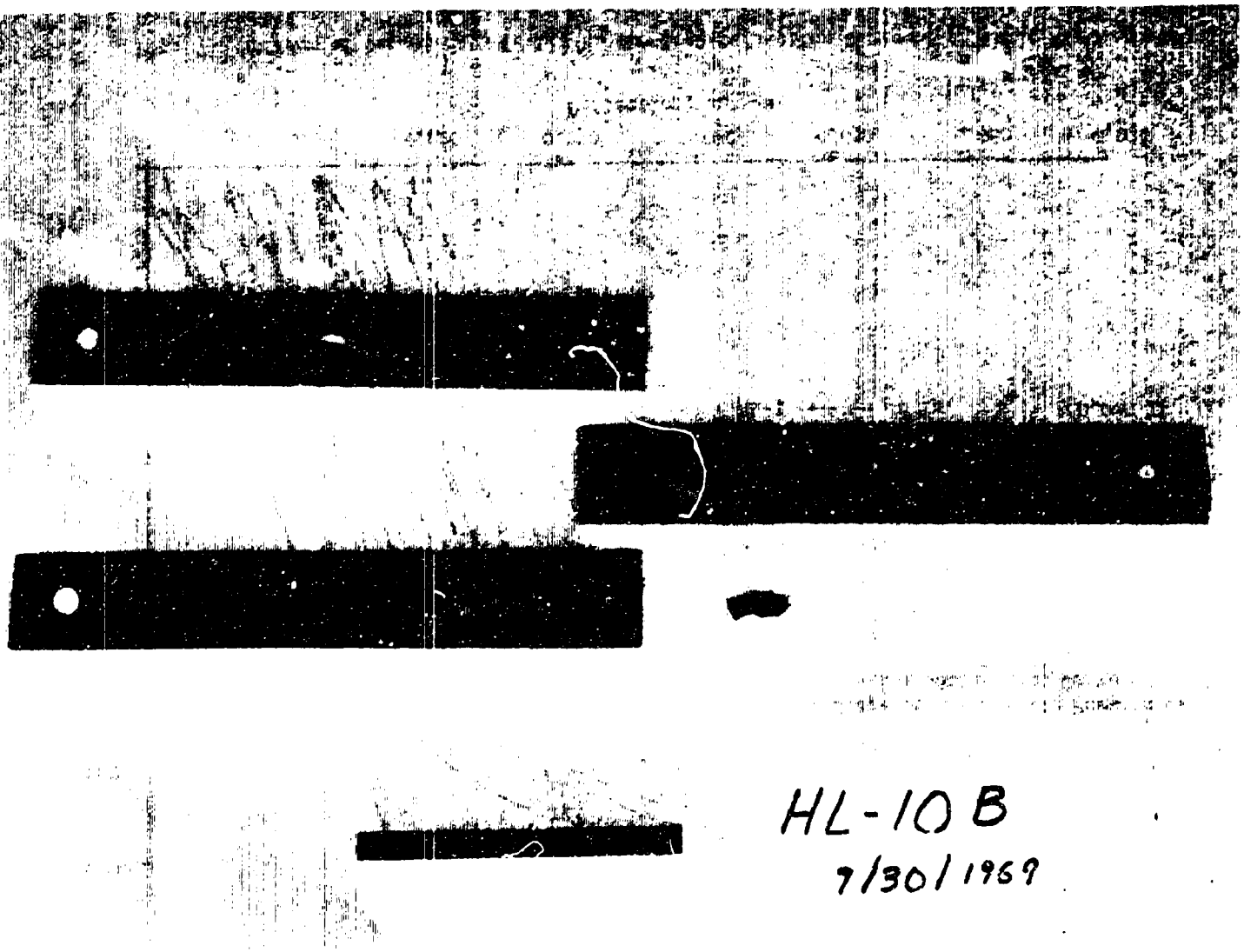

Fig. 70 Typical Failed Single Fastener Joint Specimen Showing Ovalization of the Holes and Rupture of the Fastener.

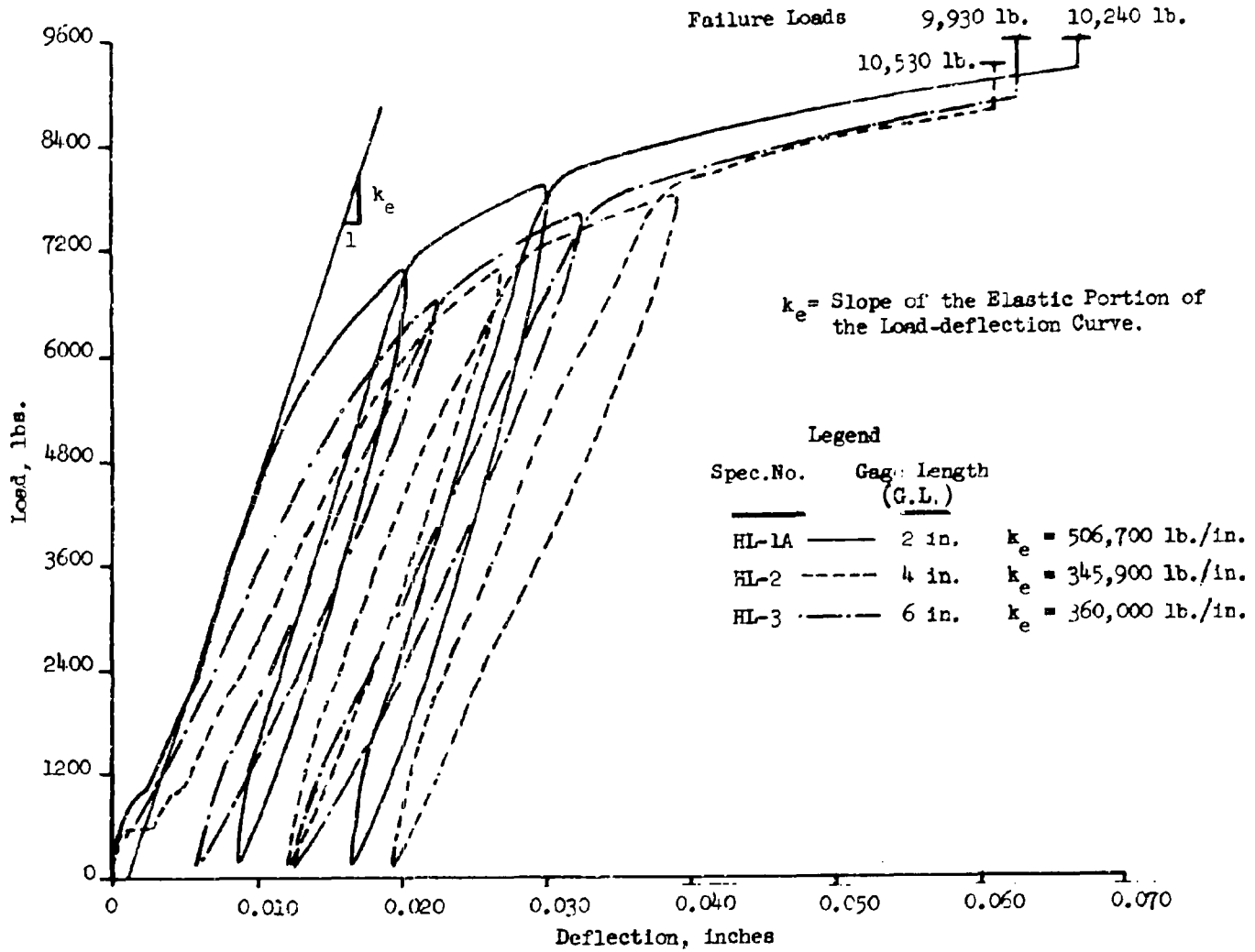

Fig. 71 Effect of Gage Length (G.L.) on the Load-Deflection Curve of a Single Fastener Joint.

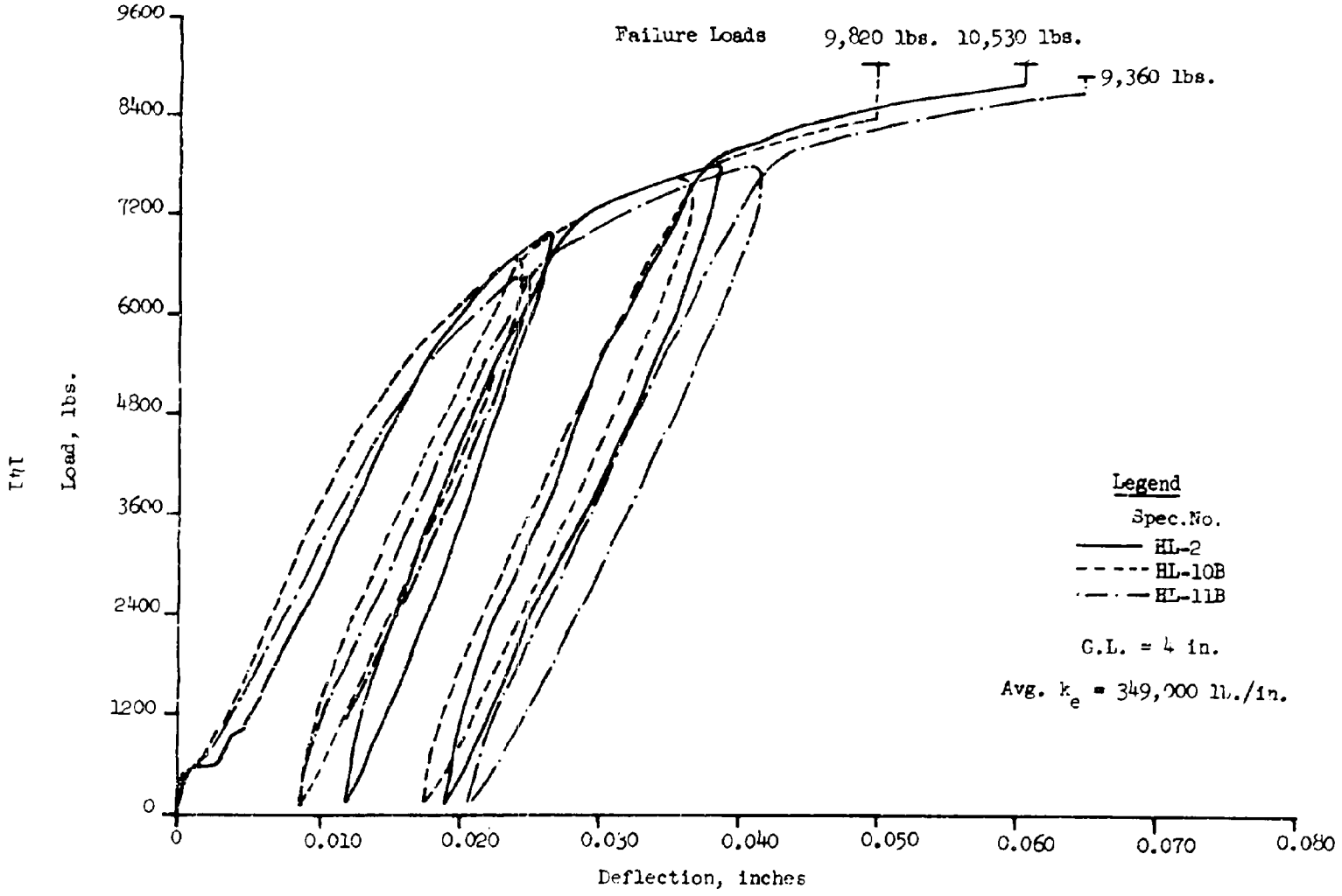

Fig. 72 Load-Deflection Curves of Single 1/4" Hi-Lok Fastener in Double Shear With Plates With No Surface Treatment

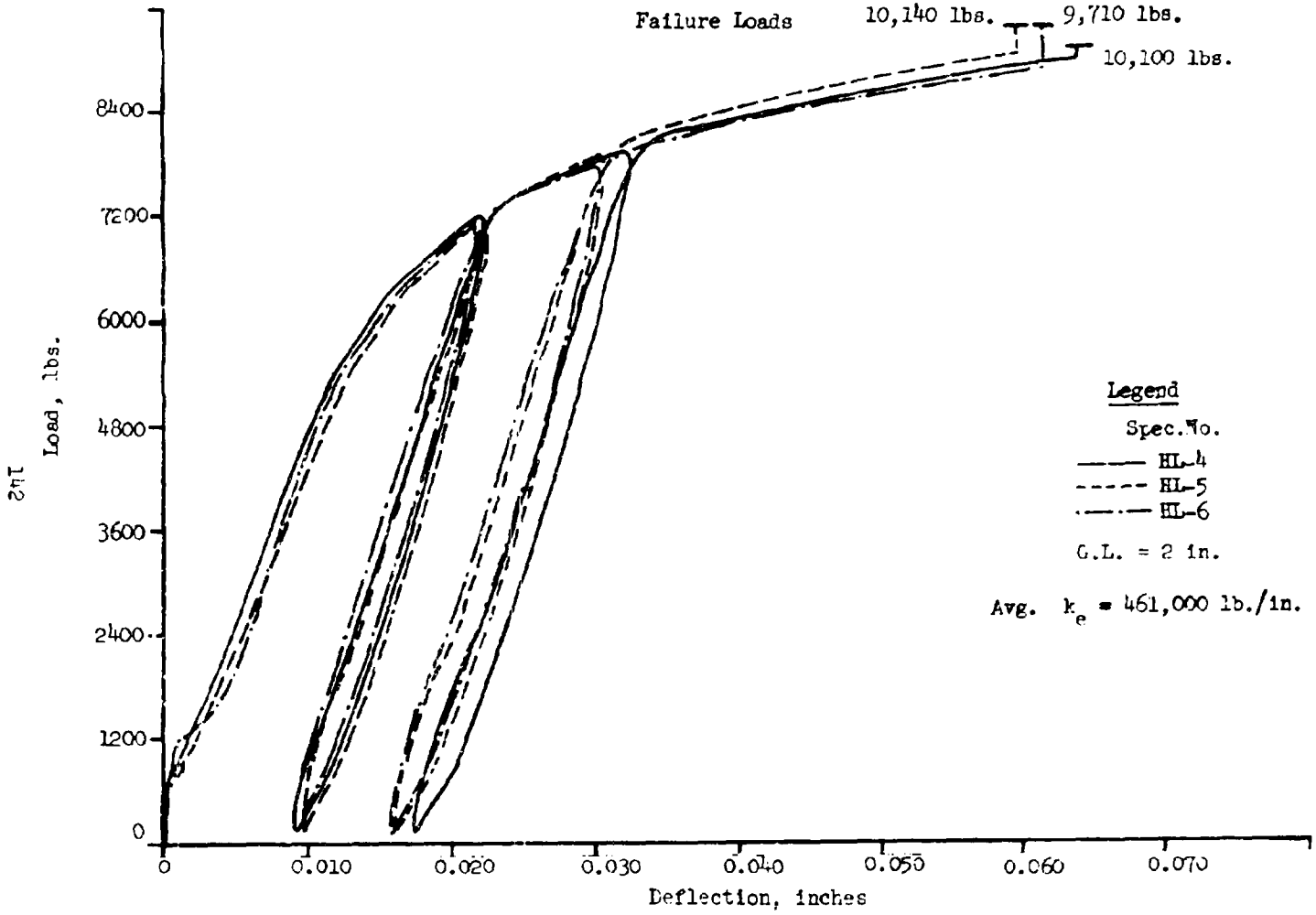

Fig. 73 Load-Deflection Curves of Single 1/4" Hi-Lok Fastener in Double Shear with Alodine Finish on Faying Surfaces of the Plates.

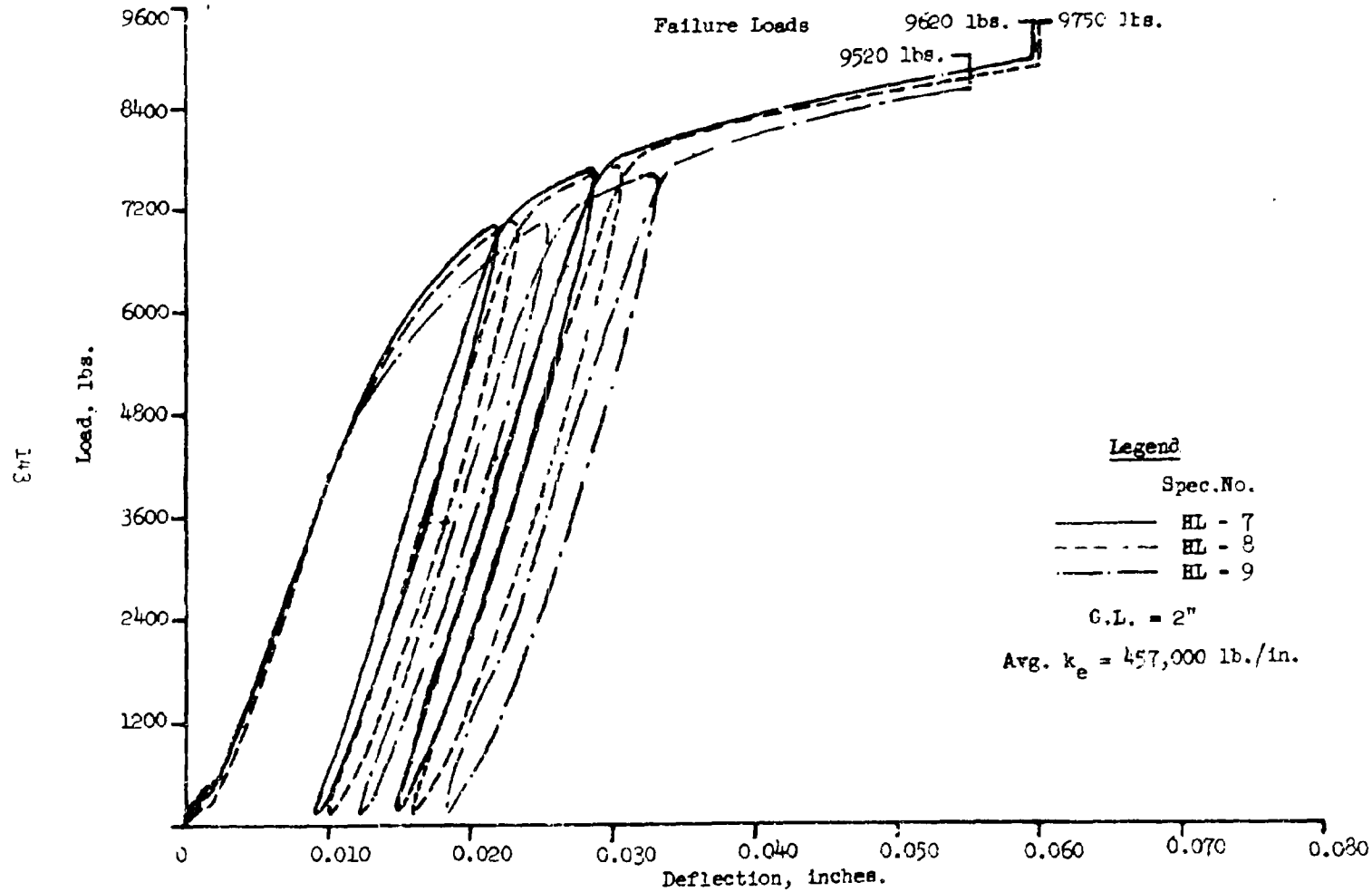

Fig. 74 Load Deflection Curves of Single 1/4" Hi-Lok Fastener in Double Shear with Teflon Coated Faying Surfaces of the Plate.

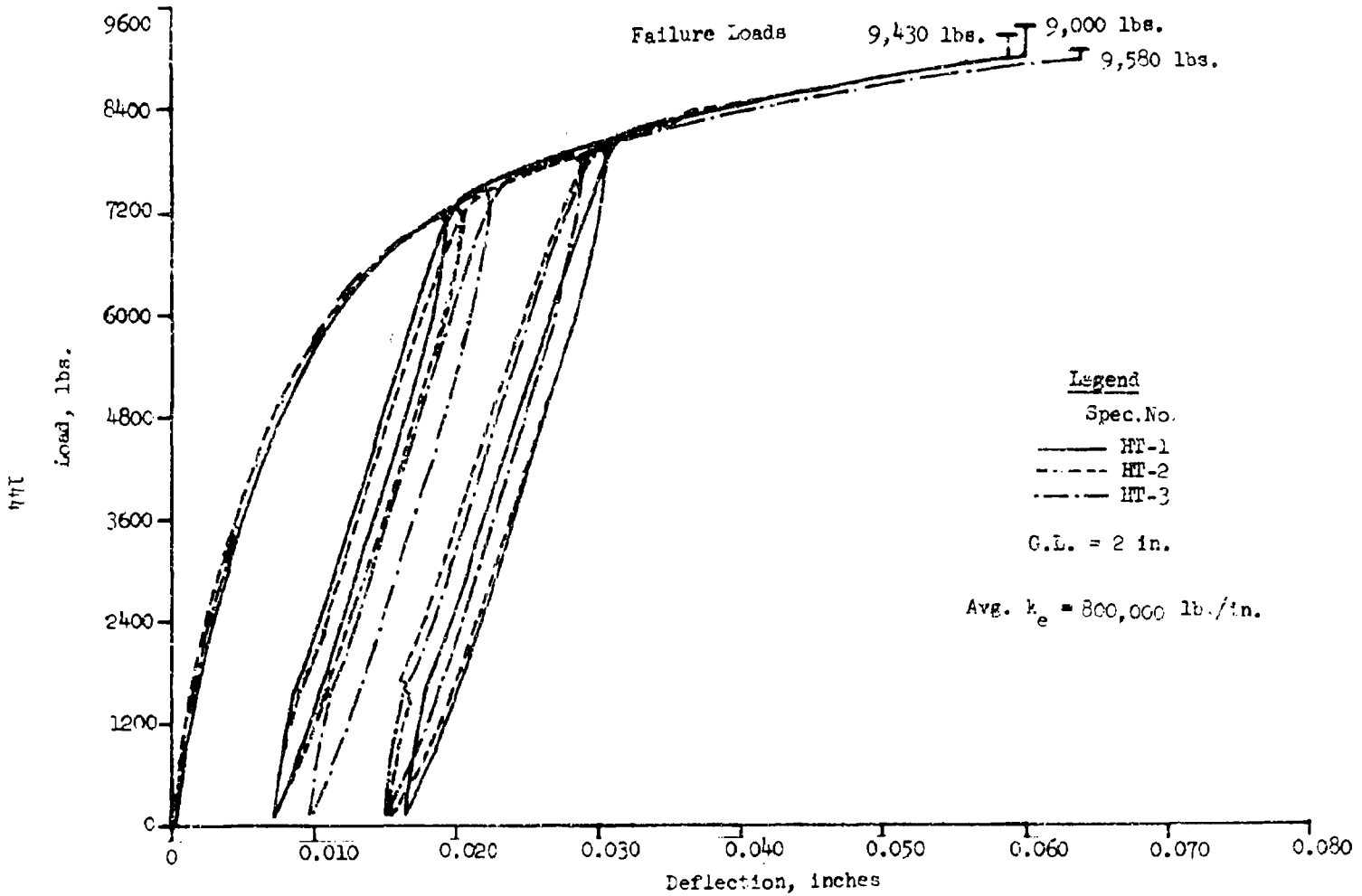

Fig. 75 Load-Deflection Curves of Single Hi-Lok-Hi-Tigue Fastener in Double Shear in 7075-T6 Aluminum Plates with no Surface Treatment

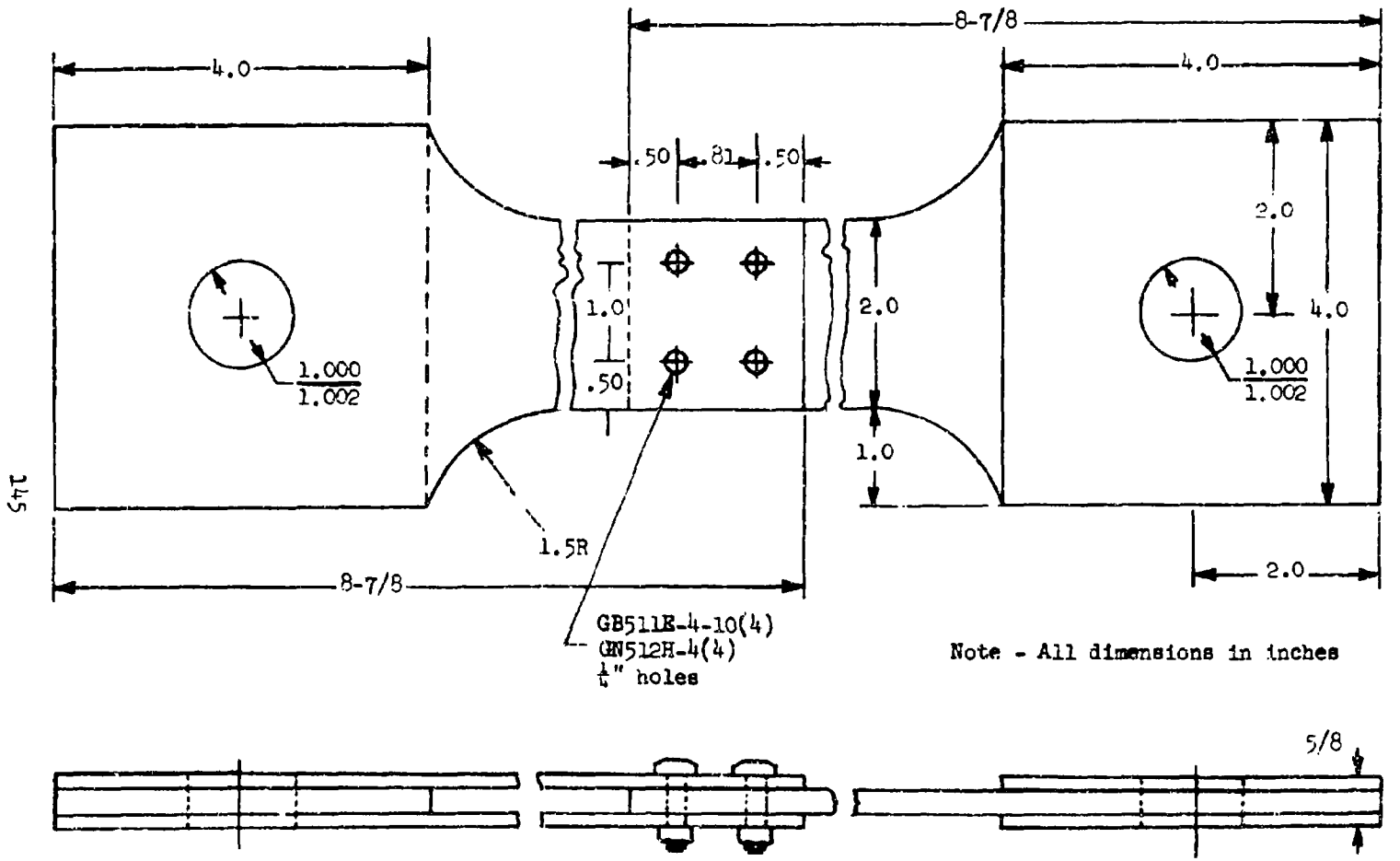

Fig. 76 Four-Fastener Joint Used to Study Clamp-up and Clearance Effects

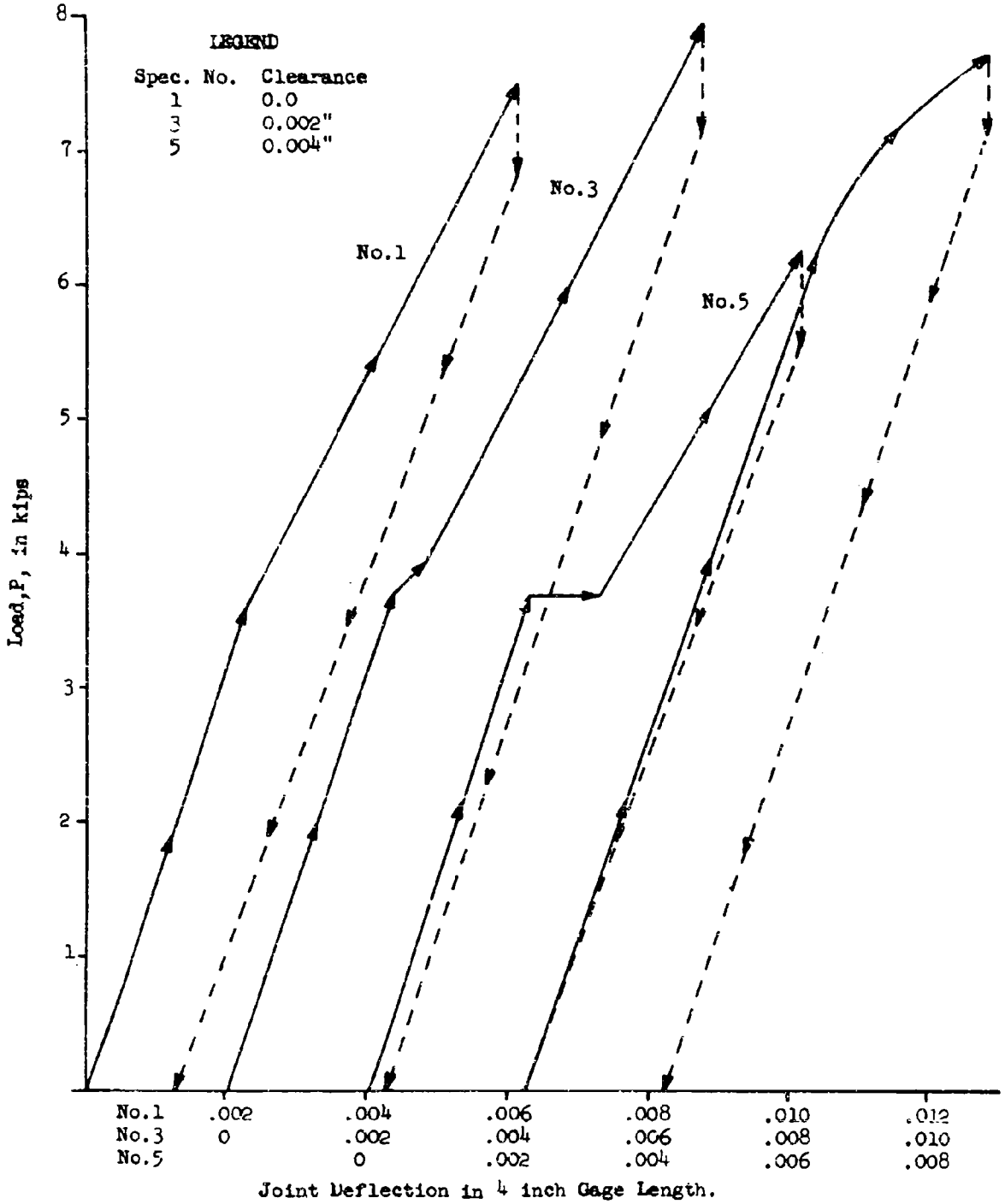

Fig. 77 Effect of Clamp up on the Static Load-Deflection Curves of Joint with Four Hi-Lok Fasteners and Three Different Amounts of Clearance

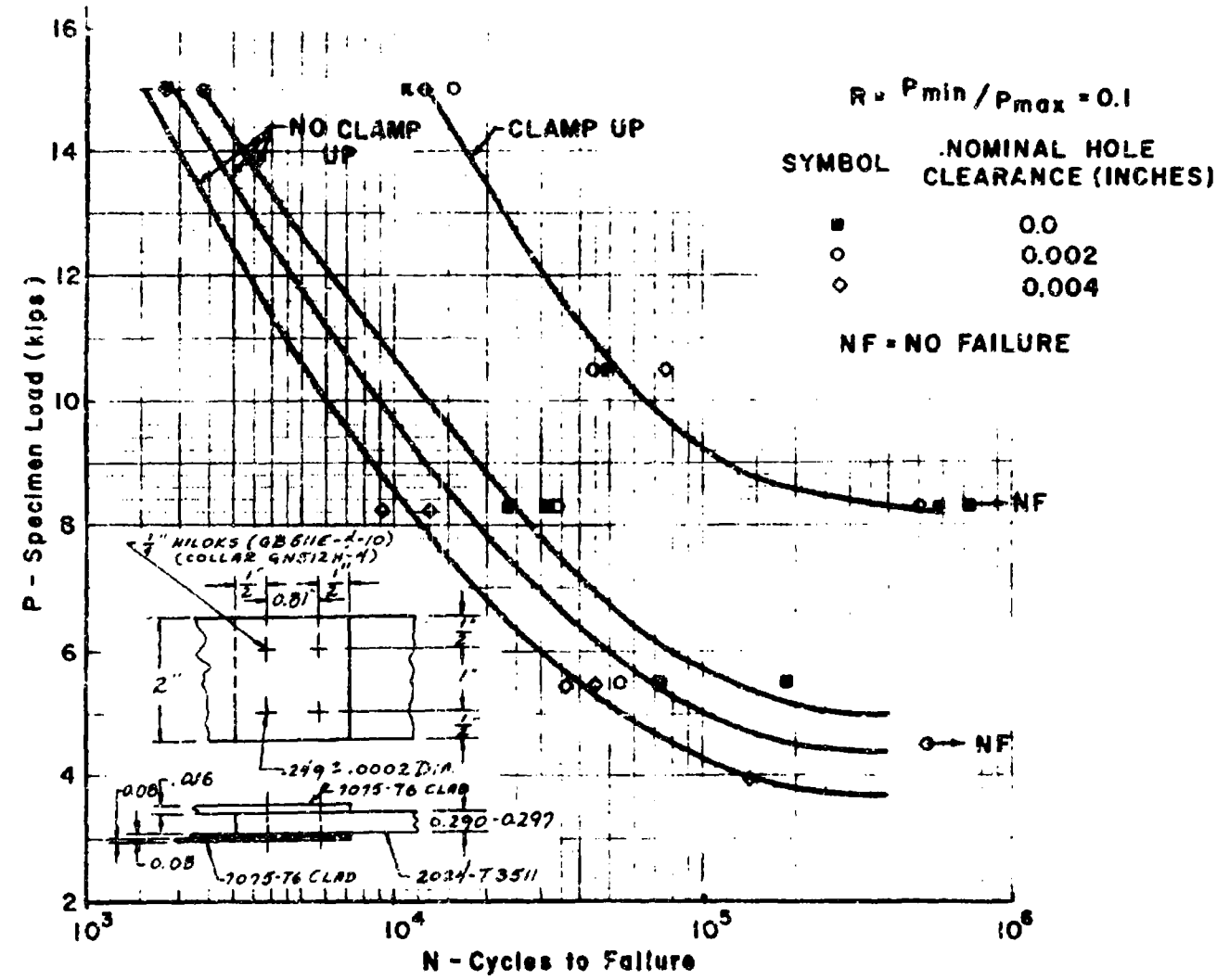

Fig. 78 Example of Fatigue Test Results Showing Effect of Interference Fit and Clamping Force

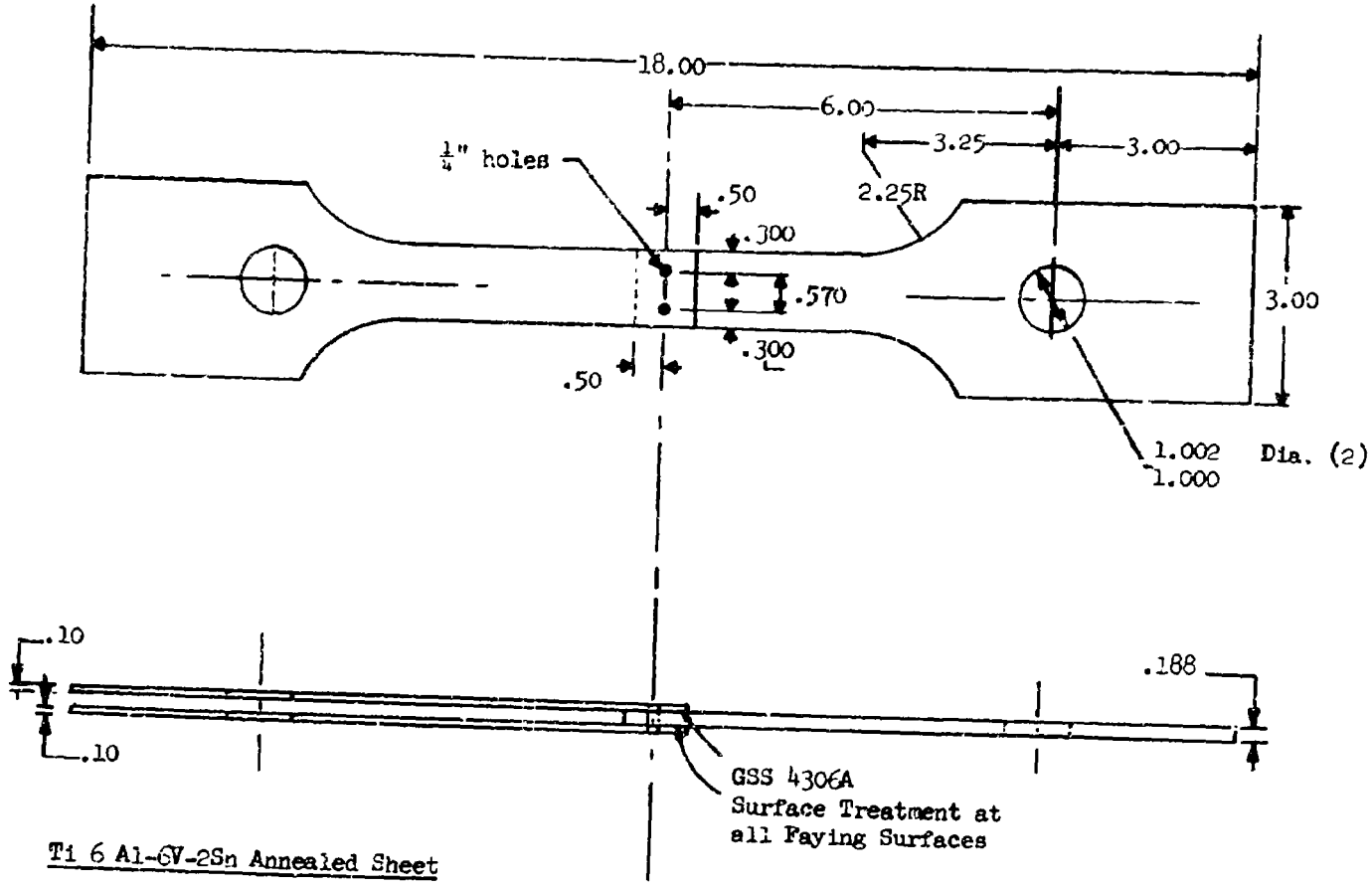

Fig. 79 - Fatigue Specimens Tested Under Spectrum Loading

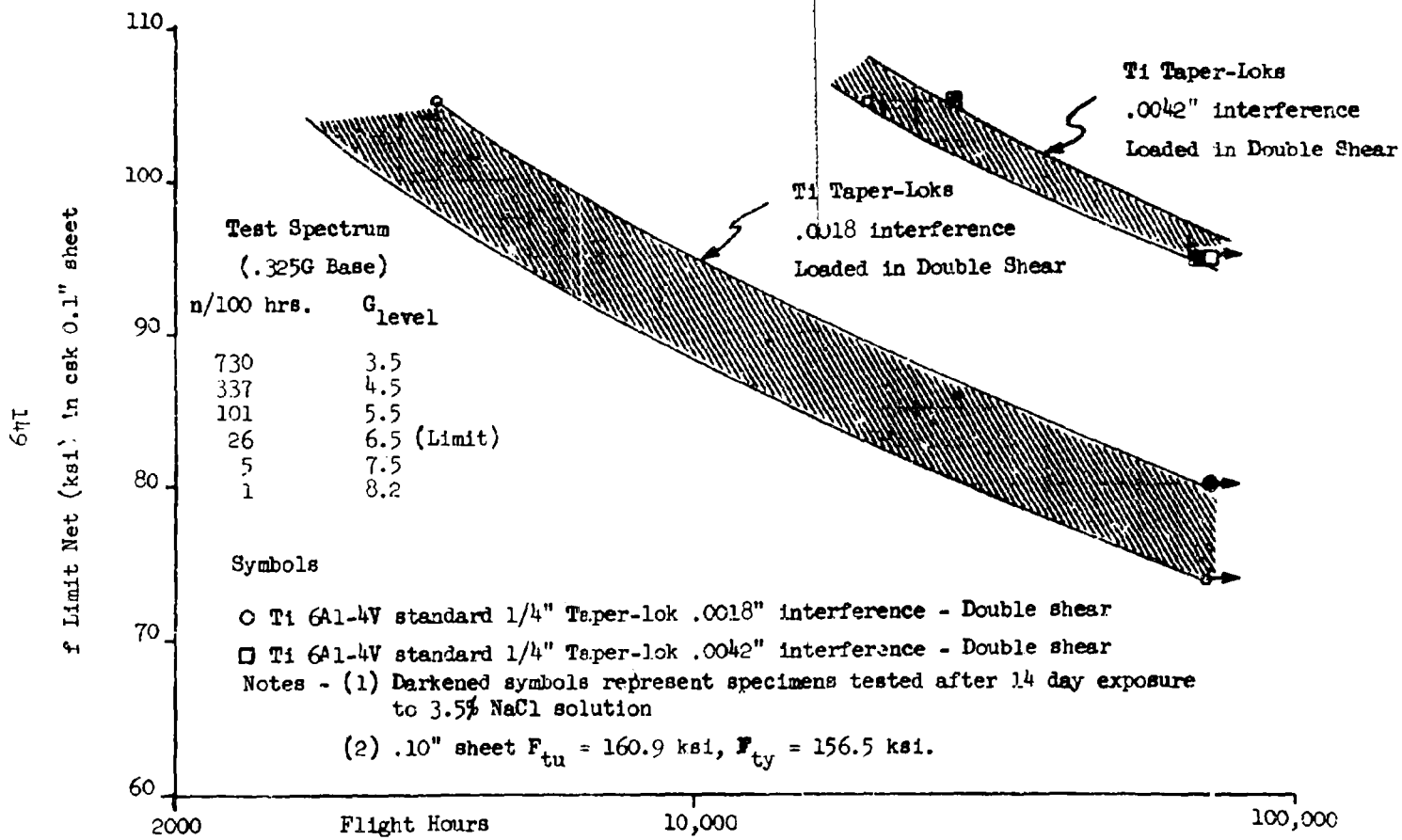

Fig. 80 Spectrum Fatigue Test Results of 1/4" Dia. Taper-Loks in Ti-6Al-6V-2Sn Annealed Sheet

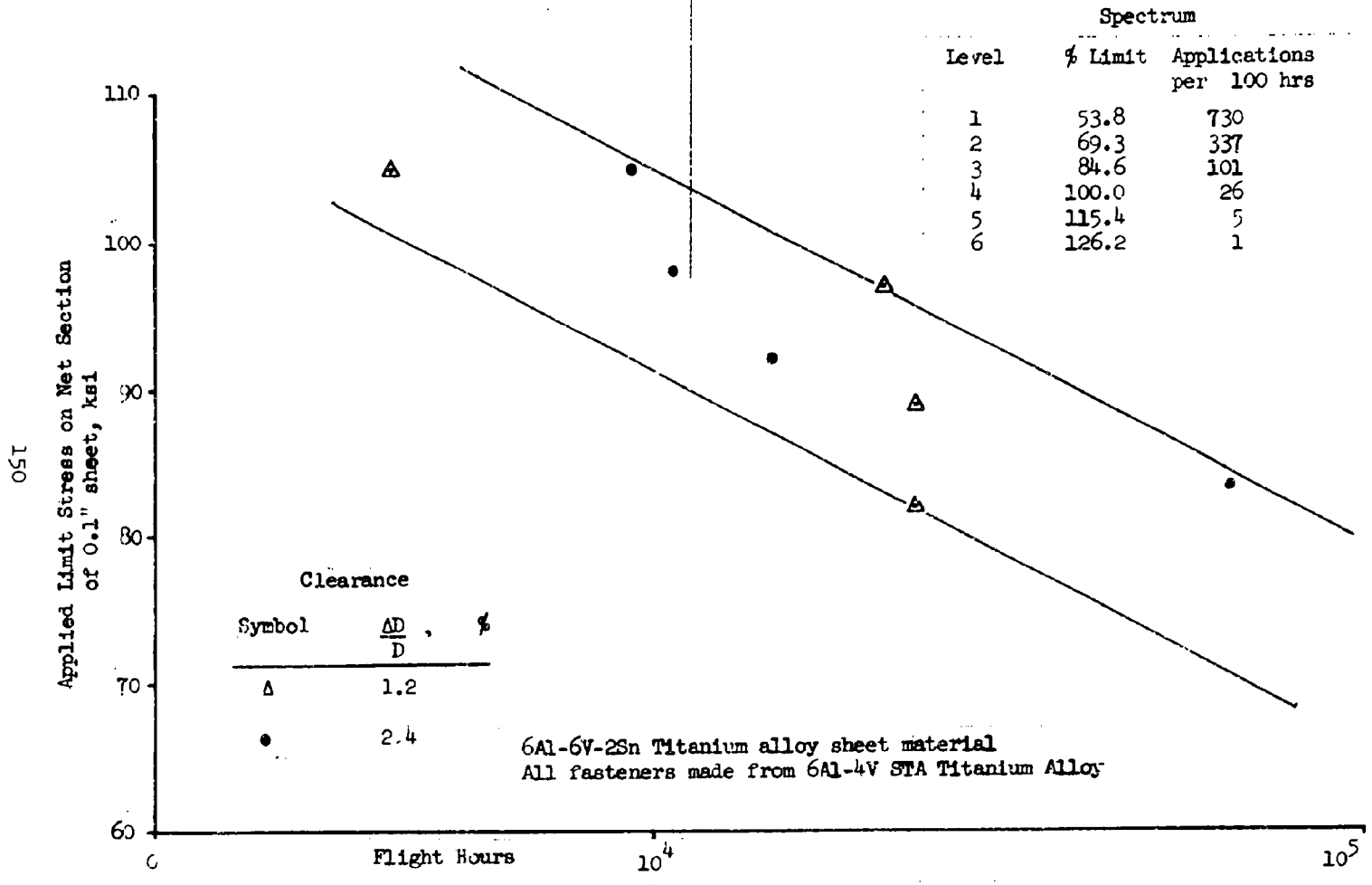

Fig. 81 Spectrum Fatigue Test Results for 1/4" D' ...s in Ti-6Al-6V-2Sn Annealed Sheets

APPENDIX A INELASTIC STRESS AND DEFLECTION ANALYSIS OF PLANAR STRUCTURES

(A) Program Description

This is a brief description of the Grumman computer program used for plastic analysis of mechanically fastened joints. This program is a modified version of deck 45128 originally written to do elastic-plastic and creep analysis of isotropic and anisotropic planar structures. (Reference 3).

The program was originally written in Fortran II for the IBM 7094. It was modified and expanded to run on the IBM System/360 (Fortran IV). On this machine, available hardware facilities permitted expansion to sixty plastic "nodes"*, after allowance was made for some additional features. The version submitted to AFFDL to operate on IBM 7094 under IBSYS control (Fortran IV) is restricted in size to thirty four plastic nodes, due to core size limitations. Use of direct-access storage (disk or drum) for the two large data matrices permits a substantial increase in problem size, at the cost of a factor of approximately ten in running time. This has been done on the IBM/360, increasing the size to 175 nodes with the increase in machine time as described.

The program includes these features. Print output may be obtained at each cycle of calculation, or at load levels which are multiples of the load increments used, as desired. The stress-strain relationship may be defined as a table of ten points on a curve, with automatic interpolation. Alternatively, it may be defined by the Ramberg-Osgood equation, with a reference stress, exponent and Young's modulus as input. The program will accept decreasing steps in applied load. Unloading follows Hooke's law when the node has been stressed in the inelastic region. At any pre-determined load level, the program can be

* The term "node" as used herein refers to either element centroids for constant strain finite elements or actual nodal points for linearly varying strain elements.

forced to spill all the memory tables and clues into a binary save tape, then exit. This permits the programmer to inspect his results and decide whether to continue the analysis from that point, or to modify or abandon the job. A timing feature is built in the coding, but temporarily patched out of the AFFDL version, to allow this save tape to be generated upon reaching a time estimate supplied with the data.

Each link of the program contains the non-IBM subroutines needed for operation. Standard input-output subroutines etc., will be taken from the library tape. As a point of information, the program contains a main program and four overlays.

(1) LKONE reads the first control card, and reads all other decimal input supplied.

(2) LKTWO is used only on a restart job. It reads the modified step table, if provided, and the binary input tape.

(3) LKFOUR is the processing link. It does all the calculation, print control, and writing of print output on tape 6.

(4) LKFIVE writes a binary tape for restart.

Sequencing and details of the data cards follow. The symbols used in the program for various items of input data are listed on page 153 and are shown on the sample key-punching sheets, pages 160 and 161.

The data cards are used in the following sequence, immediately after the $DATA card required by IBSYS:

(1) General clue card (FORMAT 1) containing KLU4, KLU7, NA, NDE, GNU, and a title or caption.

(2) Table of load steps desired. Up to ten cards defining ten steps may be used. The maximum level for each load step may be above or below the previous maximum level of load. The program verifies the algebraic sign of the increment, and corrects it if necessary. Each card

contains four variables TEMP1, TEMP2, TEMP3, TEMP4 in FORMAT 2.

(3) Data matrices. These may be provided in any sequence. Each matrix has a header card in FORMAT 3, one or more data cards in FORMAT 4, and a blank card to end it. The last input matrix on the system input tape must be followed by one added blank card (two total) to trip the program into operation.

(B) Symbols and Format of the Data Cards

(1) General Clue Card - FORMAT 1

Cols.	Field	Symbol	
1	I1	KUU4	This gives the number of input matrices on the auxiliary input tape logical #9. If all matrices are on the monitor tape, leave this blank. If using binary restart tape on #8, use a digit from 5 to 9 Maximum number of decimal input matrices on the auxiliary input tape is 4.
2	I1	KUU7	0, or blank, prints output on cycles indicated by the step table; 1 prints on all cycles.
3-5	I3	NA	This sets the frame size for the problem to be handled. NA is three times the number of nodes. Maximum value is 102 (34 nodes).
6-8	I3	NDE	This indicates the number of load conditions for deflection calculations.
9-14	F6.3	GNU	Poisson's ratio "nu"

(B) Symbols and Format of the Data Cards - (Continued)

(1) General Clue Card - FORMAT 1 (Continued)

Cols.	Field	Symbol	
15-80	11A6	TA	Any 66 characters of alpha-numeric text to be printed as a heading for identification purposes.

(2) Table of Steps (limited to ten entries) - FORMAT 2

Cols.	Field	
1-6	6X	Not used.
7-10	A4	LOAD indicates a load step, TAPE indicates write memory on a save-tape on logical #11 then exit. ESTM indicates a time estimate in minutes to automatically terminate run. ESTM does not count as one of the ten load steps. FINS or blank indicates end of table (this may be the 11th card in the table).
11-20	E10.6	Upper limit of step in pounds or estimated time in minutes.
21-30	E10.1	Interval or increment for calculation.
31-40	E10.1	Interval or increment for print output. Prints are generated on tape 6 for the current cycle when the current load level is an integral multiple of the print interval. If the print interval is left blank, no prints are generated for cycles in this step. If print interval is

(B) Symbols and Format of the Data Cards - (Continued)

(2) Table of Steps (limited to ten entries) - FORMAT 2 (Continued)

Cols.	Field	
31-40	E10.1	very small compared to the current level, then numeric problems sometimes occur in the print control subroutine (OUTPUT), and it may be necessary to re-run with the every-cycle print control "1" for KLU7 punched in the first control card.
41-80		Ignored.

(3) Data Matrices - Header Card - FORMAT 3

Cols.	Field	
1-6	6X	Not used.
7-10	4X	Not used. We use the letters MTRX for compatibility with the GISMO Matrix System, which reads and writes matrices in this format.
11	1X	Not used.
12-17	A6	This is the identification name for the input matrices and must correspond exactly with one of the following names:

bbbSIM } Matrix of stresses for applied loads
or SIMbbb } maximum size 102x1

bbbSIJ } Matrix of stresses for member strains
or SIJbbb } maximum size 102x102

bTSIGN Table of stress values 11x1 }
bTEPSN Table of strain values 11x1 }

(B) Symbols and Format of the Data Cards - (Continued)

(3) Data Matrices - Header Card - FORMAT 3 - (Continued)

Cols.	Field	
		These two matrices define the stress-strain curve as a series of chords. The data is entered in this format, merely to conform to the format of the SIM-SIJ matrices which were generated using the GISMO Matrix System. Note that the first value in both TSIGN and TEPSN must be zero to avoid upsetting the interpolation procedure.
	bbbDIM / DIMbbb	Matrix of deflection for applied loads maximum size 102x1
	or	
	bbbDIJ / DIJbbb	Matrix of deflection for unit induced strains - maximum size 102x102
	or	
	RAMOSG	three parameters for Ramberg-Osgood equation - reference stress, exponent and Young's modulus.
18	1X	Not used.
19-21	I3	Number of rows in this matrix.
22-24	I3	Number of columns in this matrix.
25-80		Not used.

(B) Symbols and Format of the Data Cards - (Continued)

(4) Data Matrices - Data Cards - FORMAT 4

Cols.	Field	
1	1X	Not used.
2-4	I3	Row index for the first element.
5-7	I3	Column index for the first element.
8-23	E16.8	The first element on this card.
24	1X	Not used.
25-27	I3	Row index for the second element.
28-30	I3	Column index for the second element.
31-46	E16.8	The second element on this card.
47	1X	Not used.
48-50	I3	Row index for the third element.
51-53	I3	Column index for the third element.
54-69	E16.8	The third element on this card.
70-80		Not used.

The last card of a matrix must be completely blank (tested in Col. 2-4). The last matrix on the Monitor input tape 5 must be followed by one added blank card (two total) to trip the program into operation.

The input matrices on the Monitor tape may be in any sequence as long as each matrix starts with a header card, has all its data cards next, and ends with a blank card.

(C) Ramberg-Osgood Equation

If a run encounters the name RAMOSG in the data matrices, an internal clue (KLUJ) is set and the run will use the three input parameters with the Ramberg-Osgood equation for stress-

(C) Ramberg-Osgood Equation - (Continued)

strain relationships. Note that the second value in TSIGN (TSIGN(2)) must be provided to indicate the effective stress for start of plasticity. Without this value, plasticity is assumed to start at zero stress level.

(D) Stress-Strain Curve

If a run has not found the Ramberg-Osgood parameters, it will calculate Young's Modulus from the first two points in Tables TSIGN and TEPSN (Table of SIGma sub N and Table of EPSilon sub N). TSIGN (2) is also used to define the start of plasticity.

(E) Restart Procedure

If the run being set up is a restart, the input deck can be in several forms. The first control card must have a digit from 5 to 9 in KUU4 so that the program will read tape 8; KUU7 is read from this card. The other factors are carried from the previous run.

The table of steps may be read in again (modified) if the previous run is stopped due to the time estimate, or it may be retained and continued from the previous run. However, if the previous run is stored on tape by using a TAPE card in the step table, then a new step table must be read in.

In either case, the last data card on a restart job must be FINS or blank in columns 7-10. This means a restart data deck will have a minimum of two cards (clue card and a blank), or a maximum of 12 cards (clue card, 10 step cards and a FINS or blank).

(F) Time Estimates

For time estimates, allow 3.5 minutes to compile the Fortran, 1.5 minutes to read the input tape, 2.0 seconds per cycle printed, and 100 to 110 cycles of calculation per minute.

(G) Special Input Formats and Options

The plastic analysis program was set up to use common matrix card formats for the auxiliary tape as well as the system input tape, due to the simplicity of the logic required to switch between the units. Original formats were those used in the GISMO matrix package. The formats used on the auxiliary tape were modified (as an option at "compile time") to accept formats from a later matrix package (COMAP card images) on the auxiliary tape. The option has been extended to include FORMAT matrix package card images on the auxiliary tape only, still using the original card formats on the system input tape. The option is selected when compiling the program. It is not set by clues at execution time. The card formats are illustrated on the sample key punch sheets pgs. 160 and 161.

Internal clue NFC is set to 0 to use the original card formats (#3 and #4) for the auxiliary tape as well as on the system input tape. If NFC = 40, the program will expect COMAP card formats (#43 and #44) only on the auxiliary tape. If NFC = 42, the program will expect FORMAT cards (#45 and #46) only on the auxiliary tape. Note that all these clues, formats and modified lists are provided in the program, with identifying comment cards. It is only necessary to reproduce the desired card for NFC dropping out the C from column 1 (and adding C to the conflicting card) and the program logic will be modified.

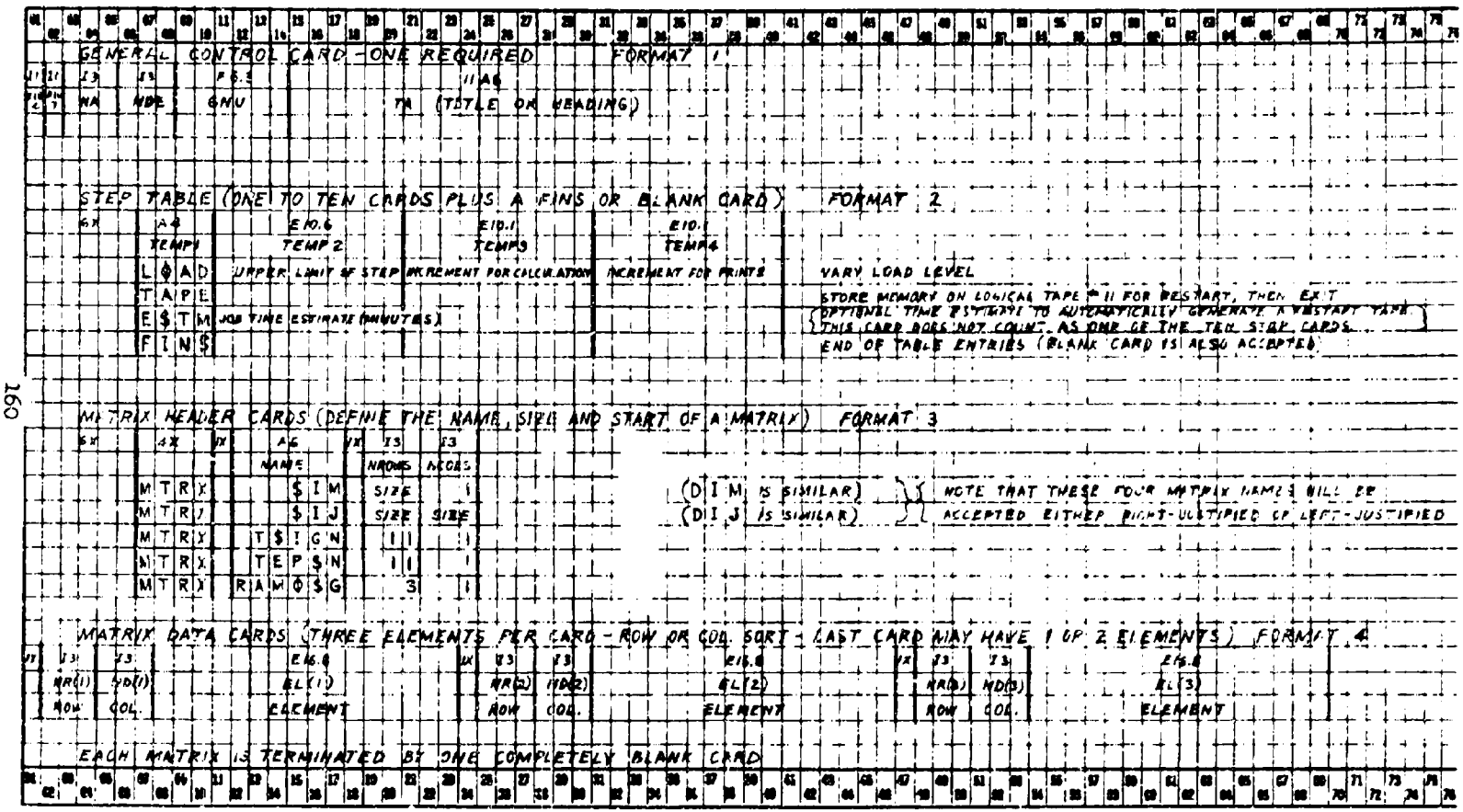

160

FORMATS FOR INELASTIC ANALYSIS PROGRAM

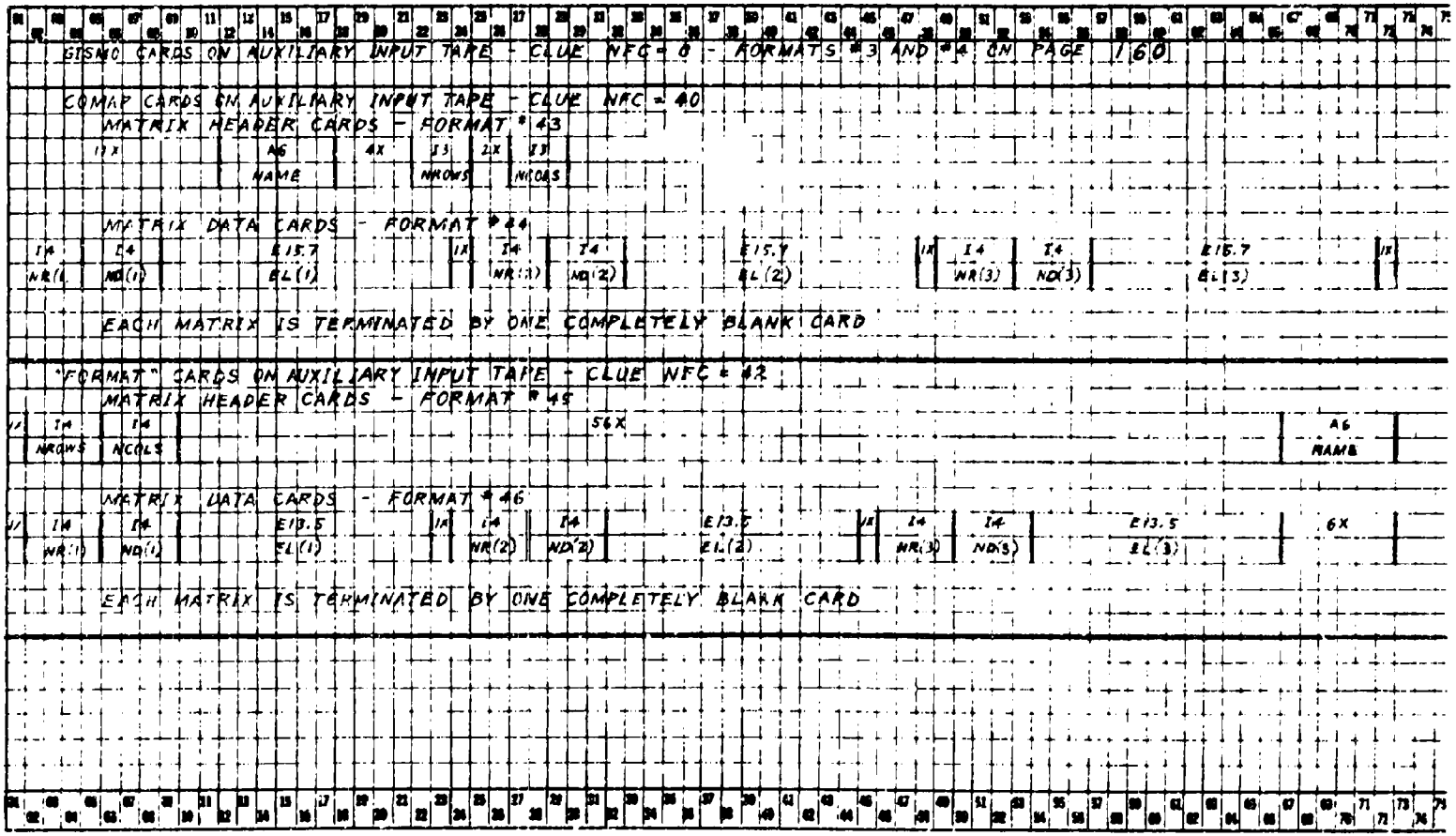

SPECIAL INPUT FORMATS FOR INELASTIC ANALYSIS PROGRAM

APPENDIX B INELASTIC STRUCTURAL ANALYSIS PROGRAM - FLOW CHARTS

The Main Program is Simply an Overlay Caller. The Clue (IEXIT) to Direct the Main Program is Set in Each Overlay, as Determined by the Data and the Execution of the Problem.

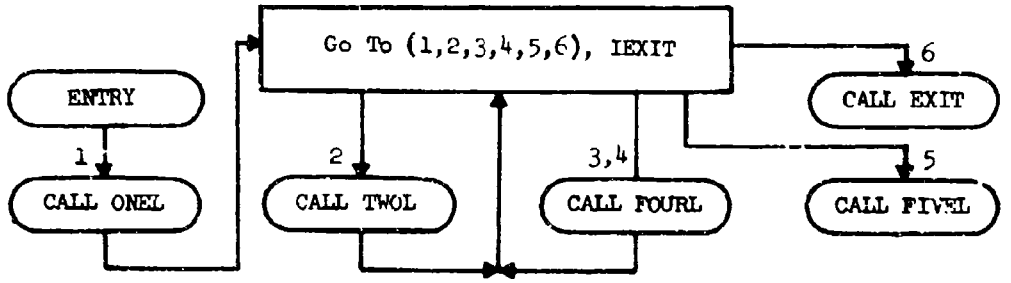

MAIN PROGRAM

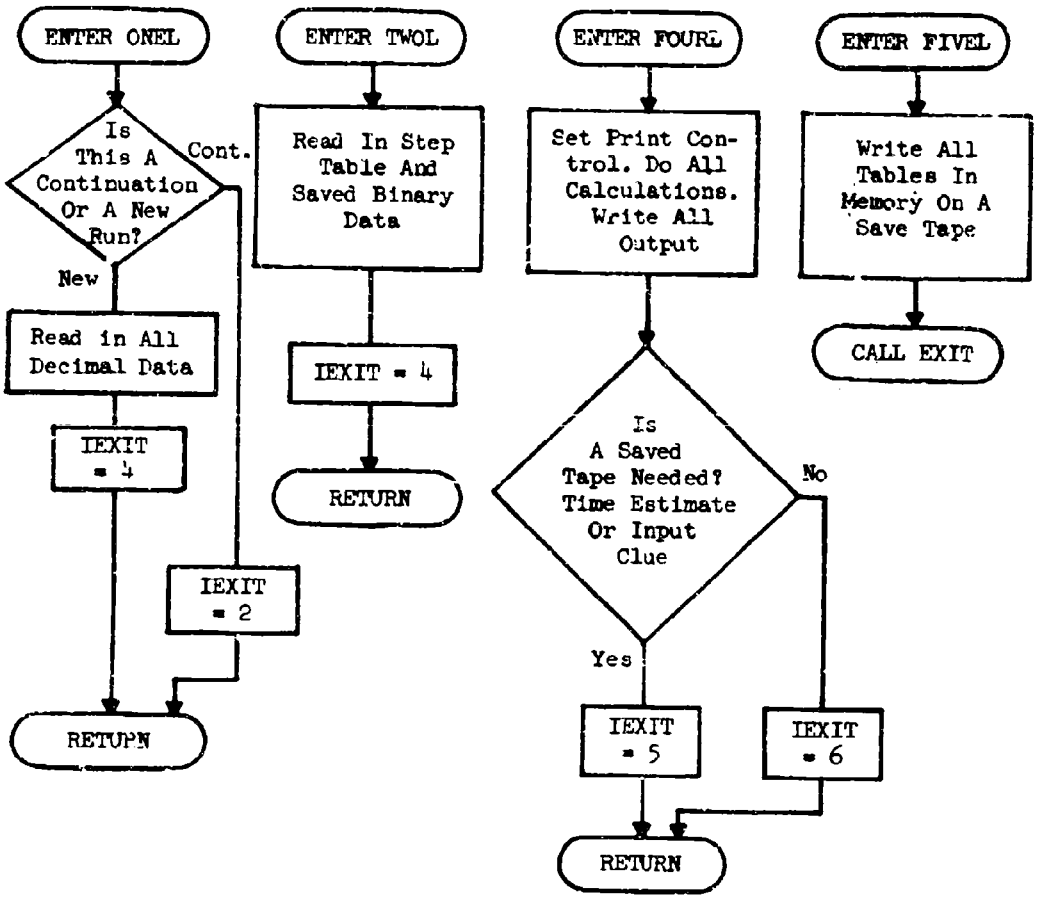

OVERLAY LOGIC

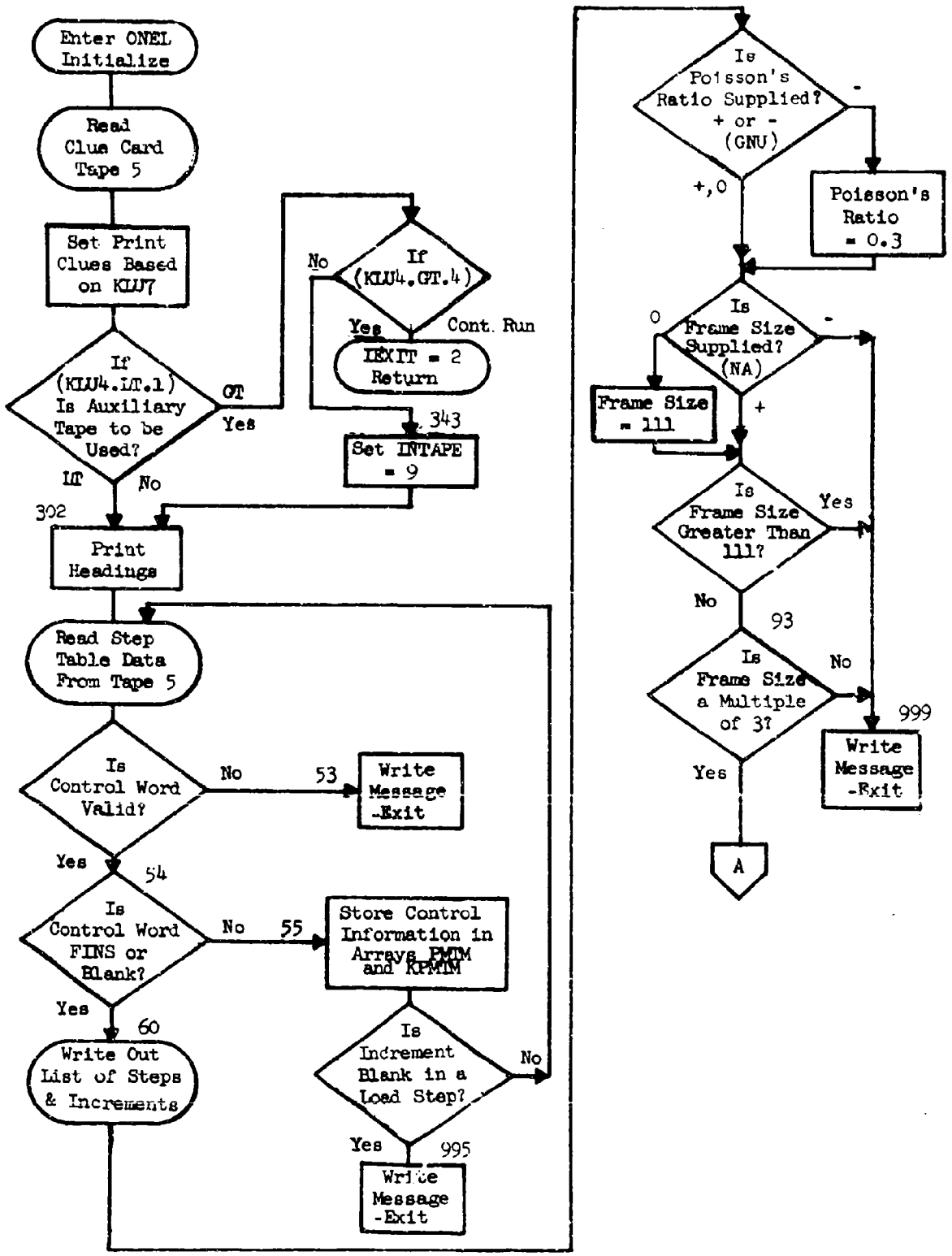
Enter ONEL Initialize
Read Clue Card Tape 5
Set Print Clues Based on KLU7
If (KLU4.LT.1) Is Auxiliary Tape to be Used?
LT
No
GT
Yes
If (KLU4.GT.4)
No
Yes
Cont. Run
IEXIT = 2 Return
343
Set INTAPE = 9
302
Print Headings
Read Step Table Data From Tape 5
Is Control Word Valid?
No
53
Write Message -Exit
Yes
54
Is Control Word FINS or Blank?
No
55
Store Control Information in Arrays PMTM and KPMTM
Yes
60
Write Out List of Steps & Increments
Is Increment Blank in a Load Step?
No
Yes
995
Write Message -Exit
Is Poisson's Ratio Supplied? + or - (GNU)
-
+,0
Poisson's Ratio = 0.3
Is Frame Size Supplied? (NA)
0
-
+
Frame Size = 111
Is Frame Size Greater Than 111?
Yes
No
93
Is Frame Size a Multiple of 3?
No
999
Write Message -Exit
Yes
A

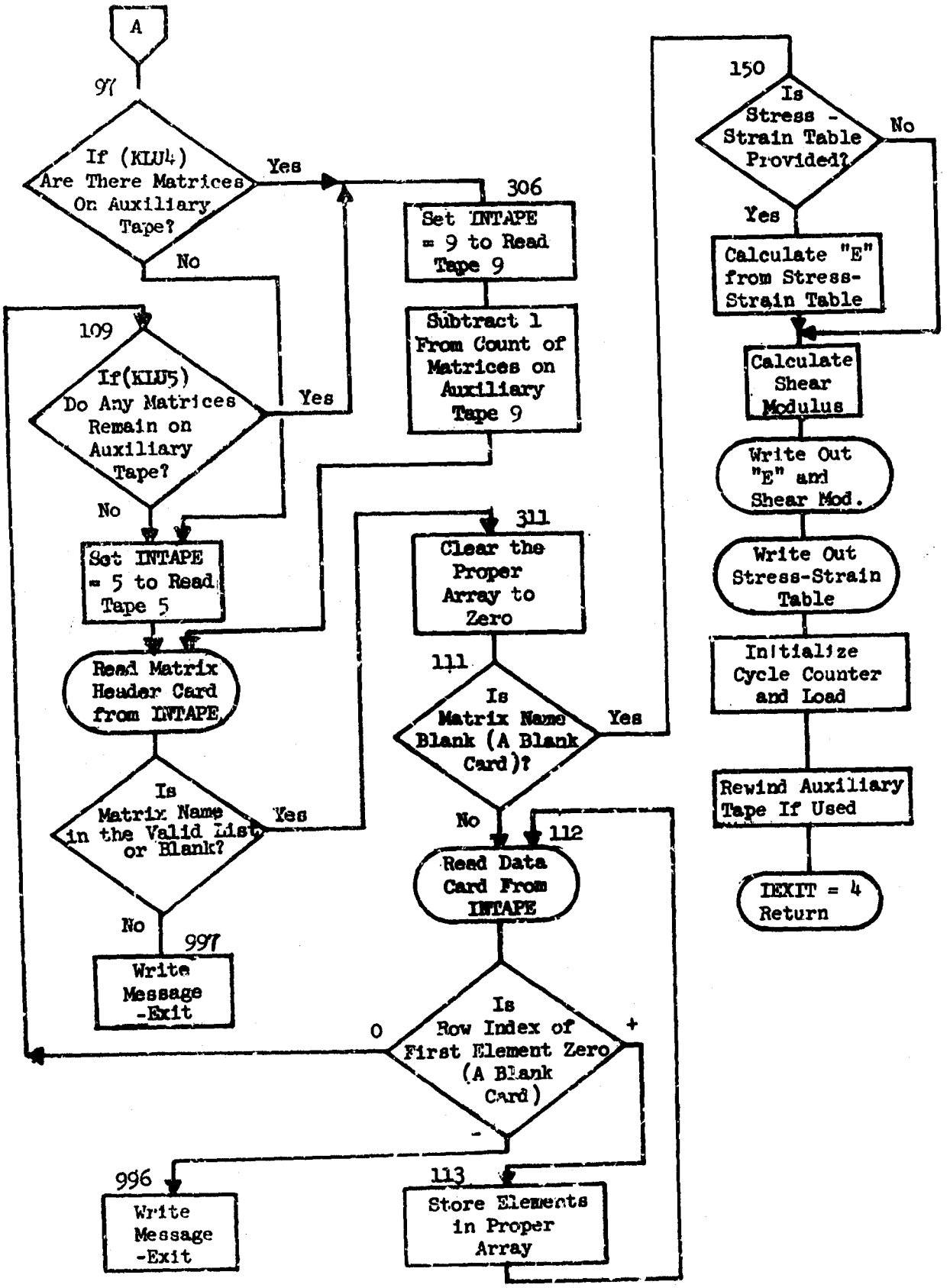
A
97
If (KLU4) Are There Matrices On Auxiliary Tape?
Yes
No
306
Set INTAPE = 9 to Read Tape 9
Subtract 1 From Count of Matrices on Auxiliary Tape 9
109
If(KLU5) Do Any Matrices Remain on Auxiliary Tape?
Yes
No
Set INTAPE = 5 to Read Tape 5
Read Matrix Header Card from INTAPE
Is Matrix Name in the Valid List or Blank?
Yes
No
997
Write Message -Exit
311
Clear the Proper Array to Zero
111
Is Matrix Name Blank (A Blank Card)?
Yes
No
112
Read Data Card From INTAPE
Is Row Index of First Element Zero (A Blank Card)
0
+
-
996
Write Message -Exit
113
Store Elements in Proper Array
150
Is Stress - Strain Table Provided?
No
Yes
Calculate "E" from Stress-Strain Table
Calculate Shear Modulus
Write Out "E" and Shear Mod.
Write Out Stress-Strain Table
Initialize Cycle Counter and Load
Rewind Auxiliary Tape If Used
IEXIT = 4 Return

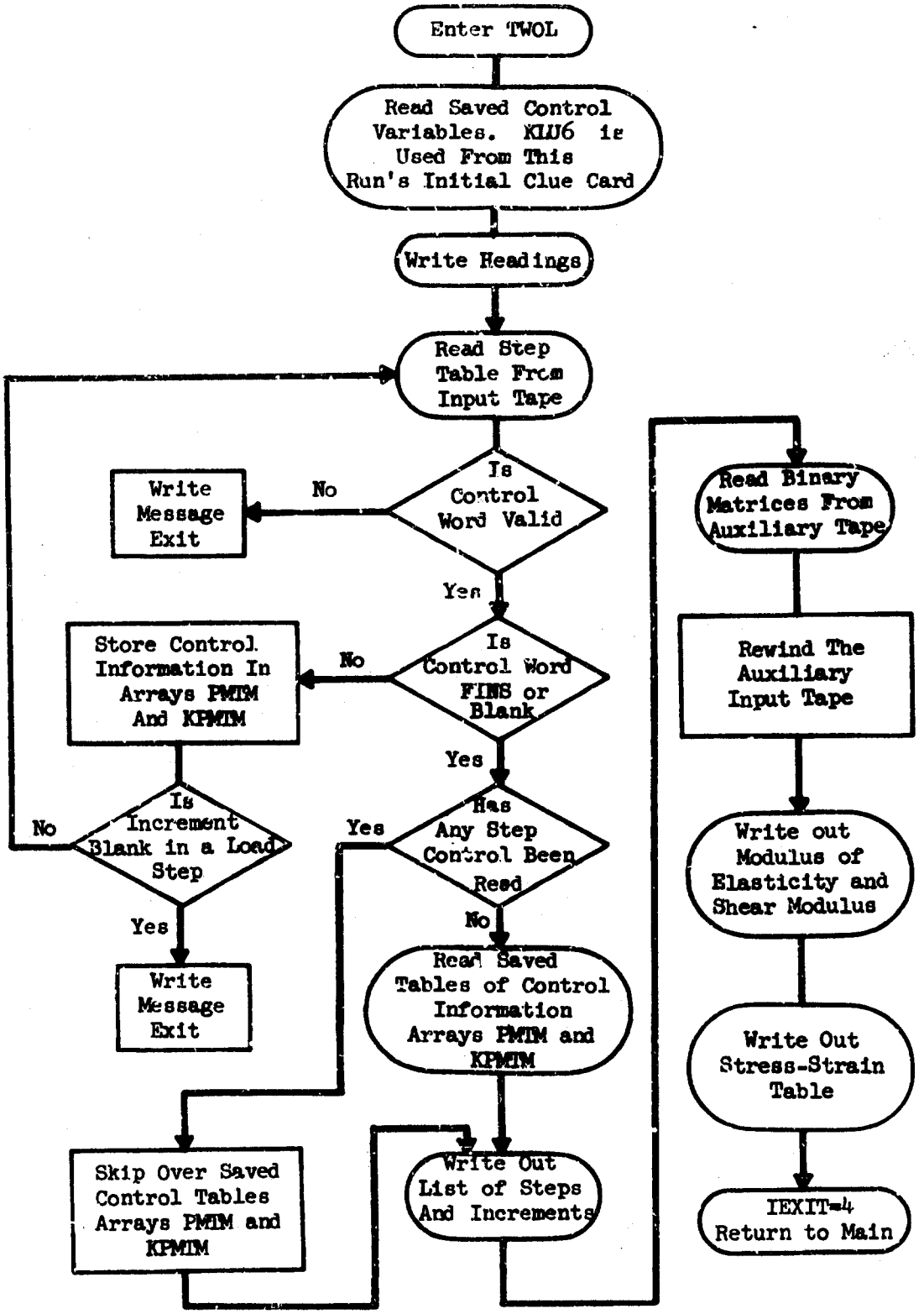
Enter TWOL
Read Saved Control Variables. KLU6 is Used From This Run's Initial Clue Card
Write Headings
Read Step Table From Input Tape
Is Control Word Valid
No
Write Message Exit
Yes
Is Control Word FINS or Blank
No
Store Control Information In Arrays PMTM And KPMTM
Yes
Has Any Step Control Been Read
Yes
No
Is Increment Blank in a Load Step
No
Yes
Write Message Exit
Read Saved Tables of Control Information Arrays PMTM and KPMTM
Skip Over Saved Control Tables Arrays PMTM and KPMTM
Write Out List of Steps And Increments
Read Binary Matrices From Auxiliary Tape
Rewind The Auxiliary Input Tape
Write out Modulus of Elasticity and Shear Modulus
Write Out Stress-Strain Table
IEXIT=4 Return to Main

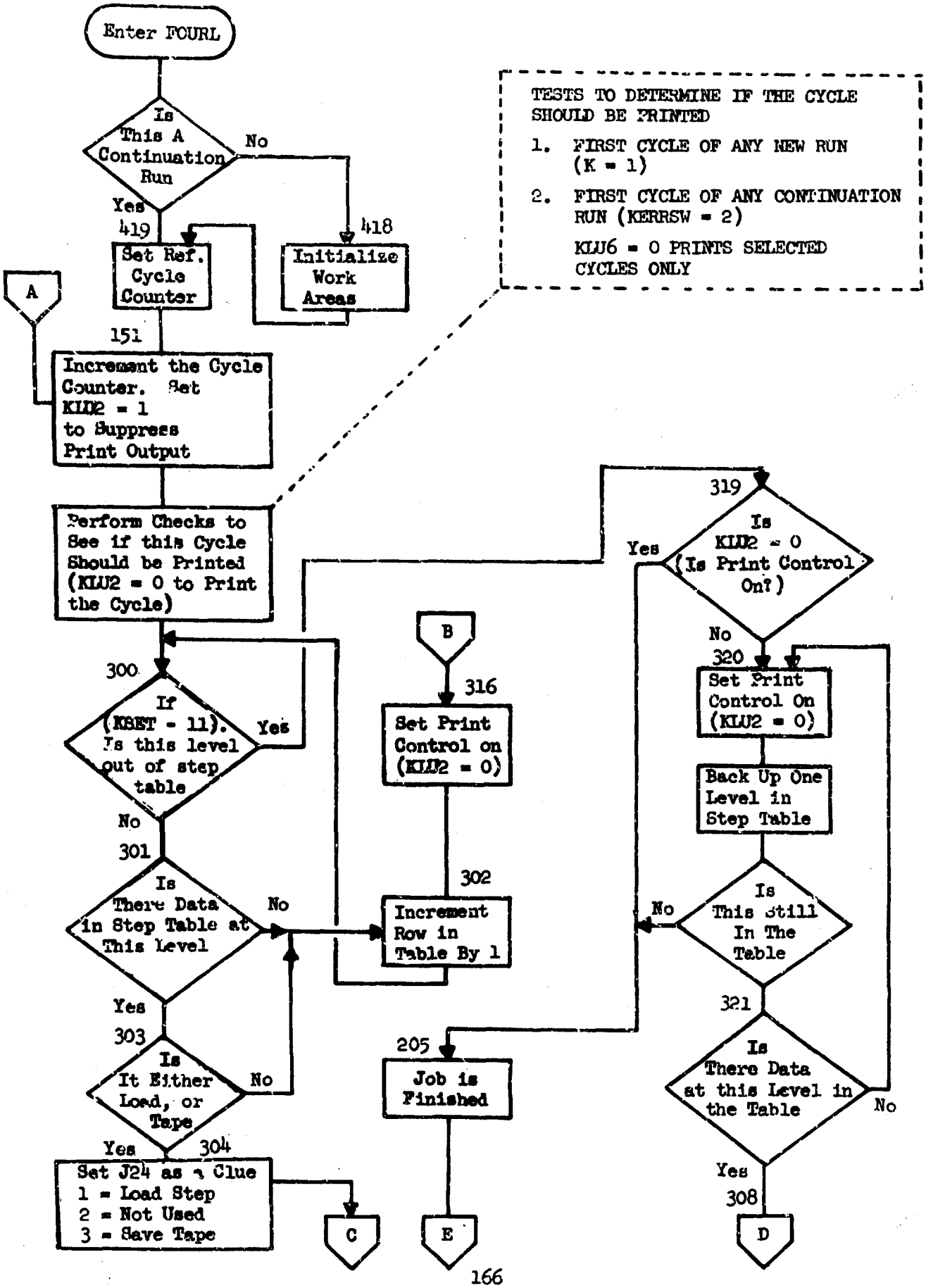
Enter FOURL
Is This A Continuation Run
No
Yes
418
Initialize Work Areas
419
Set Ref. Cycle Counter
A
151
Increment the Cycle Counter. Set KUU2 = 1 to Suppress Print Output
Perform Checks to See if this Cycle Should be Printed (KUU2 = 0 to Print the Cycle)
TESTS TO DETERMINE IF THE CYCLE SHOULD BE PRINTED
1. FIRST CYCLE OF ANY NEW RUN (K = 1)
2. FIRST CYCLE OF ANY CONTINUATION RUN (KERRSW = 2)
KUU6 = 0 PRINTS SELECTED CYCLES ONLY
300
If (KSET - 11). Is this level out of step table
Yes
No
301
Is There Data in Step Table at This Level
No
Yes
303
Is It Either Load, or Tape
No
Yes
304
Set J24 as a Clue
1 = Load Step
2 = Not Used
3 = Save Tape
C
B
316
Set Print Control on (KUU2 = 0)
302
Increment Row in Table By 1
205
Job is Finished
E
319
Is KUU2 = 0 (Is Print Control On?)
Yes
No
320
Set Print Control On (KUU2 = 0)
Back Up One Level in Step Table
Is This Still In The Table
No
321
Is There Data at this Level in the Table
No
Yes
308
D

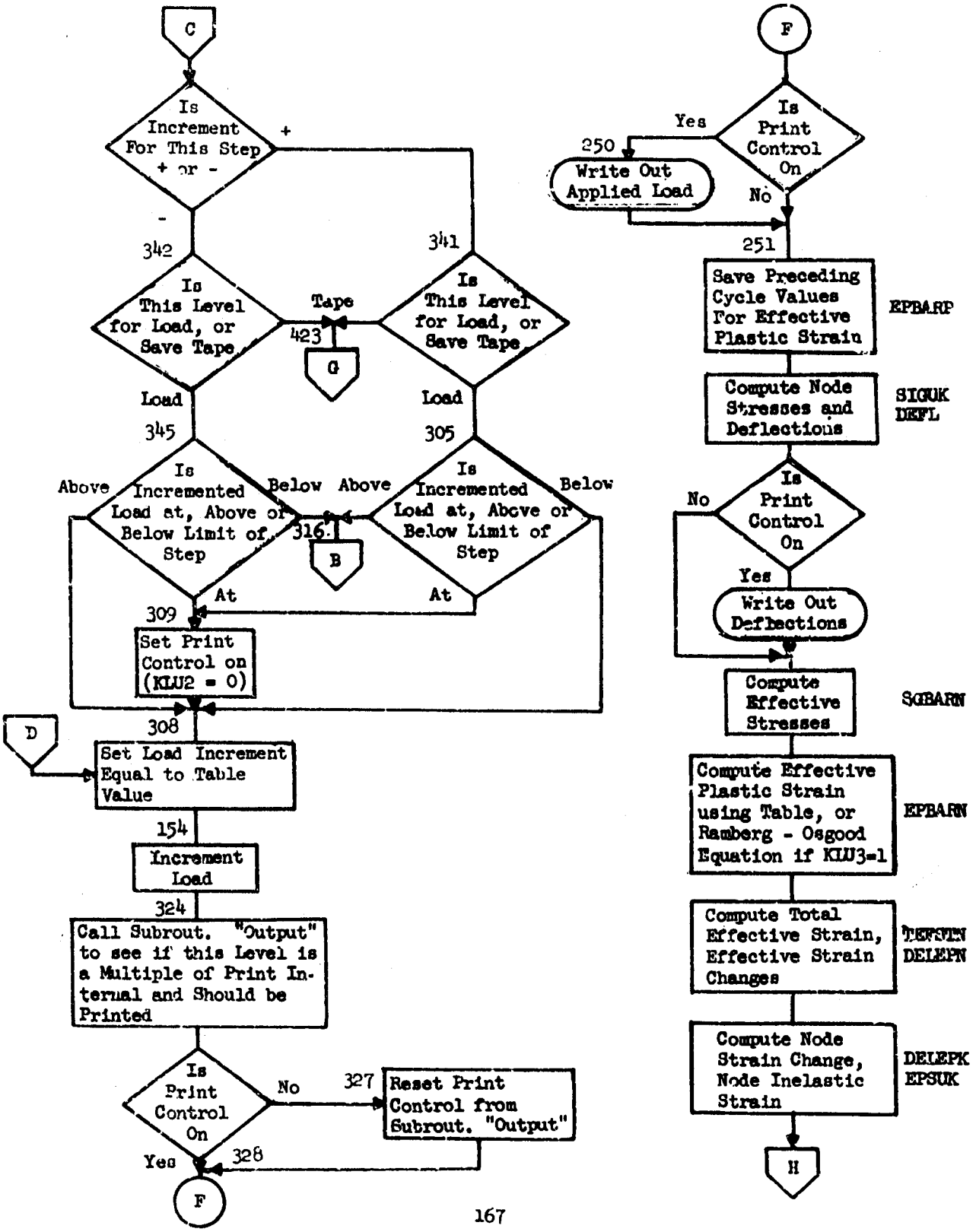
C
Is Increment For This Step + or -
+
-
342
341
Is This Level for Load, or Save Tape
Tape
423
G
Is This Level for Load, or Save Tape
Load
Load
345
305
Is Incremented Load at, Above or Below Limit of Step
Above
Below
316
B
Above
Below
Is Incremented Load at, Above or Below Limit of Step
At
At
309
Set Print Control on (KUU2 = 0)
D
308
Set Load Increment Equal to Table Value
154
Increment Load
324
Call Subrout. "Output" to see if this Level is a Multiple of Print Interval and Should be Printed
Is Print Control On
No
327
Reset Print Control from Subrout. "Output"
Yes
328
F
F
Is Print Control On
Yes
250
Write Out Applied Load
No
251
Save Preceding Cycle Values For Effective Plastic Strain
EPBARP
Compute Node Stresses and Deflections
SIGUK
DEFL
Is Print Control On
No
Yes
Write Out Deflections
Compute Effective Stresses
SGBARN
Compute Effective Plastic Strain using Table, or Ramberg - Osgood Equation if KUU3=1
EPBARN
Compute Total Effective Strain, Effective Strain Changes
DEPSTN
DELEPN
Compute Node Strain Change, Node Inelastic Strain
DELEPK
EPSUK
H

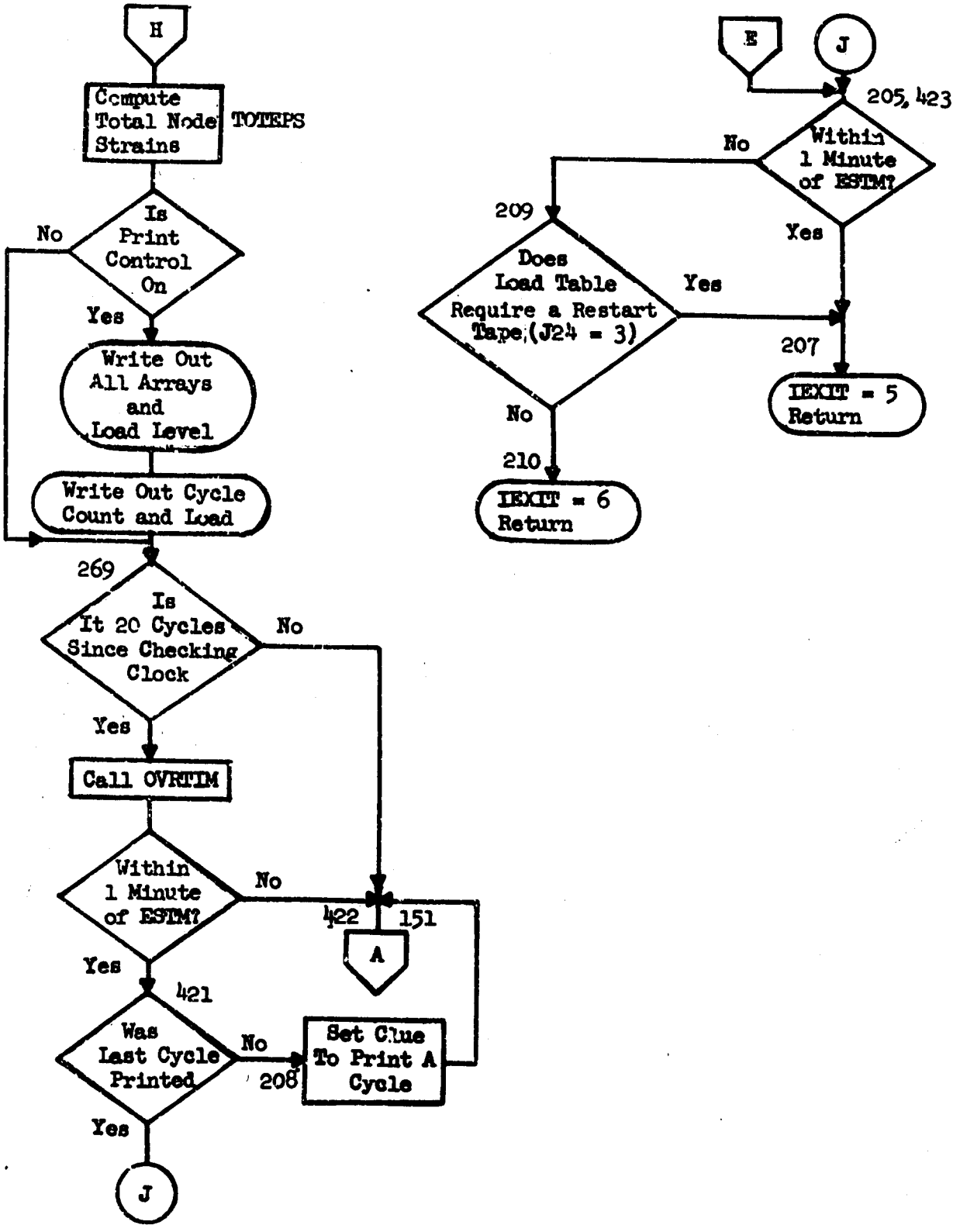
H
Compute Total Node Strains
TOTEPS
Is Print Control On
No
Yes
Write Out All Arrays and Load Level
Write Out Cycle Count and Load
269
Is It 20 Cycles Since Checking Clock
No
Yes
Call OVRTIM
Within 1 Minute of ESTM?
No
422
151
A
Yes
421
Was Last Cycle Printed
No
208
Set Clue To Print A Cycle
Yes
J
E
J
205, 423
Within 1 Minute of ESTM?
No
Yes
209
Does Load Table Require a Restart Tape (J24 = 3)
Yes
207
IEXIT = 5
Return
No
210
IEXIT = 6
Return

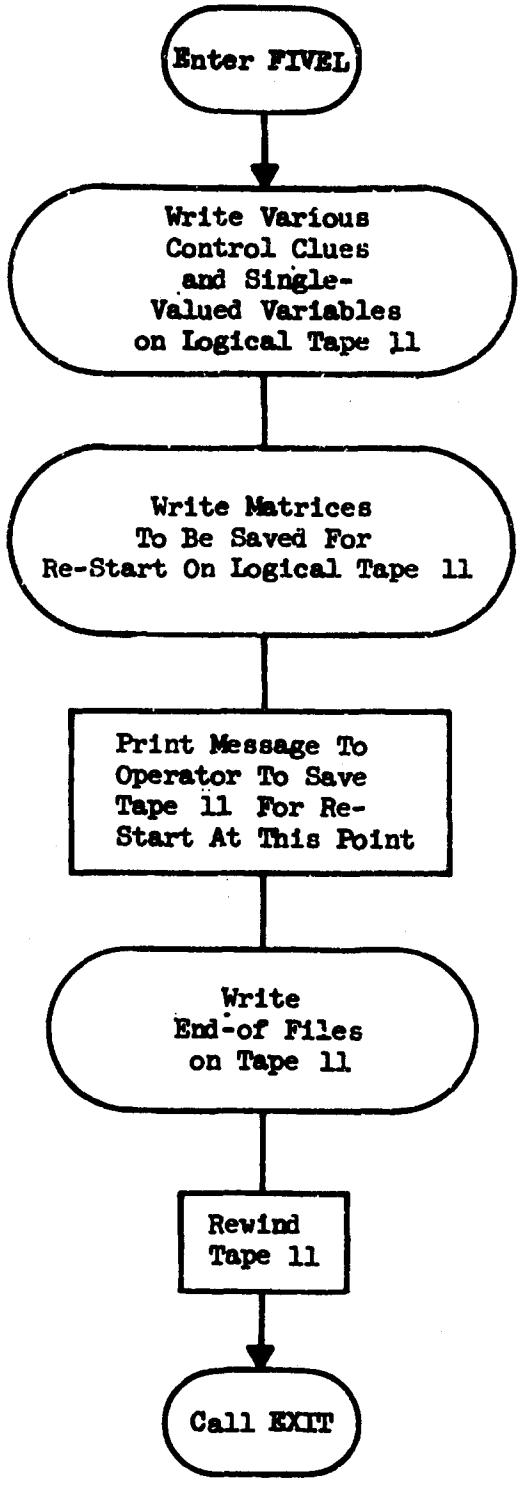
Enter FIVEL
Write Various Control Clues and Single-Valued Variables on Logical Tape 11
Write Matrices To Be Saved For Re-Start On Logical Tape 11
Print Message To Operator To Save Tape 11 For Re-Start At This Point
Write End-of Files on Tape 11
Rewind Tape 11
Call EXIT

APPENDIX C FORTRAN LISTING OF INELASTIC STRUCTURAL ANALYSIS PROGRAM

```
$GROUP          OPNCT=01,BUFCT=001,'UNIT04','UNIT08','UNIT10'
$GROUP          OPNCT=01,BUFCT=001,'UNIT01','UNIT02','UNIT11'
$*      TAPE 08 IS USED FOR A BINARY INPUT TAPE (SAVED FROM PREVIOUS RUN)
$IBMAP  TAPE08
        ENTRY   .UN08.
.UN08.  PZE     UNIT08
UNIT08  FILE    ,LB3,MOUNT,INPUT,BLK=256,BIN
        END
$*      TAPE 09 IS USED FOR A BCD MATRIX INPUT TAPE (AUXILIARY TAPE)
$IBMAP  TAPE09
        ENTRY   .UN09.
.UN09.  PZE     UNIT09
UNIT09  FILE    ,CK1,MOUNT,INPUT,BLK=14,BCD
        END
$*      TAPE 11 IS USED FOR A BINARY SAVE TAPE (FOR CONTINUATION RUN)
$IBMAP  TAPE11
        ENTRY   .UN11.
.UN11.  PZE     UNIT11
UNIT11  FILE    ,LB4,READY,OUTPUT,BLK=256,BIN
        END
```

APPENDIX C FORTRAN LISTING OF INELASTIC STRUCTURAL ANALYSIS PROGRAM

```
$GROUP          OPNCT=01,BUFCT=001,'UNIT04','UNIT08','UNIT10'
$GROUP          OPNCT=01,BUFCT=001,'UNIT01','UNIT02','UNIT11'
$*      TAPE 08 IS USED FOR A BINARY INPUT TAPE (SAVED FROM PREVIOUS RUN)
$IBMAP  TAPE08
        ENTRY   .UN08.
.UN08.  PZE     UNIT08
UNIT08  FILE    ,LB3,MOUNT,INPUT,BLK=256,BIN
        END
$*      TAPE 09 IS USED FOR A BCD MATRIX INPUT TAPE (AUXILIARY TAPE)
$IBMAP  TAPE09
        ENTRY   .UN09.
.UN09.  PZE     UNIT09
UNIT09  FILE    ,CK1,MOUNT,INPUT,BLK=14,BCD
        END
$*      TAPE 11 IS USED FOR A BINARY SAVE TAPE (FOR CONTINUATION RUN)
$IBMAP  TAPE11
        ENTRY   .UN11.
.UN11.  PZE     UNIT11
UNIT11  FILE    ,LB4,READY,OUTPUT,BLK=256,BIN
        END
```

```
C      GRUMMAN AEROSPACE CORP.   DECK NO. 45128   MAIN PROGRAM
C      MATRIX ANALYSIS FOR ISOTROPIC INELASTIC STRUCTURES
C      IN THE PLASTIC REGIME
C
C
C      THIS PROGRAM WRITTEN FOR AIR FORCE CONTRACT F33615-69-C-1263
C
C      * * *                  TABLE OF SYMBOLS USED                  * * *
C
C           * * ARRAYS * *
C      DEFL   - MATRIX OF NODE DEFLECTIONS
C      DELEPK - MATRIX OF NODE STRAIN CHANGES (DELTA EPSILON)
C               FOR THE X AND Y DIRECTIONS, AND THE SHEAR STRAIN CHANGE
C      DELEPN - MATRIX OF EFFECTIVE INELASTIC STRAIN CHANGES
C      DIJ    - MATRIX OF DEFLECTIONS FOR MEMBER STRAINS
C      DIN    - MATRIX OF DEFLECTIONS FOR APPLIED LOADS
C      EPBARN - MATRIX OF EFFECTIVE INELASTIC STRAINS (EPSILON BAR SUB N)
C               FOR K-TH CYCLE
C      EPBARP - MATRIX OF EFFECTIVE INELASTIC STRAINS (EPSILON BAR SUB N)
C               FOR K-1 CYCLE (THE PRECEDING CYCLE)
C      EPSUK  - MATRIX OF NODE PLASTIC STRAINS (EPSILON SUB U) FOR THE
C               X, Y AND SHEAR STRAINS, FOR THE K-TH CYCLE
C      KPNTN  - TABLE OF CONTROL CLUES (LOAD STEP, WRITE SAVE
C               TAPE)   READ-IN CONTROL INFORMATION USED WITH PNTN
C      PNTN   - TABLE OF LOAD INCREMENTS, PRINT CONTROL INCREMENTS AND
C               UPPER LOAD LEVEL PER STEP (CONTROL INFORMATION)
C      SGBARN - MATRIX OF EFFECTIVE NODE STRESSES FOR LAST CYCLE THAT
C               SHOWED AN INCREASE AT A PARTICULAR NODE
C      SGBARN - MATRIX OF EFFECTIVE NODE STRESSES FOR CURRENT CYCLE
C      SGBARP - MATRIX OF EFFECTIVE NODE STRESSES FOR PREVIOUS CYCLE
C      SIGUK  - MATRIX OF NODE STRESSES (SIGMA SUB U) FOR K-TH CYCLE
C      SIJ    - MATRIX OF STRESSES FOR MEMBER STRAINS
C      SIN    - MATRIX OF STRESSES FOR APPLIED LOADS
C      TEFSTN - MATRIX OF TOTAL EFFECTIVE STRAINS
C      TEPSN  - TABLE OF STRAIN VALUES DEFINING THE STRESS-STRAIN CURVE
C      TOTEPS - MATRIX OF TOTAL NODE STRAINS
C      TSIGN  - TABLE OF STRESS LEVELS DEFINING THE STRESS-STRAIN CURVE
C
C           * * VARIABLES AND CLUES * *
C      E      - MODULUS OF ELASTICITY
C      EXP    - INPUT EXPONENT FOR RAMBERG-OSGOOD EQUATION
C      GNU    - POISSONS RATIO
C      INTAPE - THE DATA INPUT TAPE (MAY BE AN AUXILIARY TAPE OR
C               THE SYSTEM INPUT TAPE - VARIES DURING INPUT PHASE)
C      K      - THE CYCLE COUNTER
C      KERRSW - CLUE USED FOR TEMPORARY INDICATOR BETWEEN LINKS
C               - ALSO AS AN ERROR INDICATOR FOR LINK 1 ONLY
C      KLU3   - CLUE INDICATING USE OF RAMBERG-OSGOOD EQUATION
C      KLU4   - CLUE INDICATING TOTAL COUNT OF MATRICES ON AUXILIARY TAPE
C      KLU5   - CLUE INDICATING MATRICES STILL NOT READ FROM AUXIL. TAPE
C      KLU6   - CLUE FOR PRINT CONTROL (WHICH CYCLES)
C      KLU7   - INPUT CLUE FOR PRINT CONTROL (1 TO PRINT ALL CYCLES)
C      KSET   - CLUE FOR THE LOAD LEVEL CURRENTLY IN USE
C      NA     - 3 TIMES THE NODE COUNT (INPUT)
C      NC     - NUMBER OF NODES
```

```
C      NAUX    - THE AUXILIARY MATRIX DATA INPUT TAPE
C      NIN     - THE SYSTEM INPUT TAPE
C      NOUT    - THE SYSTEM PRINT OUTPUT TAPE
C      PM      - CURRENT LOAD LEVEL
C      SHRMOD  - SHEAR MODULUS
C      S7      - INPUT REFERENCE STRESS FOR RAMBERG-OSGOOD EQUATION
C
C      OUTPUT - SUBROUTINE TO CONTROL PRINTING AT VARYING LOAD LEVELS
C
C      ELASTIC UNLOADING (FOLLOWS HOOKES LAW WHEN UNLOADING)
C
       DIMENSION TALF12(11),TALF23(11),TALF31(11),TALF44(11)
       DIMENSION AL1212(34),AL1223(34),AL1231(34),ALFA44(34)
       DIMENSION PMTM(10,3),KPMTM(10),SIM(102),SIJ(102,102),TSIGN(11)
       DIMENSION TEPSN(11),SIGUK(102),EPSUK(102),SGBARN(34),SGBARP(34)
       DIMENSION SGBARN(34),EPBARN(34),EPBARP(34),DELEPN(34)
       DIMENSION            DIM(102),DIJ(102,102),DEFL(102)
       COMMON /COMA/  KLU3,KLU4,KLU5,KLU6,NA,NC,NDE,INTAPE,NIN,NOUT,NAUX
      2 , K       , KERRSW , KSET    , RUNEST , E       , EXP     , S7
      3 , GNU     , SHRMOD , PM
      4 , PMTM    , KPMTM  , SIM     , DIM    , DEFL    , TSIGN   , TEPSN
      5 , TALF12  , TALF23 , TALF31  , TALF44 , AL1212  , AL1223  , AL1231
      6 , ALFA44  , SIGUK  , EPSUK   , SGBARN , SGBARP  , SGBARM  , EPBARN
      7 , EPBARP  , DELEPN , SIJ     , DIJ
      1 CALL ONEL(IEXIT)
        GO TO 10
      2 CALL TWOL(IEXIT)
        GO TO 10
      3 CONTINUE
      4 CALL FOURL(IEXIT)
        GO TO 10
      5 CALL FIVEL(IEXIT)
     10 CONTINUE
        WRITE(6,11) IEXIT
        GO TO (1,2,3,4,5,6) ,IEXIT
      6 CONTINUE
        CALL EXIT
     11 FORMAT(10H1 IEXIT = ,I2)
        STOP
         END
```

Note: Subroutine OVRTIM, listed on Page 190, is put in the root segment of the program, after the main program, so it will be accessable to all its callers.

```
      SUBROUTINE ONEL(IEXIT)
C     GRUMMAN AEROSPACE CORP.   DECK NO. 45128   LINK 1
      DIMENSION TALF12(11),TALF23(11),TALF31(11),TALF44(11)
      DIMENSION AL1212(34),AL1223(34),AL1231(34),ALFA44(34)
      DIMENSION PMTM(10,3),KPMTM(10),SIM(102),SIJ(102,102),TSIGN(11)
      DIMENSION TEPSN(11),SIGUK(102),EPSUK(102),SGBARN(34),SGBARP(34)
      DIMENSION SGBARM(34),EPBARN(34),EPBARP(34),DELEPN(34)
      DIMENSION           DIM(102),DIJ(102,102),DEFL(102)
      DIMENSION BL(6),ID(12),NR(3),ND(3),EL(3),TA(11)
      DIMENSION PSTEP(3)
      DIMENSION NFA(1),NFB(1)
      COMMON /COMA/  KLU3,KLU4,KLU5,KLU6,NA,NC,NDE,INTAPE,NIN,NOUT,NAUX
     2 , K       , KERRSW , KSET    , RUNEST , E       , EXP     , S7
     3 , GNU     , SHRMOD , PM
     4 , PMTM    , KPMTM  , SIM     , DIM    , DEFL    , TSIGN   , TEPSN
     5 , TALF12  , TALF23 , TALF31  , TALF44 , AL1212  , AL1223  , AL1231
     6 , ALFA44  , SIGUK  , EPSUK   , SGBARN , SGBARP  , SGBARM  , EPBARN
     7 , EPBARP  , DELEPN , SIJ     , DIJ
      DATA BL/36HLOAD   VOID   TAPE   FINS          ESTM  /
      DATA ID/ 72H    SIM    SIJ TSIGN TEPSN    DIM    DIJRAMOSG       SIM
     1SIJ    DIM    DIJ    /
      KERRSW = 1
      INTAPE = NIN
      NFA(1)  = 3
      NFB(1)  = 4
C
C     * * SELECT CLUE NFC AS APPROPRIATE WHEN COMPILING          * *
C     NFC  =  0 FOR GISMO CARD FORMATS ON AUXIL. TAPE (SIM,SIJ,DIM,DIJ)
C     NFC  =  0
C     NFC  = 40 FOR COMAP FORMAT CARDS WHEN DEBUGGING (SIM,SIJ,DIM,DIJ)
      NFC  = 40
C     NFC  = 42 FOR FORMAT PACKAGE DECIMAL MATRIX CARD FORMATS ON
C               AUXILIARY TAPE 9 ONLY (SIM,SIJ,DIM,DIJ) FOR AFFDL
C     NFC  = 42
C
C     KLU3 = 1 WILL INDICATE USE OF THE RAMBERG-OSGOOD EQUATION
C              FOR STRAINS, NOT A TABLE INTERPOLATION
      KLU3 = 0
      KLU5 = 0
      KLU6 = 0
      PSTEP(1) = 0.0
      PSTEP(2) = 0.0
      PSTEP(3) = 0.0
      RUNEST = 120.
      K = 0
      K000FX = 3
C     TIMING ROUTINE DISABLED
C     IT = ICHRON(K000FX)
      DO 51 J22=1,10
   51 KPMTM(J22) = 0
      LROW = 0
      READ (NIN,1) KLU4,KLU7,NA,NDE,GNU,(TA(I),I=1,11)

      WRITE (NOUT,21) (TA(I),I=1,11)
C     KLU7 (INPUT) = 0 TO PRINT ON SELECTED CYCLES
```

```
C       KLU7 (INPUT) = 1 TO PRINT ON ALL CYCLES
        IF(KLU7)384,384,382
  382   KLU6 = 1
C       KLU6 (OUTPUT) = 1 TO PRINT EACH CYCLE. 0 TO PRINT SELECTED CYCLES
  384   CONTINUE
C       KLU4 = 5 TO 9 FOR A CONTINUATION RUN
C            = 1 TO 4 FOR INPUT ON AUXILIARY MATRIX TAPE NAUX (9)
C       DECIMAL INPUT CARDS MUST ALWAYS BE IN INPUT STREAM
C       DECIMAL INPUT TAPE MOUNTS ON LOGICAL UNIT NAUX (9)
        IF(KLU4.LT.1) GO TO 302
        IF(KLU4.GT.4) GO TO 344
        GO TO 343
  344   CONTINUE
C       SAVED TAPE FROM PREVIOUS RUN OF INELASTIC PLATE
C       THIS RUN IS A CONTINUATION
        IEXIT = 2
        RETURN
  343   CONTINUE
C       SEPARATE MATRIX INPUT TAPE - NOT IN INPUT STREAM
C       THIS RUN IS A NEW ONE
        INTAPE = NAUX
        KLU5 = KLU4
  302   CONTINUE
C       NEW RUN - ALL THE INPUT IS DECIMAL IN THE INPUT STREAM
        WRITE (NOUT,9)
   52   READ (NIN,2) TEMP1,TEMP2,TEMP3,TEMP4
        LROW = LROW + 1
        DO 53 J22=1,6
        IF(TEMP1.EQ.BL(J22)) GO TO 54
   53   CONTINUE
C       BAD CONTROL CARD
        WRITE (NOUT,12) LROW
        WRITE (NOUT,2) TEMP1,TEMP2,TEMP3,TEMP4
        GO TO 998
   54   GO TO (55,66,55,60,60,65),J22
   55   IF(LROW-10)56,56,53
C       KPMTM( N ) = 1 FOR A LOAD STEP
C       KPMTM( N ) = 2 NOT USED
C       KPMTM( N ) = 3 TO DUMP MEMORY INTO A SAVE TAPE
C       PMTM (N,1) = UPPER LIMIT OF STEP
C       PMTM (N,2) = INTERVAL (INCREMENT) FOR CALCULATION
C       PMTM (N,3) = INTERVAL (INCREMENT) FOR PRINT OUTPUT
   56   KPMTM(LROW) = J22
        PMTM(LROW,1)= TEMP2
        TEMP5       = TEMP2-PSTEP(J22)
        PMTM(LROW,2)= SIGN(TEMP3,TEMP5)
        PSTEP(J22)  = TEMP2
        IF(PPTM(LROW,2))57,63,57
   63   GO TO(995,995,57),J22
   57   CONTINUE
        PMTM(LROW,3)= TEMP4
        GO TO 52
   65   RUNEST = TEMP2 - 1.0
   66   LROW   = LROW - 1
        GO TO 52
   60   CONTINUE
```

```
      DO 361 J23 = 1,10
      IF(KPMTM(J23))361,361,362
  362 IF(KPMTM(J23)-4)363,361,361
  363 J24 = KPMTM(J23)
      GO TO (364,364,368),J24
  364 WRITE (NOUT,22) PMTM(J23,2),PMTM(J23,1)
      IF(PMTM(J23,3))361,361,365
  365 WRITE (NOUT,23) PMTM(J23,3)
      GO TO 361
  368 WRITE (NOUT,27)
  361 CONTINUE
      IF(GNU)86,87,87
   86 GNU = .3
   87 CONTINUE
      IF(NA)999,91,92
   91 NA  = 102
   92 IF(NA-102) 93,93,999
   93 CONTINUE
   96 IF(NA-3*(NA/3))959,97,999
   97 NC  = NA/3
      DO 303 I21 = 1,11
      TSIGN(I21) = 0.0
  303 TEPSN(I21) = 0.0
      IF(KLU4) 308,308,306
  306 CONTINUE
      INTAPE = NAUX
      KLU5   = KLU5 - 1
C     STATEMENT 108 READS INPUT STREAM OR AUXILIARY TAPE NAUX (9)
  108 CONTINUE
      IF(INTAPE.EQ.NIN) GO TO 1108
      IF(NFC-40) 1108,2108,3108
C     GISMC FORMAT CARD READING LIST
 1108 READ (INTAPE, 3) NAME,NROWS,NCOLS
      GO TO 1001
C     COMAP FORMAT CARD READING LIST
 2108 READ (INTAPE,43) NAME,NROWS,NCOLS
      GO TO 1001
C     AFFDL FORMAT CARD READING LIST
 3108 READ (INTAPE,45) NROWS,NCOLS,NAME
 1001 CONTINUE
      DO 110 I21 = 1,12
      IF(NAME-ID(I21))110,311,110
  110 CONTINUE
C     BAD INPUT - MATRIX NAME NOT ACCEPTABLE
      GO TO 997
  311 GO TO (321,322,323,324,325,326,472,111,321,322,325,326),I21
  321 DO 331 I1 = 1,NA
  331 SIM(I1) = 0.0
      WRITE (NOUT,20) NAME,NROWS,NCOLS,INTAPE
      IF(NROWS.NE.NA) KERRSW=2
      IF(NCOLS.NE.1) GO TO 990
      GO TO 111
  322 DO 332 I1 = 1,NA
      DO 332 I2 = 1,NA
  332 SIJ(I1,I2) = 0.0
      WRITE (NOUT,20) NAME,NROWS,NCOLS,INTAPE
```

```
      IF(NROWS.EQ.NCOLS) GO TO 433
      WRITE (NOUT,33) NAME,NROWS,NCOLS
      KERRSW = 2
      GO TO 468
  433 CONTINUE
  468 CONTINUE
      GO TO 111
  323 DO 333 I1 = 1,11
  333 TSIGN(I1) = 0.0
      GO TO 111
  324 DO 334 I1 = 1,11
  334 TEPSN(I1) = 0.0
      GO TO 111
  325 DO 335 I1 = 1,NROWS
  335 DIM(I1) = 0.0
      WRITE (NOUT,20) NAME,NROWS,NCOLS,INTAPE
      IF(NCOLS.NE.1) GO TO 590
      IF(NROWS.EQ.NDE) GO TO 449
      KERRSW = 2
      WRITE (NOUT,40) NROWS,NAME,NDE
  449 CONTINUE
      GO TO 111
  326 DO 336 I1 = 1,NROWS
      DO 336 I2 = 1,NCOLS
  336 DIJ(I1,I2)= 0.0
      WRITE (NOUT,20) NAME,NROWS,NCOLS,INTAPE
      IF(NROWS.EQ.NDE) GO TO 461
      KERRSW = 2
      WRITE (NOUT,40) NROWS,NAME,NDE
  461 CONTINUE
      GO TO 111
  472 S7   = 0.0
      EXP  = 0.0
      E    = 0.0
      KLU3= 1
      WRITE (NOUT,37)
      GO TO 111
  111 IF(I21.EQ.8) GO TO 150
  112 CONTINUE
      IF(INTAPE.EQ.NIN) GO TO 1112
      IF(NFC-40) 1112,2112,3112
C     GISMC FORMAT CARD READING LIST
 1112 READ (INTAPE, 4) (NR(I22),ND(I22),EL(I22),I22=1,3)
      GO TO 1002
C     COMAP FORMAT CARD READING LIST
 2112 READ (INTAPE,44) (NR(I22),ND(I22),EL(I22),I22=1,3)
      GO TO 1002
C     AFFDL FORMAT CARD READING LIST
 3112 READ (INTAPE,46) (NR(I22),ND(I22),EL(I22),I22=1,3)
 1002 CONTINUE
      IF(NR(1))996,109,113
  109 IF(KLU5)308,308,306
  308 INTAPE  = NIN
      GO TO 108
  113 GO TO (121,122,125,126,201,202,474,150,121,122,201,202),I21
C     READ IN ARRAY SIGMA-IM
```

```
  121 MROW = NR(1)
      WRITE (NOUT,4) (NR(I22),ND(I22),EL(I22),I22=1,3)
      SIM   (MROW) = EL(1)
      IF(EL(2))127,128,127
  127 MROW = NR(2)
      SIM   (MROW) = EL(2)
  128 IF(EL(3))129,112,129
  129 MROW = NR(3)
      SIM   (MROW) = EL(3)
      GO TO 112
C     READ IN ARRAY SIGMA-IJ
  122 MROW = NR(1)
      MCOL = ND(1)
      SIJ   (MROW,MCOL) = EL(1)
      IF(EL(2))130,131,130
  130 MROW = NR(2)
      MCOL = ND(2)
      SIJ   (MROW,MCOL) = EL(2)
  131 IF(EL(3))132,112,132
  132 MROW = NR(3)
      MCOL = ND(3)
      SIJ   (MROW,MCOL) = EL(3)
      GO TO 112
C     READ IN ARRAY TSIGN (TABLE OF SIGMA BAR N)
  125 MROW = NR(1)
      TSIGN(MROW) = EL(1)
      IF(EL(2))139,140,139
  139 MROW = NR(2)
      TSIGN(MROW) = EL(2)
  140 IF(EL(3))141,112,141
  141 MROW = NR(3)
      TSIGN(MROW) = EL(3)
      GO TO 112
C     READ IN ARRAY TEPSN (TABLE OF EPSILON BAR N)
  126 MROW = NR(1)
      TEPSN(MROW) = EL(1)
      IF(EL(2))142,143,142
  142 MROW = NR(2)
      TEPSN(MROW) = EL(2)
  143 IF(EL(3))144,112,144
  144 MROW = NR(3)
      TEPSN(MROW) = EL(3)
      GO TO 112
C     READ IN ARRAY DIM
  201 MROW = NR(1)
      WRITE (NOUT,4) (NR(I22),ND(I22),EL(I22),I22=1,3)
      DIM(MROW) = EL(1)
      IF(EL(2))221,222,221
  221 MROW = NR(2)
      DIM(MROW) = EL(2)
  222 IF(EL(3))223,112,223
  223 MROW = NR(3)
      DIM(MROW) = EL(3)
      GO TO 112
C     READ IN ARRAY DIJ
  202 MROW = NR(1)
```

```
      MCOL  = ND(1)
      DIJ(MROW,MCOL) = EL(1)
      IF(EL(2))224,225,224
  224 MROW  = NR(2)
      MCOL  = ND(2)
      DIJ(MROW,MCOL) = EL(2)
  225 IF(EL(3))226,112,226
  226 MROW  = NR(3)
      MCOL  = ND(3)
      DIJ(MROW,MCOL) = EL(3)
      GO TO 112
C     READ IN CONSTANTS FOR RAMBERG-OSGOOD EQUATION
  474 S7    = EL(1)
      EXP   = EL(2)
      E     = EL(3)
      WRITE (NOUT,38) S7,EXP,E
      GO TO 112
  150 CONTINUE
C     END OF LOOP THAT READS DECIMAL MATRICES
      IF(KLU4.GE.1) REWIND NAUX
  165 DO 166 I = 1,11
      TALF12(I)= 0.5
      TALF23(I)= 0.5
      TALF31(I)= 0.5
  166 TALF44(I)= 1.0
C *** IF(KLU3.EQ.1) TSIGN(2) = START OF INELASTICITY      *****
C     TSIGN(2) MUST BE SUPPLIED OR THE PROGRAM ASSUMES PLASTICITY
C              STARTS AT ZERO EFFECTIVE STRESS
      IF(KLU3.EQ.1) GO TO 81
      E = TSIGN(2)/TEPSN(2)
      IE = IFIX(E/100.)
      E  = FLOAT(100*IE)
   81 SHRMOD = E/(2.0*(1.0+GNU))
      WRITE (NOUT,5)  E,SHRMOD,GNU
      WRITE (NOUT,6)
      DO 149 I1=1,11
  149 WRITE (NOUT,7) I1,TSIGN(I1),TEPSN(I1)
      K    = 0
      PM   = 0.0
  152 IEXIT = 4
      CALL OVRTIM(KOOOFX)
      IF(KERRSW.EQ.2) GO TO 993
      RETURN
  990 WRITE (NOUT,33) NAME,NROWS,NCOLS
      GO TO 998
  993 WRITE (NOUT,34)
      GO TO 998
  995 WRITE (NOUT,16) LROW
      GO TO 998
  996 CONTINUE
      WRITE (NOUT,14) NAME
      WRITE (NOUT,4) (NR(I22),ND(I22),EL(I22),I22=1,3)
      GO TO 998
  997 CONTINUE
      WRITE (NOUT,13) NAME
  998 IF(KLU4.GE.1) REWIND NAUX
```

```
      CALL EXIT
  999 WRITE (NOUT,11) NA
      GO TO 998
    1 FORMAT(2I1,2I3,F6.3,11A6)
    2 FORMAT(6X,A4,E10.6,E10.1,E10.1)
C   * GISMC CARD FORMATS FOR TAPE 9
    3 FORMAT(11X, A6,1X,2I3)
    4 FORMAT(3(1X,2I3,E16.8)  )
    5 FORMAT(26H1 MODULUS OF ELASTICITY = ,F11.0,4H PSI,6X,16HSHEAR MODU
     1LUS = ,F11.0,4H PSI,3X,5HNU = ,F6.3)
    6 FORMAT(41H0 TABLE OF VALUES FOR STRESS-STRAIN CURVE  //
     15X,29HPOINT  STRESS LEVEL    STRAIN/16X,3HPSI,9X,7HIN./IN.//)
    7 FORMAT(6X,I3,F13.2,F15.8)
    9 FORMAT(//79H THIS   ISOTROPIC RUN USES ELASTIC UNLOADING (HOOKES L
     1AW) WITH STRAIN HARDENING)
   11 FORMAT(10H ERROR NA=I4)
   12 FORMAT(26H ERROR- INCREMENT CARD NO.,I3,5H N.G.)
   13 FORMAT(14H ERROR-MATRIX ,A6)
   14 FORMAT(17H ERROR-NEG.INDEX A6)
   16 FORMAT(33H ERROR-NO INTERVAL-INCREMENT CARD,I3)
   20 FORMAT(//5X,7HMATRIX ,A6,1X,I3,8H ROWS X ,I3,19H COLUMNS FROM TAPE
     1 ,I2)
   21 FORMAT(1H1,29X,11A6)
   22 FORMAT(5X,16HLOAD INCREMENTS ,F9.2,11H POUNDS TO ,F10.2,7H POUNDS)
   23 FORMAT(1H+,61X,15HPRINT OUTPUT EVERY ,F9.2,7H POUNDS)
   27 FORMAT(5X,35HSTORE MEMORY ON TAPE  11, THEN EXIT)
   31 FORMAT(10X,I2)
   33 FORMAT(14H INPUT MATRIX ,A6,2I4,46H ON TAPE IS NEITHER SQUARE NOR
     1A COLUMN VECTOR)
   34 FORMAT(74H INPUT ERROR - INDEX IN INPUT   MATRIX DOES NOT MATCH CL
     1UE IN CONTROL CARD)
   37 FORMAT(//5X,24HRAMBERG-OSGOOD CONSTANTS)
   38 FORMAT(5X,22HINPUT REFERENCE STRESS,E16.7/5X,14HINPUT EXPONENT,
     1F10.5/5X,15HYOUNG'S MODULUS,F11.0)
   40 FORMAT(//5X,I3,16H ROWS IN MATRIX ,A6,15H DOES NOT MATCH,I4,
     119H ROWS IN INPUT CLUE/5X,21HRUN WILL NOT CONTINUE//)
C   * COMAP CARD FORMATS FOR TAPE 9
   43 FORMAT(11X,A6,4X,I3,2X,I3)
   44 FORMAT(3(2I4,E15.7,1X))
C   * SPECIAL FORMATS FOR AFFDL FORMAT INPUT ON AUXILIARY TAPE 9 * *
   45 FORMAT(1X,2I4,57X,A6)
   46 FORMAT(1X,3(2I4,E13.5,1X))
      END
```

```
      SUBROUTINE TWOL(IEXIT)
C     GRUMMAN AEROSPACE CORP.    DECK NO. 45128   LINK 2
C        MATRIX ANALYSIS OF INELASTIC PLATE   LINK 2
C     THIS LINK READS IN A SAVED BINARY TAPE - FIRST PART
      DIMENSION TALF12(11),TALF23(11),TALF31(11),TALF44(11)
      DIMENSION AL1212(34),AL1223(34),AL1231(34),ALFA44(34)
      DIMENSION PMTM(10,3),KPMTM(10),SIM(102),SIJ(102,102),TSIGN(11)
      DIMENSION TEPSN(11),SIGUK(102),EPSUK(102),SGBARN(34),SGBARP(34)
      DIMENSION SGBARM(34),EPBARN(34),EPBARP(34),DELEPN(34)
      DIMENSION            DIM(102),DIJ(102,102),DEFL(102)
      COMMON /COMA/  KLU3,KLU4,KLU5,KLU6,NA,NC,NDE,INTAPE,NIN,NOUT,NAUX
     2 , K       , KERRSW , KSET    , RUNEST , E       , EXP     , S7
     3 , GNU     , SHRMOD , PM
     4 , PMTM    , KPMTM  , SIM     , DIM    , DEFL    , TSIGN   , TEPSN
     5 , TALF12  , TALF23 , TALF31  , TALF44 , AL1212  , AL1223  , AL1231
     6 , ALFA44  , SIGUK  , EPSUK   , SGBARN , SGBARP  , SGBARM  , EPBARN
     7 , EPBARP  , DELEPN , SIJ     , DIJ
      DIMENSION BL(6)
      DIMENSION PSTEP(3)
      DATA BL/36HLOAD  VOID  TAPE  FINS        ESTM  /
      INTAPE = NAUX - 1
      READ (INTAPE)  KLU3,KLU4,KLU5,      NA,NC,NDE,        NIN,NOUT
     2 , K       , KERRSW , KSET    , RUNEST , E       , EXP     , S7
     3 , GNU     , SHRMOD , PM
C     KLU6 = 1 WILL PRINT EVERY CYCLE, 0 WILL PRINT ONLY SELECTED CYCLES


      WRITE (NOUT,9)
      NCLU = 1
      KERRSW = 2
      DO 51 I42 = 1,10
   51 KPMTM(I42) = 0
      PSTEP(1) = 0.0
      PSTEP(2) = 0.0
      PSTEP(3) = 0.0
      LROW = 0
   52 READ (NIN,2) TEMP1,TEMP2,TEMP3,TEMP4
      LROW = LROW + 1
      DO 53 J22=1,6
      IF(TEMP1.EQ.BL(J22)) GO TO 54
   53 CONTINUE
C     BAD CONTROL CARD
      WRITE (NOUT,12) LROW
      WRITE (NOUT,2)  TEMP1,TEMP2,TEMP3,TEMP4
      CALL EXIT
   54 GO TO (55,66,55,60,60,65),J22
   55 IF(LROW-10)56,56,53
C     KPMTM( N ) = 1 FOR A LOAD STEP
C     KPMTM( N ) = 2 NOT USED
C     KPMTM( N ) = 3 TO DUMP MEMORY INTO A SAVE TAPE
C     PMTM (N,1) = UPPER LIMIT OF STEP
C     PMTM (N,2) = INTERVAL (INCREMENT) FOR CALCULATION
C     PMTM (N,3) = INTERVAL (INCREMENT) FOR PRINT OUTPUT
   56 KPMTM(LROW) = J22
      NCLU = 2
```

```
      KSET = 1
      PMTM(LROW,1)= TEMP2
      TEMP5       = TEMP2-PSTEP(J22)
      PMTM(LROW,2)= SIGN(TEMP3,TEMP5)
      PSTEP(J22)  = TEMP2
      IF(PMTM(LROW,2))57,63,57
   63 GO TO (995,995,57),J22
   57 CONTINUE
      PMTM(LROW,3)= TEMP4
      GO TO 52
   65 RUNEST = TEMP2 - 1.0
   66 LROW   = LROW - 1
      GO TO 52
   60 CONTINUE
      GO TO (61,62),NCLU
   62 CONTINUE
      READ (INTAPE) JUNK
      READ (INTAPE) JUNK
      GO TO 64
   61 CONTINUE
      READ (INTAPE) PMTM
      READ (INTAPE) KPMTM
   64 CONTINUE
      WRITE (NOUT,1)
      DO 361 J23 = 1,10
      IF(KPMTM(J23))361,361,362
  362 IF(KPMTM(J23)-4)363,361,361
  363 J24 = KPMTM(J23)
      GO TO (364,364,368),J24
  364 WRITE (NOUT,22) PMTM(J23,2),PMTM(J23,1)
      IF(PMTM(J23,3))361,361,365
  365 WRITE (NOUT,23) PMTM(J23,3)
      GO TO 361
  368 WRITE (NOUT,27)
  361 CONTINUE
      READ (INTAPE) SIM
      READ (INTAPE) S..
      READ (INTAPE) DIM
      READ (INTAPE) DIJ
      READ (INTAPE) DEFL
      READ (INTAPE) TSIGN
      READ (INTAPE) TEPSN
      READ (INTAPE) TALF12
      READ (INTAPE) TALF23
      READ (INTAPE) TALF31
      READ (INTAPE) TALF44
      READ (INTAPE) AL1212
      READ (INTAPE) AL1223
      READ (INTAPE) AL1231
      READ (INTAPE) ALFA44
      READ (INTAPE) SIGUK
      READ (INTAPE) EPSUK
C     GRUMMAN AEROSPACE CORP.   DECK NO. 45128   LINK 3
C        MATRIX ANALYSIS OF INELASTIC PLATE   LINK 3
C     THIS IS THE SECOND HALF OF OLD LINK 2
C     THIS LINK READS IN A SAVED BINARY TAPE - SECOND PART
```

```
      READ (INTAPE) SGBARN
      READ (INTAPE) SGBARP
      READ (INTAPE) SGBARM
      READ (INTAPE) EPBARN
      READ (INTAPE) EPBARP
      READ (INTAPE) DELEPN
      REWIND INTAPE
      WRITE (NOUT,5) E,SHRMOD,GNU
      IF(KLU3.NE.1) GO TO 140
      WRITE (NOUT,37)
      WRITE (NOUT,38) ST,EXP,E
  140 CONTINUE
      WRITE (NOUT,6)
      DO 149 II=1,11
  149 WRITE (NOUT,7) II,TSIGN(II),TEPSN(II)
      IEXIT = 4
      CALL OVRTIM(K000FX)
      RETURN
  995 WRITE (NOUT,16) LROW
      CALL EXIT
      STOP
    1 FORMAT(1H0,29X,37HCONTINUATION RUN - INELASTIC ANALYSIS)
    2 FORMAT(6X,A4,E10.6,E10.1,E10.1)
    5 FORMAT(26H0 MODULUS OF ELASTICITY = ,F11.0,4H PSI,6X,16HSHEAR MODU
     1LUS = ,F11.0,4H PSI,6X,5HNU = ,F6.3)
    6 FORMAT(41H0 TABLE OF VALUES FOR STRESS-STRAIN CURVE  //
     15X,29HPOINT  STRESS LEVEL     STRAIN/16X,3HPSI,9X,7HIN./IN.//)
    7 FORMAT(6X,I3,F13.2,F15.8)
    9 FORMAT(//79H THIS   ISOTROPIC RUN USES ELASTIC UNLOADING (HOOKES L
     1AW) WITH STRAIN HARDENING)
   12 FORMAT(26H ERROR- INCREMENT CARD NO.,I3,5H N.G.)
   16 FORMAT(33H ERROR-NO INTERVAL-INCREMENT CARD,I3)
   22 FORMAT(5X,16HLOAD INCREMENTS ,F9.2,11H POUNDS TO ,F10.2,7H POUNDS)
   23 FORMAT(1H+,61X,19HPRINT OUTPUT EVERY ,F9.2,7H POUNDS)
   27 FORMAT(5X,35HSTORE MEMORY ON TAPE A-6, THEN EXIT)
   37 FORMAT(//5X,24HRAMBERG-OSGOOD CONSTANTS)
   38 FORMAT(5X,22HINPUT REFERENCE STRESS,E16.7/5X,14HINPUT EXPONENT,
     1F10.5/5X,15HYOUNG'S MODULUS,F11.0)
      END
```

```
      SUBROUTINE FIVEL(IEXIT)
C     GRUMMAN AEROSPACE CORP.   DECK NO. 45128   LINK 5
C        MATRIX ANALYSIS OF INELASTIC PLATE   LINK 5
C     THIS LINK WRITES A SAVE TAPE FOR RESTART
      DIMENSION TALF12(11),TALF23(11),TALF31(11),TALF44(11)
      DIMENSION AL1212(34),AL1223(34),AL1231(34),ALFA44(34)
      DIMENSION PMTM(10,3),KPMTM(10),SIM(102),SIJ(102,102),TSIGN(11)
      DIMENSION TEPSN(11),SIGUK(102),EPSUK(102),SGBARN(34),SGBARP(34)
      DIMENSION SGBARM(34),EPBARN(34),EPBARP(34),DELEPN(34)
      DIMENSION            DIM(102),DIJ(102,102),DEFL(102)
      COMMON /CONA/  KLU3,KLU4,KLU5,KLU6,NA,NC,NDE,INTAPE,NIN,NOUT,NAUX
     2 , K       , KERRSW , KSET    , RUNEST , E       , EXP     , S7
     3 , GNU     , SHRMOD , PN
     4 , PMTM    , KPMTM  , SIM     , DIM    , DEFL    , TSIGN   , TEPSN
     5 , TALF12  , TALF23 , TALF31  , TALF44 , AL1212  , AL1223  , AL1231
     6 , ALFA44  , SIGUK  , EPSUK   , SGBARN , SGBARP  , SGBARM  , EPBARN
     7 , EPBARP  , DELEPN , SIJ     , DIJ
      NSTAPE = 11
      WRITE (NSTAPE) KLU3,KLU4,KLU5,      NA,NC,NDE,        NIN,NOUT
     2 , K       , KERRSW , KSET    , RUNEST , E       , EXP     , S7
     3 , GNU     , SHRMOD , PN
      WRITE (NSTAPE) PMTM
      WRITE (NSTAPE) KPMTM
      WRITE (NSTAPE) SIM
      WRITE (NSTAPE) SIJ
      WRITE (NSTAPE) DIM
      WRITE (NSTAPE) DIJ
      WRITE (NSTAPE) DEFL
      WRITE (NSTAPE) TSIGN
      WRITE (NSTAPE) TEPSN
      WRITE (NSTAPE) TALF12
      WRITE (NSTAPE) TALF23
      WRITE (NSTAPE) TALF31
      WRITE (NSTAPE) TALF44
      WRITE (NSTAPE) AL1212
      WRITE (NSTAPE) AL1223
      WRITE (NSTAPE) AL1231
      WRITE (NSTAPE) ALFA44
      WRITE (NSTAPE) SIGUK
      WRITE (NSTAPE) EPSUK
      WRITE (NSTAPE) SGBARN
      WRITE (NSTAPE) SGBARP
      WRITE (NSTAPE) SGBARM
      WRITE (NSTAPE) EPBARN
      WRITE (NSTAPE) EPBARP
      WRITE (NSTAPE) DELEPN
      WRITE (NOUT,25) NSTAPE
      PRINT 25,NSTAPE
      END FILE NSTAPE
      REWIND NSTAPE
      WRITE (NOUT,25) NSTAPE
      CALL OVRTIM(K000FX)
      CALL EXIT
      RETURN
   25 FORMAT(19H SAVE LOGICAL TAPE ,I3, 10H FOR RERUN///)
```

```
      SUBROUTINE FOURL(IEXIT)
C     GRUMMAN AEROSPACE CORP.   DECK NO. 45128   LINK 4
C        MATRIX ANALYSIS OF INELASTIC PLATE   LINK 4
C     THIS LINK DOES THE CALCULATION AND WRITES PRINT OUTPUT
      DIMENSION TALF12(11),TALF23(11),TALF31(11),TALF44(11)
      DIMENSION AL1212(34),AL1223(34),AL1231(34),ALFA44(34)
      DIMENSION PMTM(10,3),KPMTM(10),SIM(102),SIJ(102,102),TSIGN(11)
      DIMENSION TEPSN(11),SIGUK(102),EPSUK(102),SGBARN(34),SGBARP(34)
      DIMENSION SGBARM(34),EPBARN(34),EPBARP(34),DELEPN(34)
      DIMENSION             DIM(102),DIJ(102,102),DEFL(102)
      DIMENSION             TEPSTN(34),TOTEPS(102),DELEPK(102)
      COMMON /COMA/  KLU3,KLU4,KLU5,KLU6,NA,NC,NDE,INTAPE,NIN,NOUT,NAUX
     2 , K       , KERRSW , KSET    , RUNEST , E       , EXP     , S7
     3 , GNU     , SHRMOD , PM
     4 , PMTM    , KPMTM  , SIM     , DIM    , DEFL    , SIGUK   , TEPSN
     5 , TALF12  , TALF23 , TALF31  , TALF44 , AL1212  , AL1223  , AL1231
     6 , ALFA44  , SIGUK  , EPSUK   , SGBARN , SGBARP  , SGBARM  , EPBARN
     7 , EPBARP  , DELEPN , SIJ     , DIJ
      GO TO (418,419),KERRSW
C     INITIALIZE WORK AREAS
  418 DO 102 I1 = 1,NA
      EPSUK (I1) = 0.0
  102 SIGUK(I1) = 0.0
      DO 103 I1 = 1,NC
      DELEPN(I1) = 0.0
      SGBARN(I1) = 0.0
      SGBARP(I1) = 0.0
      SGBARM(I1) = 0.0
      EPBARP(I1) = 0.0
      AL1212(I1)= 2.0*TALF12(2)
      AL1223(I1)= TALF12(2) + TALF23(2)
      AL1231(I1)= TALF12(2) + TALF31(2)
      ALFA44(I1)= TALF44(2)
  103 EPBARN(I1) =0.0
      DO 105 I1 = 1,NDE
  105 DEFL(I1)  = 0.0
      KSET = 1
  419 CONTINUE
      KREF = K
      IF(KLU3.EQ.0) GO TO 151
      AA = 3.*((1./S7)**(EXP-1.))/7.
  151 K    = K + 1
      KLU2 = 1
C     IF KLU2 = 0, THE CYCLE OF OPERATIONS WILL BE PRINTED
C     KLU6 = 1 WILL PRINT EVERY CYCLE, 0 WILL PRINT ONLY SELECTED CYCLES
      IF(KLU6)248,248,249
  249 KLU2 = 0
  248 CONTINUE
      IF(K-1)270,270,271
  270 KLU2 = 0
  271 CONTINUE
      GO TO (416,417),KERRSW
  417 KLU2 = 0
      KERRSW = 1
  416 CONTINUE
```

```
C      KSET IS THE ROW OF KPMTM OR PMTM BEING USED (CURRENT LOAD LEVEL)
  300  IF(KSET-11)301,319,319
  301  IF(KPMTM(KSET))302,302,303
  302  KSET = KSET + 1
       GO TO 300
  303  IF(KPMTM(KSET)-4)304,302,302
C      VARIABLE (J24) INDICATES A LOAD CYCLE (1) OR WRITE MEMORY ON
C      A SAVE TAPE (3). (2) IS NOT USED.
  304  J24  = KPMTM(KSET)
       IF(PMTM(KSET,2))342,342,341
  341  GO TO (305,305,423),J24
  342  GO TO (345,345,423),J24
  305  IF(PMTM(KSET,1)-(PM+PMTM(KSET,2))) 316,309,308
  345  IF(PMTM(KSET,1)-(PM+PMTM(KSET,2))) 308,309,316
  309  KLU2  = 0
  308  DELPM = PMTM(KSET,2)
       GO TO 154
  316  KLU2  = 0
       GO TO 302
  319  IF(KLU2)205,205,320
  320  KLU2  = 0
       KSET  = KSET - 1
       IF(KSET)205,205,321
  321  IF(KPMTM(KSET)) 320,320,308
  154  CONTINUE
  335  CONTINUE
  502  PM    = PM    + DELPM
  324  CALL OUTPUT(PM,PMTM(KSET,3),KLU1)
  326  IF(KLU2)327,328,327
  327  KLU2 = KLU1
  328  CONTINUE
       IF(KLU2)250,250,251
  250  CONTINUE
C      LABEL = APPLIED LOAD
       WRITE (NOUT,22) PM
  251  CONTINUE
C      SAVE PRECEDING CYCLE VALUES OF EPBARN
       DO 152 I1 = 1,NC
  152  EPBARP(I1) = EPBARN(I1)
C      CALCULATE NODE STRESSES - MATRIX SIGUK - FRAME SIZE 105 X 1
C      COMPUTATION OF STRESSES AND DEFLECTIONS IN THE INELASTIC RANGE
C      REDUCE SIJ*EPSUK MULTIPLICATION BY SELECTING THE COLUMNS OF SIJ
C      CORRESPONDING TO THE NON-ZERO ELEMENTS OF EPSUK
       DO 861 I5=1,NA
  861  SIGUK(I5)= SIM(I5)*PM
       DO 631 I5=1,NDE
  631  DEFL(I5) = DIM(I5)*PM
       DO 641 I4=1,NA
       IF (EPSUK(I4).EQ.0.0) GO TO 641
       DO 643 I2=1,NA
  643  SIGUK(I2)= SIGUK(I2) + SIJ(I2,I4)*EPSUK(I4)
       DO 644  I3=1,NDE
  644  DEFL(I3)=DEFL(I3) +DIJ(I3,I4)*EPSUK(I4)
  641  CONTINUE
       IF(KLU2)254,254,255
  254  CONTINUE
```

```
C       LABEL DEFLECTIONS
        WRITE (NOUT,23)
        KNDE = NDE/2
        DO 665 II = 1,KNDE
        KNDE2  = 2*II
        KNDE1  = KNDE2-1
        WRITE (NOUT,24) II,DEFL(KNDE1),DEFL(KNDE2)
  665 CONTINUE
  255 CONTINUE
C       CALCULATE MAGNITUDE AND SIGN OF EFFECTIVE STRESS AT EACH NODE
C       CALCULATE EFFECTIVE STRESSES - MATRIX SGBARN -  SAME SIZE 35 X 1
        DO 166 I7 = 1,NC
        SGBARP(I7) = SGBARN(I7)
        M3         = 3*I7
        M32        = M3-2
        M31        = M3-1
        SGBARN(I7)=SQRT(AL1223(I7)*SIGUK(M32)**2-AL1212(I7)*SIGUK(M32)* SI
       1GUK(M31)+AL1223(I7)*SIGUK(M31)**2+3.0*ALFA44(I7)*SIGUK(M3)**2)
  166 CONTINUE
C       LABEL = EFF. STRESSES
C       CALCULATE EFFECTIVE INELASTIC STRAIN FOR EACH NODE - INTERPOLATE
C       IN TABLE (TSIGN VS. TEPSN)
        DO 181 I8 = 1,NC
C       SGBARP IS EFFECTIVE STRESS OF PREVIOUS CYCLE
        IF(SGBARN(I8)-SGBARP(I8))411,401,401
C       EFFECTIVE STRESS IS ABOVE PREVIOUS LEVEL
C       SGBARM IS EFFECTIVE STRESS OF LAST CYCLE TO SHOW AN INCREASE
  401 IF(SGBARN(I8)-SGBARM(I8))411,402,402
C       EFFECTIVE STRESS IS ABOVE KNEE OF PREVIOUS DROP-OFF, IF ANY
  402 CONTINUE
  403 SGBARM(I8) = SGBARN(I8)
        ESUPRK =(SGBARN(I8)/E) + EPBARP(I8)
        IF(KLU3.EQ.1) GO TO 670
        DO 171 I9 = 1,11
        IF(ESUPRK-TEPSN(I9))173,172,171
  171 CONTINUE
        GO TO 998
  172 BARSGN = TSIGN(I9)
        IF(SGBARN(I8)-TSIGN(2))178,177,177
  177 AL1212(I8)= 2.0*TALF12(I9)
        AL1223(I8)= TALF12(I9)+ TALF23(I9)
        AL1231(I8)= TALF12(I9)+ TALF31(I9)
        ALFA44(I8)= TALF44(I9)
  178 CONTINUE
        GO TO 174
  173 KKK2 = I9
        KKK1 = I9 - 1
        STNRAT    = (ESUPRK-TEPSN(KKK1))/(TEPSN(KKK2)-TEPSN(KKK1))
        BARSGN    = TSIGN(KKK1)+(TSIGN(KKK2)-TSIGN(KKK1))*STNRAT
        IF(SGBARN(I8)-TSIGN(2))176,175,175
  175 CONTINUE
        ALFA12    = TALF12(KKK1)+(TALF12(KKK2)-TALF12(KKK1))*STNRAT
        ALFA23    = TALF23(KKK1)+(TALF23(KKK2)-TALF23(KKK1))*STNRAT
        ALFA31    = TALF31(KKK1)+(TALF31(KKK2)-TALF31(KKK1))*STNRAT
        ALFA44(I8)=TALF44(KKK1)+(TALF44(KKK2)-TALF44(KKK1))*STNRAT
        AL1212(I8)= 2.0*ALFA12
```

```
      AL1223(I8)= ALFA12 + ALFA23
      AL1231(I8)= ALFA12 + ALFA31
  176 CONTINUE
      GO TO 174
  670 CONTINUE
      BSGN1  = SGBARN(I8)
      DO 674 II=1,10
      F1BSN  = AA*BSGN1**EXP*BSGN1-E*ESUPRK
      F2BSN  = AA*EXP*BSGN1**(EXP-1.)*1.
      BARSGN = BSGN1 - F1BSN/F2BSN
      TEST   = BARSGN/BSGN1
      BSGN1  = BARSGN
      IF(TEST.LT..99999) GO TO 674
      IF(TEST.GT.1.00001) GO TO 674
      GO TO 676
  674 CONTINUE
  676 CONTINUE
  174 EPBARN(I8) = 0.0
      IF(SGBARN(I8).GT.TSIGN(2)) EPBARN(I8)=ESUPRK-BARSGN/E
C     CALCULAYE TOTAL EFFECTIVE STRAIN - MATRIX TEFSTN - FRAME SIZE 35X1
      TEFSTN(I8) = ESUPRK
C     CALCULATE EFFECTIVE STRAIN CHANGES - MATRIX DELEPN - FRAME 35 X 1
C     CALCULATE INCREMENTAL EFFECTIVE INELASTIC STRAIN
      DELEPN(I8) = EPBARN(I8) - EPBARP(I8)
      GO TO 181
C     DROP-OFF OF EFFECTIVE STRESS
C     OR STILL BELOW THE KNEE OF PREVIOUS DROP-OFF
  411 EPBARN(I8) = EPBARP(I8)
      TEFSTN(I8) = EPBARP(I8)+(SGBARN(I8)/E)
      DELEPN(I8) = 0.0
  181 CONTINUE
C
C
      IF(KLU3.EQ.0) GO TO 680
C     USE OF THE RAMBERG-OSGOOD EQUATION IS ONLY VALID FOR
C     ISOTROPIC ANALYSIS
      DO 679 I8 = 1,NC
      AL1212(I8) = 1.0
      AL1223(I8) = 1.0
      AL1231(I8) = 1.0
      ALFA44(I8) = 1.0
  679 CONTINUE
  680 CONTINUE
C
C     LABEL = EFF.PLASTIC STRAIN
C     LABEL = TOTAL EFF. STRAIN


C     CALCULATE NODE STRAIN CHANGE - MATRIX DELEPK - FRAME SIZE 105 X 1
      DO 191 III = 1,NC
      TEMPA =          DELEPN(III)/ SGBARN(III)
      M3    = 3*III
      M32   = M3-2
      M31   = M3-1
      DELEPK(M32)=TEMPA*(AL1231(III)*SIGUK(M32)-.5*AL1212(III)*SIGUK(M31
     1))
```

```
      DELEPK(M31)=TEMPA*(AL1223(III)*SIGUK(M31)-.5*AL1212(III)*SIGUK(M32
     1))
      DELEPK(M3) =TEMPA*(3.0*ALPA3(III)*SIGUK(M3))
  191 CONTINUE
C     CALCULATE NODE PLASTIC STRAIN - MATRIX EPSUK - FRAME SIZE 105 X 1
C     CALCULATE NODE POINT STRAINS
      DO 192 I23=1,NA
      EPSUK(I23) = EPSUK(I23) + DELEPK(I23)
  192 CONTINUE
C     LABEL = EFF.STRAIN CHANGES
C     LABEL = NODE STRAIN CHANGE
C     LABEL = NODE INELAS.STRAIN
C     CALCULATE TOTAL NODE STRAINS - MATRIX TOTEPS - FRAME SIZE 105 X 1
      DO 201 I14=1,NC
      M32 = 3*I14-2
      M31 = 3*I14-1
      M3  = 3*I14
      TOTEPS(M32)=EPSUK (M32)+SIGUK(M32)/E -GNU*SIGUK(M31)/E
      TOTEPS(M31)=EPSUK (M31)+SIGUK(M31)/E -GNU*SIGUK(M32)/E
  201 TOTEPS(M3 )=EPSUK (M3 )+SIGUK(M3 )/SHRMOD
      IF(KLU2)262,262,263
  262 CONTINUE
C     LABEL = TOT. NODE STRAINS
      WRITE (NOUT,41)
      WRITE (NOUT,42)
      DO 258 I8 = 1,NC
      J3 = 3*I8
      J2 = J3-1
      J1 = J3-2
      WRITE (NOUT,46) I8,SIGUK(J1),SIGUK(J2),SIGUK(J3),TOTEPS(J1),
     1 TOTEPS(J2),TOTEPS(J3)
  258 CONTINUE
      WRITE (NOUT,43)
      WRITE (NOUT,44)
      DO 259 I8 = 1,NC
      J3 = 3*I8
      J2 = J3-1
      J1 = J3-2
      WRITE (NOUT,46) I8,EPSUK(J1),EPSUK(J2),EPSUK(J3),DELEPK(J1),
     1 DELEPK(J2),DELEPK(J3)
  259 CONTINUE
      WRITE (NOUT,45)
      DO 260 I8 = 1,NC
      WRITE (NOUT,46) I8,SGBARN(I8),TEPSTN(I8),DELEPN(I8),EPBARN(I8)
  260 CONTINUE
  263 CONTINUE
      IF(KLU2)268,268,269
  268 CONTINUE
      WRITE (NOUT,31) K,PM
  269 CONTINUE
      IF(K.LE.(KREF+20)) GO TO 422
      KREF = K
      CALL OVRTIM(K000FX)
C     K000FX = 1 TO FORCE AN EXIT
       GO TO(421,422),K000FX
  422 CONTINUE
```

```
      GO TO 151
C     STATEMENT 421 IS REACHED IF THE RUNNING TIME IS ONE MINUTE
C     BELOW THE LINE ESTIMATE
  421 IF(KLU2)423,423,208
  423 CONTINUE
  205 CONTINUE
      CALL OVRTIM(K000FX)
       GO TO(207,209),K000FX
  209 IF(J24-3)210,207,210
  207 CONTINUE
      IEXIT = 5
      RETURN
  210 CONTINUE
      IEXIT = 6
      RETURN
  208 KERRSW = 2
C     KERRSW SET TO 2 TO MAKE KLU. = 0 AND PRINT A CYCLE
      GO TO 151
  998 CONTINUE
      WRITE (NOUT,12) ESUPRX,SGBARN(I8)
      WRITE (NOUT,13) K,I8,PM
      GO TO 205
   12 FORMAT(46H VALUE NOT FOUND IN TABLE FOR EPSILON BAR N = ,E15.8,
     119H   ( SIGMA BAR N = ,E15.8,2H ) )
   13 FORMAT(16H CYCLE NUMBER = ,I5,20H    ELEMENT INDEX = ,I4,17H    LO
     1AD LEVEL = ,F9.2)
   21 FORMAT(// 1X,4A4,A2,5(1PE16.7)/(19X,5E16.7))
   22 FORMAT(//21H APPLIED LOAD          ,F12.2)
   23 FORMAT(//9X,30HDEFLECTIONS AT GEOMETRIC NODES//14X,4HNODE,6X
     1,7HDELTA X,9X,7HDELTA Y)
   24 FORMAT(15X,I4,2E16.7)
   31 FORMAT(2H0 ,I6,27H CYCLES COMPLETED -- LOAD = ,F9.2)
   41 FORMAT(/22X,13HNODE STRESSES,33X,18HTOTAL NODE STRAINS)
   42 FORMAT(98H NODE      SIGMA X          SIGMA Y           TAU XY
     1 EPSILON X        EPSILON Y         GAMMA XY)
   43 FORMAT(/18X,22HNODE INELASTIC STRAIN ,29X,18HNODE STRAIN CHANGE)
   44 FORMAT(98H NODE     EPSILON X        EPSILON Y         GAMMA XY
     1 EPSILON X        EPSILON Y         GAMMA XY)
   45 FORMAT(/27X,39HTOTAL          EFFECTIVE        EFFECTIVE/9X,56HEFFEC
     1TIVE       EFFECTIVE         STRAIN           PLASTIC/64H NODE      S
     2TRESSES         STRAIN           CHANGES          STRAIN)
   46 FORMAT(1X,I3,1X,6(1PE16.7))
       END
```

```
      SUBROUTINE OVRTIM(K00OFX)
C     SUBROUTINE TO TEST THE SYSTEM CLOCK AND FORCE GENERATION OF A
C     RESTARTABLE SAVE TAPE WHEN THE TIME ESTIMATE IS REACHED
      COMMON /COMA/  KLU3,KLU4,KLU5,KLU6,NA,NC,NDE,INTAPE,NIN,NOUT,NAUX
     2 , K      , KERRSW , KSET   , RUNEST , E      , EXP    , S7
     3 , GNU    , SHRMOD , PM
C     K000FX = 1 TO TERMINATE THE RUN
C            = 2 TO LET THE RUN CONTINUE
      LIM = RUNEST*600.
      N   = 0
C     TIMING ROUTINE DISABLED PENDING INFORMATION ON WPAFB CLOCK ROUTINE
      K000FX = 2
      IT = 0
      IF( IT.EQ.0) GO TO 102
C     END OF PATCH
C     IT = ICHRON(N)
      K000FX = 2
      IF( IT.GT.90000) GO TO 102
      IF( IT.LT.LIM) GO TO 100
      K000FX = 1
  100 TI  = IT
      TIME = TI/600.
      WRITE (NOUT,1) TIME,K
  102 RETURN
    1 FORMAT(20H ELAPSED TIME READS ,F10.4,18H MINUTES ON CYCLE ,I5)
      END
```

NOTE: Subroutine OVRTIM is a portion of the root segment of the program.

```
      SUBROUTINE OUTPUT(VALUE1,STEP1,KLU1)
C     THIS SUBROUTINE SETS KLU1 = 0 IF THE CURRENT CYCLE IS TO BE PRINTE
      VALUE = ABS(VALUE1)
      STEP = ABS(STEP1)
  102 IF(VALUE-STEP)131,100,100
  100 NTEST1 = (VALUE/STEP)*1.00001
      NTEST2 = (VALUE/STEP)+.998
      IF(NTEST1-NTEST2)131,130,131
  130 KLU1   = 0
      GO TO 135
  131 KLU1   = 1
  135 RETURN
      END
```

TEST PROBLEM FOR IBM 7094 VERSION - 34 NODE CHECK RUN FEB. 3,1970

THIS ISOTROPIC RUN USES ELASTIC UNLOADING (HOOKES LAW) WITH STRAIN HARDENING

LOAD INCREMENTS	500.00 POUNDS TO	5000.00 POUNDS	PRINT OUTPUT EVERY 2500.00 POUNDS
LOAD INCREMENTS	100.00 POUNDS TO	8000.00 POUNDS	PRINT OUTPUT EVERY 1000.00 POUNDS
LOAD INCREMENTS	100.00 POUNDS TO	16000.00 POUNDS	PRINT OUTPUT EVERY 4000.00 POUNDS
LOAD INCREMENTS	100.00 POUNDS TO	17000.00 POUNDS	PRINT OUTPUT EVERY 200.00 POUNDS
LOAD INCREMENTS	50.00 POUNDS TO	18000.00 POUNDS	PRINT OUTPUT EVERY 200.00 POUNDS

MATRIX DIM 94 ROWS 1 COLUMNS FROM TAPE 9

2	1	0.19614226E-07	-0 -0 -0.	-0 -0 -0.
3	1	-0.13014546E-07	-0 -0 -0.	-0 -0 -0.
4	1	0.64942148E-08	-0 -0 -0.	-0 -0 -0.
5	1	-0.62691242E-07	-0 -0 -0.	-0 -0 -0.
6	1	0.51411592E-07	-0 -0 -0.	-0 -0 -0.
7	1	-0.11024622E-06	-0 -0 -0.	-0 -0 -0.
8	1	0.13732514E-06	-0 -0 -0.	-0 -0 -0.
9	1	-0.15446535E-06	-0 -0 -0.	-0 -0 -0.
10	1	0.24953737E-06	-0 -0 -0.	-0 -0 -0.
11	1	-0.17998633E-06	-0 -0 -0.	-0 -0 -0.
12	1	0.39266776E-06	-0 -0 -0.	-0 -0 -0.
13	1	-0.18051048E-06	-0 -0 -0.	-0 -0 -0.
14	1	0.54804689E-06	-0 -0 -0.	-0 -0 -0.
15	1	-0.15513211E-06	-0 -0 -0.	-0 -0 -0.
16	1	0.69905966E-06	-0 -0 -0.	-0 -0 -0.
17	1	-0.11119954E-06	-0 -0 -0.	-0 -0 -0.
18	1	0.92801373E-06	-0 -0 -0.	-0 -0 -0.
19	1	-0.57381599E-07	-0 -0 -0.	-0 -0 -0.
20	1	0.51226651E-06	-0 -0 -0.	-0 -0 -0.
22	1	0.55023758E-06	-0 -0 -0.	-0 -0 -0.
24	1	0.24243548E-07	-0 -0 -0.	-0 -0 -0.
25	1	-0.33752845E-08	-0 -0 -0.	-0 -0 -0.
26	1	0.70235836E-08	-0 -0 -0.	-0 -0 -0.
27	1	-0.21506342E-07	-0 -0 -0.	-0 -0 -0.
28	1	0.68590054E-07	-0 -0 -0.	-0 -0 -0.
29	1	-0.92677329E-07	-0 -0 -0.	-0 -0 -0.
30	1	0.16561074E-06	-0 -0 -0.	-0 -0 -0.
31	1	-0.16393784E-05	-0 -0 -0.	-0 -0 -0.
32	1	0.27405577E-04	-0 -0 -0.	-0 -0 -0.
33	1	-0.30747265E-06	-0 -0 -0.	-0 -0 -0.
34	1	0.39202108E-06	-0 -0 -0.	-0 -0 -0.
35	1	-0.19502477E-06	-0 -0 -0.	-0 -0 -0.
36	1	0.50954276E-05	-0 -0 -0.	-0 -0 -0.
37	1	-0.13522580E-06	-0 -0 -0.	-0 -0 -0.
38	1	0.64545152E-06	-0 -0 -0.	-0 -0 -0.
39	1	-0.80114750E-07	-0 -0 -0.	-0 -0 -0.

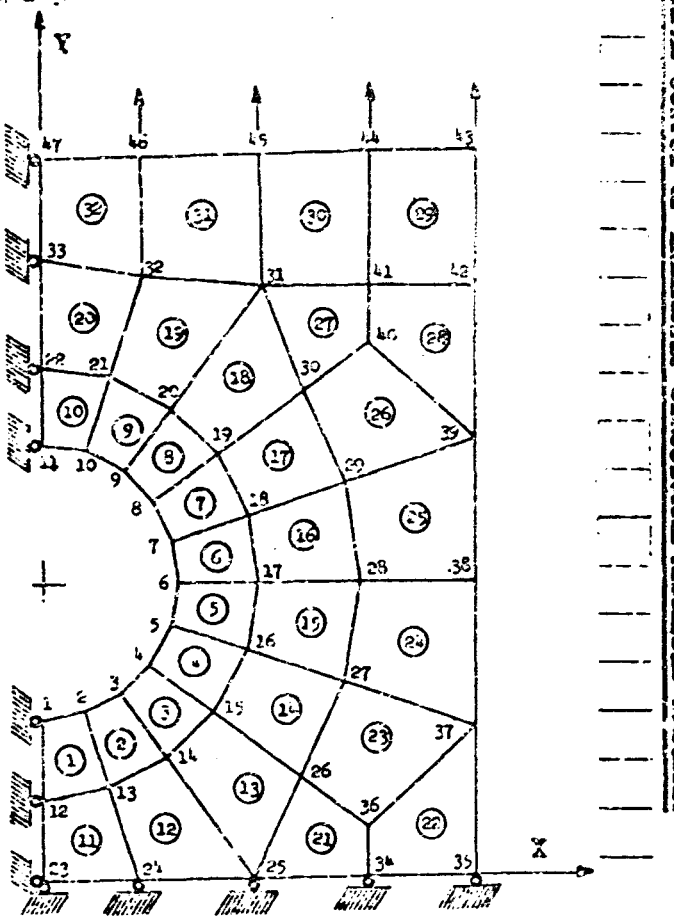

40	1	0.795310158E-05	-0 -0 -0.	-0 -0 -0.
41	1	-0.19593205E-07	-0 -0 -0.	-0 -0 -0.
42	1	0.516442216-06	-0 -0 -0.	-0 -0 -0.
44	1	0.566937026-06	-0 -0 -0.	-0 -0 -0.
47	1	-0.5740E259E-08	-0 -0 -0.	-0 -0 -0.
49	1	-0.43044237E-07	-0 -0 -0.	-0 -0 -0.
51	1	-0.10025294E-06	-0 -0 -0.	-0 -0 -0.
52	1	0.102E3906E-05	-0 -0 -0.	-0 -0 -0.
53	1	-0.1[illegible]413E-06	-0 -0 -0.	-0 -0 -0.
54	1	0.2[illegible]265E-06	-0 -0 -0.	-0 -0 -0.
55	1	-0.2[illegible]E-06	-0 -0 -0.	-0 -0 -0.
56	1	0.[illegible]E-06	-0 -0 -0.	-0 -0 -0.
57	1	-0.[illegible]E-05	-0 -0 -0.	-0 -0 -0.
58	1	0.[illegible]E-06	-0 -0 -0.	-0 -0 -0.
59	1	-0.12885652E-06	-0 -0 -0.	-0 -0 -0.
60	1	0.641116286-06	-0 -0 -0.	-0 -0 -0.
61	1	-0.47273757E-07	-0 -0 -0.	-0 -0 -0.
62	1	0.60748929E-06	-0 -0 -0.	-0 -0 -0.
63	1	-0.12300820E-07	-0 -0 -0.	-0 -0 -0.
64	1	0.53601289E-06	-0 -0 -0.	-0 -0 -0.
66	1	0.565E8587E-06	-0 -0 -0.	-0 -0 -0.
67	1	-0.12540402E-06	-0 -0 -0.	-0 -0 -0.
69	1	-0.16244166E-06	-0 -0 -0.	-0 -0 -0.
71	1	-0.12824369E-06	-0 -0 -0.	-0 -0 -0.
72	1	0.90845227E-07	-0 -0 -0.	-0 -0 -0.
73	1	-0.20089534E-06	-0 -0 -0.	-0 -0 -0.
74	1	0.2051630RE-06	-0 -0 -0.	-0 -0 -0.
75	1	-0.26091772E-06	-0 -0 -0.	-0 -0 -0.
76	1	0.36732427E-06	-0 -0 -0.	-0 -0 -0.
77	1	-0.22063284E-06	-0 -0 -0.	-0 -0 -0.
78	1	0.40893229E-06	-0 -0 -0.	-0 -0 -0.
79	1	-0.12329541E-06	-0 -0 -0.	-0 -0 -0.
80	1	0.64223928E-06	-0 -0 -0.	-0 -0 -0.
81	1	-0.57678536E-07	-0 -0 -0.	-0 -0 -0.
82	1	0.67980730E-06	-0 -0 -0.	-0 -0 -0.
83	1	-0.12250906E-06	-0 -0 -0.	-0 -0 -0.
84	1	0.61747611E-06	-0 -0 -0.	-0 -0 -0.
85	1	0.1226E174E-07	-0 -0 -0.	-0 -0 -0.
86	1	0.78612787E-06	-0 -0 -0.	-0 -0 -0.
87	1	0.35562034E-07	-0 -0 -0.	-0 -0 -0.
88	1	0.85571610E-06	-0 -0 -0.	-0 -0 -0.
89	1	0.53927116E-07	-0 -0 -0.	-0 -0 -0.
90	1	0.97824431E-06	-0 -0 -0.	-0 -0 -0.
91	1	0.36283374E-07	-0 -0 -0.	-0 -0 -0.
92	1	0.10658923E-05	-0 -0 -0.	-0 -0 -0.
94	1	0.10918055E-05	-0 -0 -0.	-0 -0 -0.

MATRIX DIJ 94 ROWS X 96 COLUMNS FROM TAPE 9

MATRIX SIM 96 ROWS X 1 COLUMNS FROM TAPE 9

1	1	0.22051536E-00	-0 -0 -0.	-0 -0 -0.
2	1	0.61378789E 00	-0 -0 -0.	-0 -0 -0.
3	1	0.11614404E-00	-0 -0 -0.	-0 -0 -0.
4	1	-0.16628405E 01	-0 -0 -0.	-0 -0 -0.
5	1	0.62109423E 00	-0 -0 -0.	-0 -0 -0.
6	1	0.42355019E-00	-0 -0 -0.	-0 -0 -0.
7	1	-0.52512552E 00	-0 -0 -0.	-0 -0 -0.
8	1	0.31677780E 01	-0 -0 -0.	-0 -0 -0.
9	1	0.75245333E 00	-0 -0 -0.	-0 -0 -0.
10	1	0.30618185E-00	-0 -0 -0.	-0 -0 -0.
11	1	0.6831298?E 01	-0 -0 -0.	-0 -0 -0.
12	1	0.53093573E 00	-0 -0 -0.	-0 -0 -0.
13	1	0.505104?4E 00	-0 -0 -0.	-0 -0 -0.
14	1	0.59245489E 01	-0 -0 -0.	-0 -0 -0.
15	1	0.14196408E-00	-0 -0 -0.	-0 -0 -0.
16	1	0.12056302E 01	-0 -0 -0.	-0 -0 -0.
17	1	0.10601959E 02	-0 -0 -0.	-0 -0 -0.

18	1	-0.12255783E 01	-0 -0 -0.	-0 -0 -0.
19	1	0.12486060E 01	-0 -0 -0.	-0 -0 -0.
20	1	0.84726819E 01	-0 -0 -0.	-0 -0 -0.
21	1	-0.21087273E 01	-0 -0 -0.	-0 -0 -0.
22	1	0.40350556E-00	-0 -0 -0.	-0 -0 -0.
23	1	0.49795274E 01	-0 -0 -0.	-0 -0 -0.
24	1	-0.20217408E 01	-0 -0 -0.	-0 -0 -0.
25	1	-0.12437858E 01	-0 -0 -0.	-0 -0 -0.
26	1	0.12116406E 01	-0 -0 -0.	-0 -0 -0.
27	1	-0.11964[illegible]E 01	-0 -0 -0.	-0 -0 -0.
28	1	-0.20092813E 01	-0 -0 -0.	-0 -0 -0.
29	1	0.29256300E-00	-0 -0 -0.	-0 -0 -0.
30	1	-0.36649203E-00	-0 -0 -0.	-0 -0 -0.
31	1	-0.55601031E 00	-0 -0 -0.	-0 -0 -0.
32	1	0.76635863E-01	-0 -0 -0.	-0 -0 -0.
33	1	-0.29490650E-00	-0 -0 -0.	-0 -0 -0.
34	1	-0.53254112E-00	-0 -0 -0.	-0 -0 -0.
35	1	0.24567261E 01	-0 -0 -0.	-0 -0 -0.
36	1	-0.22846148E-00	-0 -0 -0.	-0 -0 -0.
37	1	-0.11633939E 01	-0 -0 -0.	-0 -0 -0.
38	1	0.51622256E 01	-0 -0 -0.	-0 -0 -0.
39	1	0.73989938E-02	-0 -0 -0.	-0 -0 -0.
40	1	-0.49086726E-00	-0 -0 -0.	-0 -0 -0.
41	1	0.65816440E 01	-0 -0 -0.	-0 -0 -0.
42	1	-0.74351984E-00	-0 -0 -0.	-0 -0 -0.
43	1	0.57886416E 00	-0 -0 -0.	-0 -0 -0.
44	1	0.66630563E 01	-0 -0 -0.	-0 -0 -0.
45	1	-0.56367997E 00	-0 -0 -0.	-0 -0 -0.
46	1	0.67363727E-00	-0 -0 -0.	-0 -0 -0.
47	1	0.64682445E 01	-0 -0 -0.	-0 -0 -0.
48	1	-0.34052330E-00	-0 -0 -0.	-0 -0 -0.
49	1	0.89090111E-01	-0 -0 -0.	-0 -0 -0.
50	1	0.65220727E 01	-0 -0 -0.	-0 -0 -0.
51	1	-0.10004899E-00	-0 -0 -0.	-0 -0 -0.
52	1	-0.74729051E 00	-0 -0 -0.	-0 -0 -0.
53	1	0.57992791E 01	-0 -0 -0.	-0 -0 -0.
54	1	-0.58869335E 00	-0 -0 -0.	-0 -0 -0.
55	1	-0.64703017E 00	-0 -0 -0.	-0 -0 -0.
56	1	0.41281175E 01	-0 -0 -0.	-0 -0 -0.
57	1	-0.16386002E 01	-0 -0 -0.	-0 -0 -0.
58	1	-0.36979400E-00	-0 -0 -0.	-0 -0 -0.
59	1	0.18133201F 01	-0 -0 -0.	-0 -0 -0.
60	1	-0.51672026E 00	-0 -0 -0.	-0 -0 -0.
61	1	-0.50945470E 00	-0 -0 -0.	-0 -0 -0.
62	1	0.62208836E 01	-0 -0 -0.	-0 -0 -0.
63	1	-0.33301412E-00	-0 -0 -0.	-0 -0 -0.
64	1	-0.30685431E-00	-0 -0 -0.	-0 -0 -0.
65	1	0.69792469E 01	-0 -0 -0.	-0 -0 -0.
66	1	-0.37222034E-00	-0 -0 -0.	-0 -0 -0.
67	1	-0.32247268E-00	-0 -0 -0.	-0 -0 -0.
68	1	0.64089822E 01	-0 -0 -0.	-0 -0 -0.
69	1	-0.59730778E 00	-0 -0 -0.	-0 -0 -0.
70	1	0.30813503E-00	-0 -0 -0.	-0 -0 -0.
71	1	0.52626106E 01	-0 -0 -0.	-0 -0 -0.
72	1	-0.11141205E 01	-0 -0 -0.	-0 -0 -0.
73	1	0.21072656E-00	-0 -0 -0.	-0 -0 -0.
74	1	0.45575528E 01	-0 -0 -0.	-0 -0 -0.
75	1	0.40620426E-02	-0 -0 -0.	-0 -0 -0.
76	1	-0.16477048E-00	-0 -0 -0.	-0 -0 -0.
77	1	0.51395853E 01	-0 -0 -0.	-0 -0 -0.
78	1	0.56683767E 00	-0 -0 -0.	-0 -0 -0.
79	1	-0.16256534E-00	-0 -0 -0.	-0 -0 -0.
80	1	0.55062751E 01	-0 -0 -0.	-0 -0 -0.
81	1	-0.42365104E-00	-0 -0 -0.	-0 -0 -0.
82	1	-0.43814982E-01	-0 -0 -0.	-0 -0 -0.
83	1	0.45753306E 01	-0 -0 -0.	-0 -0 -0.
84	1	0.27397618E-01	-0 -0 -0.	-0 -0 -0.
85	1	0.10101712E-01	-0 -0 -0.	-0 -0 -0.
86	1	0.45253629E 01	-0 -0 -0.	-0 -0 -0.
87	1	-0.67868736E-01	-0 -0 -0.	-0 -0 -0.

88	1	0.15930474E-00	-0	-0	-0.	-0	-0	-0.
89	1	0.45977c58E 01	-0	-0	-0.	-0	-0	-0.
90	1	-0.[illegible]346E 00	-0	-0	-0.	-0	-0	-0.
91	1	0.[illegible]RC5E 00	-0	-0	-0.	-0	-0	-0.
92	1	0.[illegible] 01	-0	-0	-0.	-0	-0	-0.
93	1	-0.[illegible] 00	-0	-0	-0.	-0	-0	-0.
94	1	0.[illegible]342E 01	-0	-0	-0.	-0	-0	-0.
95	1	0.36053390E 01	-0	-0	-0.	-0	-0	-0.
96	1	-0.50621923E 00	-0	-0	-0.	-0	-0	-0.

MATRIX SIJ 96 ROWS X 96 COLUMNS FROM TAPE 9

MODULUS OF ELASTICITY = 9727600. PSI SHEAR MODULUS = 3741385. PSI NU = 0.300

TABLE OF VALUES FOR STRESS-STRAIN CURVE

POINT	STRESS LEVEL PSI	STRAIN IN./IN.
1	0.	0.
2	40000.00	0.00411200
3	45000.00	0.00475000
4	50000.00	0.00560000
5	55000.00	0.00700000
6	59000.00	0.00875000
7	60000.00	0.01031999
8	80000.00	0.06569999
9	100000.00	0.42800000
10	120000.00	2.22199997
11	140000.00	8.86399994

IEXIT = 2

APPLIED LOAD 300.00

DEFLECTIONS AT GEOMETRIC NODES

NODE	DELTA X	DELTA Y
1	0.	0.98074135E-05
2	-0.68C7273E-05	0.2747107E-03
3	-0.3134562E-04	0.2570560E-04
4	-0.8512311E-04	0.[illegible]6457E-04
5	-0.1674268E-04	0.1247687E-03
6	-0.8999316E-04	0.1964039E-03
7	-0.9025524E-04	0.2740234E-03
8	-0.7756605E-04	0.3495030E-03

9	-0.6555577E-04	0.4142569E-03
10	-0.2869370E-04	0.4591328E-03
11	0.	0.4754188E-03
12	0.	0.1212177E-04
13	-0.1687642E-05	0.3911792E-05
14	-0.1575417E-04	0.3423503E-04
15	-0.4633667E-04	0.8280537E-04
16	-0.8196892E-04	0.1395279E-03
17	-0.1037364E-03	0.1960105E-03
18	-0.9751238E-04	0.2549714E-03
19	-0.6781490E-04	0.3227288E-03
20	-0.3305737E-04	0.3965521E-03
21	-0.9756602E-05	0.4582211E-03
22	0.	0.4829685E-03
23	0.	0.
24	-0.2870415E-05	0.
25	-0.2152212E-04	0.
26	-0.9412647E-04	0.5141973E-04
27	-0.9404206E-04	0.1193203E-03
28	-0.1197896E-03	0.1836848E-03
29	-0.1061724E-03	0.2461006E-03
30	-0.6442826E-04	0.3205581E-03
31	-0.2363688E-04	0.4037446E-03
32	-0.6150410E-05	0.4680064E-03
33	0.	0.4929429E-03
34	-0.6270201E-04	0.
35	-0.8122083E-04	0.
36	-0.6414194E-04	0.2542261E-03
37	-0.1004477E-03	0.1025815E-03
38	-0.1304589E-03	0.1836621E-03
39	-0.1103164E-03	0.2444661E-03
40	-0.6164771E-04	0.3211120E-03
41	-0.4883927E-04	0.3399037E-03
42	-0.6125498E-04	0.3087391E-03
43	0.6134087E-05	0.3930639E-03
44	0.1778102E-04	0.4278589E-03
45	0.2696356E-04	0.4891222E-03
46	0.1814169E-04	0.5329461E-03
47	0.	0.5459028E-03

NODE STRESSES

NODE	SIGMA X	SIGMA Y	TAU XY
1	1.1[illegible]E 02	3.0[illegible]E 02	5.9072019E 01
2	-9.3[illegible]E 02	3.1[illegible]E 02	2.1177509E 02
3	-2.[illegible]E 02	1.[illegible]E 03	3.[illegible]E 02
4	1.[illegible]E 02	3.4[illegible]E 03	4.6546786E 02
5	1.[illegible]E 02	4.[illegible]E 03	7.0982039E 01
6	0.[illegible]E 02	3.[illegible]E 03	-6.1278914E 02

TOTAL NODE STRAINS

NODE	EPSILON X	EPSILON Y	GAMMA XY
1	1.6698859E-06	2.8148487E-05	1.5788812E-05
2	-9.5047547E-05	5.7505403E-05	5.6603401E-05
3	[illegible]	[illegible]	[illegible]
4	-3.9601120E-05	3.4640837E-04	1.2441059E-04
5	-1.0651445E-04	4.9618464E-04	1.8972131E-05
6	9.7401078E-05	5.2511770E-04	-1.6378673E-04

7	6.2440[illegible]E 02	4.2363409E 03	-1.0743637E 03	-6.6460304E-05	4.1624039E-04	-2.8715671E-04
8	2.0175276E 02	2.4897637E 03	-1.0108704E 03	-5.6044278E-05	2.4972633E-04	-2.7018618E-04
9	6.2189294E 02	5.6582029E 02	-5.9821269E 02	-9.3716744E-05	1.1846582E-04	-1.5989072E-04
10	-1.1046417E 03	1.4628190E 02	-1.8324601E 02	-1.3862887E-04	5.5273078E-05	-4.8978127E-05
11	-2.7800515E 02	3.8419931E 01	-1.4745325E 02	-2.9763881E-05	1.2523282E-05	-3.9411411E-05
12	-4.6627056E 02	1.2283630E 03	1.1423084E 02	-8.5815561E-05	1.4065585E-04	3.0531701E-05
13	-5.8169699E 02	2.5836148E 03	3.6979969E 00	-1.3947751E-04	2.8353590E-04	9.8840330E-07
14	-2.4543363E 02	3.2908220E 03	-3.7175991E 02	-1.2671987E-04	3.4586661E-04	-9.9364260E-05
15	2.8943208E 02	3.3315262E 03	-4.8183398E 02	-7.2990907E-05	3.3355591E-04	-1.2878654E-04
16	4.3682688E 02	3.2341222E 03	-1.7026165E 02	-5.4834674E-05	3.1899680E-04	-4.5507657E-05
17	2.9545055E 01	3.2610364E 03	-9.5024493E 01	-9.7533393E-05	3.3432427E-04	-2.5398216E-05
18	-3.7364545E 02	2.8956395E 03	-4.9432667E 02	-1.2783598E-04	3.0960701E-04	-1.3212399E-04
19	-3.2351908E 02	2.0640588E 03	-8.1925009E 02	-9.6913185E-05	2.2216305E-04	-2.1896976E-04
20	-1.8489700E 02	9.0666008E 02	-4.5836013E 02	-4.6968936E-05	9.6907148E-05	-1.2251083E-04
21	-4.5472734E 02	3.1144418E 03	-1.6650706E 02	-1.4279574E-04	3.3418932E-04	-4.4504129E-05
22	-1.5342715E 02	3.4856244E 03	-1.8611017E 02	-1.2339266E-04	3.6346607E-04	-4.9743661E-05
23	-1.6123643E 02	3.2044911E 03	-2.7865389E 02	-1.1540192E-04	3.3439512E-04	-7.4478813E-05
24	1.5406751E 02	2.6314053E 03	-5.5706024E 02	-6.5314575E-05	2.6575774E-04	-1.4889147E-04
25	1.0536228E 02	2.2789764E 03	2.0314213E 00	-5.9452448E-05	2.3103000E-04	5.4295975E-07
26	-2.2385237E 01	2.5657932E 03	2.8361883E 02	-8.7721859E-05	2.6671622E-04	7.5752391E-05
27	-4.1282[illegible]E 01	2.7531376E 03	-2.1182552E 02	-9.3262873E-05	2.8553007E-04	-5.6616879E-05
28	-2.1907491E 01	2.2876653E 03	1.3698809E 01	-7.2803884E-05	2.3584826E-04	3.6614276E-06
29	5.0508564E 00	2.2626815E 03	-3.3834367E 01	-6.9262055E-05	2.3244852E-04	-5.0432744E-06
30	7.5652369E 01	2.2588829E 03	-2.5139673E 02	-6.2709454E-05	2.3386532E-04	-6.9999948E-05
31	4.5123404E 02	2.1082911E 03	-4.9156138E 02	-1.8632888E-05	2.0281682E-04	-1.3138488E-04
32	8.5[illegible]6714E 02	1.8026695E 03	-2.5410962E 02	3.1864620E-05	1.5907720E-04	-6.7918603E-05

NODE	NODE INELASTIC STRAIN EPSILON X	EPSILON Y	GAMMA XY	NODE STRAIN CHANGE EPSILON X	EPSILON Y	GAMMA XY
1	0.	0.	0.	-0.	0.	0.
2	0.	0.	0.	-0.	0.	0.
3	0.	0.	0.	-0.	0.	0.
4	0.	0.	0.	-0.	0.	0.
5	0.	0.	0.	-0.	0.	0.
6	0.	0.	0.	-0.	0.	-0.
7	0.	0.	0.	-0.	0.	-0.
8	0.	0.	0.	-0.	0.	-0.
9	0.	0.	0.	-0.	0.	-0.
10	0.	0.	0.	-0.	0.	-0.
11	0.	0.	0.	-0.	0.	-0.
12	0.	0.	0.	-0.	0.	0.
13	0.	0.	0.	-0.	0.	0.
14	0.	0.	0.	-0.	0.	-0.
15	0.	0.	0.	-0.	0.	-0.
16	0.	0.	0.	-0.	0.	-0.
17	0.	0.	0.	-0.	0.	-0.
18	0.	0.	0.	-0.	0.	-0.
19	0.	0.	0.	-0.	0.	-0.
20	0.	0.	0.	-0.	0.	-0.
21	0.	0.	0.	-0.	0.	-0.

22	0.	0.	0.	-0.	0.	-0.
23	0.	0.	0.	-0.	0.	-0.
24	0.	0.	0.	-0.	0.	-0.
25	0.	0.	0.	-0.	0.	0.
26	0.	0.	0.	-0.	0.	0.
27	0.	0.	0.	-0.	0.	-0.
28	0.	0.	0.	-0.	0.	0.
29	0.	0.	0.	-0.	0.	-0.
30	0.	0.	0.	-0.	0.	-0.
31	0.	0.	0.	-0.	0.	-0.
32	0.	0.	0.	-0.	0.	-0.

NODE	EFFECTIVE STRESSES	TOTAL EFFECTIVE STRAIN	EFFECTIVE STRAIN CHANGES	EFFECTIVE PLASTIC STRAIN
1	2.8804816E 02	2.0611431E-05	0.	0.
2	1.0F648C6E 03	1.1169053E-04	0.	0.
3	1.8438251E 03	1.9005974E-04	0.	0.
4	3.4376116E 03	3.5338743E-04	0.	0.
5	4.7537771C 03	4.8868562E-04	0.	0.
6	5.1217747E 03	5.2651986E-04	0.	0.
7	4.3765342E 03	4.4990894E-04	0.	0.
8	2.9659661E 03	3.0500494E-04	0.	0.
9	1.7302519E 03	1.7787038E-04	0.	0.
10	1.4195320E 03	1.4592828E-04	0.	0.
11	3.9328268E 02	4.0425569E-05	0.	0.
12	1.5291107E 03	1.5719301E-04	0.	0.
13	2.9182801E 03	3.0000001E-04	0.	0.
14	3.4802359C 03	3.5770922E-04	0.	0.
15	3.3028022E 03	3.4563179E-04	0.	0.
16	3.0536178E 03	3.1391273E-04	0.	0.
17	3.2959342E 03	3.3415582E-04	0.	0.
18	3.2193228E 03	3.3094720E-04	0.	0.
19	2.6544805E 03	2.7288134E-04	0.	0.
20	1.2161338E 03	1.3221491E-04	0.	0.
21	3.1772652E 03	3.4718381E-04	0.	0.
22	3.5631410E 03	3.6836845E-04	0.	0.
23	3.1233093E 03	3.4163712E-04	0.	0.
24	2.7337821E 03	2.8103356E-04	0.	0.
25	2.2281667E 03	2.2905616E-04	0.	0.
26	2.6576500E 03	2.7321127E-04	0.	0.
27	2.0186461E 03	2.0675760E-04	0.	0.
28	2.3528168E 03	2.3631932E-04	0.	0.
29	3.2EC9199E 03	3.3242319E-04	0.	0.
30	2.3051822E 03	2.3697338E-04	0.	0.
31	2.1C28715E 03	2.1617578E-04	0.	0.
32	1.6C.290I6E 03	1.6662946E-04	0.	0.

1 CYCLES COMPLETED - LOAD = 500.00

APPLIED LOAD 5000.00

DEFLECTIONS AT GEOMETRIC NODES

NODE	DELTA X	DELTA Y
1	-0.	0.9751782E-04
2	-0.6819702E-04	0.2709466E-04
3	-0.3137A26E-03	0.2562855E-03
4	-0.5619135E-03	0.6601230E-03
5	-0.7679278E-03	0.1244639E-02
6	-0.8999C12E-03	0.1965615E-02
7	-0.9041115E-03	0.2752182E-02
8	-0.7778574E-03	0.3505041E-02
9	-0.5573C60E-03	0.4152337E-02
10	-0.2875716E-03	0.4601115E-02
11	-0.	0.4764025E-02
12	-0.	0.1205512E-03
13	-0.1055C59E-04	0.3883887E-04
14	-0.1577292E-03	0.3421780E-03
15	-0.4637262E-03	0.8266096E-03
16	-0.8207240E-03	0.1393606E-02
17	-0.1045774E-02	0.1961724E-02
18	-0.9781868E-03	0.2558090E-02
19	-0.6776040E-03	0.3236209E-02
20	-0.3314501E-03	0.3974965E-02
21	-0.5833552E-04	0.4591980E-02
22	-0.	0.4839611E-02
23	-0.	-0.
24	-0.2871761E-04	-0.
25	-0.2142653E-03	-0.
26	-0.5409221E-03	0.5142463E-03
27	-0.9417250E-03	0.1195004E-02
28	-0.1201777E-02	0.1840009E-02
29	-0.1064576E-02	0.2484597E-02
30	-0.6449034E-03	0.3211716E-02
31	-0.2361642E-03	0.4046455E-02
32	-0.6147018E-04	0.4689589E-02
33	-0.	0.4930317E-02
34	-0.6265564E-03	-0.
35	-0.6121352E-03	-0.
36	-0.6411183E-03	0.2545001E-03
37	-0.1005527E-02	0.1029098E-02
38	-0.1308330E-02	0.1839042E-02
39	-0.1105638E-02	0.2447632E-02
40	-0.6166593E-03	0.3216094E-02
41	-0.4882694E-03	0.3404184E-02
42	-0.2124588E-03	0.3091050E-02
43	0.6394C913E-04	0.3934705E-02
44	0.1803593E-03	0.4283975E-02
45	0.2716215E-03	0.4898887E-02
46	0.1824233E-03	0.5330499E-02
47	-0.	0.5466438E-02

NODE STRESSES

NODE	SIGMA X	SIGMA Y	TAU XY
1	1.0588[illegible]E 03	3.0709793E 03	5.6930054E 02
2	-9.3277622E 03	3.0818824E 03	2.1026550E 03
3	-2.[illegible]E 03	1.5792547E 04	3.7384235E 03
4	1.[illegible]E 03	3.4044860E 04	4.6597701E 03
5	[illegible]	[illegible]	7.1901753E 02
6	[illegible]	[illegible]	-6.0897180E 03
7	[illegible]	[illegible]	[illegible]
8	2.0018993[illegible]E 03	2.4[illegible]E 04	-1.0090006E 04
9	-6.2505366E 03	9.6416703E 03	-8.9708816E 03
10	-1.3[illegible]E 04	1.4[illegible]E 03	-1.8284360E 03
11	-2.7[illegible]E 03	3.7026424E 02	-1.4778715E 03
12	-4.[illegible]E 03	1.2250581E 04	1.1349745E 03
13	-5.8161802E 03	2.9756110E 04	3.6309244E 01
14	-2.4759411E 02	3.2893768E 04	-3.7022674E 03
15	2.8913819E 03	3.3421163E 04	-4.8240502E 03
16	4.4[illegible]E 03	3.2533126E 04	-1.7238590E 03
17	2.6[illegible]E 02	3.2616957E 04	-9.7832627E 02
18	-3.7[illegible]E 03	2.8970164E 04	-4.9611542E 03
19	-3.2432[illegible]E 03	2.0621797E 04	-8.1970438E 03
20	-1.8612209E 03	9.0551850E 03	-4.5834204E 03
21	-4.5453457E 03	3.1153412E 04	-1.6643811E 03
22	-1.[illegible]E 03	3.4964802E 04	-1.9686290E 03
23	-1.6200762E 03	3.2096846E 04	-2.7877741E 03
24	1.5470076E 03	2.6350002E 04	-5.6011828E 03
25	1.0[illegible]E 03	2.2753857E 04	3.0263770E 01
26	-8.[illegible]E 02	2.5744161E 04	2.8934653E 03
27	-8.[illegible]E 02	2.7543151E 04	-2.1387192E 03
28	-2.2[illegible]E 02	2.2859020E 04	1.3694021E 02
29	5.1732861E 01	2.2635767E 04	-3.4372819E 02
30	8.0[illegible]E 02	2.2[illegible]E 04	-2.6325993E 03
31	4.5[illegible]E 03	2.1[illegible]E 04	-4.9257184E 03
32	8.5330017E 03	1.8021406E 04	-2.5435980E 03

TOTAL NODE STRAINS

NODE	EPSILON X	EPSILON Y	GAMMA XY
1	1.[illegible]E-05	2.8180[illegible]E-04	1.[illegible]
2	-9.5114183E-04	5.7364725E-04	5.6200183E-04
3	-7.5852715E-04	1.7049334E-03	9.9920855E-04
4	-8.9771208E-04	3.4545250E-03	1.2454667E-03
5	-1.1380473E-03	5.1144526E-03	2.0610853E-04
6	-1.0[illegible]E-03	5.9[illegible]	-1.7479372E-03
7	[illegible]	[illegible]	[illegible]
8	-5.6082703E-04	2.4936689E-03	-2.6568642E-03
9	-9.3994795E-04	1.1839450E-02	-1.5359016E-03
10	-1.3900636E-03	5.8320856E-04	-4.8870563E-04
11	-2.9804153E-04	1.2465003E-04	-3.9500558E-04
12	-8.5718397E-04	1.4031757E-03	3.0335681E-04
13	-1.3934591E-03	2.8321685E-03	9.7547613E-06
14	-1.2693852E-03	3.4579701E-03	-9.8954471E-04
15	-7.3347657E-04	3.3465344E-03	-1.2693780E-03
16	-5.4949391E-04	3.2082653E-03	-4.6075429E-04
17	-9.7829337E-04	3.3467380E-03	-2.6148776E-04
18	-1.2784765E-03	3.0936512E-03	-1.3240209E-03
19	-9.6938827E-04	2.2199455E-03	-2.1909118E-03
20	-4.7059669E-04	9.8027574E-04	-1.2250599E-03
21	-1.4280166E-03	3.3427583E-03	-6.4485648E-04
22	-1.2367501E-03	3.6419212E-03	-4.9944853E-04
23	-1.1564137E-03	3.3495280E-03	-7.4311828E-04
24	-6.5360345E-04	2.6610777E-03	-1.4970882E-03
25	-5.9369168E-04	2.3105232E-03	8.0889225E-06
26	-8.7983634E-04	2.6742722E-03	7.5890228E-04
27	-9.3323798E-04	2.8565650E-03	-5.7163842E-04
28	-7.2922148E-04	2.3609258E-03	3.6601478E-05
29	-6.9277079E-04	2.3253677E-03	-9.1871920E-05
30	-6.2616267E-04	2.0385681E-03	-7.0364306E-04
31	-1.8291989E-04	2.0270351E-03	-1.3162823E-03
32	3.2141071E-04	1.8894587E-03	-6.7985471E-04

NODE INELASTIC STRAIN

NODE	EPSILON X	EPSILON Y	GAMMA XY
1	0.	0.	0.
2	0.	0.	0.
3	0.	0.	0.
4	0.	0.	0.
5	-7.9[illegible]745E-05	1.8622640E-04	8.6903001E-06
6	-1.3705703E-04	3.4[illegible]598E-04	-1.2642044E-04
7	-2.5295384E-05	6.6209016E-05	-5.4783029E-05
8	0.	0.	0.
9	0.	0.	0.
10	0.	0.	0.
11	0.	0.	0.
12	0.	0.	0.

NODE STRAIN CHANGE

NODE	EPSILON X	EPSILON Y	GAMMA XY
1	-0.	0.	0.
2	-0.	0.	0.
3	-0.	0.	0.
4	-0.	0.	0.
5	-0.	[illegible]E-04	6.[illegible]E-06
6	-0.	2.[illegible]E-04	-8.[illegible]E-05
7	-0.	[illegible]E-05	-5.4783029E-05
8	-0.	0.	-0.
9	-0.	0.	-0.
10	-0.	0.	-0.
11	-0.	0.	-0.
12	-0.	0.	0.

13	0.	0.	0.	-0.	0.	0.
14	0.	0.	0.	-0.	0.	-0.
15	0.	0.	0.	-0.	0.	-0.
16	0.	0.	0.	-0.	0.	-0.
17	0.	0.	0.	-0.	0.	-0.
18	0.	0.	0.	-0.	0.	-0.
19	0.	0.	0.	-0.	0.	-0.
20	0.	0.	0.	-0.	0.	-0.
21	0.	0.	0.	-0.	0.	-0.
22	0.	0.	0.	-0.	0.	-0.
23	0.	0.	0.	-0.	0.	-0.
24	0.	0.	0.	-0.	0.	-0.
25	0.	0.	0.	-0.	0.	0.
26	0.	0.	0.	-0.	0.	0.
27	0.	0.	0.	-0.	0.	-0.
28	0.	0.	0.	-0.	0.	0.
29	0.	0.	0.	-0.	0.	-0.
30	0.	0.	0.	-0.	0.	-0.
31	0.	0.	0.	-0.	0.	-0.
32	0.	0.	0.	-0.	0.	-0.

200

NODE	EFFECTIVE STRESS	TOTAL EFFECTIVE STRAIN	EFFECTIVE STRAIN CHANGES	EFFECTIVE PLASTIC STRAIN
1	[illegible] 03	[illegible]	0.	0.
2	[illegible]	[illegible]	0.	0.
3	1.8439429E 04	1.8955785E-03	0.	0.
4	3.4265756E 04	3.5256133E-03	0.	0.
5	4.7218144E 04	4.9054842E-03	1.3152447E-04	1.8703635E-04
6	5.0605765E 04	5.2264305E-03	2.2811361E-04	3.5184615E-04
7	4.3156589E 04	4.4924327E-03	7.3927920E-05	7.3927920E-05
8	2.9624120E 04	3.0458678E-03	0.	0.
9	1.7269126E 04	1.7753550E-03	0.	0.
10	1.4227504E 04	1.4625913E-03	0.	0.
11	3.9264372E 03	4.0466684E-04	0.	0.
12	1.5258820E 04	1.5685480E-03	0.	0.
13	2.5142656E 04	2.5858937E-03	0.	0.
14	3.4757158E 04	3.5771617E-03	0.	0.
15	3.2143860E 04	3.4071981E-03	0.	0.
16	3.0711324E 04	3.1571327E-03	0.	0.
17	3.2527552E 04	3.3438414E-03	0.	0.
18	3.2161432E 04	3.3082603E-03	0.	0.
19	2.6537412E 04	2.7280534E-03	0.	0.
20	1.2858561E 04	1.3218431E-03	0.	0.
21	3.3760301E 04	3.4726244E-03	0.	0.
22	3.5906471E 04	3.6911952E-03	0.	0.
23	3.3288835E 04	3.4221015E-03	0.	0.
24	2.7387441E 04	2.8154366E-03	0.	0.

25	2.2[illegible]16E 04	2.2935797E-03	0.	0.
26	2.6629[illegible]E 04	2.7376455E-03	0.	0.
27	2.9200308E 04	2.0493795E-03	0.	0.
28	2.3C1[illegible]94E 04	2.3687422E-03	0.	0.
29	2.2317702E 04	2.3281143E-03	0.	0.
30	2.3C[illegible]E 04	2.3659204E-03	0.	0.
31	2.1024[illegible]E 04	2.1613600E-03	0.	0.
32	1.6224609E 04	1.6678327E-03	0.	0.

10 CYCLES COMPLETED - LOAD = 5000.00

APPLIED LOAD 16000.00

DEFLECTIONS AT GEOMETRIC NODES

NODE	DELTA X	DELTA Y
1	-0.	0.1834266E-02
2	-0.1354204E-03	0.9840871E-03
3	-0.2131713E-02	0.4376436E-02
4	-0.6105047E-02	0.1413375E-01
5	-0.1056513E-01	0.2926615E-01
6	-0.1288031E-01	0.4364013E-01
7	-0.1157194E-01	0.5883652E-01
8	-0.7744429E-02	0.7330976E-01
9	-0.4176802E-02	0.8408169E-01
10	-0.1592816E-02	0.8981841E-01
11	-0.	0.9109615E-01
12	-0.	0.2215896E-02
13	0.6514695E-04	0.9628529E-03
14	-0.1305631E-02	0.4983438E-02
15	-0.7127649E-02	0.1570879E-01
16	-0.1411285E-01	0.2973369E-01
17	-0.1760520E-01	0.4362269E-01
18	-0.1505574E-01	0.5673531E-01
19	-0.6557570E-02	0.7091255E-01
20	-0.3030400E-02	0.8274529E-01
21	-0.4429239E-03	0.8784958E-01
22	-0.	0.9163623E-01
23	-0.	-0.
24	-0.1081097E-03	-0.
25	-0.2365713E-02	-0.
26	-0.1078470E-01	0.1109740E-01
27	-0.2058212E-01	0.2741802E-01
28	-0.2547245E-01	0.4260798E-01
29	-0.2128427E-01	0.5701762E-01
30	-0.1101842E-01	0.732802 E-01
31	-0.4555645E-02	0.8644432E-01
32	-0.1389738E-02	0.9176628E-01
33	-0.	0.9280031E-01
34	-0.1248564E-01	-0.
35	-0.1977993E-01	-0.
36	-0.1363704[illegible]-01	0.5702420E-02
37	-0.[illegible]E-01	0.2233164E-01
38	-0.[illegible]E-01	0.[illegible]E-01
39	-0.2426897E-01	0.5762441E-01
40	-0.1197417E-01	0.7400623E-01
41	-0.9267265E-02	0.7758912E-01
42	-0.1224470E-01	0.7139266E-01
43	-0.4246746E-02	0.8306547E-01
44	-0.2048812E-02	0.8764596E-01
45	0.1253593E-03	0.9449336E-01
46	0.3358787E-03	0.9747484E-01
47	-0.	0.9785107E-01

NODE STRESSES				TOTAL NODE STRAINS		
NODE	SIGMA X	SIGMA Y	TAU XY	EPSILON X	EPSILON Y	GAMMA XY
1	1.4508088E 04	1.4228640E 04	6.9880750E 03	1.052[illegible]E-03	1.0152784E-03	1.8677778E-03
2	-2.1555422E 04	1.7739039E 04	2.4416703E 04	-9.780[illegible]E-03	1.1527116E-02	1.7179011E-02
3	-8.9731385E 03	7.5316840E 04	1.7862140E 04	-2.7071201E-02	4.8794462E-02	3.5084694E-02
4	8.3002466E 03	1.0151915E 05	9.3442271E 03	-3.7230509E-02	6.5670739E-02	3.0285604E-02
5	1.7372501E 04	1.0947562E 05	1.3569608E 03	-3.8409002E-02	1.0825[illegible]79E-01	6.2776454E-03
6	1.6521826E 04	1.0815106E 05	-3.1287073E 03	-3.6997817E-02	1.0545023E-01	-1.7616362E-02
7	9.8023131E 03	1.0047675E 05	-1.1437973E 04	-3.4263436E-02	8.8403459E-02	-3.9851675E-02
8	-2.5498406E 02	7.8238656E 04	-2.2330953E 04	-2.3524571E-02	4.9760257E-02	-4.6734130E-02
9	-1.4677704E 04	4.3057543E 04	-2.3472471E 04	-1.3238312E-02	1.7541306E-02	-2.8934352E-02
10	-4.3554083E 04	1.5768084E 04	-1.4566204E 04	-7.2386625E-03	4.4034375E-03	-5.3401092E-03
11	3.2518612E 03	3.4168291E 04	-5.6671171E 02	-7.1946071E-04	3.4122227E-03	-1.5147112E-04
12	-9.5641956E 03	6.5308785E 04	6.4651716E 03	-9.5505785E-03	2.0259312E-02	5.5893118E-03
13	-1.3716366E 04	7.7586634E 04	2.3089051E 03	-3.2107606E-02	5.2957940E-02	7.7514830E-03
14	9.3313143E 02	9.5552619E 04	-1.2945508E 03	-3.5999758E-02	7.5738037E-02	-5.8170959E-03
15	1.0355209E 04	9.9400467E 04	-3.4412467E 03	-2.9001316E-02	7.4769365E-02	-1.1184506E-02
16	9.2033799E 03	9.8133469E 04	1.2712433E 03	-2.7916404E-02	7.0808588E-02	1.0890223E-03
17	8.1679448E 02	9.4109449E 01	-1.1964001E 03	-3.4000587E-02	7.2394625E-02	-2.4729502E-03
18	-4.4787615E 03	8.2655283E 04	-9.7430657E 03	-2.9492462E-02	5.4133062E-02	-2.0813946E-02
19	1.8617439E 03	7.1564380E 04	-1.6911892E 04	-1.5028462E-02	3.0925777E-02	-2.5832348E-02
20	2.9859340E 02	6.1071254E 04	-1.4407938E 04	-5.6642358E-03	1.3072707E-02	-1.0259439E-02
21	-2.9599522E 03	9.1400709E 04	-6.4285762E 03	-3.5157801E-02	6.9325117E-02	-1.3628222E-02
22	-7.0348868E 03	9.0611372E 04	-6.5701942E 03	-4.0993457E-02	7.7256289E-02	-1.5517909E-02
23	-2.2594351E 03	9.2813559E 04	-7.7228555E 03	-3.6944289E-02	7.3816285E-02	-1.7173950E-02
24	3.1509409E 03	8.8109823E 04	-1.5701006E 04	-2.6126802E-02	5.9796288E-02	-3.2827374E-02
25	2.7019047E 03	8.8081665E 04	6.9725612E 02	-2.4382556E-02	5.4646192E-02	1.5825503E-03
26	1.8927714E 03	8.7083228E 04	1.0579429E 04	-2.6591619E-02	5.7273250E-02	2.0595146E-02
27	1.2204454E 04	8.9277824E 04	1.7398693E 02	-1.8045175E-02	4.8523677E-02	-1.5244626E-03
28	1.0478217E 04	8.8239101E 04	5.5663302E 03	-1.8576234E-02	4.8685803E-02	7.7893626E-03
29	-7.[illegible]847E 03	6.7957775E 04	-3.1824467E 03	-1.4407811E-02	2.7761309E-02	-8.7835752E-03
30	-7.0[illegible]5009E 03	6.5349770E 04	-1.1369717E 04	-1.2270336E-02	2.3[illegible]0591E-02	-1.2210908E-02
31	9.1657012E 02	6.7282411E 04	-1.0911027E 04	-7.[illegible]7995E-03	1.8346864E-02	-8.9889227E-03
32	1.6212595E 04	7.3951444E 04	-2.4291205E 03	-2.6839480E-03	1.4484971E-02	-1.5524496E-03

	NODE INELASTIC STRAIN			NODE STRAIN CHANGE		
NODE	EPSILON X	EPSILON Y	GAMMA XY	EPSILON X	EPSILON Y	GAMMA XY
1	0.	0.	0.	0.	0.	0.
2	-6.3592898E-03	6.9804257E-03	1.0652897E-02	-3.1863937E-04	3.8023508E-04	5.7171831E-04
3	-2.3825983E-02	4.0775139E-02	3.1310488E-02	-5.9637085E-04	1.0206055E-03	6.8531652E-04
4	-3.4552918E-02	7.9450725E-02	2.7788072E-02	-7.7822191E-04	1.7846422E-03	5.1380104E-04
5	-3.6818087E-02	5.7568389E-02	5.9149618E-03	-7.4138210E-04	1.9996868E-03	8.0750255E-05
6	-3.5401958E-02	9.4854141E-02	-1.6780119E-02	-7.0950113E-04	1.9039667E-03	-1.7926613E-04
7	-3.2172406E-02	7.8376726E-02	-3.6704525E-02	-7.0545253E-04	1.6674236E-03	-5.9864487E-04
8	-2.1085483E-02	4.1709442E-02	-4.0765498E-02	-5.0778469E-04	1.0106388E-03	-8.6396519E-04
9	-1.0401542E-02	1.2662317E-02	-2.[illegible]24209E-02	-3.2544200E-04	4.5716388E-04	-7.7485217E-04
10	-2.2338815E-03	1.5069265E-03	-1.4468276E-03	-1.7634451E-04	1.2840252E-04	-1.4865588E-04
11	0.	0.	0.	-0.	0.	-0.
12	-7.0734173E-03	1.3406641E-02	3.8612761E-03	-2.8123414E-04	5.1123226E-04	1.4679461E-04
13	-2.8292445E-02	4.4517079E-02	6.8670551E-03	-6.5955530E-04	1.0616616E-03	1.2421501E-04
14	-3.3148834E-02	6.5943980E-02	-5.4710892E-03	-7.4115829E-04	1.3044628E-03	-6.1447988E-05
15	-2.7030315E-02	6.4870327E-02	-1.0254725E-02	-6.1381523E-04	1.4699513E-03	-1.6105856E-04
16	-2.[illegible]0706E-02	6.1034654E-02	7.4924350E-04	-5.9732032E-04	1.4014565E-03	5.7145675E-05
17	-3.[illegible]106E-02	[illegible]E-02	-2.1531756E-03	-6.8136125E-04	1.3005742E-03	-5.2882622E-05

18	[illegible]	[illegible]	-1.[illegible]E-02	-5.[illegible]E-04	1.07[illegible]E-03	-3.[illegible]E-04
19	[illegible]	[illegible]	[illegible]	[illegible]	[illegible]	[illegible]
20	-2.8114837E-03	6.8033490E-03	-6.4089746E-03	-2.1094012E-04	4.2500421E-04	-1.0153872E-04
21	-3.2023712E-02	5.5837811E-02	-1.1891278E-02	-7.1828491E-04	1.3710311E-03	-2.8778051E-04
22	-3.7475806E-02	6.7725058E-02	-1.3761823E-02	-8.1599231E-04	1.4674732E-03	-3.0726902E-04
23	-1.1619c40E-02	6.4205344E-02	-1.5109780E-02	-7.6445814E-04	1.4756788E-03	-2.6393624E-04
24	-2.3733703E-02	5.0836774E-02	-2.8630748E-02	-5.6679631E-04	1.1990926E-03	-6.5276680E-04
25	-2.1943F61E-02	4.5674700E-02	1.3961872E-03	-5.4800922E-04	1.1897430E-03	2.7729463E-05
26	-2.4190c91E-02	4.8379434E-02	1.7771469E-02	-5.3878614E-04	1.1142908E-03	4.1057428E-04
27	-1.8576993E-02	3.9720439E-02	-1.5704660E-03	-4.0525194E-04	1.0469680E-03	6.5819028E-06
28	-1.0932094E-02	3.0917949E-02	6.3011634E-03	-4.3184456E-04	1.0654481E-03	2.1436035E-04
29	-1.1[illegible]E-02	2.0951379E-02	-6.5965650E-03	-3.9873006E-04	6.9283423E-04	-2.3800590E-04
30	-2.4737442E-03	1.6875758E-02	-9.1720023E-03	-3.8482717E-04	6.6762376E-04	-3.3071303E-04
31	-5.3202439E-03	1.1459546E-02	-6.0726154E-03	-3.1494047E-04	6.4314446E-04	-3.1504238E-04
32	-2.0602558E-03	7.3859362E-03	-9.0319254E-04	-1.9269090E-04	6.1357281E-04	-6.7958513E-05

NODE	EFFECTIVE STRESSES	TOTAL EFFECTIVE STRAIN	EFFECTIVE STRAIN CHANGES	EFFECTIVE PLASTIC STRAIN
1	1.0788511E 04	1.9314662E-03	0.	0.
2	8.7256061E 04	1.6272532E-02	5.2493473E-04	9.8835253E-03
3	8.5942656E 04	5.2549598E-02	1.0991203E-03	4.4813790E-02
4	9.8566362E 04	8.9674506E-02	1.8139193E-03	8.1314657E-02
5	1.0155291E 05	1.0760998E-01	2.0223725E-03	9.8611578E-02
6	1.0059717E 05	1.0988988E-01	1.9272724E-03	9.6443824E-02
7	9.7975706E 04	9.0155826E-02	1.7092964E-03	8.1803193E-02
8	8.7391694E 04	5.5810050E-02	1.1270363E-03	4.7953203E-02
9	7.1647872E 04	2.5066250E-02	6.4904371E-04	1.8350773E-02
10	5.9246280E 04	8.3336813E-03	2.0154787E-04	2.4446326E-03
11	3.2678744E 04	3.3593830E-03	0.	0.
12	6.8593617E 04	2.0132056E-02	5.1914958E-04	1.3599763E-02
13	8.5663816E 04	5.2956812E-02	1.0744124E-03	4.5244400E-02
14	9.5115919E 04	7.4346099E-02	1.5049353E-03	6.6073092E-02
15	9.4836158E 04	7.3755399E-02	1.4795233E-03	6.5485739E-02
16	9.3856528E 04	6.9513835E-02	1.4069648E-03	6.1268205E-02
17	9.3726631E 04	7.1021569E-02	1.3809511E-03	6.2767397E-02
18	8.6761130E 04	5.4766661E-02	1.1009504E-03	4.6948543E-02
19	7.0511589E 04	3.3812962E-02	8.2520977E-04	2.6772760E-02
20	6.9835535E 04	1.4107476E-02	4.5928301E-04	7.7988479E-03
21	9.2595175E 04	6.8528281E-02	1.3815802E-03	6.0288236E-02
22	9.5009795E 04	7.0607472E-02	1.4812071E-03	6.8320850E-02
23	9.4510386E 04	7.3108498E-02	1.4908798E-03	6.4842503E-02
24	9.0729489E 04	6.1566045E-02	1.2574927E-03	5.3495498E-02
25	8.0770675E 04	5.3464551E-02	1.1502728E-03	4.5694774E-02
26	8.8C79834E 04	6.7381886E-02	1.1394224E-03	4.9466677E-02
27	8.3730545E 04	4.7590103E-02	1.0558385E-03	4.0038418E-02
28	8.3C49363E 04	4.7651223E-02	1.0789106E-03	4.0289844E-02
29	7.3210764E 04	2.7780651E-02	7.0983637E-04	2.0964400E-02
30	7.1875943E 04	2.4432053E-02	6.9688493E-04	1.7740121E-02
31	6.2448595E 04	1.8478952E-02	6.6841405E-04	1.2008031E-02
32	6.7425975E 04	1.3545798E-02	6.2878302E-04	7.6431725E-03

120 CYCLES COMPLETED - LOAD = 16000.00

APPENDIX E CONTACT PROBLEM - LOADED HOLE BOUNDARY COMPUTER PROGRAM

(A) Program Description

This is a brief description of the program for doing a nonlinear contact problem of a symmetric single hole plate structure which is loaded along its axis of symmetry. The program can accommodate varying amounts of clearance or interference and up to twenty points in contact on the semicircle as well as up to ten different load levels.

The program was originally written and debugged on the IBM 1130 machine and then converted to the IBM 7094. It is fully operable on the Grumman IBM 7094 system and can easily be expanded to handle more contact points around the periphery of the fastener and plate hole.

A constraint on the program as it stands at present is that the contact points must be numbered consecutively from the contact point on the center line at the bottom of the hole to the point on the center line at the top of the hole counterclockwise.

The program consists of a main program and two subroutines, one for reading and stacking input, and the other for performing the calculations. A matrix inversion routine "LINEAR" is included to avoid dependence on a library routine.

(B) Sequencing and Details of the Data Cards

The symbols used in the program for various items of input data are listed on page 205 and are shown on the sample key-punching sheet page 209.

The data cards are used in the following sequence, immediately after the $DATA card required by IBSYS:

1. A load-fit card (FORMAT 23) containing a clue K, a load QIN(1), a fit FITIN(1), and a 60 character title to be printed for identification. The clue K is ignored in this card. Up to 9 additional load-fit cards in the same

format may be provided. They are used in a slightly different manner. This title is ended by one completely blank card.

2. The four data matrices are next. They must be in proper sequence, as shown below. Each has a header card (FORMAT 1), one or more data cards (FORMAT 2) and a blank card to end it. If one of the matrices is null, it must be represented by a blank title card and a blank card to represent the end card. Required sequence is as follows:

   a) Matrix A - influence coefficient for unit radial loads, maximum size 20 x 20
   b) Matrix DL - radial displacements around hole for transfer loads, maximum size 20 x 10. Note that sequence of loads (columns) must correspond to sequence of load-fit cards already read in.
   c) Matrix THETA - angles to defined points around hole, maximum size 20 x 1
   d) Matrix DELB - radial displacements around hole due to bypass loads, maximum size 20 x 1. This matrix may be null as previously indicated. All others must be provided to give meaningful results.

(C) Symbols and Format of the Data Cards

(1) Load-fit cards - FORMAT 23

Cols.	Field	Symbol	
1	I1	K	A clue, ignored in the first card. In the other cards, any digit except 0 indicates a new fit is provided (a blank fit means 0 clearances) If K = 0, the previous fit is re-used.
2-10	E9.4	Q or QIN	This is the load to be applied with the corresponding column of matrix DL. A value must be provided. If none is provided, this is treated as a blank card (end of load table).

Cols.	Field	Symbol	
11-20	E10.4	AKFIT or FITIN	This is the fit of the pin in the hole. A positive value indicates an interference fit. A negative value indicates lack of fit (sloppy fit). Zero indicates exact or sliding fit. Fit is always accepted from the first load-fit card. It is ignored on the other cards unless Column 1 is punched to show that a new value of fit is provided. This new value is then used until a superceding value is provided.
21-80	30A2	TITLE	A title or caption that is printed to identify the run. In addition, the last 8 columns are used to identify the punched output from this run. The title is used from the first card only.

(2) Data Matrices Header Card FORMAT 1

Cols.	Field	Symbol	
1-4	I4	NROWS	The number of rows in this matrix. The number of rows in matrix A sets the size of the problem.
5-8	I4	NCOLS	The number of columns in this matrix. The number of columns in matrix DL must agree with the number of load-fit cards read in.
9-80			Ignored

(3) Data Matrices - Data Cards FORMAT 2

Cols.	Field	Symbol	
1-4	I4	MR(1)	Row index for the first element in this card. If this field is blank or zero, the card is considered bland (end of matrix)

Cols.	Field	Symbol	
5-8	I4	MC(1)	Column index for the first element in this card.
9-23	E15.7	EL(1)	The first matrix element in this card.
24	1X		Ignored
25-28	I4	MR(2)	Row index for the second element in this card. If this field is blank or zero, the element is ignored and the program looks at MR(3)
29-32	I4	MC(2)	Column index for the second element in this card.
33-47	E15.7	EL(2)	The second matrix element in this card.
48	1X		Ignored
49-52	I4	MR(3)	Row index for the third element in this card. If this field is blank or zero, the element is ignored and the program reads the next card.
53-56	I4	MC(3)	Column index for the third element in this card.
57-71	E15.7	EL(3)	The third matrix element in this card.
72	1X		Ignored
73-80	4A2		Ignored on input. For punch output, this takes 8 columns of identification from the title card.

The last card of a matrix should be completely blank (tested in Cols. 1-4 as an integer field). Note that the program does no checking on the validity of elements, their indices or their sequencing, other than checking the row index for a zero or blank as described above (negative row index is considered zero). Specifically, no checking is done for duplicate indices, column index of zero, elements out of sequence, element indices outside of the array or elements in row or column sort. Valid input is the responsibility of the user. The ability to read matrices in row or column sort, and one to three elements per card is convenient, but requires careful data preparation.

(D) Punched Output

Upon finding the points in contact for each applied load, the program calculates and prints out P_o (the center-line contact force), and then the X and Y components of the force at each point. It then punches out cards containing these values in FORMAT 2 for input as applied loads to further analysis programs. These cards carry identification in Columns 73-80 from the input title, Columns 73-80.

The punchout is described as follows. The row number corresponds to the load case (columns of matrix DL). Column 1 is the center-line contact force. Columns 2 and 3 are the X and Y components at Point 1, columns 4 and 5 are the X and Y components at point 2, etc. Thus the punched-out load matrix is N rows by M columns, where N is the input number of load cases and M is 2 times the number of points around the semicircle, plus 1.

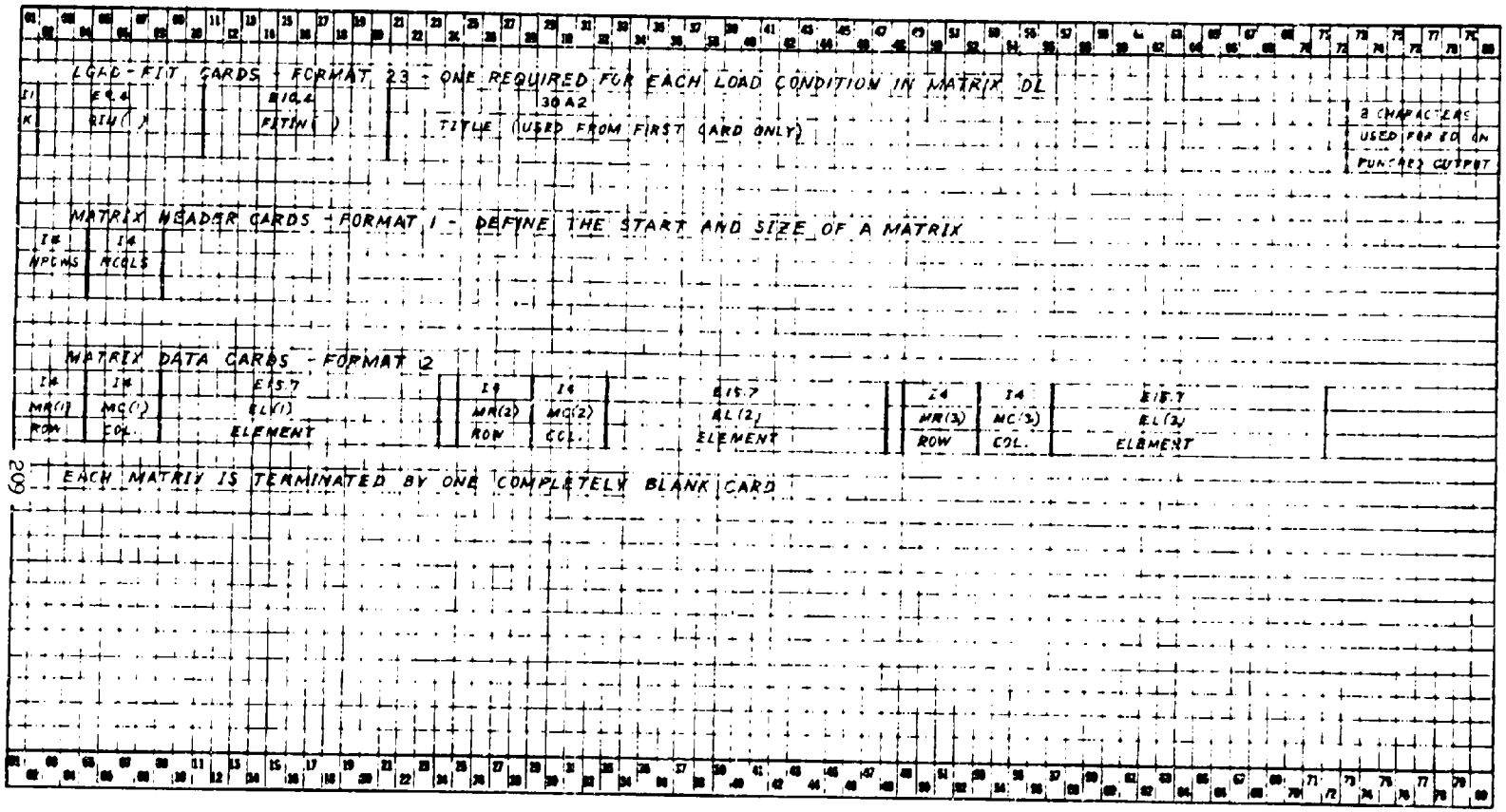

FORMATS FOR CONTACT PROBLEM COMPUTER PROGRAM

APPENDIX F CONTACT PROBLEM - LOADED HOLE BOUNDARY PROGRAM FLOW CHARTS

MAIN PROGRAM

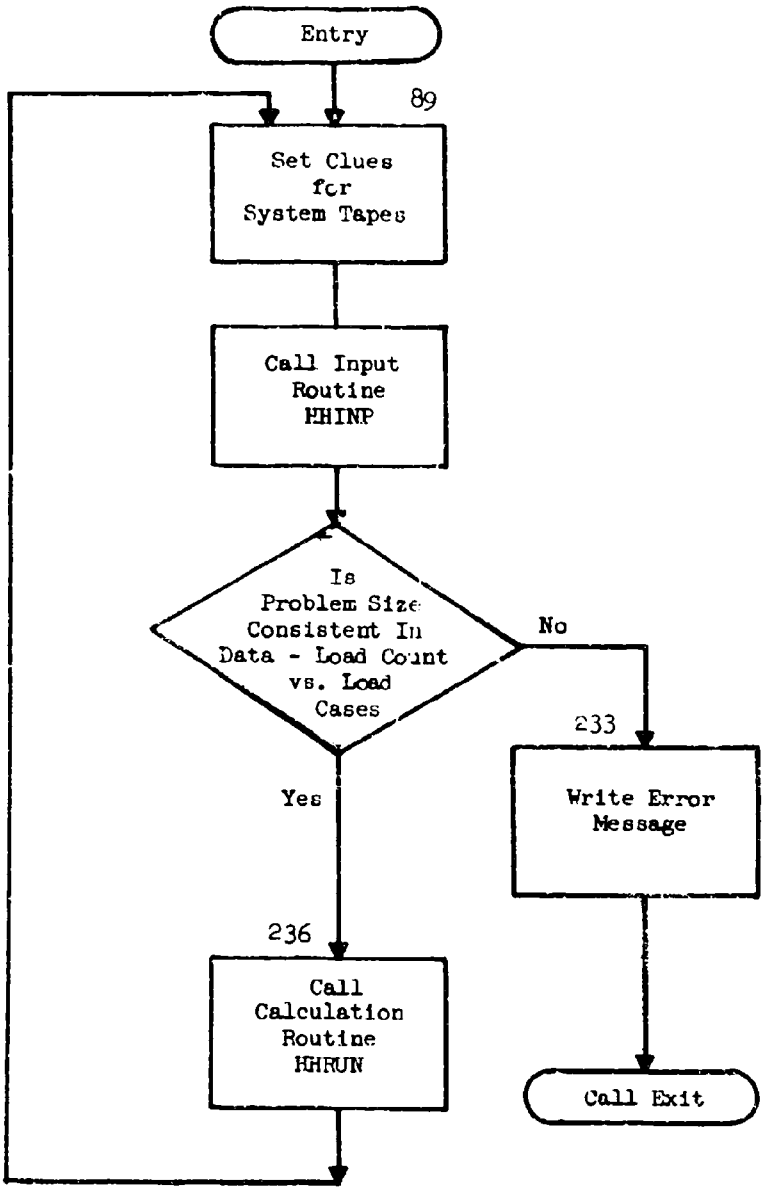

INPUT - SUBROUTINE HHINP

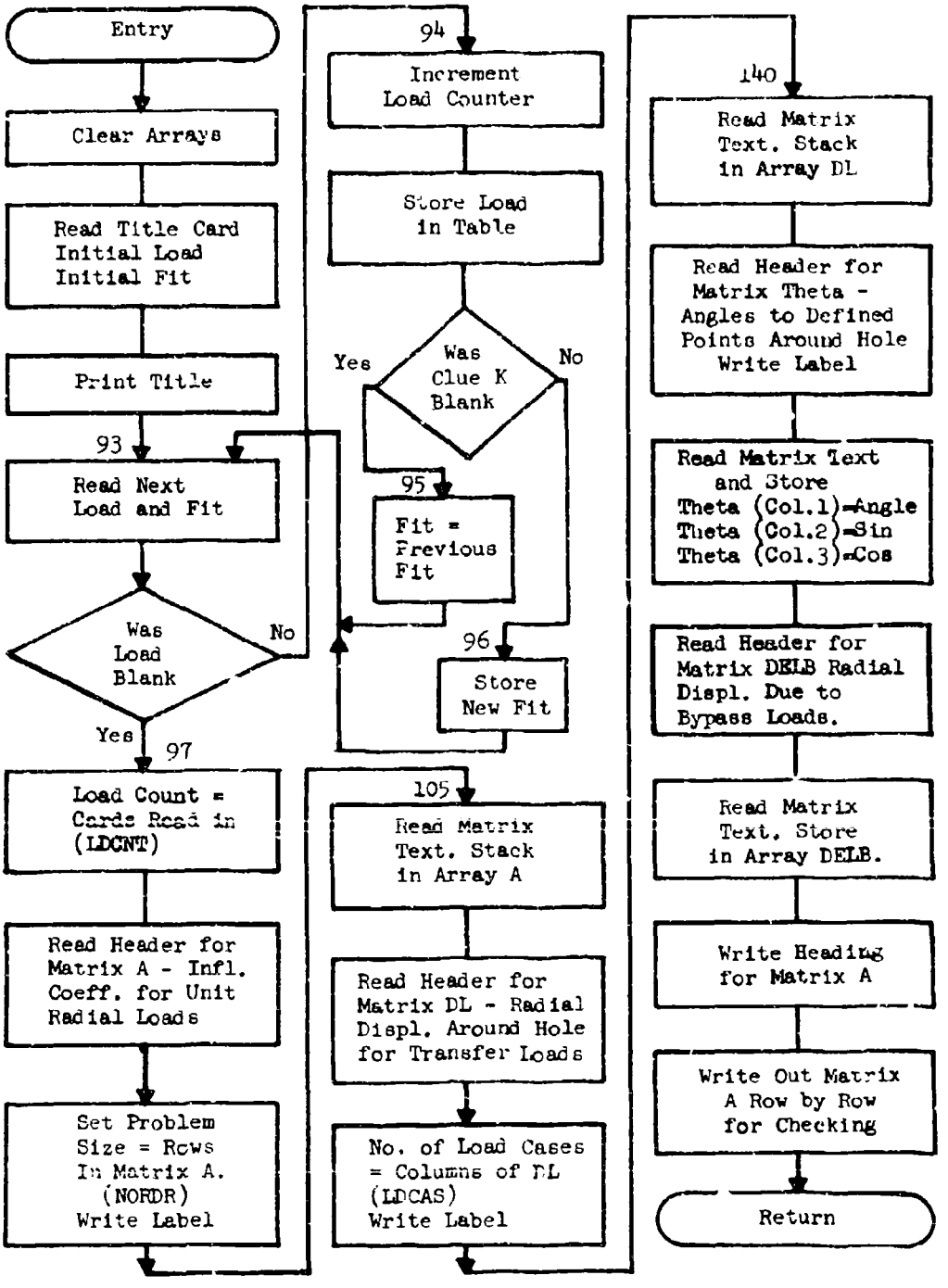

CALCULATION - SUBROUTINE HHRUN

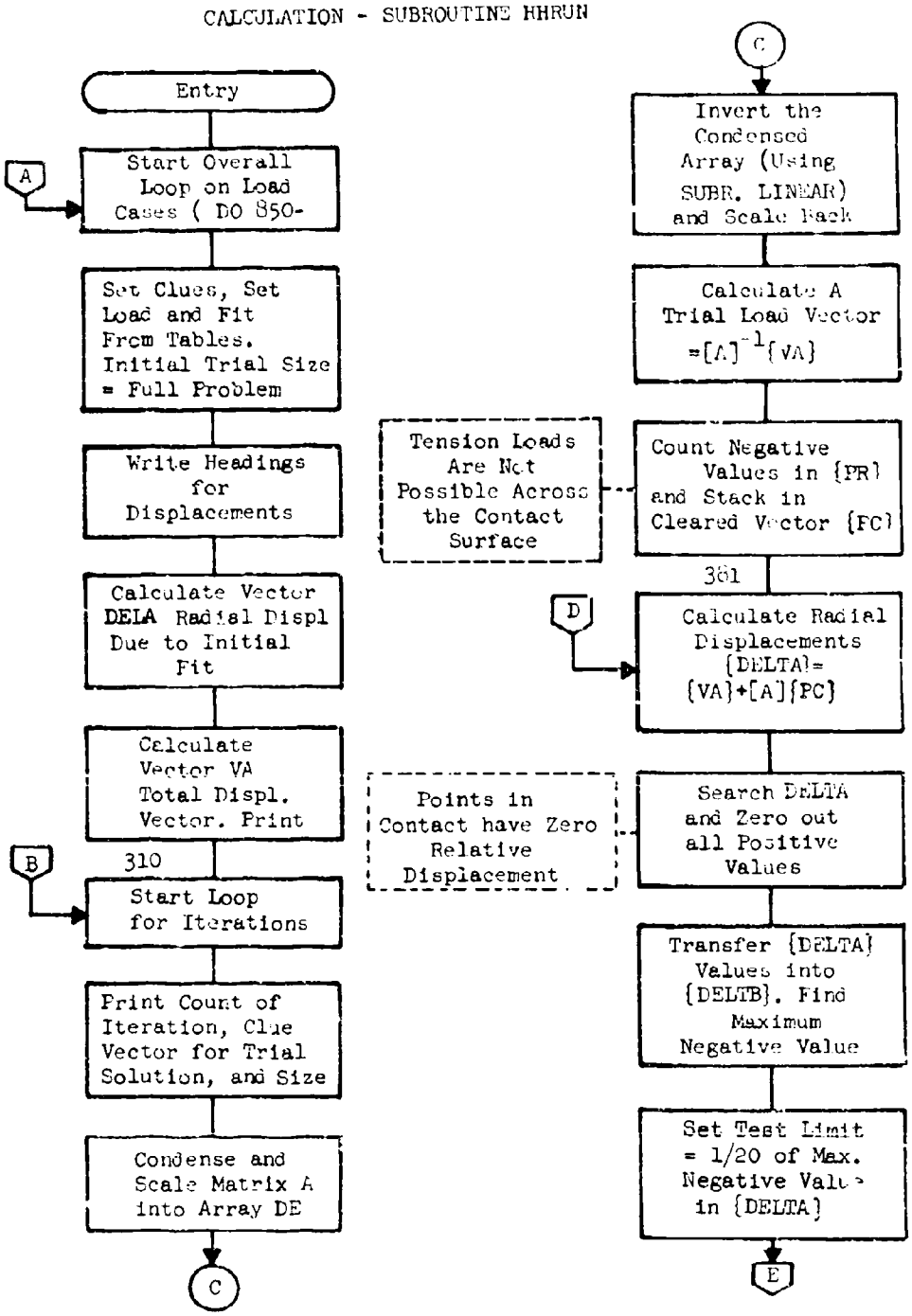

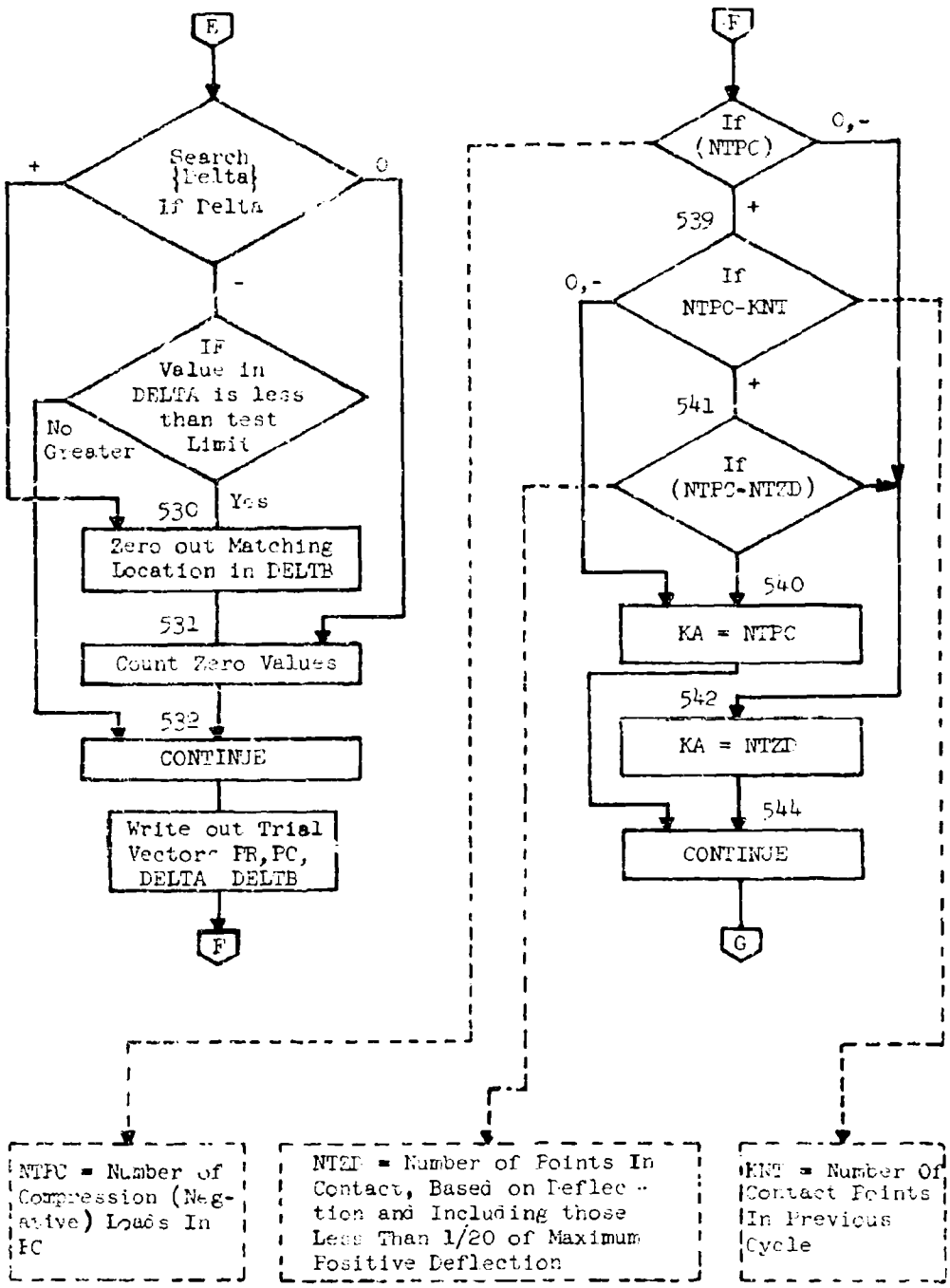
E
Search {Delta} If Delta
+
0
-
IF Value in DELTA is less than test Limit
No Greater
Yes
530
Zero out Matching Location in DELTB
531
Count Zero Values
532
CONTINUE
Write out Trial Vectors PR,PC, DELTA DELTB
F
F
If (NTPC)
0,-
+
539
If NTPC-KNT
0,-
+
541
If (NTPC-NTZD)
540
KA = NTPC
542
KA = NTZD
544
CONTINUE
G
NTPC = Number of Compression (Negative) Loads In PC
NTZD = Number of Points In Contact, Based on Deflection and Including those Less Than 1/20 of Maximum Positive Deflection
KNT = Number Of Contact Points In Previous Cycle

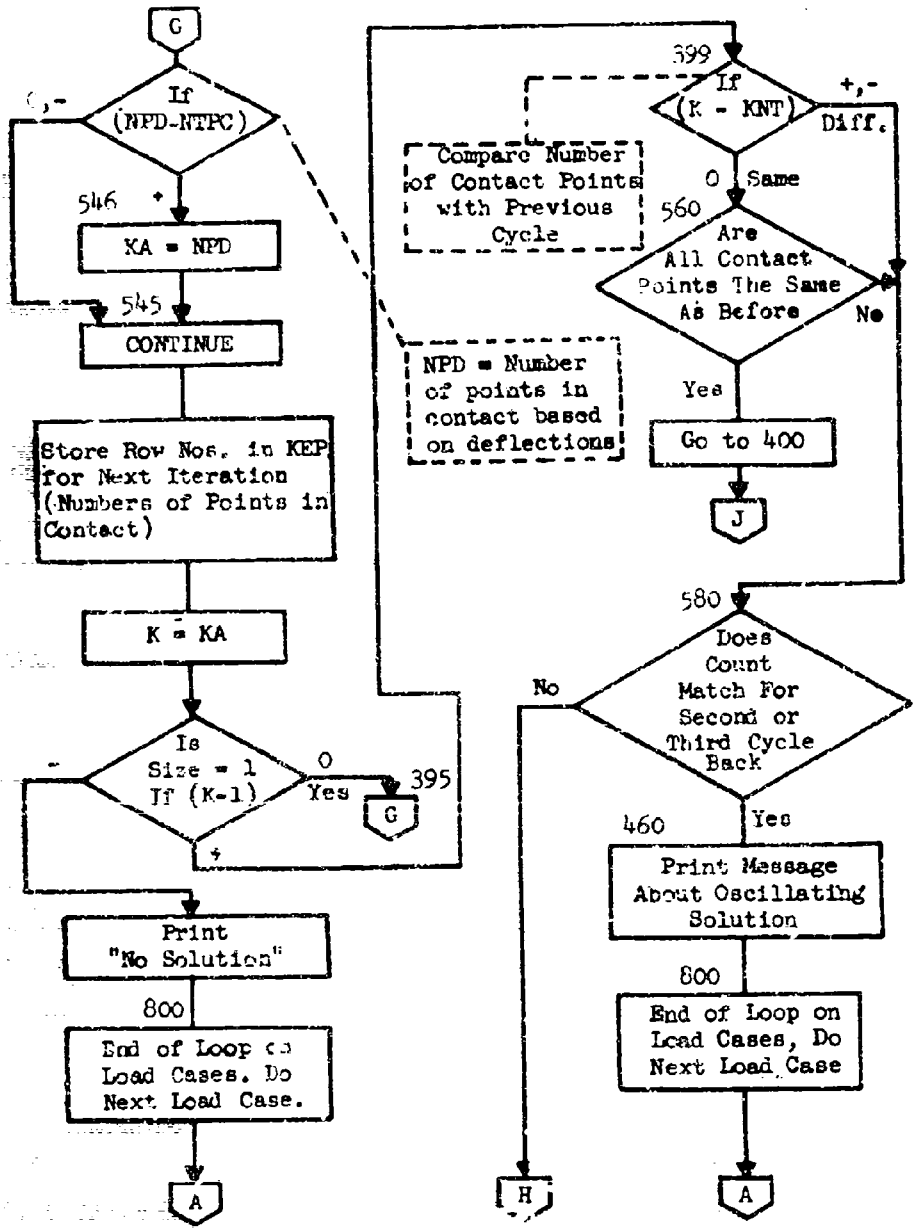
G
If (NPD-NTPC)
-,0
+
546
KA = NPD
545
CONTINUE
Store Row Nos. in KEP for Next Iteration (Numbers of Points in Contact)
K = KA
Is Size = 1 If (K-1)
-
0
Yes
395
G
+
Print "No Solution"
800
End of Loop on Load Cases. Do Next Load Case.
A
399
If (K - KNT)
+,-
Diff.
0
Same
Compare Number of Contact Points with Previous Cycle
560
Are All Contact Points The Same As Before
No
Yes
NPD = Number of points in contact based on deflections
Go to 400
J
580
Does Count Match For Second or Third Cycle Back
No
Yes
460
Print Message About Oscillating Solution
800
End of Loop on Load Cases, Do Next Load Case
H
A

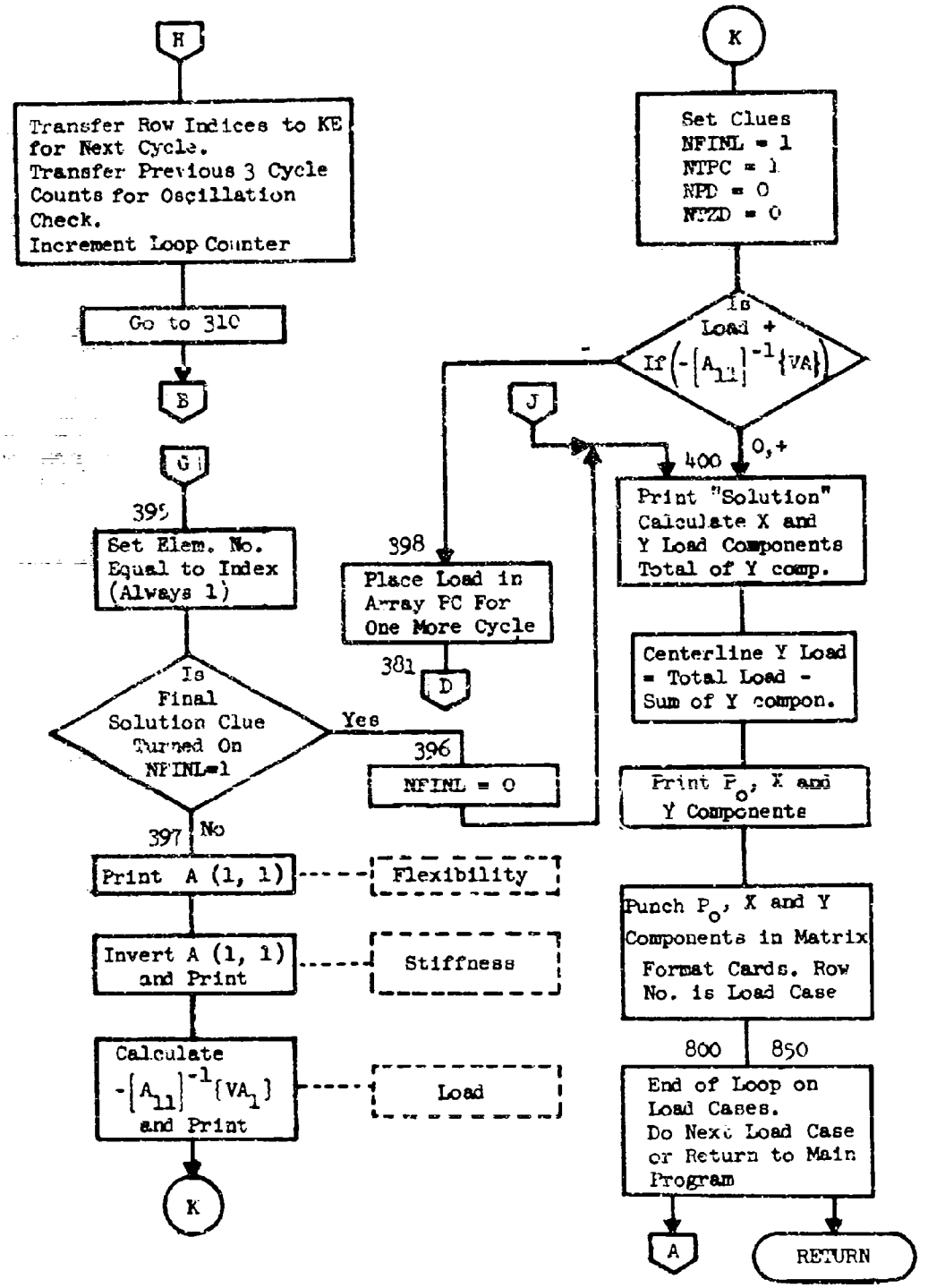
H
Transfer Row Indices to KE for Next Cycle.
Transfer Previous 3 Cycle Counts for Oscillation Check.
Increment Loop Counter
Go to 310
B
G
395
Set Elem. No. Equal to Index (Always 1)
Is Final Solution Clue Turned On NFINL=1
Yes
396
NFINL = 0
No
397
Print A (1, 1)
Flexibility
Invert A (1, 1) and Print
Stiffness
Calculate $-[A_{11}]^{-1}\{VA_1\}$ and Print
Load
K
398
Place Load in Array PC For One More Cycle
381
D
J
K
Set Clues
NFINL = 1
NTPC = 1
NPD = 0
NZD = 0
Is Load + If $\left(-[A_{11}]^{-1}\{VA\}\right)$
-
0,+
400
Print "Solution" Calculate X and Y Load Components Total of Y comp.
Centerline Y Load = Total Load - Sum of Y compon.
Print P_o, X and Y Components
Punch P_o, X and Y Components in Matrix Format Cards. Row No. is Load Case
800
850
End of Loop on Load Cases. Do Next Load Case or Return to Main Program
A
RETURN

APPENDIX G FORTRAN LISTING OF ELASTIC CONTACT PROBLEM PROGRAM

```
      COMMON NIN,NOUTP,NOUT,LDCNT,LDCAS,NORDR,Q,FIT
      COMMON     A(20,20),DL(20,10),DELA(20),DELB(20),DE(20,20),
     1 ER(20),VA(20),KE(20),KEP(20),
     2 MR(3),MC(3),EL(3),LVA(20),LVB(20)
      COMMON     PC(20),DELTA(20),THETA(20,3),TITLE(30)
      COMMON     QIN(10),FITIN(10)
   89 NIN    = 5
      NOUTP  = 7
      NOUT   = 6
      CALL HHINP
      IF (LDCNT-LDCAS) 233,236,233
  233 WRITE (NOUT,33)
      CALL EXIT
  236 CONTINUE
      CALL HHRUN
      GO TO 89
   33 FORMAT(23H INPUT ERROR-LOAD CASES)
      END

      SUBROUTINE HHINP
      COMMON NIN,NOUTP,NOUT,LDCNT,LDCAS,NORDR,Q,FIT
      COMMON     A(20,20),DL(20,10),DELA(20),DELB(20),DE(20,20),
     1 ER(20),VA(20),KE(20),KEP(20),
     2 MR(3),MC(3),EL(3),LVA(20),LVB(20)
      COMMON     PC(20),DELTA(20),THETA(20,3),TITLE(30)
      COMMON     QIN(10),FITIN(10)
      DO 91 I=1,20
      DELA(I) =  0.0
      DELB(I) =  0.0
      DE  (I) =  0.0
      VA  (I) =  0.0
      KE  (I) =  0
      KEP(I) =  0
      PC  (I) =  0.0
      DELTA(I) =  0.0
      DO 91 K = 1,3
   91 THETA(I,K) = 0.0
      DO 92 JJ = 1,10
   92 DL(I,JJ) =  0.0
      DO 91 J=1,20
      A (I,J) = 0.0
      DE(I,J) = 0.0
   91 CONTINUE
C     WORK AREAS ARE NOW CLEAR
      READ (NIN,23) K,QIN(1),FITIN(1),(TITLE(I),I=1,30)
```

```
      WRITE (NOUT,32) (TITLE(I),I=1,30)
      I = 1
   93 READ (NIN,23) K,Q,AKFIT
      IF(Q) 94,97,94
   94 I  = I + 1
      QIN(I) = Q
      IF(K) 95,95,96
   95 FITIN(I) = FITIN(I-1)
      GO TO 93
   96 FITIN(I) = AKFIT
      GO TO 93
   97 CONTINUE
      LDCNT = I
C     READ IN MATRIX (A)
      READ (NIN,1) NROWS,NCOLS
C     PROBLEM SIZE IS SET BY THE NUMBER OF ROWS IN INPUT MATRIX (A)
      NORDR = NROWS
      WRITE (NOUT,6) NROWS,NCOLS
      WRITE (NOUT,7)
  105 READ (NIN,2) (MR(I),MC(I),EL(I),I=1,3)
      IF(MR(1))130,130,110
  110 DO 120 I=1,3
      IF(MR(I))120,120,115
  115 NROW  = MR(I)
      NCOL  = MC(I)
      A(NROW,NCOL) = EL(I)
  120 CONTINUE
      WRITE (NOUT,13) (MR(I),MC(I),EL(I),I=1,3)

      GO TO 105
  130 CONTINUE
      WRITE (NOUT,5)
C     READ IN MATRIX (DL)
      READ (NIN,1) NROWS,NCOLS
      WRITE (NOUT,6) NROWS,NCOLS
      WRITE (NOUT,8)
      LDCAS = NCOLS
  140 READ (NIN,2) (MR(I),MC(I),EL(I),I=1,3)
      IF(MR(1))180,180,150
  150 DO 170 I=1,3
      IF (MR(I))170,170,160
  160 NROW  = MR(I)
      NCOL  = MC(I)
      DL(NROW,NCOL) = EL(I)
  170 CONTINUE
      WRITE (NOUT,13) (MR(I),MC(I),EL(I),I=1,3)
      GO TO 140
  180 CONTINUE
      WRITE (NOUT,5)
C     READ IN MATRIX (THETA)
      READ (NIN,1) NROWS,NCOLS
      WRITE (NOUT,6) NROWS,NCOLS
```

```
      WRITE (NOUT,9)
  190 READ (NIN,2) (MR(I),MC(I),EL(I),I=1,3)
      IF(MR(1))230,230,200
  200 DO 220 I=1,3
      IF(MR(I))220,220,210
  210 NROW = MR(I)
      THETA(NROW,1) = EL(I)
      ANGLE = .0174533*EL(I)
      THETA(NROW,2) = SIN(ANGLE)
      THETA(NROW,3) = COS(ANGLE)
  220 CONTINUE
      WRITE (NOUT,13) (MR(I),MC(I),EL(I),I=1,3)
      GO TO 190
  230 CONTINUE
      WRITE (NOUT,5)
C     READ IN MATRIX (DELB)
      READ (NIN,1) NROWS,NCOLS
      WRITE (NOUT,6) NROWS,NCOLS
      WRITE (NOUT,10)
  240 READ (NIN,2) (MR(I),MC(I),EL(I),I=1,3)
      IF(MR(1)) 280,280,250
  250 DO 270 I = 1,3
      IF(MR(I)) 270,270,260
  260 NROW = MR(I)
      DELB(NROW) = EL(I)
  270 CONTINUE
      WRITE (NOUT,13) (MR(I),MC(I),EL(I),I=1,3)
      GO TO 240
  280 CONTINUE
      WRITE (NOUTP,5)
      WRITE (NOUT,5)
C     FOUR INPUT MATRICES ARE NOW IN CORE
      WRITE (NOUT,7)

      DO 290 I = 1,NORDR
      WRITE (NOUT,16) (A(I,J),J=1,NORDR)
  290 CONTINUE
      WRITE (NOUT,5)
      RETURN
    1 FORMAT(2I4)
    2 FORMAT(3(2I4,E15.7,1X),4A2)
    5 FORMAT(1H /1H )
    6 FORMAT(13H INPUT MATRIX,6X,I4,2H X,I5)
    7 FORMAT(1H+,13X,1HA)
    8 FORMAT(1H+,13X,2HDL)
    9 FORMAT(1H+,13X,5HTHETA)
   10 FORMAT(1H+,13X,4HDELB)
   13 FORMAT(1X,3(2I4,1X,E15.7))
   16 FORMAT(/1X,7E15.7/2X,7E15.7/3X,7E15.7)
   23 FORMAT(I1,E9.4,E10.4,30A2)
   32 FORMAT(1H1,4X,30A2)
      END
```

```
      SUBROUTINE MHRUN
      DIMENSION DELTB(20),BLVB(20)
      DIMENSION LOC(20),SCALE(20)
      COMMON NIN,NOUTP,NOUT,LDCNT,LDCAS,NORDR,Q,FIT
      COMMON    A(20,20),DL(20,10),DELA(20),DELB(20),DE(20,20),
     1 PR(20),VA(20),KE(20),KEP(20),
     2 MR(3),MC(3),EL(3),LVA(20),LVB(20)
      COMMON    PC(20),DEL A(20),THETA(20,3),TITLE(30)
      COMMON    QIN(10),FITIN(10)
C     THIS IS THE START OF THE OVERALL LOOP ON LOAD CASES
      DO 850 LOOP = 1,LDCAS
      KNT   = NORDR
C     KNTB IS THE CLUE OF SIZE FROM THE SECOND ITERATION BACK
C     KNTC IS THE CLUE OF  IZE FROM THE THIRD  ITERATION BACK
C     BOTH USED TO CHECK FOR OSCILLATIONS IN THE SOLUTION
      KNTB = 25
      KNTC = 30
      NFINL = 0
      FIT = FITIN(LOOP)
      Q   = QIN  (LOOP)
      WRITE (NOUT,24) (TITLE(I),I=1,30),Q

      IF(FIT)101,103,102
  101 WRITE (NOUT,25) FIT
      GO TO 104
  102 WRITE (NOUT,26) FIT
      GO TO 104
  103 WRITE (NOUT,27)
  104 CONTINUE
C     CALCULATE MATRIX (DELA)
      DO 240 I = 1,NORDR
      DELA(I) = FIT - FIT*THETA(I,3)
  240 CONTINUE
C     FORM (DL)X(L) + (DELTA A) + DELB
      DO 300 I=1,NORDR
  300 VA(I) = DELA(I) + DELB(I) + DL(I,LOOP)
      WRITE (NOUT,28) LOOP
      DO 305 I=1,NORDR
      WRITE (NOUT,10) I,DELA(I),DELB(I),DL(I,LOOP),VA(I)
  305 KE(I)  = I
      WRITE (NOUT,5)
C     THIS IS THE START OF THE MAIN LOOP
      KLOOP = 1
  310 CONTINUE
C     KNT IS THE NUMBER OF NEGATIVE VALUES IN PRECEDING (PR)
C     ARRAY (KE) INDICATES THE ROWS AND COLUMNS OF (A) TO BE COMPACTED
      WRITE (NOUT,15) KLOOP,(KE(I),I=1,20) ,KNT
C     CONDENSE (A) ROW BY ROW
```

```
      K   = 1
      DO 320 I=1,KNT
      N   = KE(I)
      DO 315 J=1,NORDR
      DE(K,J) = A(N,J)*1.0E+07
  315 CONTINUE


      K   = K + 1
  320 CONTINUE
C     NOW CONDENSE (A) COLUMN BY COLUMN
      K   = 1
      DO 340 I=1,KNT
      N   = KE(I)
      DO 335 J=1,KNT
      DE(J,K)=DE(J,N)
  335 CONTINUE
      K   = K + 1
  340 CONTINUE
C     NOW INVERT THE CONDENSED ARRAY IN (DE)
      CALL LINEAR (DE,DE,K,T,C,0,LOC,SCALE,20)
C     INVERSE IS IN ARRAY (DE)
      DO 345 I = 1,KNT
      IF(LOC(I))345,350,345
  345 CONTINUE
      GO TO 360
  350 WRITE (NOUT,11) I
      GO TO 800
  360 CONTINUE
      DO 362 I = 1,KNT
      DO 362 J = 1,KNT
  362 DE(I,J) = DE(I,J)*1.0E+07
      DO 368 I = 1,NORDR
  363 PR(I) = 0.0
      DO 370 I =1,KNT
      KEP(I) = 0
      DO 370 J = 1,KNT
  370 PR(I)   = PR(I) - DE(I,J)*VA(J)
C     NTPC IS THE COUNT OF NEGATIVE VALUES IN P
      NTPC   = 0
C     NTZO IS THE COUNT OF POSITIVE OR ZERO VALUES IN DELTA,
C           WITH VALUES SMALLER THAN ONE-TENTH THE LARGEST NEGATIVE
C           VALUE ALSO SET TO ZERO
      NTZO   = 0
      NPO = 0
      DELMX = 0.0
C     TEST (PR) FOR NEGATIVE VALUES
C     START 'STEP 1'
      WRITE (NOUT,14) LOOP
```

```
      DO 505 I = 1,NORDR
  505 PC(I) = 0.0
      K  = 0
      DO 380 I = 1,KNT
      IF(PR(I)) 375,380,380
  375 NPC = KE(I)
      PC(NPC) = PR(I)
      NTPC = NTPC + 1
  380 CONTINUE
  381 CONTINUE
      KA   = 0
C     START *STEP 2*
      DO 514 I = 1,NORDR
      DELTA(I) = VA(I)
      DO 515 J = 1,NORDR

      DELTA(I) = DELTA(I) + A(I,J) * PC(J)
  515 CONTINUE
  514 CONTINUE
      DO 525 I = 1,NORDR
      IF(DELTA(I)) 518,517,517
  517 DELTA(I)=0.0
      NPD = NPD + 1
  518 CONTINUE
  525 CONTINUE
C     START  *STEP 3*
      DO 527 I = 1,NORDR
      DELTB(I) = DELTA(I)
      IF(DELMX-DELTA(I)) 527,527,526
  526 DELMX = DELTA(I)
  527 CONTINUE
      DELMX = 0.05*DELMX
      DO 533 I = 1,NORDR
      IF(DELTA(I)) 529,531,530
  529 IF(DELMX-DELTA(I)) 530,532,532
  530 DELTB(I) = 0.0
  531 NTZD = NTZD + 1
  532 CONTINUE
      WRITE (NOUT,18) I,KE(I),PR(I),PC(I),DELTA(I),DELTB(I)
  533 CONTINUE
C     DETERMINE SIZE FOR NEXT ITERATION
      IF(NTPC) 542,542,539
  539 CONTINUE
      IF (NTPC-KNT) 540,540,541
  541 CONTINUE
      IF(NTPC-NTZD) 542,542,540
  540 KA = NTPC
      GO TO 544
  542 KA = NTZD
```

```
  544 CONTINUE
      IF(NPD-NTPC) 545,545,546
  546 KA = NPD
  545 CONTINUE
      K = 0
      DO 550 I=1,KA
      KEP(I)=I
  550 CONTINUE
      WRITE (NOUT,5)
  552 K  = KA
  554 CONTINUE
C     IF ORDER IS REDUCED TO ONE, THIS IS THE END
      IF(K-1)480,395,399
  395 KEL   = KEP(K)
      IF(NFINL)  397,397,396
  396 NFINL = 0
      GO TO 400
  397 CONTINUE
      RA    = A(KEL,KEL)
      WRITE (NOUT,17)
      WRITE (NOUT,16) RA
      WRITE (NOUT,5)
      RAV   = 1./RA



      WRITE (NOUT,17)
      WRITE (NOUT,19)
      WRITE (NOUT,16) RAV
      WRITE (NOUT,5)
      RPR   = -RAV * VA(KEL)
      WRITE (NOUT,3) KEL,RPR
      NFINL = 1
      NTPC = 1
      NPD=0
      NTZD = 0
      IF(RPR) 398,400,400
  398 PC(KEL) = RPR
      GO TO 381
  399 CONTINUE
C     COMPARE WITH PRECEDING CYCLE
      IF(K-KNT) 580,560,580
  560 CONTINUE
      DO 565 I = 1,NORDR
      IF(KE(I)-KEP(I)) 580,565,580
  565 CONTINUE
      GO TO 400
  580 CONTINUE
      IF(K-KNTB) 585,460,585
  585 IF(K-KNTC) 590,460,590
  590 CONTINUE
```

```
      DO 385 I = 1,NORDR
  385 KE(I) = KEP(I)
      KNTC = KNTB
      KNTB = KNT
      KNT = K
C     GO BACK FOR ANOTHER ITERATION
      KLOOP = KLOOP + 1
      GO TO 310
  400 CONTINUE
      WRITE (NOUT,4) LOOP
C     STORE P(I)*SIN(THETA(I)) IN DE(I,1) ( = PIX)
C     STORE P(I)*COS(THETA(I)) IN DE(I,2) ( = PIY)
      PSUM = 0.0
      DO 410 I = 1,NORDR
      DE(I,1) =-PC(I)*THETA(I,2)
      DE(I,2) = PC(I)*THETA(I,3)
      PSUM = PSUM + DE(I,2)
  410 CONTINUE
      PZERO =-Q - PSUM
      WRITE (NOUT,29) PZERO
      WRITE (NOUT,30)
      DO 420 I = 1,NORDR
      WRITE (NOUT,31) I,DE(I,1),DE(I,2)
  420 CONTINUE
      WRITE (NOUT,5)
C     WRITE PUNCH OUTPUT FOR COMAP
      MR(1) = LOOP
      MR(2) = LOOP
      MR(3) = LOOP
      NELCT = 1
      MC(1) = 1



      MC(2) = 2
      MC(3) = 3
      EL(1) = PZERO
      EL(2) = DE(1,1)
      EL(3) = DE(1,2)
      WRITE (NOUTP,2) (MR(J),MC(J),EL(J),J=1,3),(TITLE(I),I=27,30)

      DO 440 IA = 2,NORDR
      DO 440 IB = 1,2
      EL(NELCT) = DE(IA,IB)
      MC(NELCT) = 2*IA + IB - 1
      NELCT = NELCT + 1
      IF(NELCT-3) 440,440,430
  430 NELCT = 1
      WRITE (NOUTP,2) (MR(J),MC(J),EL(J),J=1,3),(TITLE(I),I=27,30)
```

```
      DO 439 I = 1,3
      MC(I) = 0
      EL(I) = 0.0
  439 CONTINUE
  440 CONTINUE
C     PUNCH THE LAST CARD, IF ANY
      IF(NELCT-1) 455,455,450
  450 WRITE (NOUTP,2) (MR(J),MC(J),EL(J),J=1,3),(TITLE(I),I=27,30)

  455 CONTINUE
      GO TO 800
  460 WRITE (NOUT,21) LOOP
      GO TO 800
  480 WRITE (NOUT,20)
  800 CONTINUE
  850 CONTINUE
      RETURN
    2 FORMAT(3(2I4,E15.7,1X),4A2)
    3 FORMAT(1X,I3,2X,F15.7)
    4 FORMAT(4HOSOL,I4/1H0
    5 FORMAT(1H /1H )
   10 FORMAT(1X,I3,E16.7,3E18.7)
   11 FORMAT(23H)MATRIX SINGULAR AT ROW,I3)
   12 FORMAT(17H VECTOR DL + DELA)
   14 FORMAT(10HOLOAD CASE,I3,1X,8HTRIAL PR,4X,14HVECTOR PI (PC),
     111X,7HDELTA 1,11X,7HDELTA 2)
   15 FORMAT(34HOPOS.OR ZERO DELTA,OR NEG.P( CYCLE,I3,2H ),2II3)
   16 FORMAT(/1X,7E15.7/2X,7E15.7/3X,7E15.7)
   17 FORMAT(17HOMATRIX A REDUCED)
   18 FORMAT(1X,2I4,4E18.7)
   19 FORMAT(1H+,17X,12HAND INVERTED)
   20 FORMAT(7H NO NEG)
   21 FORMAT(10HOLOAD CASE,I4,11H OSCILLATES/)
   24 FORMAT(1H1,4X,30A2///7H LOAD =,E16.7,7H POUNDS///)
   25 FORMAT(22H INITIAL LACK OF FIT =,E16.7,7H INCHES//)
   26 FORMAT(19H INTERFERENCE FIT =,E16.7,7H INCHES)
   27 FORMAT(12H SLIDING FIT)
   28 FORMAT(73HOROW CALCULATED DELA       INPUT DELB          LOAD VECTOR
     1      TOTAL VECTOR/45X,6HDL (N,,I2,22H)      DELA + DELB + DL)
   29 FORMAT(9H P ZERO =,E16.7//)


   31 FORMAT(5H NODE,6X,3HPIX,14X,3HPIY)
   32 FORMAT(I4,2E17.7)
      END
```

```
      SUBROUTINE LINEAR (A,B,MO,NO,D,LOC,SCALE,MAT)
      DIMENSION A(MAT,1),B(MAT,1),LOC(1),SCALE(1)
      DIMENSION SUM(1)
      DOUBLE PRECISION  SUM
      M = MO
      N = NO
      INC = 0
      IF (N) 10,30,30
   10 IF (N + 199) 20,230,230
   20 INC = 1
   30 INC = INC + 1
      DO 60  I = 1,M
      X = 0.0
      DO 50  J = 1,M
      IF (X - ABS(A(J,I))) 40,50,50
   40 X = ABS(A(J,I))
   50 CONTINUE
      X = POWER(X)
      SCALE(I) = X
      DO 60  J = 1,M
   60 A(J,I) = A(J,I) / X
      DO 210  I = 1,M
      I1 = I - 1
      NEXTI = I + 1
      SUM(1) = -A(I,I)
      CALL DOT (I1,A(I,1),MAT,A(1,I),1,SUM)
      X = ABS(SUM)
      Y = -SNGL(SUM)
      K = I
      IF (I - M) 70,110,110
   70 DO 100  J = NEXTI,M
      SUM(1) = -A(J,I)
      CALL DOT (I1,A(J,1),MAT,A(1,I),1,SUM)
      IF (X - ABS(SUM)) 80,90,90
   80 A(K,I) = Y
      K = J
      X = ABS(SUM)
      Y = -SNGL(SUM)
      GO TO 100
   90 A(J,I) = -SNGL(SUM)
  100 CONTINUE
  110 LOC(I) = K
      IF (256.0* X - ABS(A(K,I))) 120,120,150
  120 IF (16777216.0* X - ABS(A(K,I))) 130,130,140
  130 LOC(I) = 0
      GO TO 460
  140 LOC(I) = -LOC(I)
  150 A(K,I) = Y
```

```
      IF (I - K) 160,180,130
  160 DO 170  J = 1,M
      X = A(I,J)
      A(I,J) = A(K,J)
  170 A(K,J) = X
      D = -D
  180 IF (I - M) 190,216,210

-----------------------------------------------------------------

  190 DO 200  J = NEXTI,M
      A(J,I) = A(J,I) / Y
      SUM(I) = -A(I,J)
      CALL DOT (II,A(I,1),MAT,A(1,J),1,SUM)
  200 A(I,J) = -SNGL(SUM)
  210 D = D * Y * SCALE(I)
      DO 220  I = 1,M
      DO 220  J = 1,I
  220 A(J,I) = A(J,I) * SCALE(I)
      GO TO (230,460),INC
  230 LIM= IABS(N)
      IF (LIM) 240,280,240
  240 INC = 0
      DO 270  I = 1,M
      K= IABS(LOC(I))
      IF (I - K) 250,270,130
  250 DO 260  J = 1,LIM
      X = B(I,J)
      B(I,J) = B(K,J)
  260 B(K,J) = X
  270 CONTINUE
  280 DO 300  I = 1,M
      SCALE(I) = -A(I,I)
      A(I,I) = 1.0
      DO 290  J = 1,M
  290 A(I,J) = A(I,J) / SCALE(I)
      DO 300  J = 1,I
  300 A(I,J) = -A(I,J)
      DO 330  I = 2,M
      INK = 1
      IF (LIM) 130,330,310
  310 DO 320  J = 1,LIM
      INK = INK + INC
      SUM = B(I,J)
      LIMB = I - INK
      CALL DOT (LIMB,A(I,INK),MAT,B(INK,J),1,SUM)
  320 B(I,J) = SNGL(SUM)
  330 LIM = LIM + INC
      I = M
      DO 410  MJI = 1,M
      IF (LIM) 340,360,340
  340 DO 350  K = 1,LIM
      SUM(I)= 0.D0
```

```
      CALL DOT (MI,A(I,I),MAT,B(I,K),1,SUM)
  350 B(I,K) = SNGL(SUM)
  360 IF (J) 410,370,410
  370 LIM = LIM - INC
      MI = M - I
      DO 400  K = I,M
      SUM(1)= 0.D0
      IF (K - I) 380,380,390
  380 SUM = A(I,I)
  390 CALL DOT (MI,A(I,I+1),MAT,B(I+1,K),1,SUM)
  400 SCALE(K) = SNGL(SUM)
      DO 405  K = I,M
  405 B(I,K) = SCALE(K)

  410 I = I - 1
      IF (N) 460,420,460
  420 I = M
      DO 450  MII = 1,M
      K= IABS(LOC(I))
      IF (I - K) 430,450,130
  430 DO 440  J = 1,M
      X = A(J,I)
      A(J,I) = A(J,K)
  440 A(J,K) = X
  450 I = I - 1
  460 RETURN
      END


      SUBROUTINE DOT(L,X,IX,Y,IY,SUM)
      DOUBLE PRECISION SUM
      REAL X(IX,1),Y(1)
      IF (L) 100,120,100
  100 DO 110  J = 1,L
  110 SUM = SUM + X(1,J)*Y(J)
  120 RETURN
      END
```

PROBLEM 2.3 CASE 2 .2(NEGATIVE FIT P2.3 C 2

INPUT MATRIX A 10 X 10

1	1	0.2694660E-05	1	2	0.2061993E-05	1	3	0.1653240E-05
1	4	0.9915675E-06	1	5	0.2003556E-06	1	6	-0.6277445E-06
1	7	-0.1390839E-05	1	8	-0.2000503E-05	1	9	-0.2391577E-05
1	10	-0.2526008E-05	-0	-0	-0.	-0	-0	-0.
2	1	0.2061994E-05	2	2	0.3824271E-05	2	3	0.2873731E-05
2	4	0.1936079E-05	2	5	0.6830505E-06	2	6	-0.6893550E-06
2	7	-0.1988329E-05	2	8	-0.3035310E-05	2	9	-0.3707077E-05
2	10	-0.3937564E-05	-0	-0	-0.	-0	-0	-0.
3	1	0.1653238E-05	3	2	0.2873729E-05	3	3	0.4164163E-05
3	4	0.2657554E-05	3	5	0.1235298E-05	3	6	-0.4003437E-06
3	7	-0.1960932E-05	3	8	-0.3268505E-05	3	9	-0.4095426E-05
3	10	-0.4378774E-05	-0	-0	-0.	-0	-0	-0.
4	1	0.9915666E-06	4	2	0.1936076E-05	4	3	0.2657553E-05
4	4	0.3486451E-05	4	5	0.1703253E-05	4	6	0.1929116E-06
4	7	-0.1307158E-05	4	8	-0.2536682E-05	4	9	-0.3328747E-05
4	10	-0.3595776E-05	-0	-0	-0.	-0	-0	-0.
5	1	0.2003547E-06	5	2	0.6830479E-06	5	3	0.1235296E-05
5	4	0.1703250E-05	5	5	0.2518570E-05	5	6	0.9571231E-06
5	7	-0.9822310E-07	5	8	-0.9741898E-06	5	9	-0.1533908E-05
5	10	-0.1725531E-05	-0	-0	-0.	-0	-0	-0.
6	1	-0.6277438E-06	6	2	-0.6393542E-06	6	3	-0.4003434E-06
6	4	0.1929122E-06	6	5	0.9571240E-06	6	6	0.2300309E-05
6	7	0.1448734E-05	6	8	0.1175606E-05	6	9	0.1004992E-05
6	10	0.9510716E-06	-0	-0	-0.	-0	-0	-0.
7	1	-0.1390837E-05	7	2	-0.1988326E-05	7	3	-0.1980930E-05
7	4	-0.1307157E-05	7	5	-0.9822355E-07	7	6	0.1448733E-05
7	7	0.3636777E-05	7	8	0.3560563E-05	7	9	0.3860526E-05
7	10	0.3962837E-05	-0	-0	-0.	-0	-0	-0.
8	1	-0.2000502E-05	8	2	-0.3035306E-05	8	3	-0.3268502E-05
8	4	-0.2536680E-05	8	5	-0.9741907E-06	8	6	0.1175606E-05
8	7	0.3560562E-05	8	8	0.6352545E-05	8	9	0.6566582E-05
8	10	0.6821654E-05	-0	-0	-0.	-0	-0	-0.
9	1	-0.2391574E-05	9	2	-0.3707070E-05	9	3	-0.4095423E-05
9	4	-0.3328743E-05	9	5	-0.1533908E-05	9	6	0.1004992E-05
9	7	0.3860524E-05	9	8	0.6566580E-05	9	9	0.9300023E-05
9	10	0.9143735E-05	-0	-0	-0.	-0	-0	-0.
10	1	-0.2526005E-05	10	2	-0.3937557E-05	10	3	-0.4378769E-05
10	4	-0.3595773E-05	10	5	-0.1725531E-05	10	6	0.9510720E-06
10	7	0.3962836E-05	10	8	0.6821653E-05	10	9	0.9143735E-05
10	10	0.1176686E-04	-0	-0	-0.	-0	-0	-0.

INPUT MATRIX DL 10 X 8

1	1	0.2488759E-05	1	2	0.6221896E-03	1	3	0.1244379E-02
1	4	0.2488758E-02	1	5	0.4977517E-02	1	6	0.9955034E-02
1	7	0.1119941E-01	1	8	0.1244379E-01	-0	-0	-0.
2	1	0.3812806E-05	2	2	0.9532014E-03	2	3	0.1906403E-02
2	4	0.3812806E-02	2	5	0.7625610E-02	2	6	0.1525122E-01
2	7	0.1715762E-01	2	8	0.1906403E-01	-0	-0	-0.
3	1	0.4156169E-05	3	2	0.1039042E-02	3	3	0.2078084E-02
3	4	0.4156169E-02	3	5	0.8312337E-02	3	6	0.1662467E-01
3	7	0.1870276E-01	3	8	0.2078084E-01	-0	-0	-0.
4	1	0.3304573E-05	4	2	0.8261432E-03	4	3	0.1652287E-02
4	4	0.3304573E-02	4	5	0.6609146E-02	4	6	0.1321829E-01
4	7	0.1487058E-01	4	8	0.1652287E-01	-0	-0	-0.
5	1	0.1419197E-05	5	2	0.3547992E-03	5	3	0.7095986E-03
5	4	0.1419197E-02	5	5	0.2838395E-02	5	6	0.5676787E-02
5	7	0.6386388E-02	5	8	0.7095985E-02	-0	-0	-0.
6	1	-0.1170033E-05	6	2	-0.2925082E-03	6	3	-0.5850163E-03
6	4	-0.1170033E-02	6	5	-0.2340066E-02	6	6	-0.4680131E-02
6	7	-0.5265148E-02	6	8	-0.5850162E-02	-0	-0	-0.
7	1	-0.3965521E-05	7	2	-0.9913803E-03	7	3	-0.1982761E-02
7	4	-0.3965519E-02	7	5	-0.7931042E-02	7	6	-0.1587 [illegible]8E-01
7	7	-0.1784484E-01	7	8	-0.1982760E-01	-0	-0	-0.
8	1	-0.6417691E-05	8	2	-0.1604473E-02	8	3	-0.3208945E-02
8	4	-0.6417689E-02	8	5	-0.1283578E-01	8	6	-0.2567156E-01
8	7	-0.2888051E-01	8	8	-0.3208945E-01	-0	-0	-0.
9	1	-0.8074130E-05	9	2	-0.2018532E-02	9	3	-0.4037064E-02
9	4	-0.8074127E-02	9	5	-0.1614826E-01	9	6	-0.3229652E-01
9	7	-0.3633358E-01	9	8	-0.4037065E-01	-0	-0	-0.
10	1	-0.8657122E-05	10	2	-0.2164280E-02	10	3	-0.4328560E-02
10	4	-0.8657120E-02	10	5	-0.1731424E-01	10	6	-0.3462848E-01
10	7	-0.3895704E-01	10	8	-0.4326561E-01	-0	-0	-0.

INPUT MATRIX THETA 10 X 1

1	1	0.1800000E 02	-0	-0	-0.	-0	-0	-0.
2	1	0.3600000E 02	-0	-0	-0.	-0	-0	-0.
3	1	0.5400000E 02	-0	-0	-0.	-0	-0	-0.
4	1	0.7200000E 02	-0	-0	-0.	-0	-0	-0.
5	1	0.9000000E 02	-0	-0	-0.	-0	-0	-0.
6	1	0.1080000E 03	-0	-0	-0.	-0	-0	-0.
7	1	0.1260000E 03	-0	-0	-0.	-0	-0	-0.
8	1	0.1440000E 03	-0	-0	-0.	-0	-0	-0.
9	1	0.1620000E 03	-0	-0	-0.	-0	-0	-0.
10	1	0.1800000E 03	-0	-0	-0.	-0	-0	-0.

INPUT MATRIX DELB -0 R -0

A

0.2694660E-05 0.2061693E-05 0.1655240E-05 0.9915675E-06 0.2003556E-06 -0.6277445E-06 -0.1390839E-05
-0.2000503E-05 -0.2391577E-05 -0.2526008E-05

0.2061994E-05 0.3824271E-05 0.2873731E-05 0.1936079E-05 0.6830909E-06 -0.6893550E-06 -0.1988329E-05
-0.3013510E-05 -0.3701077E-05 -0.3937564E-05

0.1655233E-05 0.2873729E-05 0.4164163E-05 0.2657554E-05 0.1239298E-05 -0.4003437E-06 -0.1980932E-05
-0.3268505E-05 -0.4095626E-05 -0.4378774E-05

0.9915666E-06 0.1936076E-05 0.2657553E-05 0.3488431E-05 0.1707253E-05 0.1929116E-06 -0.1307158E-05
-0.2536662E-05 -0.3328747E-05 -0.3594776E-05

0.2003547E-06 0.6830479E-06 0.1239196E-05 0.1707250E-05 0.2576570E-05 0.9571231E-06 -0.9822310E-07
-0.9741849E-06 -0.1533908E-05 -0.1729531E-05

-0.6277443E-06 -0.6893542E-06 -0.4003434E-06 0.1929122E-06 0.9571240E-06 0.2300309E-05 0.1448734E-05
0.1175606E-05 0.1001992E-05 0.9510716E-06

-0.1390837E-05 -0.1980326E-05 -0.1980930E-05 -0.1307157E-05 -0.9822355E-07 0.1448733E-05 0.3636777E-05
0.3560563E-05 0.3660526E-05 0.3962837E-05

-0.2000502E-05 -0.3035306E-05 -0.3268502E-05 -0.2536680E-05 -0.9741907E-06 0.1175606E-05 0.3560562E-05
0.6352543E-05 0.6856382E-05 0.6821654E-05

-0.2391574E-05 -0.3707070E-05 -0.4095402E-05 -0.3328743E-05 -0.1333908E-05 0.1001992E-05 0.3660524E-05
0.6566580E-05 0.9300023E-05 0.9143735E-05

-0.2526005E-05 -0.3937557E-05 -0.4378769E-05 -0.3599773E-05 -0.1729531E-05 0.9510726E-06 0.3962836E-05
0.6821545E-05 0.9143735E-05 0.1176686E-04

PROBLEM 2.3 CASE 2 .2(NEGATIVE FIT P2.3 C 2

LOAD = 0.1000000E 01 POUNDS

INITIAL LACK OF FIT = -0.1500000E-02 INCHES

ROW	CALCULATED DELA	INPUT DELB	LOAD VECTOR DL (N, 1)	TOTAL VECTOR DELA + DELB + DL
1	-0.7341530E-04	0.	0.2488759E-05	-0.7092654E-04
2	-0.2864748E-03	0.	0.3812606E-05	-0.2826620E-03
3	-0.6193226E-03	0.	0.4156169E-05	-0.6141664E-03
4	-0.1036475E-02	0.	0.3304573E-05	-0.1033171E-02
5	-0.1500001E-02	0.	0.1419197E-05	-0.1498582E-02

6	-0.1963527E-02	0.	-0.1170033E-05	-0.1964697E-02
7	-0.2381679E-02	0.	-0.3965521E-05	-0.2385644E-02
8	-0.2713526E-02	0.	-0.6417691E-05	-0.2719944E-02
9	-0.2926585E-02	0.	-0.8074130E-05	-0.2934659E-02
10	-0.3000000E-02	0.	-0.8657122E-05	-0.3008857E-02

POS.OR ZERO DELTA,OR NEG.PT CYCLE I) 1 2 3 4 5 6 7 8 9 10 0 0 0 0 0 0 0 0 0 0 16

LOAD CASE I	TRIAL PR	VECTOR PI (PC)	DELTA 1	DELTA 2
1 1	0.2937413E 03	0.	-0.7092651E-04	0.
2 2	0.3534691E 03	0.	-0.2826620E-03	-0.2826620E-03
3 3	0.3824068E 03	0.	-0.6141664E-03	-0.6141664E-03
4 4	0.3765388E 03	0.	-0.1933171E-02	-0.1933171E-02
5 5	0.3547668E 03	0.	-0.1496582E-02	-0.1496582E-02
6 6	0.3390201E 03	0.	-0.1964697E-02	-0.1964697E-02
7 7	0.3338007E 03	0.	-0.2385644E-02	-0.2385644E-02
8 8	0.3306488E 03	0.	-0.2719944E-02	-0.2719944E-02
9 9	0.3263674E 03	0.	-0.2934659E-02	-0.2934659E-02
10 10	0.1616084E 03	0.	-0.3008657E-02	-0.3008657E-02

MATRIX A REDUCED

0.2694660E-05

MATRIX A REDUCED AND INVERTED

0.3711043E 06

1 0.2632115E 02

SOL 1

P ZERO = -0.1000000E 01

NODE	PIX	PIY
1	-0.	0.
2	-0.	0.
3	-0.	0.
4	-0.	0.
5	-0.	-0.
6	-0.	-0.
7	-0.	-0.
8	-0.	-0.
9	-0.	-0.
10	0.	-0.

PROBLEM 2.3 CASE 2 .2(NEGATIVE FIT P2.3 C 2

LOAD = 0.2500000E 03 POUNDS

INITIAL LACK OF FIT = -0.1500000E-02 INCHES

ROW	CALCULATED DELA	INPUT DELB	LOAD VECTOR DL (N. 2)	TOTAL VECTOR DELA + DELB + DL
1	-0.7341530E-04	0.	0.6221896E-03	0.5487743E-03
2	-0.2304748E-03	0.	0.9532014E-03	0.6667267E-03
3	-0.6133226E-03	0.	0.1039042E-02	0.4257195E-03
4	-0.1036475E-02	0.	0.8261432E-03	-0.2103321E-03
5	-0.1500001E-02	0.	0.3547992E-03	-0.1145202E-02
6	-0.1963527E-02	0.	-0.2925082E-03	-0.2256035E-02
7	-0.2381679E-02	0.	-0.9913803E-03	-0.3373059E-02
8	-0.2713526E-02	0.	-0.1604473E-02	-0.4317999E-02
9	-0.2926585E-02	0.	-0.2018532E-02	-0.4945118E-02
10	-0.3000000E-02	0.	-0.2164280E-02	-0.5164280E-02

POS.OR ZERO DELTA.OR NEG.P(CYCLE 1) 1 2 3 4 5 6 7 8 9 10 0 0 0 0 0 0 0 0 0 0 10

LOAD	CASE	TRIAL PR	VECTOR PI (PC)	DELTA 1	DELTA 2
1	1	0.2812304E 03	0.	0.	0.
2	2	0.3361494E 03	0.	0.	0.
3	3	0.3637718E 03	0.	0.	0.
4	4	0.3594925E 03	0.	-0...03321E-03	0.
5	5	0.3467671E 03	0.	-0.1145202E-02	-0.1145202E-02
6	6	0.3423903E 03	0.	-0.2256035E-02	-0.2256035E-02
7	7	0.3684460E 03	0.	-0.3373059E-02	-0.3373059E-02
8	8	0.3932125E 03	0.	-0.4317999E-02	-0.4317999E-02
9	9	0.4110511E 03	0.	-0.4945118E-02	-0.4945118E-02
10	10	0.2083124E 03	0.	-0.5164280E-02	-0.5164280E-02

POS.OR ZERO DELTA.OR NEG.P(CYCLE 2) 1 2 3 0 0 0 0 0 0 0 0 0 0 0 0 0 0 0 0 0 3

LOAD	CASE	TRIAL PR	VECTOR PI (PC)	DELTA 1	DELTA 2
1	1	-0.1226254E 03	-0.1226254E 03	-0.7670546E-04	0.
2	2	-0.1430878E 03	-0.1430878E 03	-0.1333326E-03	0.
3	3	0.4639705E 02	0.	-0.1932049E-03	0.
4	0	0.	0.	-0.6089521E-03	-0.6089521E-03
5	0	0.	0.	-0.1267506E-02	-0.1267506E-02

6	0	0.	0.	-0.2080419E-02	-0.2080419E-02
7	0	0.	0.	-0.2918002E-02	-0.2918002E-02
8	0	0.	0.	-0.3638372E-02	-0.3638372E-02
9	0	0.	0.	-0.4121413E-02	-0.4121413E-02
10	0	0.	0.	-0.4291111E-02	-0.4291111E-02

POS.OR ZERO DELTA.OR NEG.P(CYCLE 3) 1 2 0 0 0 0 0 0 0 0 0 0 0 0 0 0 0 0 0 0 0 2

LOAD	CASE	2 TRIAL PR	VECTOR PI (PC)	DELTA 1	DELTA 2
1	1	-0.1195838E 03	-0.1195838C 03	0.	0.
2	2	-0.1098629E 03	-0.1098629E 03	0.	0.
3	0	0.	0.	-0.9226717E-04	0.
4	0	0.	0.	-0.5416103E-03	-0.5416103E-03
5	0	0.	0.	-0.1244203E-02	-0.1244203E-02
6	0	0.	0.	-0.2105232E-02	-0.2105232E-02
7	0	0.	0.	-0.2988294E-02	-0.2988294E-02
8	0	0.	0.	-0.3745304E-02	-0.3745304E-02
9	0	0.	0.	-0.4251854E-02	-0.4251854E-02
10	0	0.	0.	-0.4429619E-02	-0.4429619E-02

SOL 2

P ZERO = -0.4738808E 02

NODE	PIX	PIY
1	0.3695345E 02	-0.1137310E 03
2	0.6457582E 02	-0.8888093E 02
3	-0.	0.
4	-0.	0.
5	-0.	-0.
6	-0.	-0.
7	-0.	-0.
8	-0.	-0.
9	-0.	-0.
10	0.	-0.

PROBLEM 2.3 CASE 2 .2(NEGATIVE FIT) P2.3 C 2

LOAD = 0.5000000E 03 POUNDS

INITIAL LACK OF FIT = -0.1500000E-02 INCHES

ROW	CALCULATED DELA	INPUT DELB	LOAD VECTOR DL (N, 3)	TOTAL VECTOR DELA + DELB + DL
1	-0.7341530E-04	0.	0.1244379E-02	0.1170904E-02
2	-0.2864748E-03	0.	0.1904403E-02	0.1617928E-02
3	-0.6183226E-03	0.	0.2078084E-02	0.1459762E-02
4	-0.1036475E-02	0.	0.1852287E-02	0.8158113E-03
5	-0.1500001E-02	0.	0.7095986E-03	-0.7904023E-03
6	-0.1963527E-02	0.	-0.5850163E-03	-0.2548543E-02
7	-0.2331679E-02	0.	-0.1982761E-02	-0.4364439E-02
8	-0.2713526E-02	0.	-0.3208945E-02	-0.5922472E-02
9	-0.2926585E-02	0.	-0.4037064E-02	-0.6963649E-02
10	-0.3000000E-02	0.	-0.4328560E-02	-0.7328560E-02

POS.OR ZERO DELTA.OR NEG.PI CYCLE 1) 1 2 3 4 5 6 7 8 9 10 0 0 0 0 0 0 0 0 0 0 10

LOAD	CASE	3 TRIAL PR	VECTOR PI (PI)	DELTA 1	DELTA 2
1	1	0.2686693E 03	0.	0.	0.
2	2	0.3188998E 03	0.	0.	0.
3	3	0.3440579E 03	0.	0.	0.
4	4	0.3423274E 03	0.	0.	0.
5	5	0.3387352E 03	0.	-0.7904023E-03	-0.7904023E-03
6	6	0.3577983E 03	0.	-0.2548543E-02	-0.2548543E-02
7	7	0.4032305E 03	0.	-0.4364439E-02	-0.4364439E-02
8	8	0.4560279E 03	0.	-0.5922472E-02	-0.5922472E-02
9	9	0.4900540E 03	0.	-0.6963649E-02	-0.6963649E-02
10	10	0.2580034E 03	0.	-0.7328560E-02	-0.7328560E-02

POS.OR ZERO DELTA.OR NEG.PI CYCLE 2) 1 2 3 4 0 0 0 0 0 0 0 0 0 0 0 0 0 0 0 0 4

LOAD	CASE	3 TRIAL PR	VECTOR PI (PI)	DELTA 1	DELTA 2
1	1	-0.1671922E 03	-0.1671922E 03	-0.1836764E-03	0.
2	2	-0.2593273E 03	-0.2593273E 03	-0.3586351E-03	-0.3586361E-03
3	3	-0.2234298E 03	-0.2234298E 03	-0.4922812E-03	-0.4922812E-03
4	4	0.1852386E 03	0.	-0.6458248E-03	-0.6458248E-03
5	0	0.	0.	-0.1277035E-02	-0.1277035E-02
6	0	0.	0.	-0.2175372E-02	-0.2175372E-02
7	0	0.	0.	-0.3173676E-02	-0.3173676E-02
8	0	0.	0.	-0.4070585E-02	-0.4070585E-02
9	0	0.	0.	-0.4687412E-02	-0.4687412E-02
10	0	0.	0.	-0.4906768E-02	-0.4906768E-02

POS.OR ZERO DELTA.OR NEG.PI CYCLE 3) 1 2 3 0 0 0 0 0 0 0 0 0 0 0 0 0 0 0 0 0 3

LOAD CASE	3 TRIAL PR	VECTOR PI (PC)	DELTA 1	DELTA 2
1	1	-0.1806482E 03	-0.1806482E 03	0.	0.
2	2	-0.2423254E 03	-0.2423254E 03	0.	0.
3		-0.1116022E 03	-0.1116022E 03	0.	0.
4	0	0.	0.	-0.3290626E-03	-0.3290626E-03
5	0	0.	0.	-0.1129978E-02	-0.1129978E-02
6	0	0.	0.	-0.2223415E-02	2223415E-02
7	0	0.	0.	-0.3410289E-02	3410289E-02
8	0	0.	0.	-0.4460781E-02	-0.4460781E-02
9	0	0.	0.	-0.5176240E-02	-0.5176240E-02
10	0	0.	0.	-0.5429391E-02	-0.5429391E-02

SOL 3

P ZERO = -0.6654997E 02

NODE	PIX	PIY
1	0.5582337E 02	-0.1718066E 03
2	0.1424353E 03	-0.1960453E 03
3	0.9028812E 02	-0.6559810E 02
4	-0.	0.
5	-0.	-0.
6	-0.	-0.
7	-0.	-0.
8	-0.	-0.
9	-0.	-0.
10	0.	-0.

PROBLEM 2.3 CASE 2 .2(NEGATIVE FIT P2.3 C 2

LOAD = 0.1000000E 04 POUNDS

INITIAL LACK OF FIT = -0.1500000E-02 INCHES

ROW	CALCULATED DELA	INPUT DELB	LOAD VECTOR DL (N, 4)	TOTAL VECTOR DELA + DELB + DL
1	-0.7341530E-04	0.	0.2488758E-02	0.2415343E-02
2	-0.2864748E-03	0.	0.3812806E-02	0.3526331E-02
3	-0.6183226E-03	0.	0.4156169E-02	0.3537846E-02
4	-0.1036475E-02	0.	0.3304573E-02	0.2268098E-02
5	-0.1500001E-02	0.	0.1419197E-02	-0.8080369E-04
6	-0.1963527E-02	0.	-0.1170033E-02	-0.3133559E-02
7	-0.2381679E-02	0.	-0.3965519E-02	-0.6347198E-02

8	-0.2715826E-02	0.	-0.6417889E-02	-0.9131415E-02
9	-0.2926585E-02	0.	-0.8074127E-02	-0.1100071E-01
10	-0.3000000E-02	0.	-0.8657120E-02	-0.1165712E-01

POS.OR ZERO DELTA.OR NEG.P(CYCLE 1) 1 2 3 4 5 6 7 8 9 10 0 0 0 0 0 0 0 0 0 10

LOAD	CASE	4 TRIAL PR	VECTOR PI (PC)	DELTA 1	DELTA 2
1	1	0.2435470E 03	0.	0.	0.
2	2	0.2838407E 03	0.	0.	0.
3	3	0.3046300E 03	0.	0.	0.
4	4	0.3079971E 03	0.	0.	0.
5	5	0.3229715E 03	0.	-0.8080369E-04	0.
6	6	0.3766149E 03	0.	-0.3133559E-02	-0.3133559E-02
7	7	0.4727985E 03	0.	-0.6347198E-02	-0.6347198E-02
8	8	0.5816574E 03	0.	-0.9131415E-02	-0.9131415E-02
9	9	0.6666611E 03	0.	-0.1100071E-01	-0.1100071E-01
10	10	0.3483853E 03	0.	-0.1165712E-01	-0.1165712E-01

POS.OR ZERO DELTA.OR NEG.P(CYCLE 2) 1 2 3 4 0 0 0 0 0 0 0 0 0 0 0 0 0 0 0 0 4

LOAD	CASE	4 TRIAL PR	VECTOR PI (PC)	DELTA 1	DELTA 2
1	1	-0.2960439E 03	-0.2960439E 03	-0.8868687E-05	0.
2	2	-0.4416215E 03	-0.4416215E 03	-0.1731658E-04	0.
3	3	-0.4330004E 03	-0.4330004E 03	-0.23 964E-04	0.
4	4	0.8944199E 01	0.	-0.3 .8347E-04	0.
5	0	0.	0.	-0. 496E-03	-0.9866496E-03
6	0	0.	0.	-0.. 037E-02	-0.2469937E-02
7	0	0.	0.	-0.4199618E-02	-0.4199618E-02
8	0	0.	0.	-0.5783460E-02	-0.5783460E-02
9	0	0.	0.	-0.6882259E-02	-0.6882259E-02
10	0	0.	0.	-0.7274393E-02	-0.7274393E-02

POS.OR ZERO DELTA.OR NEG.P(CYCLE 3) 1 2 3 0 0 0 0 0 0 0 0 0 0 0 0 0 0 0 0 3

LOAD	CASE	4 TRIAL PR	VECTOR PI (PC)	DELTA 1	DELTA 2
1	1	-0.2966937E 03	-0.2966937E 03	0.	0.
2	2	-0.4406006E 03	-0.4406006E 03	-0.1455192E-10	0.
3	3	-0.4274009E 03	-0.4274009E 03	-0.1465572E-11	0.
4	4	0.	0.	-0.1588877E-04	0.
5	0	0.	0.	-0.9695490E-03	-0.9695490E-03
6	0	0.	0.	-0.2472257E-02	-0.2472257E-02
7	0	0.	0.	-0.4211043E-02	-0.4211043E-02
8	0	0.	0.	-0.5802301E-02	-0.5802301E-02
9	0	0.	0.	-0.6905862E-02	-0.6905862E-02
10	0	0.	0.	-0.7299627E-02	-0.7299627E-02

SOL 4

P ZERO = -0.1098752E 03

NODE	PIX	PIY
1	0.9163342E 02	-0.2821724E 03
2	0.2590962E 03	-0.3566151E 03
3	0.3459364E 03	-0.2513373E 03
4	-0.	0.
5	-0.	-0.
6	-0.	-0.
7	-0.	-0.
8	-0.	-0.
9	-0.	-0.
10	0.	-0.

PROBLEM 2.3 CASE 2 .2) NEGATIVE FIT P2.3 C 2

LOAD = 0.2000000E 04 POUNDS

INITIAL LACK OF FIT = -0.1500000E-02 INCHES

NOW CALCULATED DELA	INPUT DELB	LOAD VECTOR DL (N, S)	TOTAL VECTOR DELA + DELB + DL
1 -0.7341505E-04	0.	0.4977517E-02	0.4904101E-02
2 -0.2667748E-03	0.	0.7625610E-02	0.7339135E-02
3 -0.6102426E-03	0.	0.8312337E-02	0.7694014E-02
4 -0.1336475E-02	0.	0.6609148E-02	0.5272670E-02
5 -0.1500001E-02	0.	0.2838395E-02	0.1338394E-02
6 -0.1903527E-02	0.	-0.2340066E-02	-0.4303593E-02
7 -0.2381679E-02	0.	-0.7931042E-02	-0.1031272E-01
8 -0.2713526E-02	0.	-0.1283578E-01	-0.1554931E-01
9 -0.2920585E-02	0.	-0.1614826E-01	-0.1907484E-01
10 -0.2991808E-02	0.	-0.1731424E-01	-0.2031424E-01

POS.OF ZERO DELTA OR NEG.P(CYCLE 1) 1 2 3 4 5 6 7 8 9 10 0 0 0 0 0 0 0 0 0 10

LOAD CASE	S TRIAL PR	VECTOR PI (PC)	DELTA 1	DELTA 2
1 1	0.1933918E 03	0.	0.	0.
2 2	0.2141650E 03	0.	0.	0.
3 3	0.2257736E 03	0.	0.	0.
4 4	0.2343380E 03	0.	0.	0.
5 5	0.2405436E 03	0.	0.	0.

6	6	0.4142423E 03	0.	-0.4303593E-02	-0.4303593E-02
7	7	0.6119372E 03	0.	-0.1031272E-01	-0.1031272E-01
8	8	0.8329181E 03	0.	-0.1554931E-01	-0.1554931E-01
9	9	0.1066976E 04	0.	-0.1907484E-01	-0.1907484E-01
10	10	0.9351475E 03	0.	-0.2031424E-01	-0.2031424E-01

POS.OR ZERO DELTA,OR NEG.PI CYCLE 2) 1 2 3 4 5 0 0 0 0 0 0 0 0 0 0 0 0 0 0 0 0 5

LOAD CASE	S TRIAL PR	VECTOR PI (PC)		DELTA 1	DELTA 2
1	1	-0.4994059E 03	-0.4994059E 03	-0.1171200E-03	0.
2	2	-0.7630051E 03	-0.7630051E 03	-0.1992856E-03	0.
3	3	-0.8859670L 03	-0.8859670E 03	-0.7221094E-03	-0.7221094E-03
4	4	-0.6428867E 03	-0.6428867E 03	-0.9956577E-03	-0.9956577E-03
5	5	0.5845625E 03	0.	-0.1472262E-02	-0.1472262E-02
6	0	0.	0.	-0.3233442E-02	-0.3233442E-02
7	0	0.	0.	-0.5505633E-02	-0.5505633E-02
8	0	0.	0.	-0.7707709E-02	-0.7707709E-02
9	0	0.	0.	-0.9283548E-02	-0.9283548E-02
10	0	0.	0.	-0.9854670E-02	-0.9854670E-02

POS.OR ZERO DELTA,OR NEG.PI CYCLE 3) 1 2 3 4 0 0 0 0 0 0 0 0 0 0 0 0 0 0 0 0 4

LOAD CASE	S TRIAL PR	VECTOR PI (PC		DELTA 1	DELTA 2
1	1	-0.5537403E 03	-0.5537403E 03	-0.1818909E-10	0.
2	2	-0.8062081E 03	-0.8062081E 03	-0.2910303E-10	0.
3	3	-0.9321429E 03	-0.9321429E 03	-0.1019361E-09	0.
4	4	-0.6436436E 03	-0.6436436E 03	-0.5820766E-10	0.
5	0	0.	0.	-0.9611905E-03	-0.9611905E-03
6	0	0.	0.	-0.3125361E-02	-0.3125361E-02
7	0	0.	0.	-0.5802311E-02	-0.5802311E-02
8	0	0.	0.	-0.8337501E-02	-0.8337501E-02
9	0	0.	0.	-0.1012805E-01	-0.1012805E-01
10	0	0.	0.	-0.1077260E-01	-0.1077260E-01

SOL 5

P ZERO = -0.2140499E 03

NODE	PIX	PIY
1	0.1711177E 03	-0.5266459E 03
2	0.4733774E 03	-0.6522359E 03
3	0.6803983E 03	-0.5008767E 03
4	0.3258249E 03	-0.1061915E 03

5	-0.	-0.
6	-0.	-0.
7	-0.	-0.
8	-0.	-0.
9	-0.	-0.
10	0.	-0.

PROBLEM 2.3 CASE 2 .2(NEGATIVE P) P2.3 C 2

LOAD = 0.00000000E 04 POUNDS

INITIAL LACK OF FIT = -0.1500000E-02 INCHES

ROW	CALCULATED DELA	INPUT DELB	LOAD VECTOR DL (N, 6)	TOTAL VECTOR DELA + DELB + DL
1	-0.7341530E-0	0.	0.9955034E-02	0.9881618E-02
2	-0.2[illegible]748E-03	0.	0.1525122E-01	0.1496475E-01
3	-0.[illegible]1832260E-03	0.	0.1662467E-01	0.1600635E-01
4	-0.1036475E-02	0.	0.1321829E-01	0.1218182E-01
5	-0.1500001E-02	0.	0.5676787E-02	0.4176786E-02
6	-0.1[illegible]615275E-02	0.	-0.4680131E-02	-0.6643657E-02
7	-0.2381674E-02	0.	-0.1586208E-01	-0.1824376E-01
8	-0.2713526E-02	0.	-0.2567156E-01	-0.2838509E-01
9	-0.2[illegible]265[illegible]5E-02	0.	-0.3229652E-01	-0.3522310E-01
10	-0.3[illegible]0000[illegible]E-02	0.	-0.3462848E-01	-0.3762848E-01

POS.OR ZERO DELTA.OR NEG.P(CYCLE 1) 1 2 3 4 5 6 7 8 9 10 0 0 0 0 0 0 0 0 0 0

LOAD	CASE	TRIAL PR	VECTOR PI (PC)	DELTA 1	DELTA 2
1	1	0.9281323E 02	0.	0.	0.
2	2	0.7468850E 02	0.	0.	0.
3	3	0.6806289E 02	0.	0.	0.
4	4	0.1020185E 03	0.	0.	0.
5	5	0.2262903E 03	0.	0.	0.
6	6	0.4895084E 03	0.	-0.6643657E-02	-0.6643657E-02
7	7	0.8902127E 03	0.	-0.1824376E-01	-0.1824376E-01
8	8	0.1335437E 04	0.	-0.2838509E-01	-0.2838509E-01
9	9	0.1886107E 04	0.	-0.3522310E-01	-0.3522310E-01
10	10	0.9996737E 03	0.	-0.3762848E-01	-0.3762848E-01

POS.OR ZERO DELTA.OR NEG.P(CYCLE 2) 1 2 3 4 5 6 0 0 0 0 0 0 0 0 0 0 0 0 0 0 0 0

LOAD CASE	6 TRIAL PR	VECTOR PI (PC)	DELTA 1	DELTA 2
1	-0.1014838E 04	-0.1014838E 04	-0.1170661E-03	0.
2	-0.1492203E 04	-0.1492203E 04	-0.3091001E-03	0.
3	-0.1724234E 04	-0.1724234E 04	-0.7217734E-03	0.
4	-0.1347923E 04	-0.1347923E 04	-0.9951941E-03	-0.9951941E-03
5	0.5842902E 03	0.	-0.1471576E-02	-0.1471576E-02
6	0.	0.	-0.4547688E-02	-0.4547688E-02
7	0.	0.	-0.8687769E-02	-0.8687769E-02
8	0.	0.	-0.1277070E-01	-0.1277070E-01
9	0.	0.	-0.1571599E-01	-0.1571599E-01
10	0.	0.	-0.1676712E-01	-0.1676712E-01

POS.OR ZERO DELTA.OR NEG.PI(CYCLE 3) 1 2 3 4 0 0 0 0 0 0 0 0 0 0 0 0 0 0 0 4

LOAD CASE	6 TRIAL PR	VECTOR PI (PC)	DELTA 1	DELTA 2
1	-0.1069155E 04	-0.1069155E 04	0.	0.
2	-0.1535386E 04	-0.1535386E 04	0.	0.
3	-0.1690425E 04	-0.1690425E 04	0.	0.
4	-0.1048819E 04	-0.1048819E 04	0.	0.
5	0.	0.	-0.9607425E-03	-0.9607425E-03
6	0.	0.	-0.4439656E-02	-0.4439656E-02
7	0.	0.	-0.8984310E-02	-0.8984310E-02
8	0.	0.	-0.1340020E-01	-0.1340020E-01
9	0.	0.	-0.1656010E-01	-0.1656010E-01
10	0.	0.	-0.1770463E-01	-0.1770463E-01

SOL 6

P ZERO = -0.4233114E 03.

NODE	PIX	PIY
1	0.3303872E 03	-0.1016827E 04
2	0.9024774E 03	-0.1242153E 04
3	0.1367583E 04	-0.9936065E 03
4	0.9974867E 03	-0.3241025E 03
5	-0.	-0.
6	-0.	-0.
7	-0.	-0.
8	-0.	-0.
9	-0.	-0.
10	0.	-0.

PROBLEM 2.3 CASE 2 .2(NEGATIVE FIT P2.3 C 2

LOAD = 0.4500000E 04 POUNDS

INITIAL LACK OF FIT = -0.1500000E-02 INCHES

NO.	CALCULATED DELA	INPUT DELB	LOAD VECTOR DL (N, 7)	TOTAL VECTOR DELA + DELB + DL
1	-0.7345530E-04	0.	0.1119941E-01	0.1112600E-01
2	-0.2864748E-03	0.	0.1715762E-01	0.1687115E-01
3	-0.6183226E-03	0.	0.1870276E-01	0.1808443E-01
4	-0.1035475E-02	0.	0.1487058E-01	0.1383410E-01
5	-0.1500001E-02	0.	0.6386388E-02	0.4886387E-02
6	-0.1963527E-02	0.	-0.5265146E-02	-0.7228673E-02
7	-0.2381679E-02	0.	-0.1784484E-01	-0.2022652E-01
8	-0.2713526E-02	0.	-0.2888051E-01	-0.3159403E-01
9	-0.2926585E-02	0.	-0.3633358E-01	-0.3926017E-01
10	-0.3000000E-02	0.	-0.3895704E-01	-0.4195704E-01

T42

POS.OR ZERO DELTA,OR NEG.PI CYCLE 1) 1 2 3 4 5 6 7 8 9 10 0 0 0 0 0 0 0 0 0 0 0

LOAD	CASE	7 TRIAL PR	VECTOR PI (PC)	DELTA 1	DELTA 2
1	1	0.6769164E 02	0.	0.	0.
2	2	0.3982925E 02	0.	0.	0.
3	3	0.2863654E 02	0.	0.	0.
4	4	0.6766680E 02	0.	0.	0.
5	5	0.2102255E 03	0.	0.	0.
6	6	0.5083251E 03	0.	-0.7228673E-02	-0.7228673E-02
7	7	0.9397822E 03	0.	-0.2022652E-01	-0.2022652E-01
8	8	0.1461066E 04	0.	-0.3159403E-01	-0.3159403E-01
9	9	0.1856114E 04	0.	-0.3926017E-01	-0.3926017E-01
10	10	0.1602055E 04	0.	-0.4195704E-01	-0.4195704E-01

POS.OR ZERO DELTA,OR NEG.PI CYCLE 2) 1 2 3 4 5 0 0 0 0 0 0 0 0 0 0 0 0 0 0 5

LOAD	CASE	7 TRIAL PR	VECTOR PI (PC)	DELTA 1	DELTA 2
1	1	-0.1143695E 04	-0.1143695E 04	-0.1170519E-03	0.
2	2	-0.1674502E 04	-0.1674502E 04	-0.3990525E-03	0.
3	3	-0.1933799E 04	-0.1933799E 04	-0.7216877E-03	0.
4	4	-0.1524184E 04	-0.1524184E 04	-0.9950764E-03	-0.9950764E-03
5	5	0.5842214E 03	0.	-0.1471402E-02	-0.1471402E-02
6	6	0.	0.	-0.4876250E-02	-0.4876250E-02
7	7	0.	0.	-0.9483305E-02	-0.9483305E-02
8	8	0.	0.	-0.1403645E-01	-0.1403645E-01
9	9	0.	0.	-0.1732410E-01	-0.1732410E-01
10	10	0.	0.	-0.1852024E-01	-0.1852024E-01

POS.OR ZERO DELTA.OR NEG.PT CYCLE 3) 1 2 3 4 0 0 0 0 0 0 0 0 0 0 0 0 0 0 0 0 0 4

LOAD CASE	7 TRIAL PR	VECTOR FT (PC)	DELTA 1	DELTA 2
1	1	-0.1198006E 04	-0.1198006E 04	-0.2910383E-10	0.
2	2	-0.1717680E 04	-0.1717680E 04	0.	0.
3	3	-0.1899295E 04	-0.1899295E 04	-0.2910383E-10	0.
4	4	-0.1225115E 04	-0.1225115E 04	0.	0.
5	0	0.	0.	-0.9606296E-03	0.
6	0	0.	0.	-0.4768231E-02	-0.4768231E-02
7	0	0.	0.	-0.9779809E-02	-0.9779809E-02
8	0	0.	0.	-0.1466587E-01	-0.1466587E-01
9	0	0.	0.	-0.1816811E-01	-0.1816811E-01
10	0	0.	0.	-0.1943763E-01	-0.1943763E-01

SOL 7

P ZERO = -0.4755273E 03

NODE	PIX	PIY
1	0.3702044E 03	-0.1139371E 04
2	0.1009627E 04	-0.1389632E 04
3	0.1537128E 04	-0.1116788E 04
4	0.1155154E 04	-0.3785808E 03
5	-0.	-0.
6	-0.	-0.
7	-0.	-0.
8	-0.	-0.
9	-0.	-0.
10	0.	-0.

PROBLEM 2.3 CASE 2 .2(NEGATIVE FIT P2.3 C 2

LOAD = 0.5000000E 04 POUNDS

INITIAL LACK OF FIT = -0.1500000E-02 INCHES

ROW	CALCULATED DELA	INPUT DELB	LOAD VECTOR DL (N, S)	TOTAL VECTOR DELA + DELB + DL
1	-0.7341530E-04	0.	0.1244379E-01	0.1237038E-01
2	-0.2864748E-03	0.	0.1906403E-01	0.1877756E-01
3	-0.5183226E-03	0.	0.2078084E-01	0.2016252E-01
4	-0.1036475E-02	0.	0.1652287E-01	0.1548639E-01
5	-0.1500001E-02	0.	0.7095985E-02	0.5595984E-02

6	-0.1963527E-02	0.	-0.5850162E-02	-0.7813689E-02
7	-0.2381679E-02	0.	-0.1982760E-01	-0.2220928E-01
8	-0.2713526E-02	0.	-0.3208945E-01	-0.3480298E-01
9	-0.2926585E-02	0.	-0.4037065E-01	-0.4329724E-01
10	-0.3000000E-02	0.	-0.4328561E-01	-0.4628561E-01

POS,OR ZERO DELTA,OR NEG.PI CYCLE 1) 1 2 3 4 5 6 7 8 9 10 0 0 0 0 0 0 0 0 0 0 10

LOAD	CASE	B TRIAL PR	VECTOR PI (PC)	DELTA 1	DELTA 2
1	1	0.4256937E 02	0.	0.	0.
2	2	0.4968674E 01	0.	0.	0.
3	3	-0.1079173E 02	-0.1079173E 02	0.	0.
4	4	0.3335765E 02	0.	0.	0.
5	5	0.1941534E 03	0.	0.	0.
6	6	0.5271403E 03	0.	-0.7809369E-02	-0.7809369E-02
7	7	0.1029349E 04	0.	-0.2218790E-01	-0.2218790E-01
8	8	0.1586695E 04	0.	-0.3476771E-01	-0.3476771E-01
9	9	0.2026122E 04	0.	-0.4325304E-01	-0.4325304E-01
10	10	0.1095438E 04	0.	-0.4623835E-01	-0.4623835E-01

POS.OR ZERO DELTA,OR NEG.PI CYCLE 2) 1 2 3 4 5 0 0 0 0 0 0 0 0 0 0 0 0 0 0 5

LOAD	CASE	B TRIAL PR	VECTOR PI (PC)	DELTA 1	DELTA 2
1	1	-0.1272553E 04	-0.1272553E 04	-0.1170387E-03	0.
2	2	-0.1856803E 04	-0.1856803E 04	-0.3990066E-03	0.
3	3	-0.2143366E 04	-0.2143366E 04	-0.7216045E-03	0.
4	4	-0.1700442E 04	-0.1700442E 04	-0.9949615E-03	0.
5	5	0.5841537E 03	0.	-0.1471232E-02	-0.1471232E-02
6	0	0.	0.	-0.5204810E-02	-0.5204810E-02
7	0	0.	0.	-0.1027883E-01	-0.1027883E-01
8	0	0.	0.	-0.1530219E-01	-0.1530219E-01
9	0	0.	0.	-0.1693220E-01	-0.1693220E-01
10	0	0.	0.	-0.2025335E-01	-0.2025335E-01

POS.OR ZERO DELTA,OR NEG.PI CYCLE 3) 1 2 3 4 0 0 0 0 0 0 0 0 0 0 0 0 0 0 0 4

LOAD	CASE	B TRIAL PR	VECTOR PI (PC)	DELTA 1	DELTA 2
1	1	-0.1326858E 04	-0.1326858E 04	0.	0.
2	2	-0.1899976E 04	-0.1999976E 04	0.	0.
[illegible]	[illegible]	[illegible] 04	[illegible] 04	0.	0.
4	4	-0.1401408E 04	-0.1401408E 04	0.	0.
5	0	0.	0.	-0.9605183E-03	0.
6	[illegible]	.	0.	-0.5096804E-02	. 5096804E-02
7	[illegible]	.	0.	-0.1057531E-01	. 1057531E-01

8	0	0.	0.	-0.1593155E-01	-0.1593155E-01
9	0	0.	0.	-0.1977612E-01	-0.1977612E-01
10	0	0.	0.	-0.2117064E-01	-0.2117064E-01

SOL 8

P ZERO = -0.5279421E 03

NODE	PIX	PIY
1	0.4100217E 03	-0.1261916E 04
2	0.1116778E 04	-0.1537112E 04
3	0.1706675E 04	-0.1239971E 04
4	0.1332819E 04	-0.4330583E 03
5	-0.	-0.
6	-0.	-0.
7	-0.	-0.
8	-0.	-0.
9	-0.	-0.
10	0.	-0.

APPENDIX I CONTACT PROBLEM INPUT MATRICES

In Chapter 3 the method used to solve the contact problem was briefly described. This Appendix gives the details for setting up the matrices needed as input for the analysis. The present study uses the Grumman matrix structural analysis program called COMAP-ASTRAL but any elastic analysis computer program that has similar planar finite elements as those described in Section 2.3.1 could be used.

The first matrix to be generated is the matrix of influence coefficients, [A] which gives the radial displacements around the hole for unit redundants {P} following the notation shown in the figure below.

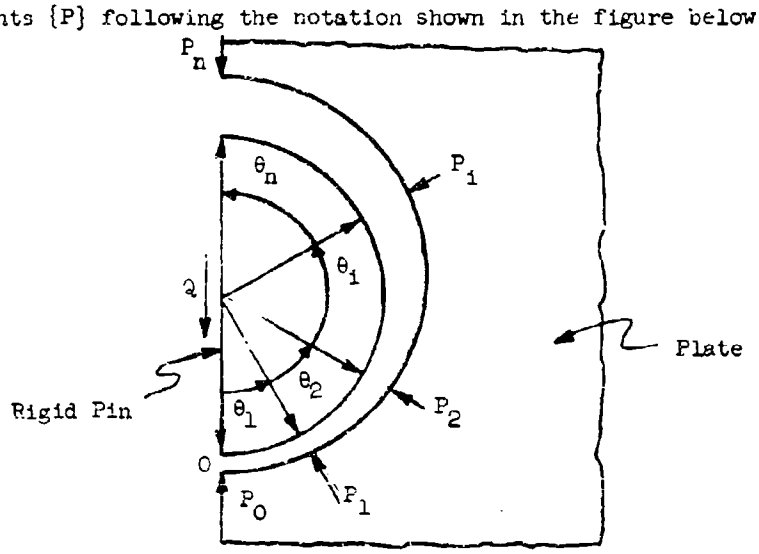

The relation of {P} to the radial displacements in the plate, $\{\delta_r\}$ is of the form:

$$\{P\} = [A] \quad \{\delta_r\} \tag{I.1}$$

where,

$$\{P\} = \begin{Bmatrix} P_0 \\ P_1 \\ \vdots \\ P_n \end{Bmatrix}$$

We can rewrite Eq. I.1 by eliminating one of the redundants from the statically determinate equilibrium condition which is:

$$P_0 = [-\cos\theta_1 \; -\cos\theta_2 \; - \ldots \; -\cos\theta_n \; - 1] \{P'\} \qquad (I.2)$$

where, $\{P'\} = \begin{Bmatrix} P_1 \\ P_2 \\ \vdots \\ P_n \\ Q \end{Bmatrix}$

Thus the new redundants are related to the old by the expression below:

$$\begin{Bmatrix} P_0 \\ P_1 \\ \vdots \\ P_n \end{Bmatrix} = \begin{bmatrix} -\cos\theta_1 & -\cos\theta_2 & \cdots & -1 \\ 1 & & & 0 \\ \vdots & & & \vdots \\ 0 & & & 0 \end{bmatrix} \begin{Bmatrix} P_1 \\ P_2 \\ \vdots \\ P_n \\ Q \end{Bmatrix} \qquad (I.3)$$

$= [\alpha] \{P'\}$, where $[\alpha]$ is a transformation matrix.

Once the order of the redundants in the compatibility equation (Eq. 10) are changed the radial displacements must be reordered. Let $\{\Delta_r\}$ be the relative radial displacements between the fastener and the plate. The relation between $\{\Delta_r\}$ and $\{\delta_r\}$ becomes:

$$\begin{Bmatrix} \Delta_{r1} \\ \Delta_{r2} \\ \vdots \\ \Delta_{rn} \\ \Delta_{rQ} \end{Bmatrix} = \begin{bmatrix} -\cos\theta_1 & 1 & & \cdots & 0 \\ -\cos\theta_2 & 0 & 1 & \cdots & 0 \\ \vdots & & & & \vdots \\ 0 & & & & 0 \end{bmatrix} \begin{Bmatrix} \delta_{r0} \\ \delta_{r1} \\ \vdots \\ \delta_{rn} \end{Bmatrix} \qquad (I.4)$$

$= [\beta] \{\delta_r\}$, where $[\beta]$ is a transformation matrix.

Note that the relative radial displacement $\Delta_{rO} = 0$ so that Δ_{rQ} or any point on the rigid fastener has zero relative displacement to point O.

The expression for relative radial displacements due to the action of of the redundant $\{P'\}$ therefore becomes:

$$\{\Delta_r\} = [\beta]\,[A]\,[\alpha]\,\{P'\} \tag{I.5}$$

APPENDIX J NONLINEAR ANALYSIS OF A SINGLE FASTENER - THREE-DIMENSIONAL EFFECTS

Starting with a load deflection curve (Figure J-1) for a single rigid fastener, (Figure J-2) as determined by finite-element methods described earlier in Chapter 2 for which the detailed sheet stresses are known (e.g. Figure J-3) for each load level, a "secant spring modulus" $\bar{k}_a$ is available. If one isolates the fastener and replaces the surrounding plate material sheets by a continuous series of non-linear transverse springs, the problem becomes quite tractable. It is emphasized here that the engineering assumption made is essentially the same as is made in "beam on elastic foundation" theory, i.e., the shear effects through the sheet thickness play only a secondary role in the load distribution and can be ignored for the present.

Continuing along these lines, Figure J-4 shows the idealization of a typical fastener in single shear. Denoting the fastener deflection adjacent to the i^{th} plate by y_i (i=1 and 2 for a fastener in single shear; i=1, 2 and 3 for a fastener in double shear, etc.) and Y_i as the plate deflection at some reference section, it becomes possible to relate $Y_i - y_i$ to the local secant spring stiffness:

$$q_i = \bar{k}_i (Y_i - y_i) \qquad (J-1)$$

where $\bar{k}_i$ and y_i may vary through the plate thickness x_i.

If the reference section is sufficiently far (i.e., several hole diameters) from the fastener, it can be assumed to remain plane, leading to the following:

$$q_i = \bar{k}_i(a_i + b_i x_i - y_i) \qquad (J-2)$$

where a_i and b_i are constants to be evaluated such that

$$P_i = \int_0^{h_i} q_i \, dx_i \tag{J-3}$$

$$M_i = \int_0^{h_i} q_i \left(\frac{h_i}{2} - x_i\right) dx_i \tag{J-4}$$

where P_i and M_i are the net force and moment at the plate reference sections.

Since the problem may be nonlinear, a step-by-step linearized numerical solution technique is proposed wherein P_i and M_i are built up simultaneously in sufficiently small steps (ΔP_i, ΔM_i), such that $\bar{k}_i$ and y_i may be approximated in the integrands of Equations (J-3) and (J-4) by values which correspond to the previous step. In this way a_i and b_i may be evaluated in terms of β_i and γ_i from Equations (J-5) and (J-6):

$$\begin{bmatrix} \alpha_{11i} & \alpha_{12i} \\ \alpha_{21i} & \alpha_{22i} \end{bmatrix} \begin{Bmatrix} a_i \\ b_i \end{Bmatrix} = \begin{Bmatrix} P_i + \beta_i \\ M_i + \gamma_i \end{Bmatrix} \tag{J-5}$$

where

$$\begin{aligned} \alpha_{11i} &= \int_0^{h_i} \bar{k}_i \, dx_i \\ \alpha_{12i} &= \int_0^{h_i} x_i \, \bar{k}_i \, dx_i \\ \alpha_{21i} &= \frac{h_i}{2} \alpha_{11i} - \alpha_{12i} \\ \alpha_{22i} &= \frac{h_i}{2} \alpha_{12i} - \int_0^{h_i} x_i^2 \, \bar{k}_i \, dx_i \end{aligned} \tag{J-6}$$

$$\beta_i = \int_0^{h_i} y_i \, k_i \, dx_i$$

$$\gamma_i = \frac{h_i}{2} \beta_i - \int_0^{h_i} x_i \, y_i \, k_i \, dx_i$$

Thus q_i, as a function of x_i, is known after each increment in the loading.

To solve for the y_i, a short thick-beam theory, such as Timoshenko's (Reference 12), appears suitable since it accounts for shear deflection. For simplicity's sake, it is assumed that the fastener-head effects may be approximated by a rotational spring and edge shear resistance to simulate head friction.

Referring to Section 4.3, the beam-segment equations, corresponding to each plate, are:

$$\frac{d}{dx_i}\left(EI_i \frac{d\psi_i}{dx_i}\right) + \lambda G A_i \left(\frac{dy_i}{dx_i} - \psi_i\right) = 0 \qquad \text{(J-7)}$$

and

$$\frac{d}{dx_i}\left(A_i \left[\frac{dy_i}{dx_i} - \psi_i\right]\right) = -\frac{q_i}{\lambda G} \qquad \text{(J-8)}$$

where ψ_i is the cross-sectional beam rotation under the usual assumption that plane sections remain plane, A_i is the cross-sectional area, E and G are the material stiffnesses, I_i the bending moment of inertia, and λ is a factor which depends on the geometry of the beam cross-section.

The interface boundary conditions are

$$y_i = -y_{i+1}, \quad \psi_i = \psi_{i+1}$$

$$\frac{d\psi_i}{dx_i} = -\frac{d\psi_{i+1}}{dx_{i+1}}, \quad \frac{dy_i}{dx_i} - \psi_i = \frac{dy_{i+1}}{dx_{i+1}} - \psi_{i+1} \qquad \text{(J-9)}$$

and the boundary conditions at the fastener heads can be written as

$$C_{1i}\, EI \frac{d\psi_i}{dx_i} + C_{2i}\, \psi_i = 0$$

$$\lambda A_i\, G\left(\frac{dy_i}{dx_i} - \psi_i\right) = F \qquad \text{(J-10)}$$

where the C's are adjusted to account for head effects and F is the shear load between fastener and head. For example, if the head rotational stiffness is a constant, say S, $C_{2i} = S$ and $C_{1i} = 1$ regardless of the level of P_i and M_i. In general, these C's as well as F, must be approximated by engineering means or be empirically adjusted to permit correlation with test data.

Equations (J-7) through (J-10) may be solved numerically by finite difference techniques. However, because of the nature of the assumptions and degree of approximation to this point, an analytical solution is easily available if the coefficients of the differential equation are assumed constant, i.e., A_i and I_i are assumed constant. Thus, the y_i are evaluated as functions of x_i for each step in the P_i, M_i iteration process.

Once a solution for q_i as a function of the plate thickness is obtained in terms of the final P_i,M_i combination, the stresses through the sheets near the fastener holes may be determined by reference to the previous two-dimensional stress solution at each thickness level. Furthermore, an effective fastener spring rate, including fastener shear and rotation, may be defined in terms of relative deflections on a given fastener.

Linearization: As a first step to the overall problem, the equations may be greatly simplified if, as appears justified from Chapter 3,

the elastic foundation springs, corresponding to each plate, are assumed to have constant rates. Thus, the first three integrations required by Equations (J-6) may be performed explicitly once and for all, and a_i and b_i become uniquely determined function of integrals in y_i. Substituting these into Equation (J-2) and thence into Equation (J-8) yields

$$\frac{d}{dx_i}\left(A_i\left[\frac{dy_i}{dx_i} - \psi_i\right]\right) + \frac{k_i}{\lambda G} y_i = \frac{k_i a_i}{\lambda G} + \frac{k_i b_i}{\lambda G} x_i \qquad \text{(J-11)}$$

where Equation (J-11) will involve integrals of y_i.

For constant area, A_i, and bending inertia, I_i, it becomes a simple matter to obtain closed-form analytic solutions to Equations (J-7) and (J-11) subject to linear boundary Equations (J-10). In this way, once the y_i are known the stress variation through the thickness, q_i, may be computed.

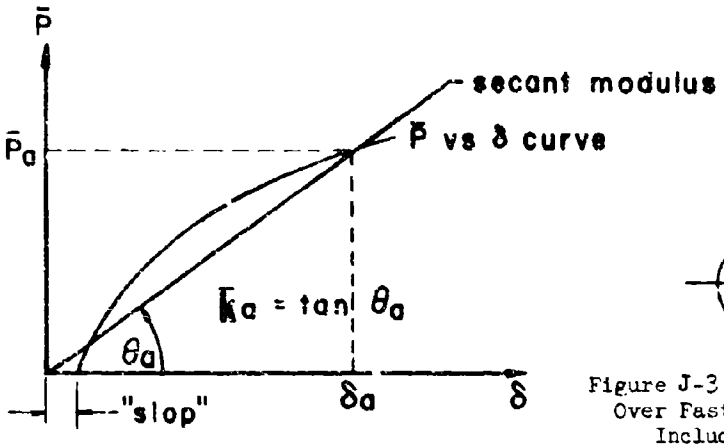

Figure J-1 - Load Deflection Curve for A Typical Fastener. Includes Local Planar Effects Only.

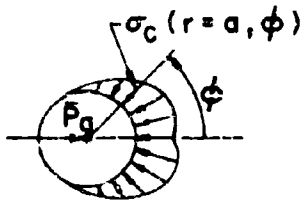

Figure J-3 - Typical Compressive Stresses Over Fastener-Plate Contact Region. Includes Planar Effects Only.

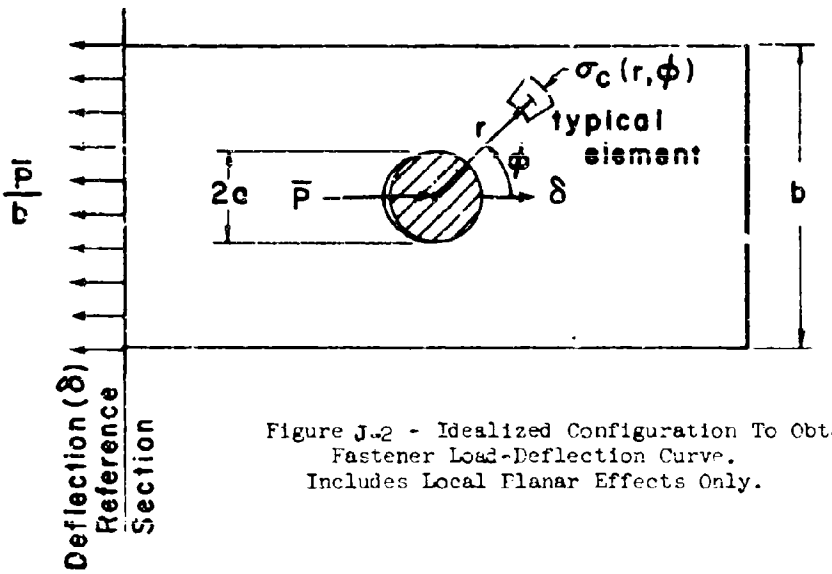

Figure J-2 - Idealized Configuration To Obtain Fastener Load-Deflection Curve. Includes Local Planar Effects Only.

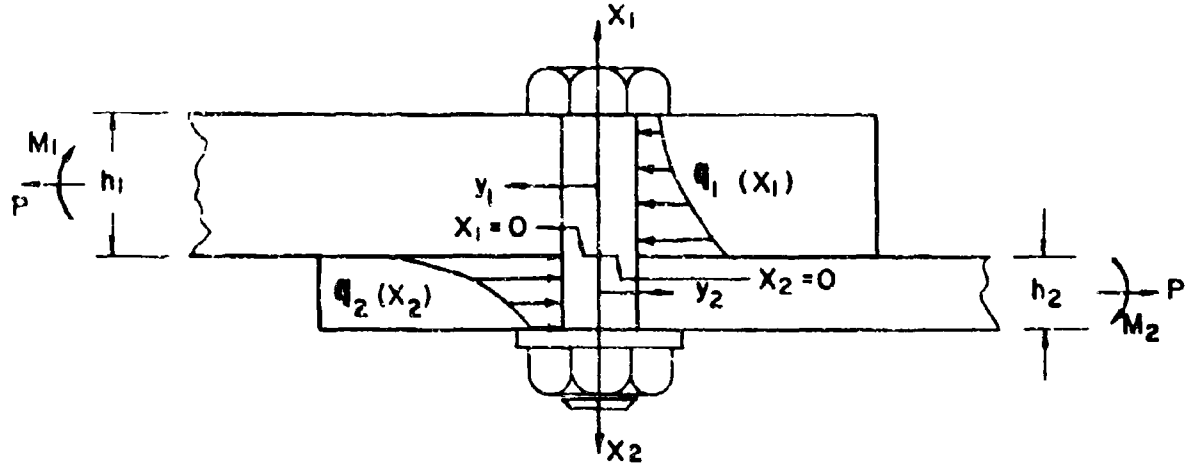

(a) Plate-Fastener Load Interaction Through Plate Thickness

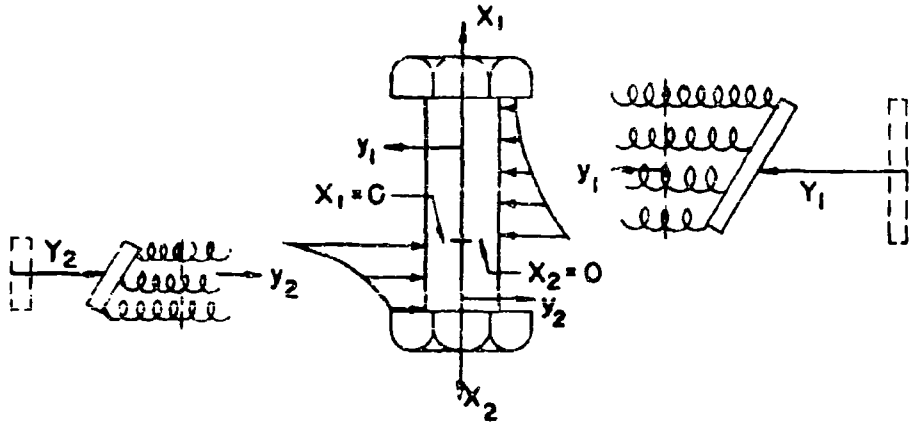

(b) Idealized Model of Plate as a Nonlinear Elastic Foundation Interacting With a Short Beam

Figure J-4 - Idealized Model Including Local Effects Along the Fastener Length and Through the Plate's Thickness

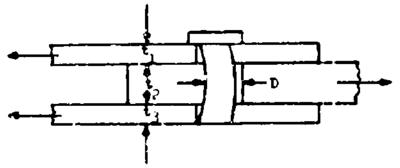

Section Through Fastener

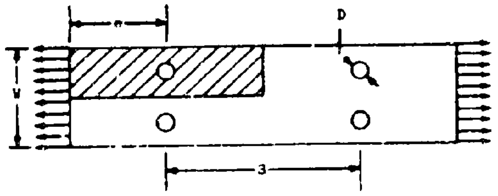

Typical Dimensions

$$\delta = \frac{P}{k_e} + A\left(\frac{P}{P_j}\right)^B$$

Basic Relationship

PLATE DATA							FASTENER DATA						MEASURED INTERFERENCE			LOAD-DEFLECTION PARAMETERS						TEST INFORMATION		IDENTIFICATION			
Material	E	t_1	t_2	t_3	e	e/D	Material	E	Dia (D)	Head Type	Torque	No. Fast	(-ve) "slop"	(0) zero	(+ve) pos.	k_e	δ_0	P_1	P_j	A	B	Gage L'gth	Type Rec.	Ref.	Date	[illegible]	Test No.
	$\times 10^6$ psi	in.	in.	in.	in.	in.		$\times 10^6$ psi	in.		in-lb		in.	in.	in.	$\times 10^{-3}$ lb/in	in.	lb.	lb.	in.		in.					
1	2	3	4	5	6	7	8	9	10	11	12	13	14	15	16	17	18	19	20	21	22	23	24	25	26	27	28
7075-T6	10.5	.072	.102	.072			EL1870		5/32			1		0		273		2050	2330	.005	7.15	2	Auto	Ref. 1		III	
"	"	"	"	"			"		"			"	.005			181		2225	2460	"	9.13	"	"	"		III-[illegible]	4
"	"	"	"	"			[illegible] AN 320		.250		0	"		0		285		2750	3175	"	6.38	"	"	"		III-C	4
"	"	"	"	"			"		"		35	"		"		275		3225	3500	"	11.20	"	"	"		III-D	4
"	"	"	"	"			"		"		0	"	.005			263		2700	3125	"	6.27	"	"	"		III-[illegible]	4
"	"	"	"	"			"		"		35	"	"			240		3100	3450	"	8.57	"	"	"		III-[illegible]	4

FASTENER "SPRING CONSTANTS" - REDUCTION OF EXPERIMENTAL LOAD-DEFLECTION CURVES

PLATE DATA							FASTENER DATA						MEASURED INTERFERENCE			LOAD-DEFLECTION PARAMETERS						TEST INFORMATION		IDENTIFICATION			
Material	E	t_1	t_2	t_3	e	e/D	Material	E	Dia (D)	Head Type	Torque	No. Fast	(-ve) sion	(0) zero	(+ve) pos.	k_e	δ_0	P_1	P_2	A	B	Gage L'gth	Type Rec.	Ref.	Date	Spec.	Test No.
	$\times 10^{-7}$ psi	in.	in.	in.	in.	in.		$\times 10^{-7}$ psi	in.		in-lb		in.	in.	in.	$\times 10^{-3}$ lb/in	in.	lb.	lb.	in.		in.					
1	2	3	4	5	6	7	8	9	10	11	12	13	14	15	16	17	18	19	20	21	22	23	24	25	26	27	28
7075-T6	105	.072	.072	None			HL1870		5/32			1		0		106		1325	1460	.005	9.44	2	Auto	Ref.1		II-4	1
"	"	.102	.102	"			"		"			"		"		130		1550	1830	"	5.52	"	"	"		II-4	2
"	"	.102	.072	"			"		"			"		"		117		1390	1530	"	9.55	"	"	"		II-4	3
"	"	.072	.072	"			"		"			"	.005			85		1250	1400	"	7.78	"	"	"		III-4	1
"	"	.102	.102	"			"		"			"	"			108		1610	1825	"	7.31	"	"	"		III-4	2
"	"	.102	.072	"			"		"			"	"			88		1400	1595	"	7.03	"	"	"		III-4	3
"	"	.072	.072	"			NAS 464		.250		0	"		0		125		1800	2025	"	7.78	"	"	"		III-4	1
"	"	.102	.102	"			"		"		"	"		"		158		2525	2850	"	7.57	"	"	"		III-4	2
"	"	.102	.072	"			"		"		"	"		"		140		1860	2150	"	5.88	"	"	"		III-4	3
"	"	.072	.072	"			"		"		3'	"		"		120		1975	2235	"	7.41	"	"	"		III-4	1
"	"	.102	.102	"			"		"		"	"		"		163		2660	3050	"	6.70	"	"	"		III-4	2
"	"	.102	.072	"			"		"		"	"		"		160		2080	2400	"	6.40	"	"	"		III-4	3
"	"	.072	.072				"		"		0	"	.005			120		1725	2040	"	5.46	"	"	"		III-4	1
"	"	.102	.102				"		"		0	"	"			150		2310	2750	"	5.26	"	"	"		III-4	2
"	"	.102	.072				"		"		0	"	"			141		1960	2250	"	6.58	"	"	"		III-4	3
"	"	.072	.072				"		"		35	"	"			120		2025	2300	"	7.40	"	"	"		III-4	1
"	"	.102	.102				"		"		"	"	"			153		2690	3150	"	5.80	"	"	"		III-4	2
																136		2100	2425	"	6.37	"	"	"		...	3

FASTENER "SPRING CONSTANTS" - REDUCTION OF EXPERIMENTAL LOAD-DEFLECTION CURVES

PLATE DATA							FASTENER DATA						MEASURED INTERFERENCE			LOAD-DEFLECTION PARAMETERS						TEST INFORMATION		IDENTIFICATION			
Material	E	t_1	t_2	t_3	c	[illegible]	Material	E	Dia (D)	Head Type	Torque	No Fast	(-ve) slop	(o) zero	(+ve) pos.	K_e	δ_0	P_1	P_3	A	F	Gage Length	Type Rec.	Ref.	Date	Code	Test
	$\times 10^6$ psi	in.	in.	in.	in.	in.		$\times 10^6$ psi	in.		in-lb		in.	in.	in.	lb/in	in.	lb.	lb.	in.		in.					
1	2	3	4	5	6	7	8	9	10	11	12	13	14	15	16	17	18	19	20	21	22	23	24	25	26	27	28
Aluminum	10.5	.124	.256	.124	.625	.9375	Titanium	15	.25	CSK		1				292500	.0018	6180	7140	.0102	8.22	4.0	Auto	*			[illegible]
"	"	.124	.257	.124	"	.9400	"	"		"		"				440000	.0011	6300	7380	.0107	6.49	2.0	"	*			[illegible]
Aluminum	10.5	.124	.256	.124	.625	.9400	Titanium	15		CSK		1				450000	.0013	6810	7710	.0107	8.5[illegible]	2.0	Auto	*			[illegible]
"	"	.124	.256	.124	"	.9400	"	"		"		"				480000	.0017	6400	7500	.0103	7.17	2.0	"	*			[illegible]
	.														Average	415625	.0015	6423	7433	.0105	7.56	2.5					
Aluminum	10.5	.124	.255	.124	.625	.9400	Titanium	15		CSK		1				744000	0.0	6040	7260	.0120	4.75	2.0	Auto	*			[illegible]
"	"	.124	.256	.124	"	.9400	"	"				"				839000	0.0	5965	7175	.0120	4.74	2.0	"	*			[illegible]
"	"	.124	.255	.124	"	.9400	"	"				"				795000	0.0	5725	7020	.0120	4.29	2.0	"	*			[illegible]
															Average	803000	0.0	5910	7152	.0120	4.59	2.0					
Aluminum	10.5	.125	.257	.125	.625	.9400	Titanium	15		CSK		1				480000	0.0	6585	7775	.0123	8.17	2.0	Auto	*			[illegible]
"	"	.125	.257	.125	"	.9400	"	"		"		"				403000	-.0006	7200	8010	.0126	7.50	2.0	"	*			[illegible]
"	"	.125	.258	.125	"	.9400	"	"		"		"				504000	.0012	6600	7605	.0110	7.13	2.0	"	*			[illegible]
															Average	461334	.00013	6928	7797	.0119	7.63	2.0					
Aluminum	10.5	.124	.255	.124	.625		Titanium	15		CSK		1				505667	.0013	6720	7300	.0107	7.12	2.0	Auto	*			[illegible]
"	"	.124	.255	.124	"	.9400	"	"		"		"				345880	.0020	6690	7530	.0100	10.17	4.0	"	*			[illegible]
"	"	.124	.255	.124	"	.9400	"	"		"		"				360000	.0004	6815	7680	.0116	7.74	6.0	"	*			[illegible]
"	"	.124	.255	.124	"	.9400	"	"		"		"				384000	.0005	6240	7305	.0115	5.95	4.0	"	*			[illegible]
"	"	.124	.255	.124	"	.9400	"	"		"		"				317645	.0005	6540	7440	.0015	7.27	4.0	"	*			[illegible]
															Average	382838	.00094	6601	7551	.0111	7.65	4.5					

* Present Study

FASTENER "SPRING CONSTANTS" - REDUCTION OF EXPERIMENTAL LOAD-DEFLECTION CURVES

Sample

[illegible]

PLATE DATA							FASTENER DATA						MEASURED INTERFERENCE			LOAD-DEFLECTION PARAMETERS						TEST INFORMATION		IDENTIFICATION			
Material	E	t_1	t_2		e	w/?	Material	E	Dia (D)	Head Type	Torque	No. Test	(-ve) slop	(+) zero	(+ve) pos.	k_e	A_0	P_1	P_2	A	B	Gage Length	Type Rec.	Ref.	Date	Code	Test No.
	$\times 10^6$ psi	in.	in.	in.	in.	in.		$\times 10^6$ psi	in.		in-lb		in.	in.	in.	lb/in	in.	lb.	lb.	in.		in.					
1	2	3	4	5	6	7	8	9	10	11	12	13	14	15	16	17	18	19	20	21	22	23	24	25	26	27	28
Ti-6Al-4V	15	0.127	0.129	None	.375	9/16	Titanium	15	.188	CSK	0	1		0		135,000	-.0010	2668	2880	.0130	11.207	4	Auto	31	6/1/68	[illegible]	
"		0.126	0.126	"	"	"	"		"	"	"	"		"		115,385	-.0020	2742	2892	.0140	8.084	11	"		"	[illegible]	
"		0.126	0.127	"	"	"	"		"	"	"	"		"		175,385	-.0008	2485	2710	.0126	9.355	11	"		"	[illegible]	
															Average	141,923	-.0012	2638	2827	.0132	9.549	4					
"	15	0.187	0.186	None	.375	9/16	Titanium	15	.188	CSK	0	1		0		214,285	-.0005	2520	2815	.0125	7.416	4	Auto		6/7/68	[illegible]	
"		0.189	0.187	"	"	"	"		"	"	"	"		"		190,000	-.0006	2585	2820	.0126	9.308	11	"		"	[illegible]	
		0.189	0.189	"	"	"	"		"	"	"	"		"		226,667	-.0008	2592	2815	.0123	10.297	11	"		"	[illegible]	
															Average	210,317	-.0006	2566	2817	.0125	[illegible]	4					
"	15	0.187	0.188	None	.750	1-1/8	Titanium	15	.375	CSK	0	1		0		338,182	-.0027	9670	10675	.0147	4.1116	4	Auto		6/7/68	[illegible]	
		0.185	0.186	"	"	"	"		"	"	"	"		"		316,364	.0006	9804	10680	.0125	5.598	11	"		"	[illegible]	
		0.187	0.185	"	"	"	"		"	"	"	"		"		316,364	-.0023	9800	10800	.0143	7.727	11	"		"	[illegible]	
															Average	323,637	-.0018	9725	10652	.0138	7.910	4					
	15	0.128	0.128	None	.750	1-1/8	Titanium	15	.375	CSK	0	1		0		372,000	-.0004	5785	7020	.0124	4.296	4	Auto		6/18/68	[illegible]	
		0.129	0.128	"	"	"	"		"	"	"	"		"		420,000	-.0008	6444	7440	.0128	5.507	11	"		"	[illegible]	
		0.127	0.128	"	"	"	"		"	"	"	"		"		349,090	0.0	6552	7620	.0120	5.797	11	"		"	[illegible]	
															Average	380,364	-.0004	6260	7360	.0124	5.200	4					
	15	.093	.092	None	.750	1-1/8	Titanium	15	.375	CSK	0	1		0		126,667	-.0084	5134	5808	.0205	3.675	4	Auto		6/19/68	[illegible]	
		.093	.094	"	"	"	"		"	"	"	"		"		128,000	-.0017	4590	5268	.0137	5.199	11	"		"	[illegible]	
		.094	.095	"	"	"	"		"	"	"	"		"		145,714	-.0013	4164	4060	.0133	4.834	11	"		"	[illegible]	
															Average	133,460	-.0038	4646	5712	.0158	4.701	4					
	15	.123	.122	None	.750	1-1/8	Titanium	15	.375	CSK	0	1		0		217,500	-.0004	5940	6995	.0124	5.084	4	Auto		6/18/68	[illegible]	
		.123	.121	"	"	"	"		"	"	"	"		"		189,474	-.0018	6480	7715	.0136	6.587	11	"		"	[illegible]	
		.121	.122	"	"	"	"		"	"	"	"		"		213,333	-.0004	6360	7295	.0124	6.060	11	"		"	[illegible]	
															Average	206,769	-.0009	6260	7368	.0129	5.910	4					
Ti-6Al-4V	15	.069	.069	None	.312	15/32	Titanium	15	.156	CSK	0	1		0		107,143	0.0	1620	1790	.0120	8.775	4	Auto		6/20/68	[illegible]	
"	"	.066	.066	"	"	"	"	"	"	"	"	"		"		86,667	-.0013	1713	1775	.0133	21.016	11	"		"	[illegible]	
"	"	.065	.064	"	"	"	"	"	"	"	"	"		"		76,667	-.003	1800	1880	.0150	4.455	"	"		"	[illegible]	
															Average	90,159	-.0014	1711	1815	.0134	4.748						
Ti-6Al-4V	15	.065	.065	None	.375	9/16	Titanium	15	.188	PRUD	0	1		0		126,667	-.0823	2710	2895	.0153	9.216	4	Auto		6/4/68	[illegible]	
"	"	.065	.064	"	"	"	"	"	"	"	"	"		"		140,000	-.0736	2795	2890	.0156	15.090	"	"	31	"	[illegible]	

FASTENER "SPRING CONSTANTS" - REDUCTION OF EXPERIMENTAL LOAD-DEFLECTION CURVES

PLATE DATA							FASTENER DATA						MEASURED INTERFERENCE			LOAD-DEFLECTION PARAMETERS						TEST INFORMATION		IDENTIFICATION			
Material	F^{tu}	t_1	t_2	t_3	e	$\frac{w}{t}$	Material	E	Dia (D)	Head Type	Torque	No. Parts	(-ve) "slop"	0 zero	(+ve) pos.	k_e	δ_0	P_1	P_2	A	B	Shear Length	Type Insp.	Ref	Date	Code	Test No.
	$\times 10^3$ psi	in.	in.	in.	in.	in.		$\times 10^7$ psi	in.		in-lb		in.	in.	in.	lb/in	in.	lb.	lb.	in.		in.					
1	2	3	4	5	6	7	8	9	10	11	12	13	14	15	16	17	18	19	20	21	22	23	24	25	26	27	28
Ti-6Al-4V	15	0.155	0.153	None	.312	15/32	Titanium	15	.156	CSK	0	1		0		126,667	-.0008	1818	1920	.0128	14.501	4	Auto	31	6/19/69		BT-1
															Appr.	126,079	.0005	1749	1879	.0124	11.00?						
Ti-6Al-4V	15	.040	.040	None	.312	15/32	Titanium	25	.156	PROT	0	1		0		93,333	-.0004	1572	1752	.0124	7.433	4	Auto		6/20/68	[illegible]	BT-1
"	"	.041	.041	"	"	"	"	"	"	"	"	"		"		85,000	0.0	1670	1810	.0120	10.875	"	"		"		BT-2
"	"	.041	.041	"	"	"	"	"	"	"	"	"		"		96,000	-.0007	1625	1795	.0127	8.051	"	"		"		BT-3
															Appr.	91,444	-.0008	1622	1788	.0124	8.786						
Ti-6Al-4V	15	.078	.076	None	.312	15/32	Titanium		.156	PROT	0	1		0		116,230	.0008	1776	1932	.0118	10.683	4	Auto		6/20/68	[illegible]	BT-1
"	"	.077	.077	"	"	"	"		"	"	"	"		"		140,000	.0009	1735	1900	.0111	10.962	"	"		"		BT-2
"	"	.077	.078	"	"	"	"		"	"	"	"		"		137,143	0.0	1773	1908	.0120	11.930	"	"		"		BT-3
															Appr.	131,131	.0005	1761	1913	.0116	11.199						
Ti-6Al-4V	15	.401	.400	None	.750	1 1/8	Titanium	15	.500	CSK	0	1		0		1,050,000	-.0003	7730	20580	.0123	5.647	4	Auto		3/3/68	[illegible]	BT-1
"	"	.398	.399	"	"	"	"	"	"	"	"	"		"		1,237,500	-.0004	8740	19200	.0124	6.062	"	"		"		BT-2
"	"	.393	.401	"	"	"	"	"	"	"	"	"		"		1,237,500	-.0011	7670	19880	.0131	6.221	"	"		"		BT-3
															Appr.	1,175,000	-.0008	7380	19880	.0126	5.977						
Ti-6Al-4V	15	.408	.407	None	.500	3/4	Titanium	15	.375	CSK	0	1		0		445,714	-.0030	3040	11736	.0150	10.232	4	Auto		8/6/68	[illegible]	BT-1
"		.407	.408	"	"	"	"	"	"	"	"	"		"		405,000	-.0037	11005	11495	.0157	13.552	"	"	31	"		BT-4

FASTENER "SPRING CONSTANTS" - REDUCTION OF EXPERIMENTAL LOAD-DEFLECTION CURVE.

PLATE DATA							FASTENER DATA						MEASURED INTERFERENCE			LOAD-DEFLECTION PARAMETERS						TEST INFORMATION		IDENTIFICATION			
Material	E	t_1	t_2	t_3	e	$\frac{h}{t}$	Material	E	Dia (D)	Head Type	Torque	No. Past	(-ve) "slop"	(0) zero	(+ve) pos.	k_e	δ_0	P_1	P_2	A	B	Gage L'gth	Type Rec.	Ref.	Date	Code	Test No.
	$\times 10^{-6}$ psi	in.	in.	in.	in.	in.		$\times 10^{-6}$ psi	in.		in-lb		in.	in.	in.	lb/in	in.	lb.	lb.	in.		in.					
1	2	3	4	5	6	7	8	9	10	11	12	13	14	15	16	17	18	19	20	21	22	23	24	25	26	27	28
Ti-6Al-4V	15	.08"	.08"	HOKE	.375	9/6	Titanium	15	"	"	0	"		"		170000		2010	2310	.005	6.59	4"	AUTO	31	5/6/68		
		"	"	"	"	"			"	"	"	"		"		138000		2340	2580	"	9.38	"	"		"		
		.188"	.188"	"	.500	3/4			.250"	"	"	"		"		210000		3480	3600	"	27.03	"	"		5/23/68		
		"	"	"	"	"			"	"	"	"		"		288000		3540	3960	"	8.17	"	"		5/24/68		
		.156"	.156"	"	.500	3/4			"	"	"	"		"		192000		3480	3560	"	7.09	"	"		5/25/68		
		"	"	"	"	"			"	"	"	"		"		330000		4080	4440	"	9.22	"	"		"		
		"	"	"	.500	3/4				"	"	"		"		180000		2760	3060	"	8.88	"	"		5/22/68		
		"	"	"	"	"				"	"	"		"		234000		2730	2960	"	11.33	"	"		"		
		.188	.188	"	.375	9/16			.188	"	"	"		"		174000		2580	26.80		8.33	"	"		5/31/68		
		"	"	"	"	"			"	"	"	"		"		150000		2820	3060	"	11.22	"	"		"		
		"	"	"	"	"			"	"	"	"		"		168000		2670	2880	"	12.10	"	"		"		
		.125"	.125"	"	.375	9/16			"	"	"	"		"		180000		2640	2880	"	10.53	"	"		5/29/68		
		"	"	"	"	"			"	"	"	"		"		132000		2580	2760	"	13.59	"	"		5/28/68		
		"	"	"	"	"			"	"	"	"		"		144000		2700	2880	"	[illegible]	"	"		"		
		.09"	.09"	"	.37"	9/16			"	"	"	"		"		105000		2085	2340	"	7.94	"	"		5/27/68		
		"	"	"	"	"			"	"	"	"		"		195000		2205	2400	"	10.83	"	"		"		
		"	"	"	"	"			"	"	"	"		"		108000		2005	2250	"	7.35	"	"		"		
		.063	.063	"	.375	9/16			"	"	"					105000		1530	1800	"	5.68	"	"		5/31/68		
		"	"	"	"	"			"	"	"	"		"		111000		1470	1680	"	6.86	"	"		"		
		"	"	"	"	"			"	"	"	"		"		102000		1620	1980	"	5.39	"	"		"		
		.125	.125	HOKE	.500	3/4		15	.250"	DRK	0	1		0		114000		3060	3290	.005	8.64	4"	AUTO		8/29/68		
		"	"	"	"	"			"	"	"	"		"		126000		2760	3080	"	8.11	"	"		"		
		"	"	"	.250	"		15	.175"	"	"	"		"		117000		1120	1200		11.28	"	"		6/5/68		
		"	"	"	"	"			"	"	"	"		"		144000		1050	1170	"	8.47	"	"		"		
		"	"	"	"	"			"	"	"	"		"		111000		1070	1200	"	7.58	"	"		6/3/68		
		.08	.08	"	.250	3/8			"	"	"	"		"		98000		1140	1200	"	9.86	"	"		6/3/68		
		"	"	"	"	3/8			"	"	"	"		"		69000		1110	1185	"	6.01	"	"		"		
		"	"	"	"	"			"	"	"	"		"		126000		1050	1170	"	8.47	"	"				
		.061"	.063	"	.250"	3/8			"	"	"	"		"		84000		1070	1140	"	6.46	"	"		6/4/68		
Ti-6Al-4V	15	"	"	"	"	"	Titanium	15	"	"	"	"		"		69000		1110	1130	"	3317	"	"	31	"		

FASTENER "SPRING CONSTANTS" - REDUCTION OF EXPERIMENTAL LOAD-DEFLECTION CURVES

PLATE DATA							FASTENER DATA						MEASURED INTERFERENCE			LOAD-DEFLECTION PARAMETERS						TEST INFORMATION		IDENTIFICATION			
Material	E	t_1	t_2	t_3	c	$\frac{w}{2}$	Material	E	Dia (1A)	Head Type	Torque	No. Fast	(-ve) "slop"	(0) zero	(+ve) pos.	k_e	δ_0	P_1	P_2	A	B	Gage Length	Type Rec.	Ref.	Date	Code	Test No.
	x10⁶ psi	in.	in.	in.	in.	in.		x10⁶ psi	in.		in-lb		in.	in.	in.	lb/in	in.	lb.	lb.	in.		in.					
1	2	3	4	5	6	7	8	9	10	11	12	13	14	15	16	17	18	19	20	21	22	23	24	25	26	27	28
Ti-6Al-4V	15	.063	.063	KORE	.250	3/8	Titanium	15	.171	CSK		1		C		105000		1060	1140	1	12.59	4	AUTO	31	5/3/68		
		"	"	"	"	"			"	"		"		"		87000		1120	1200	"	13.28	"	"		"		
		.04	.04	"	.250	3/8			"	"		"		"		74400		1008	10098	"		"	"		"		
		"	"	"	"	"			"	"		"		"		85200		1032	1120	"	11.20	"	"		"		
		"	"	"	"	"			"	"		"		"		79000		1080	1150	"	14.59	"	"		"		
		.02	.02	"	.250	3/8			"	"		"		"		50400		900	960	"	14.20	"	"		5/21/68		
		"	"	"	"	"			"	"		"		"		51600		864	954	"	9.25	"	"		"		
		"	"	"					"	"		"		"		45600		894	978	"	10.20	"	"		5/22/68		
		.156	.156	"	.312	15/32			.156	FHCT		"		"		126000		1680	1800	"	13.28	"	"		5/9/68		
		"	"	"	"	"			"	"		"		"		141070		1800	1890	"	18.78	"	"		"		
		"	"	"	"	"			"	"		"		"		150000		1640	1800	"	9.84	"	"		"		
		.08	.08	"	.312	15/32			"	"		"		"		123000		1670	1800	"	12.22	"	"		"		
		"	"	"	"	"			"	"		"		"		144000		1640	1755	"	13.52	"	"		5/20/68		
		"	"	"	"	"			"	"		"		"		144020		1650	1670	"	16.05	"	"		"		
		.04	.04	"	.312	15/32			"	"		"		"		93000		1350	1500	"	8.70	"	"		"		
		"	"	"	"	"			"	"		"		"		75000		1575	1695	"	12.48	"	"		"		
		"	"	"	"	"			"	"		"		"		84000		1420	1620	"	0.95	"	"		"		
		.188	.188	"	.375	9/16			.188	"		"		"		88000		1245	1340	"	12.46	"	"		6/5/68		
		"	"	"	"	"			"	"		"		"		87000		1230	1330	"	11.72	"	"		"		
		"	"	"	"	"			"	"		"		"		97500		1215	1320	"	11.05	"	"		"		
		.09	.09	"	.375	9/16			"	"		"		"		135000		2490	2670	"	13.13	"	"		6/27/68		
		"	"	"	"	"			"	"		"		"		152000		2550	2735	"	12.43	"	"		"		
		.063	.063	"	.375	9/16			"	"		"		"		130500		2360	2550	"	11.83	"	"		6/6/68		
		"	"	"	"	"			"	"		"		"		141000		2385	2610	"	10.16	"	"		"		
		"	"	"	"	"			"	"		"		"		138000		2205	2540	"	6.98	"	"		"		
		.04	.04	"	.375	9/16			"	"		"		"		96000		1890	2100	"	8.70	"	"		5/21/68		
		"	"	"	"	"			"	"		"		"		108000		1890	2100	"	8.70	"	"		"		
Ti-6Al-4V	15	"	"	"	"	"	Titanium	15	"	"		"		"		171000		1910	2130	"	6.70	"	"	31	"		

FASTENER "SPRING CONSTANTS" - REDUCTION OF EXPERIMENTAL LOAD-DEFLECTION CURVES

PLATE DATA							FASTENER DATA						MEASURED INTERFERENCE			LOAD-DEFLECTION PARAMETERS						TEST INFORMATION		IDENTIFICATION			
Material	E	t_1	t_2	t_3	e	$\frac{w}{2}$	Material	E	Dia (D)	Head Type	Torque	No. Fast.	(-ve) "slop"	(0) zero	(+ve) pen.	k_e	δ_0	P_1	P_j	A	B	Gage L'gth	Type Rec.	Ref.	Date	Code	Test No.
	$\times 10^6$ psi	in.	in.	in.	in.	in.		$\times 10^6$ psi	in.		in-lb		in.	in.	in.	lb/in	in.	lb.	lb.	in.		in.					
1	2	3	4	5	6	7	8	9	10	11	12	13	14	15	16	17	18	19	20	21	22	23	24	25	26	27	28
Ti-6Al-4V	15	.063"	.063"	NONE	.250	3/8	Titanium	15	.175	CSK	0	1		0		87000		1020	1130	.005	8.84	4"	AUTO	31	6/A/68		
"	"	.08	.08	"	.250	3/8	"	"	"	"	"	"		"		45000		840	970	"	6.37	"	"	"	"		
"	"	"	"	"	"	"	"	"	"	"	"	"		"		45000		915	1005	"	9.77	"	"	"	"		
"	"	"	"	"	"	"	"	"	"	"	"	"		"		54000		775	900	"	6.23	"	"	"	5/21/68		
"	"	.156	.156	"	.312	15/32	"	"	.156	"	"	"		"		123000		1530	1650	"	12.18	"	"	"	"		
"	"	"	"	"	"	"	"	"	"	"	"	"		"		123000		1200	1270	"	3.12	"	"	"	"		
"	"	"	"	"	"	"	"	"	"	"	"	"		"		138000		1650	1770	"	13.05	"	"	"	6/A/68		
"	"	.10	.10	"	.312	15/32	"	"	"	"	"	"		"		84000		1700	1815	"	14.00	"	"	"	"		
"	"	"	"	"	"	"	"	"	"	"	"	"		"		120000		1650	1770	"	13.05	"	"	"	6/20/68		
"	"	"	"	"	"	"	"	"	"	"	"	"		"		93000		1700	1800		16.05	"	"	"	"		
"	"	.063	.063	"	.312	15/32	"	"	"	"	"	"		"		211000		1350	1605		5.30	"	"	"	"		
"	"	"	"	"	"	"	"	"	"	"	"	"		"		85500		1590	1690		15.02	"	"	"	"		
"	"	"	"	"	"	"	"	"	"	"	"	"		"		81000		1615	1720		14.55	"	"	"	"		
"	"	.188	.188	"	.375	9/16	"	"	"	"	"	"		"		168000		2400	2630		10.01	"	"	"	6/A/68		
"	"	"	"	"	"	"	"	"	"	"	"	"		"		168000		2400	2670		8.59	"	"	"	"		
"	"	"	"	"	"	"	"	"	"	"	"	"		"		210000		2400	2640		9.61	"	"	"	6/17/68		
"	"	.125	.125	"	.375	"	"	"	"	"	"	"		"		154000		2400	2690		9.61	"	"	"	"		
"	"	"	"	"	"	"	"	"	"	"	"	"		"		147000		2400	2640		9.61	"	"	"	"		
"	"	"	"	"	"	"	"	"	"	"	"	"		"		168000		2310	2500		13.59	"	"	"	"		
"	"	.09	.09	"	.375	9/16	"	"	"	"	"	"		"		102000		2000	2250		8.12	"	"	"	"		
"	"	.375	.375	"	.750	1 1/8	"	"	.375	"	"	"		"		590000		11700	12450		14.75	"	"	"	"		
"	"	"	"	"	"	"	"	"	"	"	"	"		"		720000		11900	12000		10.95	"	"	"	6/27/68		
"	"	"	"	"	"	"	"	"	"	"	"	"		"		750000		10500	12000		6.86	"	"	"	7/3/68		
"	"	.250	.250	"	.750	1 1/8	"	"	"							650000		10650	11700		9.74	"	"	"	"		
"	"	"	"	"	"	"	"	"	"	"	"	"		"		635000		10500	11400		11.14	"	"	"	"		
"	"	"	"	"	"	"	"	"	"	"	"	"		"		680000		10650	11600		10.72	"	"	"	6/A/68		
"	"	.188	.188	"	.750	1 1/8	"	"	"	"	"	"		"		388000		7180	8150		7.23	"	"	"	"		
"	"	"	"	"	"	"	"	"	"	"	"	"		"		466000		6180	7500		4.72	"	"	"	"		
"	"	"	"	"	"	"	"	"	"	"	"	"		"		588000		8160	9100		8.40	"	"	"	6/A/68		
Ti-6Al-4V	15	.125	.125	"			Titanium	15	"	"	"	"		"		388000		5980	6180		8.13	"	"	31	"		

FASTENER "SPRING CONSTANTS" - REDUCTION OF EXPERIMENTAL LOAD-DEFLECTION CURVES

MATL. DATA							FASTENER DATA						MEASURED INTERFERENCE			LOAD-DEFLECTION PARAMETERS						TEST INFORMATION		IDENTIFICATION			
Material	E	t_1	t_2	t_3	e	$\frac{w}{2}$	Material	E	Dia (D)	Head Type	Torque	No. Fast.	(-ve) slop*	(0) zero	(+ve) pos.	k_e	δ_0	P_1	P_j	A	B	Gage Length	Type Rec.	Ref.	Date	Code	Test No.
	$\times 10^6$ psi	in.	in.	in.	in.	in.		$\times 10^6$ psi	in.		in-lb		in.	in.	in.	lb/in	in.	lb.	lb.	in.		in.					
1	2	3	4	5	6	7	8	9	10	11	12	13	14	15	16	17	18	19	20	21	22	23	24	25	26	27	28
Ti-6Al-4V	15	.125	.125	same			Titanium	15	.375	CSK		1		0		360000		5850	6660	.005	7.16	4	AUTO	31	6/8/68		2
		"	"	"					"	"		"		"		300000		5860	6660	"	7.16	"	"		"		3
		.5	.5	"	100	1 1/2			.5	"		"		"		810000		19500	20500	"	38.32	"	"		7/8/68		
		"	"	"	"	"			"	"		"		"		810000		19500	21000	"	42.36	"	"		"		2
		"	"	"	"	"			"	"		"		"		760000		20400	21600	"	36.03	"	"		"		3
		.375	.375	"	100	1 1/2			"	"		"		"		780000		17400	19800	"	7.09	"	"		8/23/68		
		"	"	"	"				"	"		"		"		840000		15900	17700	"	6.54	"	"		8/26/68		
		"	"	"	"	"			"	"		"		"		870000		16500	18200	"	9.34	"	"		"		
		.09	.09	"	.375	9/16		15	.188	"		"		"		108000		2040	2325	"	7.01	"	"		8/27/68		
		.063	.063	"	.375	9/16		"	"	"		"		"		84000		1680	1875	"	8.34	"	"		8/23/68		
		"	"	"	"	"		"	"	"		"		"		79200		1740	1950	"	8.04	"	"		"		
		"	"	"	"	"			"	"		"		"		84000		1650	1910	"	6.26	"	"		"		
		.125	.125	"	.250	3/8		"	.172	"		"		"		55500		829	880	"	38.20	"	"		8/27/68		
		"	"	"	"	"			"	"		"		"		66000		840	900	"	33.28	"	"		"		
		.063	.063	"	.250	3/8			"	"		"		"		52800		786	900	"	6.77	"	"		"		
		"	"	"	"	"			"	"		"		"		45600		822	888	"	31.86	"	"		"		
		.04	.04	"	.250	3/8			"	"		"		"		32400		600	732	"	4.61	"	"		"		
		"	"	"	"	"			"	"		"		"		31200		696	768	"	30.11	"	"		8/28/68		
		.156	.156	"	.312	25/32			.156	"		"		"						"		"	"		8/29/68		
		"	"	"	"	"			"	"		"		"		84000		1275	1340	"	2.95	"	"		"		
		.063	.063	"	.438	25/32			"	"		"		"		111000		1270	1350	"	25.00	"	"		"		
		"	"	"	"	"			"	"		"		"		60000		1230	1320	"	12.9	"	"		"		
		.188	.188	"	.375	9/16			.188	"		"		"		165000		2100	2190		21.89	"	"		8/29/68		
		"	"	"	"	"			"	"		"		"		108000		1800	1950		11.45	"	"		"		
		.063	.063	"	.375	9/16			"	"		"		"		117000		1200	1600		3.29	"	"		8/30/68		
		"	"	"	"	"			"	"		"		"		87000		1500	1790		5.18	"	"		"		
		.125	.125	"	.250	3/8			.125	shoT		"		"		97500		1095	1185		21.58	"	"		9/4/68		
		"	"	"	"	"			"	"		"		"		108000		1090	1200		9.53	"	"		"		
		"	"	"	"	"			"	"		"		"		110000		1080	1200		8.70	"	"		9/6/68		
Ti-6Al-4V	15	.063	.063	"	.250	3/8	Titanium	15								90000		1110	1117		17.41	"	"	31	8/3/68		

FASTENER "SPRING CONSTANTS" - REDUCTION OF EXPERIMENTAL LOAD-DEFLECTION CURVES

PLATE DATA							FASTENER DATA						MEASURED INTERFERENCE			LOAD-DEFLECTION PARAMETERS						TEST INFORMATION		IDENTIFICATION			
Material	E	t_1	t_2	t_3	e	w/2	Material	E	Dia (D)	Head Type	Torque	No. Fast	(-ve) -Lap	(o) zero	(+ve) pos.	k_e	δ_o	P_1	P_2	A	B	Gage L'gth	Type Rec.	Ref.	Ins'n	Code	Test No.
	x10⁶ psi	in.	in.	in.	in.	in.		x10⁶ psi	in.		in-lb		in.	in.	in.	lb/in	in.	lb.	lb.	in.		in.					
1	2	3	4	5	6	7	8	9	10	11	12	13	14	15	16	17	18	19	20	21	22	23	24	25	26	27	28
TSS-T6		0.188	0.188	NONE	3/4	1 1/8	HS-47-12		.373	CSK		1		0		175,000		5500	6350	.005	7.29	4	READ	30			
"		"	"	"	"	"	"		"	"		"		"		185,700		5380	5780	"	02.78	"	"	"			
"		0.102	0.102	"	2	1	HS-48-6		.188	PROD		"		"		118,200		2200	2780	"	3.32	"	"	"			
"		"	"	"	"	"	"		"	"		"		"		120,000		1600	2040	"	3.78	"	"	"			
"		"	"	"	"	"	"		"	"		"		"		110,000		1600	2180	"	3.09	"	"	"			
"		0.188	0.188	"	"	"	HS-48-10		.313	"		"		"		208,000		4250	5100	"	5.03						
"		"	"	"	"	"	"		"	"		"	"	"		200,000		4670	5650	"	4.81	"	"	"			
"		"	"	"	"	"	"		"	"		"	"	"		200,000		4800	5740	"	5.12	"	"	"			
"		"	"	"	"	"	HS-48-12		.375	"		"	"	"		215,300		6500	7200	"	8.55	"	"	"			
"		"	"	"	"	"	"		"	"		"	"	"		210,000		5770	7400	"	10.30	"	"	"			
TSS-T6		"	"	"	"	"	"		"	"		"	"	"		250,000		6000	6900	"	6.56	"	"	"			
R301-T6		.040	.040	NONE	3/8	9/16	HS-48-6		.375	PROD		1		0		37,000		750	830	.005	9.04	4	READ	30			
"		"	"	"	"	"	"		"	"		"		"		53,000		700	780	"	8.47	"	"	"			
"		"	"	"	"	"	"		"	"		"		"		44,450		730	845	"	6.26	"	"	"			
"		.051	.051	"	"	"	"		"	"		"		"		55,000		940	1060	"	7.63	"	"	"			
"		"	"	"	"	"	"		"	"		"		"		49,000		1100	1200	"	10.53	"	"	"			
"		"	"	"	"	"	"		"	"		"		"		54,000		1100	1120	"	8.09	"	"	"			
"		.063	.063	"	"	"	"		"	"		"		"		62,000		1280	1390	"	11.11	"	"	"			
"		"	"	"	"	"	"		"	"		"		"		48,000		1180	1300	"	9.46	"	"	"			
R301-T6		"	"	"	"	"	"		"	"		"		"		60,000		1270	1380	"	11.03	"	"	"			
TSS-T6		.102	.102	NONE	2	1	HS-48-6		.188	PROD		1		0		80,000		2120	2340	.005	9.28	4	READ	30			
"		"	"	"	"	"	"		"	"		"		"		90,000		1960	2190	"	8.26	"	"	"			
"		"	"	"	"	"	"		"	"		"		"		88,000		1840	2100	"	6.93	"	"	"			
"		.188	.188	"	"	"	HS-48-10		.313	"		"		"		198,000		4920	5550	"	7.60	"	"	"			
"		"	"	"	"	"	"		"	"		"		"		200,000		4540	5300	"	5.92	"	"	"			
"		"	"	"	"	"	"		"	"		"		"		190,000		4800	5600	"	5.95	"	"	"			
TSS-T6		.125	.125	NONE	2	1	HS-48-8		.25	PROD		1		0		152,000		3120	3560	.005	6.95	4	READ	30			

FASTENER "SPRING CONSTANTS" - REDUCTION OF EXPERIMENTAL LOAD-DEFLECTION CURVES

PLATE DATA							FASTENER DATA						MEASURED INTERFERENCE			LOAD-DEFLECTION PARAMETERS						TEST INFORMATION		IDENTIFICATION			
Material	E	t_1	t_2	t_3	e	$\frac{t}{D}$	Material	E	Dia (D)	Head Type	Torque	No. Fast	(-ve) "slop"	(0) zero	(+ve) pos.	k_e	δ_0	P_1	P_2	A	B	Gage Length	Type Rec.	Ref.	Date	Code	Test No.
	$\times 10^6$ psi	in.	in.	in.	in.	in.		$\times 10^6$ psi	in.		in-lb		in.	in.	in.	lb/in	in.	lb.	lb.	in.		in					
1	2	3	4	5	6	7	8	9	10	11	12	13	14	15	16	17	18	19	20	21	22	23	24	25	26	27	28
TS8-5		0.102	0.102	RIVET	2	1	BS-48-6		.188	TROP		1		0		118200		2200	2780	.005	3.98	4	HEAD	30			3
"		"	"	"	"	"	"		"			"		"		120000		1600	2040	"	3.78	"	"	"			2
"		"	"	"	"	"	"		"			"		"		110000		1620	2180	"	3.09	"	"	"			
"		0.188	0.186	"	"	"	BS-48-10		.330			"	+.0005 -.002			208000		4250	5100	"	5.05	"	"	"			
"		"	"	"	"	"	"		"			"	"			200000		4670	5650	"	4.81	"	"	"			
"		"	"	"	"	"	"		"			"	"			200000		4800	5700	"	5.12	"	"	"			
"		"	"	"	"	"	BS-48-12		.375			"	"			215300		6500	7200	"	8.56	"	"	"			
"		"	"	"	"	"	"		"			"	"			210000		6770	7400	"	10.30	"	"	"			
TS8-R6		"	"	"	"	"	"		"			"	"			250000		6400	6900		6.56	"	"	"			
R301-R6		.060	.060	"	3/8	3/16	BS-A86					"		0		47000		750	830	"	9.08	"	"	"			
"		"	"	"	"	"	"					"		"		53000		700	780		8.46	"	"	"			
"		"	"	"	"	"	"		"			"		"		44450		730	845	"	6.26						
"		.0513	.0513	"	"	"	"					"		"		55000		940	1060	"	7.63	"	"	"			A
"		"	"	"	"	"	"					"		"		49000		1100	1200	"	10.53	"	"	"			B
"		.063	.063	"	"	"	"					"		"		54000		1000	1320	"	8.79	"	"	"			C
"		"	"	"	"	"	"					"		"		62000		1280	1390	"	11.11	"	"	"			
"		"	"	"	"	"	"					"		"		48000		1188	1370		9.46	"	"				
R301-R6		"	"	"	"	"	"					"		"		60000		1270	1380	"	11.03	"	"	"			
TS8-R6		.102	.102	"	2	1	"		.188			"			-.003 to -.005	80000		2120	2340	"	9.28	"	"	"			
"		"	"	"	"	"	"		"			"			"	90000		1960	2190	"	8.28	"	"	"			
"		"	"	"	"	"	"		"			"			"	88000		1840	2100	"	6.93	"	"	"			
"		.188	.188	"	"	"	BS-48-10		.320			"			"	196000		4500	5550	"	7.60	"	"	"			
"		"	"	"	"	"	"		"			"			"	200000		4540	5300	"	5.98	"	"	"			
"		"	"	"	"	"	"		"			"			"	190000		4800	5600	"	5.95	"	"	"			
"		.125	.125	"	"	"	BS-48-8		.25			"			"	152000		3120	3560	"	6.95	"	"	"			
"		"	"	"	"	"	"		"			"			"	160000		2880	3400	"	5.52	"	"	"			
TS8-16		"	"	"	"	"	"		"			"			"	156000		2960	3300	"	8.43	"	"	"			
"		10.5	.188	"	"	"	BS-48-12		.375	TROT		"			"	210000		6400	7200	"	7.78	"	"	"			
"		"	"	"	"	"	"		"	"		"			"	32000		6000	7070	"	6.98	"	"	30			

FASTENER "SPRING CONSTANTS" - REDUCTION OF EXPERIMENTAL LOAD-DEFLECTION CURVES

PLATE DATA							FASTENER DATA						MEASURED INFLEXPERENCE			LOAD-DEFLECTION PARAMETERS						TEST INFORMATION		IDENTIFICATION			
Material	E	t_1	t_2	t_3	e	w/2	Material	E	Dia (D)	Head Type	Torque	No. Fast.	(-ve) slop	(0) zero	(+ve) pos.	k_e	δ_0	P_i	P_j	A	B	Gage Length	Type Rec.	Ref.	Date	Code	Test No.
	$\times 10^6$ psi	in.	in.	in.	in.	in.		$\times 10^6$ psi	in.		in-lb		in.	in.	in.	lb/in	in.	lb.	lb.	in.		in.					
1	2	3	4	5	6	7	8	9	10	11	12	13	14	15	16	17	18	19	20	21	22	23	24	25	26	27	28
75S-T6		.188	.183	Plane	2	1	NB-48-12		.375	PROD		1			[illegible]	210000		6000	6560	.005	5.42	4	Read	30		6.1.1 3-7	
R30-T6		.031	.031	"	3/8	9/16	NB-48-6					"		0		41000		625	695	"	3.63	"	"	"		6.1.1 3-7	
"		"	"	"	"	"	"					"		"		29900		515	585	"	7.18	"	"	"			
"		"	"	"	"	"	"					"		"		30000		610	660	"	1.63	"	"	"			
"		.100	.100	"	"	"	"					"		"		89000		1600	1750	"	3.23	"	"	"		6.1.1 3-2	
"		"	"	"	"	"	"					"		"		99000		1700	1910	"	7.87	"	"	"			
"		"	"	"	"	"	"					"		"		72500		1725	1890	"	3.03	"	"	"			
"		.092	.092	"	"	"	"					"		"		90000		1550	1760	"	9.92	"	"	"		6.1.1 3-11	
"		"	"	"	"	"	"					"		"		95000		1600	1775	"	3.83	"	"	"			
"		"	"	"	"	"	"					"		"		82500		1800	2040	"	7.32	"	"	"			
"		.187	.187	"	3/4	9/8	NB-48-12		3/8			"		"		235000		4500	5300	"	3.60	"	"	"		6.1.1 3-15	
"		"	"	"	"	"	"		"			"		"		270000		4800	5500	"	3.73	"	"	"			
"		"	"	"	"	"	"		"			"		"		230000		5100	5670	"	1.68	"	"	"			
"		.125	.125	"	"	"	"		"			"		"		155000		3550	4000	"	7.68	"	"	"		6.1.1 3-19	
"		"	"	"	"	"	"		"			"		"		210000		3500	3970	"	0.99	"	"	"			
		"	"	"	"	"	"		"			"		"		195000		3600	4100	"	7.05	"	"	"			
"		.090	.090	"	"	"	"		"			"		"		190000		3000	3350	"	8.30	"	"	"		6.1.1 3-17	
"		"	"	"	"	"	"		"			"		"		140000		2800	3190	"	7.03	"	"	"			
"		"	"	"	"	"	"		"			"		"		170000		2970	3300	"	8.70	"	"	"			
"		.0692	.0695	"	"	"	"		"			"		"		155000		2200	2550	"	6.21	"	"	"		6.1.1 3-27	
"		"	"	"	"	"	"		"			"		"		135000		2100	2400	"	5.86	"	"	"			
"		"	"	"	"	"	"		"			"		"		115000		2400	2675	"	8.45	"	"	"			
75S-T6		.188	.188	"	"	"	NB-47-12		.373	CSK		"		"		210000		4200	5000	"	5.26	"	"	"		6.1.1 3-1	
"		"	"	"	"	"	"		"	"		"		"		220000		4200	5100	"	4.72	"	"	"			
"		"	"	"	"	"	"		"	"		"		"		220000		4200	5100	"	4.72	"	"	"			
"		.128	.128	"	"	"	"		.376	"		"		"		160000		3200	3600	"	7.78	"	"	"		6.1.1 3-1	
"		"	"	"	"	"	"		"	"		"		"		160000		3600	4000	"	8.70	"	"	"			
"		"	"	"	"	"	"		"	"		"		"		130000		4100	4500	"	9.81	"	"	"			
"		.375	.375	"	.750	1 1/8			.375	"		"		"		496000		9600	10440	"	10.98	"	"	"	[illegible]		
		"	"	"	"	"			"	"		"		"		384000		9600	10960	"	9.61	"	"	30	"		

Unclassified

Security Classification

DOCUMENT CONTROL DATA - R & D

(Security classification of title, body of abstract and indexing annotation must be entered when the overall report is classified)

1. ORIGINATING ACTIVITY (Corporate author) Grumman Aerospace Corporation Bethpage, New York	2a. REPORT SECURITY CLASSIFICATION Unclassified 2b. GROUP

3. REPORT TITLE

Stress and Deflection Analysis of Mechanically Fastened Joints

4. DESCRIPTIVE NOTES (Type of report and inclusive dates)

Final Report - January 1969 - January 1970

5. AUTHOR(S) (First name, middle initial, last name)

Harry G. Harris
Irving U. Ojalvo
Reginald E. Hooson

6. REPORT DATE	7a. TOTAL NO. OF PAGES	7b. NO. OF REFS
May 1970	285	32

8a. CONTRACT OR GRANT NO.	9a. ORIGINATOR'S REPORT NUMBER(S)
F 33615-69-C-1263 b. PROJECT NO. 1467 c. Task No. 146704 d.	None 9b. OTHER REPORT NO(S) (Any other numbers that may be assigned this report) AFFDL-TR-70-49

10. DISTRIBUTION STATEMENT

This report has been approved for release; its distribution is unlimited.

11. SUPPLEMENTARY NOTES	12. SPONSORING MILITARY ACTIVITY
	Air Force Flight Dynamics Laboratory Wright Patterson AFB, Ohio 45433

13. ABSTRACT

This report presents analytical techniques for predicting both the linear and nonlinear stresses and deformations of mechanically fastened joints. The idealization used is a set of stacked parallel plates which transfer planar loads among themselves by means of transverse fasteners. The plates are treated by finite element methods of matrix structural analysis in which each element is assumed to be in plane stress for both elastic and plastic stress states. The fasteners, which are treated by short-beam theory, interact with the plates under the assumption that the plates may be represented by an equivalent elastic foundation.

Application of the present analytical techniques was made to a variety of problems including: the combined elastic-plastic behavior of plates with unloaded holes, the load-deflection behavior of single-fastener joints, the residual stress distributions in plates with squeeze rivets, the effect of fastener bending and shear deformation on the bearing stress distribution between the fastener and the plate, and the prediction of the fatigue life of typical mechanically fastened joints. In all these cases, comparisons with test results generally gave very good correlation.

Parametric studies were performed to determine the effects on stress and deflection distributions of variables such as: initial clearance or interference between fastener and hole, load level, geometry and material properties. The effect of these variables upon fatigue life of single and multi-fastener joints under realistic loadings was also assessed.

For the range of parameters studied, the effects of hole clearance and fastener interference and geometric configuration appear to play the dominant roles in determining the stress distribution and hence, the fatigue life of mechanically fastened joints.

DD FORM 1 NOV 1473

Unclassified

Security Classification

14. KEY WORDS	LINK A		LINK B		LINK C	
	ROLE	WT	ROLE	WT	ROLE	WT
Aircraft Structural Joints						
Fastener Load Deflection Data						
Mechanically Fastened Joint Analysis						
Fatigue of Joints						
Stress Concentration Problems						
Finite Element Applications						
Plastic Analysis of Structural Joints						